Order Number 9200500

The Lower Silurian Brassfield Formation: A condensed sequence of punctuated deposition?

Norrish, Winston Alfred, Ph.D.

University of Cincinnati, 1991

U·M·I
300 N. Zeeb Rd.
Ann Arbor, MI 48106

THE LOWER SILURIAN BRASSFIELD FORMATION: A CONDENSED SEQUENCE OF PUNCTUATED DEPOSITION?

A DISSERTATION SUBMITTED TO
DIVISION OF GRADUATE STUDIES AND RESEARCH
UNIVERSITY OF CINCINNATI

IN PARTIAL FULFILLMENT OF THE REQUIREMENTS FOR THE DEGREE OF

DOCTOR OF PHILOSOPHY

DEPARTMENT OF GEOLOGICAL SCIENCES
COLLEGE OF ARTS AND SCIENCES

1991

BY

WINSTON A. NORRISH

B.A., COLLEGE OF WOOSTER, 1982
M.S., UNIVERSITY OF CINCINNATI, 1985

UNIVERSITY OF CINCINNATI

28 May 19 91

I hereby recommend that the thesis prepared under my supervision by Winston A. Norrish

entitled The Lower Silurian Brassfield Formation: A Condensed Sequence of Punctuated Deposition?

be accepted as fulfilling this part of the requirements for the degree of Doctor of Philosophy

Approved by:

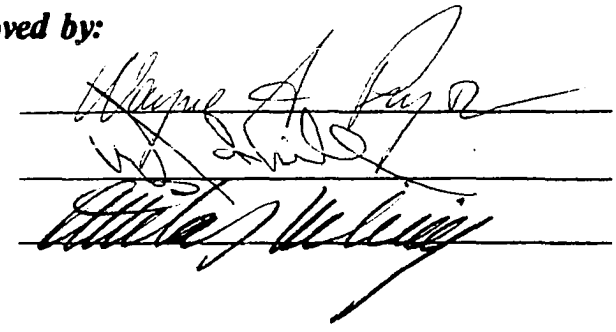

ABSTRACT

The Brassfield Formation is a very thin, highly condensed carbonate unit that encompasses most of the Llandovery (8.5 MMYR) and covers much of the eastern midcontinent. Fifty six Brassfield outcrops exposed around the flanks of the Cincinnati arch comprise three members, four facies tracts, and seven lithofacies. The three types of condensation recognized in the Brassfield (dynamic bypass, punctuated deposition, and sediment starvation) are related to sea level fluctuations, manifested as a hierarchy of sequence orders, that ultimately controlled the spatial and temporal distribution of facies.

The Brassfield is itself a third order sequence. It contains two fourth order sequences, the older comprising facies tracts one (the Belfast Member -- a shallow, peritidal, silty dolomite), and facies tracts two and three (the Middle Member -- distal to proximal tempestites, carbonate shoals, and very shallow ferruginous carbonate sand sheets). The younger fourth order sequence contains only facies tract four (the Lee Creek Member, or facies VII -- fine grained glauconitic and collophane rich, deep water dolomite). All other facies are fifth order sequences. The facies themselves can be separated into sixth order sequences. Third order bounding surfaces can be correlated far from the study area. Fourth and fifth order sequence boundaries are correlative at least within, and possibly away from the study area, and sixth order sequences and their bounding surfaces vary between outcrops.

Condensation marked by moderate to rapid accumulations of sediment punctuated by periods of non-deposition and erosion (punctuated deposition), is most common at the base of fifth or sixth order shallowing upward sequences, as in Brassfield facies II, III, IV and V. These are characterized by interbedded shales and limestones with reworked glauconitic bioclasts and pellets, hardgrounds, intense bioturbation, and erosional surfaces. Individual beds are relatively thin. Reworking, amalgamation and sedimentary bypass (dynamic bypass) are associated with the tops of shallowing upward sixth, fifth or fourth order cycles. Brassfield examples include the top of facies III, V, and the sixth order sequences they contain, and the entire thickness of facies VI. Lithologies include oolitic ironstones and altered glauconitic bioclasts, enrichment of durable clasts, and relatively coarse grained, thick beds. Continuous low sedimentation rates (sediment starvation) are associated with moderate to major transgressions and deep "starved basin" conditions. Such conditions in the Brassfield have been identified only in the upper fourth order sequence, the Lee Creek Member. It has has a patchy distribution and is composed of very fine grained dolomite with well formed glauconite pellets and collophane fragments.

TABLE OF CONTENTS

ACKNOWLEDGEMENTS

Special thanks go to Dr Wayne A. Pryor, my principal advisor, who, through out this project, provided guidance, insight, and an occasional kick in the pants. Thanks also to research committee members Dr. Arnie Miller and Dr. Barry Maynard for their encouragement, suggestions and manuscript review. Acknowledged also are Bruce Brasswell for his help in the field (and on my car), and David Jennette, who engaged me in many constructive discussions of sequence stratigraphy and sedimentary condensation. Dr. Barry Cohn (BP Exploration) kindly provided use of support staff at BP to help with final manuscript preparation, in particular, Lane, who patiently typed, and retyped, and those in the Drafting Department at BP, with whom all were a pleasure to work.

Finally, thanks to my parents, Bob and Nancy, who encouraged me through out graduate school. They were always able to put their own troubles aside to help me out.

LIST OF FIGURES

INTRODUCTION

Stratigraphically condensed intervals are an integral part of all dynamic depositional systems. Recognition of unconformable surfaces is essential to sequence correlation and condensed intervals are, themselves, a form of unconformity. Clearly, condensed deposits are diverse, and individual depositional systems comprise more than one process of condensation (e.g., Kidwell, 1989). Shallow water, high energy condensation may be at least as common as deep water, sediment-starved condensation on carbonate ramp and platform systems typical of Paleozoic continental epeiric seas.

As we learn more about stratigraphic sequences, how they form, and how they correlate on a broad regional scale, we advance stratigraphy toward a higher level of organization based on a hierarchy of relative sea level fluctuations. The recognition of condensed sequences, widely correlative unconformable surfaces, the dynamics of their formation, and their diversity, are essential to a greater understanding of all that is contained in the stratigraphic record.

The Lower Silurian Brassfield Formation has been the subject of geologic study for over a century-and-a-half, yet its most remarkable characteristic -- a thickness greatly reduced relative to coeval strata -- has remained essentially unexplored. The Brassfield Formation was the cornerstone of many early stratigraphic Silurian studies because it marks the base of the Silurian system over a broad area of the North American eastern

midcontinent (Locke, 1838; Owne, 1856; Orton, 1869-1884; Foerste, 1935). More recent Brassfield work has addressed stratigraphy (Warn, 1941; Holbrook, 1964; Rexroad, 1965, 1967; Rexroad and Nicolle, 1968; Kallio, 1976), paleontology (Laub, 1979, Harrison, 1974; Grey and Boucot, 1972; Ausich, 1984a, 1984b, 1985, 1986a-c), and petrology (Rago, 1952; Byrne, 1961; Elhers and Hoover, 1961; O'Donnel, 1967; Frost, 1977; Sheehy, 1979; Hendrix, 1983; Gordon and Ettensohn, 1984; Adenuga, 1985).

This study documents sedimentary condensation in the Brassfield Formation within the framework of the dynamic sedimentological regime that evolved on the eastern midcontinent prior to and through the Llandovery. On a regional scale, this study builds on the Paleozoic stratigraphic and depositional history of the North American eastern midcontinent. More importantly, it provides a look at the variety of condensed sedimentary intervals developed in typical carbonate platform systems, and how they relate to the sedimentological regime.

CONCLUSIONS

(1) The Brassfield Formation is divisible into three members: (1) the Belfast Member, (2) the Middle Member, and (3) the Lee Creek Member. These comprise seven lithofacies:

I shallow peritidal silty dolomite

II distal to proximal tempestites

III distal to proximal tempesities capped by ironstones

IV shallow carbonate shoals

V shallow platform sand sheets with small bioherms commonly capped by ironstones

VI very shallow water amalgamated ferruginous sand sheets, and

VII fine grained, glauconitic and phosphatic, deep, starved basin dolomite

(2) The seven facies are grouped into four facies tracts which record an overall transgression through the Llandovery:

Tract	Facies
1	I (Belfast Member)
2	II, IV, (VI) (Middle Member, lower)
3	III, V, VI (Middle Member, upper)
4	VII (Lee Creek Member)

(3) The Brassfield Formation represents a hierarchy of four sequence orders as described by Vail et al. (1977) and Busch and Rollins (1984). The entire Brassfield is contained in a third order sequence. This is divisible into two fourth order sequences, the first of which comprises facies I through VI (facies tracts 1 through 3), and the second of which contains facies VII only (facies tract 4). Facies tracts 1, 2, and 3 are fifth order sequences. Fifth order sequences cannot be resolved in the highly condensed beds of facies tract 4. Facies tracts 1, 2, and 3 each contain sixth order sequences which appear as small scale shallowing-upward tempestite packages, sand sheets, or intertidal flat parasequences.

All sequences in the study area are bound by unconformable or paraconformable surfaces. Major sequence bounding surfaces are more widely correlative than minor sequences bounding surfaces. Third order sequences are roughly equivalent to stages and are very widely correlative. Fourth and fifth order sequences in the Brassfield can probably be traced away from the study area, but are obscured in subsurface. Deposition of third, fourth, and fifth order sequences are controlled by processes that operate on at least a basin wide scale. Sixth order sequences show a high degree of local variability and are not correlative within the bounds of the study area. Therefore, sixth order sequences are affected by local, rather than basin wide processes.

(4) Facies orientation and paleocurrent data from the Middle Member are consistent with previous interpretations of a north northeast - south

southwest trending depositional strike (Gordon and Ettensohn, 1984; Lukasik, 1988). This coincides with the eastern edge of the interbasin platform, which deepens to the east. Facies tract 4, the Lee Creek Member, represents deeper water deposition and records a gentle regional westward deepening of the platform.

(5) Condensation in the Brassfield Formation has three forms that can be related to depositional conditions. The degree of condensation is greatest where coincident with major sequence boundaries. Rapid depositional events punctuated by periods of nondeposition are typical at the base of shallowing-upward sequences. The tops of shallowing upward sequences and broad, very shallow platforms are susceptible to amalgamation, reworking, and sedimentary bypass. These horizons are typified by a mixture of reworked, durable clasts (e.g., hematitic ooliths, glauconitized bioclasts, and phosphatized clasts) and non-reworked clasts. The third type of condensed deposit accumulates slowly under sediment starved, relatively deep water conditions, and is represented in the Brassfield by facies VII, the Lee Creek Member. Sediment starved deposits are fine grained, bioturbated or laminated, and contain well formed glauconite pellets, collophane fragments, chertified bioclasts, and quartz silt. This type of condensed deposit can probably be traced toward the sediment source, grading first into condensed deposits formed under punctuated sedimentary conditions, and eventually into condensed deposits accumulated under conditions of sedimentary bypass.

(6) Clay minerals in the Brassfield include illite, glauconite, kaolinite, and chlorite, and their distribution as described in previous studies (Ehlers and Hoover, 1961' O'Donnel, 1967) is verified in this study. Illite and glauconite are present around the outcrop belt. Glauconite is associated with condensed horizons. Kaolinite and chlorite are found in the southeast quadrant of the outcrop belt, and may be related to source area proximity.

Glauconite in the Brassfield occurs as well formed pellets associated with sediments deposited under starved conditions. Less well developed glauconitized bioclasts are commonly associated with condensed deposits formed under punctuated and sediment starved conditions. All Brassfield glauconite is shown by x-ray diffraction analysis to be an iron rich, mixed layer illite.

(7) Analysis of dolomite in the Brassfield reveals at least two dolomitizing events. Facies I, the Belfast Member, represents early stage peritidal, possibly intertidal dolomitization. The second, late stage is associated with dolomite in facies II through VII. Dolomitization in this stage was complete (replacing the entire rock) to the south and partial (replacing only micrite) to the north. The transition between the northern and southern zones is sharp and may be related to uplift and exposure of Silurian and Ordovician sediments in the Devonian, which was more intense in southern parts of the study area. Circulation of normal marine waters through these strata over a long period of time (as described by Hardie, 1987) may have been sufficient to drive the second stage

dolomitization process, rather than the mixing zone, or "Dorag" model evoked by previous workers.

BACKGROUND

Condensed sections are thin units deposited over relatively long periods of time. They are products of low net rates of sedimentation formed either by prolonged periods of slow continuous deposition, short periods of rapid deposition punctuated by long periods of nondeposition or erosion, or rapid and frequent deposition combined with reworking, amalgamation and bypass of sediments.

The following section addresses the formation of sedimentary strata in the context of geologic time. The first part of the discussion focuses on the historical development of fundamental geologic concepts that have affected our perception of how sedimentation occurs in time. The second part addresses current concepts relative to the formation of condensed sections.

HISTORICAL DEVELOPMENT

Uniformity or Catastophism

The development of the uniformitarian concept has dramatically influenced our understanding of sedimentary processes. Before James Hutton laid the foundation for uniformitariansim at the end of the eighteenth century, earth history was thought to have been the product of divine intervention. Hutton knew that if geologic interpretations were to be based on natural laws, then those laws must have remained constant through geologic history. Fifty years after Hutton published Theory of the Earth (1795), Charles Lyell (1833) introduced the concept of uniformitarianism with *Principles of Geology.* The role

of religion in geology was formulated in the writings of Buckland (1837) and Cuvier (1817) who, as Catastrophists, believed the earth had been shaped by a series of grand cataclysms brought about by supernatural forces. Lyellian uniformitariansim had two aspects, each of which were specifically designated to undermine the main weaknesses of catastrophism. The first aspect, *substantive uniformitariansim*, involved the contention that rates and energies involved in geologic processes do not vary through time, implying that catastrophic events do not occur. The second aspect, *actualistic uniformitariansim*, suggested that physical laws do not change in time or space, thus rejecting the notion that divine influence was necessary to drive earth evolution (Gould, 1985, 1965; Hsu, 1983). Actualistic uniformitariansim is, of course, shared by all sciences.

The earth-shaping catastrophic events suggested by Buckland, Cuvier, and others were simply not observable (at least on the scale of a human life time) and the increasing awareness of the vastness of geologic time led Lyell to conclude that geologic features of the earth had formed as a consequence of slow and continuous processes. Reaction to catastrophic theory brought about the uniformitarian concepts that were to shape geologic thought for a century to follow.

Darwin, who first formalized his theories on evolutionary processes in The Origin of Species (1859), was obviously influenced by uniformitariansim. Just as Lyell considered geology to be driven by steady processes, Darwin saw biological evolution as gradual. If geologic and evolutionary rates were indeed slow, as embodied by the concept of substantive uniformitariansim, then abrupt

stratigraphic and paleontologic changes were surely manifestations of an incomplete geologic record, rather than punctuated geologic process.

The Fallacy of Substantive Sedimentation

Lydell and Darwin both observed disparities between rates of modern geological and biological processes and the ancient record, which led them to conclude that the stratigraphic record was incomplete. This disparity also inspired Barrell's (1917) treatise entitled Rhythms and the Measurement of Geologic Time. Barrell, too, stressed the incompleteness of the stratigraphic record, but recognized the existence of breaks in deposition represented by bedding planes with "values from seasonal cessations of sedimentation to those which approach geologic epochs in duration" (p. 78). Barrell called these breaks "diastems" and contended they were characteristic of all stratigraphic sections. One of Barrell's main theses was based on his observation that the frequency and duration of stratigraphic breaks appeared to increase with the age of deposit: "The proportion of lost intervals (to preserved) increases with the more distant eras" (p. 891). He attributed this trend in part to an increase through time in orogenic activity which resulted in an acceleration in sedimentation rate. However, Sadler (1981) and Salop (1977) pointed out that an increase in tectonism would result not only in an increase in sedimentation rate, but in sedimentary discontinuity as well. Therefore, the apparent increase in sedimentation rate toward the present must have another explanation.

Saddler (1981) examined in depth the issue of sedimentation rates relative to time. He found that apparent sedimentation rates increase as the intervals over which they are determined decrease. For example, the rate of

sedimentation during a geologically instantaneous event, such as a storm, would be vastly greater than the sedimentation rate measured over the span of time available for the deposition of a geologic formation. The formation, however, might consist of many geologically instantaneous storm events separated by long periods of depositional hiatus.

Geologic studies that stress the importance of depositional hiatus, like those of Barrell and Sadler, expose the fallacy of substantive uniformitarianism, and cast doubt on the notion of continuous, gradual deposition. Some older geologic theories anchored in substantive uniformitariansim have been reevaluated in this light. Darwin's view of evolution as a gradual process has been at least partially replaced by the concept of punctuated equilibrium (Eldredge and Gould, 1972) where long period of phenotypic stability are thought to be interrupted by rapid, or punctuated, evolutionary events. Similarly, where it was one thought that the sedimentary record was nearly complete in deep ocean basins, records from the Glomar Challenger indicate that less than half of the last 125 million years has been recorded in the deep south Atlantic (van Andel, 1981).

Several papers addressing the effects of non-uniform sedimentation, published in the late 1970's and early 1980's, (e.g., Ager, 1981; van Andel, 1981; Sadler, 1981; Dott, 1983, Hsu, 1983), emphasize the importance of stratigraphic gaps caused by breaks in deposition. In an interesting, philosophical discussion on stratigraphy, Ager (1981, p. 35) likens the sedimentary record to a musical score where "the intervals between the notes are every bit as important as the notes themselves." Stratigraphic gaps caused

by depositional hiatus -- the intervals between the notes -- rarely appear significant, and may be impossible to detect, particularly if paleontological evidence is inconclusive. The chance that a boundary between two stratigraphic units will be preserved is especially slim for rapidly deposited units (Newell, 1967; van Andel, 1981; Barrell, 1971). Sedimentologists must learn to detect these depositional breaks and incorporate them into their depositional models. This is an important step in the evaluation of condensed sequences.

The Rare Event

Almost without exception, stratigraphic accumulations do not form by continuous sedimentation, but rather from depositional events that would be considered rare on the scale of human life. Gretener (1967) defines a rare geologic event (such as the deposition and preservation of a significant sedimentary package) as physically possible, but requiring the improbable coincidence of several favorable factors. The significance of rare events in geology becomes clear when they are placed within the framework of geologic time. Consider, for example, that an event with a one-in-a-million chance of happening once in a year has a 98% certainty of happening five times in one million years (Gretener, 1967).

Given the dynamic nature of most depositional systems, it would be wrong to assume that sedimentation has been inactive between recorded events. The magnitude and occurrence of depositional events is sporadic. Substantive uniformitarianism simply does not apply. However, deposition is a

continual process, and it may be the depositional event large enough to be recorded and survive subsequent reworking that is rate (Hsu, 1983).

Cyclic Repetition of Rare Events

Depositional events are commonly recorded at semi-regular stratigraphic intervals, and are inferred to represent cyclic processes. These cycles show a tremendous range in scale. They can be as small as those represented by diurnal lamination in stromatolites, and tidalites. They are recorded in annual varve deposits. Major global stratigraphic patterns, on the other hand, may be associated with cycles that have enormous periods, such as the first order sea level cycles described by Vail, et al. (1977; see below).

The tendency to impose the rigidity of cycles on natural depositional systems may stem from geology's deep roots in uniformitariansim. "Cyclicity", wrote Dott (1983), "is a special subtle form of uniformity." True Markovian cyclicity is probably uncommon in depositional systems and may be restricted to cosmically controlled pulses such as those described by Milankovitch (1941). It is important to keep in mind, however, that the earth has been shaped by episodic phenomena that have varied widely in terms of magnitude and frequency, and stratigraphic patterns signal repetitive depositional conditions, be they cyclic in a Markovian sense or not.

Several models have been proposed to explain seemingly cyclic patterns in carbonate lithologies. Such models are commonly driven by relative sea level change, and invoke a transgressive phase associated with a break in

sedimentation (Goodwin and Anderson, 1980; Wilkinson, 1982; James, 1984). It is not clear how small to moderate sea level fluctuations cause sedimentologic breaks in carbonate systems, however. Carbonate production is an autocthonus (or parautocthonus) process, and carbonate growth rate potential has been calculated to be several orders of magnitude higher than rates of sea level rise caused by transgressions (Schlager, 1981), though this idea is subject to question. Thus, it is difficult to envisage carbonate deposition lagging behind sea level rise, resulting in nondepositional periods. Schlager suggests that superimposed on long period sea level oscillations are pulses that are small in magnitude and more rapid than rates of autochthonus carbonate sedimentation. These pulses could account for the deeper water phases of the carbonate cycles, and "lag time" (the time required for carbonate production to recover after a transgression) could account for nondepositional periods (see Schlager, 1981; Read, et al., 1986).

Vail, et al. (1977) described a series of sea level curves based on the recognition of discrete stratigraphic units deposited on continental shelves world wide. These stratigraphic units are "relatively conformable successions of genetically related strata bounded on their tops and bottoms by unconformities or correlative conformities." They range in thickness from centimeters to hundreds or thousands of meters. The bounding surfaces are directly related to breaks in transgression-induced nondeposition. Sloss (1963) described six major unconformities separating seven major stratigraphic units. Vail borrowed from Sloss' definition of a stratigraphic sequence as a rock stratigraphic unit ranked higher than group, mega group, or super group (mega- and

supergroups are informal stratigraphic units higher in rank than group and that represent major events in the course of geologic history), traceable over large areas of the continent, and bounded by interregional unconformities. Because these are discrete rock bodies bounded by relatively synchronous surfaces, they are chronostratigraphically significant.

Vail (1977) described three orders of sea level curves. First order cycles have durations of 200-300 million years. Second order cycles have durations of 10-80 million years and are roughly correlative to systems. Third order cycles encompass from 1-10 million years and are roughly correlative to stages. Smaller, fifth and sixth order cycles (as described by Busch and Rollins, 1984) have been identified with punctuated aggradational cycles (PACs of Goodwin and Anderson, 1980, 1984).

The pervasive occurrence of shallowing upward carbonate sequences (see James, 1984, for a review) suggests that cyclic carbonate production commonly involves rapid transgressions followed by slow regressions, at least on the scale described by Goodwin and Anderson (1980).

Wilkinson (1982) reviewed two general models of cyclicity in cratonic carbonate sequences that could generate shallowing upward packages. The models take into account both relative sea level changes and autocthonus carbonate production rates.

"Allocyclic" carbonate production is driven by relative sea level changes controlled by processes not directly related to sedimentation, such as non-

uniform basin subsidence and/or eustatic sea level fluctuation. When relative sea level rises fast enough to outpace carbonate production, the shelf or platform is quickly shifted to a deeper water setting. Consequently, deeper water sediments (deep water hemicycle, or half cycle) directly overlie shallow (shallow water hemicycle). More often than not, the change is suggestive of an instantaneous, rather than gradual, transgression. If the sea level rise is gradual, then it is apparently accompanied by minimal deposition. PACs form in this manner, and because they are bound by isochronous boundaries and are commonly basin wide, they can be used for correlation across a basin (Goodwin and Anderson, 1980).

Aigner (1985) has recognized 1-7 meter thick packages that thicken and coarsen upward in the Upper Triassic Muschelkalk of Germany. The base of the packages represent distal tempestites, and the top proximal. As with the models described by Wilkinson (1982) and Goodwin and Anderson (1980), rapid sea level rise leaves little evidence of transgression. Aigner suggests that these tempestite cycles, like PACs, are time stratigraphic markers.

"Autocyclic" deposition depends on variations in autocthonus carbonate production. Like allocyclic deposition, the autocyclic deep water hemicycles from eustatic sea level rise or basin subsidence. However, when carbonate accretion exceeds sea level rise, relative water depth will decrease. Eventually, the water becomes too shallow and the carbonate factory shuts down. Sea level rise then outpaces carbonate production until water depth becomes sufficient for the cycle to begin anew.

Read, et al. (1986) used computer modeling to quantify carbonate cyclicity. The following variables were incorporated into the model:

- depth dependent sedimentation rate;
- amplitude and period of sea level oscillation;
- linear rate of subsidence; and
- lag time (the time it takes a carbonate system to recover after it has shut down).

A short lag time results in deposits with thin deep-, and thick shallow-water hemicycles. A long lag time will result in a thicker deep water hemicycle. Hard grounds, glauconite, and other condensation lithologies can be incorporated into the shallow water hemicycle, given a long lag time.

Asymmetrical sea level oscillations have a greater effect on sedimentary cyclicity than symmetrical fluctuations. If sea level rises rapidly enough to out pace sedimentation and is followed by a slow regression, well defined shallowing-upward cycles will be developed. Hays, et al. (1976) and Read, et al. (1986) have shown these to be more typical of glacio-eustatic fluctuations. If sea level rise is slow and sedimentation is maintained, cycles may be difficult or impossible to identify. Furthermore, low amplitude oscillations will result in thin subtidal facies and thick tidal flat caps, where as an increase in amplitude results in thicker subtidal facies. The greater (and faster) the rise in the sea level, the longer it takes the system to aggrade to tidal flat conditions, hence, the thicker subtidal facies. Thick subtidal facies may also indicate the influence of storms (Read, et al., 1980).

CONDENSED DEPOSITS

Whether of autocyclic or allocylic origin, vertical stratal patterns in carbonates almost always result from relative changes in water depth, because with changes in sea level come great variations in the style and rate of depositional processes.

It was suggested earlier that sedimentation is a sporadic process and produces a stratigraphic record riddled with depositional breaks. The wide variation in depositional conditions that result from relative changes in sea level should be taken into account when interpreting how stratigraphic breaks fit into the depositional history of a particular deposit. The origins of depositional breaks, apparent low sedimentation rates, and condensed sequences vary with the depositional system.

Condensed strata are thin, commonly widespread deposits that appear to represent exceedingly low rates of deposition. Jenkyns (1971, p. 330) defined a condensed deposit as "a bed that is considerably reduced in thickness relative to another of equal age and whose origin is the product of minimal net sedimentation." This is a useful working definition because it allows for variations in the effect of, for example, relative sea level change, depositional energy and rate, sedimentary amalgamation and bypass, paleotopography, proximity to source area, and biological production. It does not require that the sedimentation rate be continuously low over long periods of time.

Examples of chronostratigraphic deposits that show significant variation in thickness across a basin or among basins are common. For instance,

Paleozoic sediments in the Unita Basin of Utah measure 40,000 feet to the west and 8,000 feet on the eastern side of the basin. Baker (1949) attributed the thinning to long breaks in sedimentation. Lower Silurian sands and shales in the Appalachian Basin of Pennsylvania and West Virginia are over 1,000 feet thick, while their carbonate equivalents in the Illinois Basin, Michigan Basin, and Cincinnati Arch region to the west measure less than 100 feet. Ager (1981) listed many similar European examples in his argument for the incompleteness of the record, including a case in the Upper Jurassic Purbeckian Stage where over 550 feet of sediments south of London thin to less than 3 feet 30 miles away from the French cliffs near Boulogne, with no obvious sedimentary breaks.

We must look closely at condensed deposits to construct their depositional history. Does a particular condensed deposit represent a persistence of slow sedimentary rates, rapid depositional events punctuated by long periods of depositional hiatus, or rapid deposition combined with reworking, amalgamation and sedimentary bypass? Given the discussion to this point one would expect that even those intervals appearing to represent continuous sedimentation will, upon closer inspection, reveal a history marked by at least some depositional hiatus.

Low Energy Condensation

One of the first models for the formation of basin-wide condensed deposits involving slow continuous sedimentation was the "barred basin" (Wollnough, 1942). Woolnough speculated that at certain times in geologic history land masses were extremely eroded (a condition he called ultra base-leveling or ultra peneplanation) and terrigenous sediment input to the ocean

basins slowed dramatically. Stagnant bottom conditions on shelves resulted in the deposition of thin pelagic limestones, radiolorites, and manganese nodules in red clay. Sediment transported to the ocean by sluggish streams could not bypass near shore barriers that "cut off free access of deeper oceanic circulation while permitting more or less unrestricted inflow of surface waters." This ultimately led to euxinic bottom conditions (Wollnough, 1942, p. 785).

Rich (1951) divided the marine realm into unda (shelf), cline (slope), and fondo (basin) environments. His "fondothem" consisted of fine grained, massive and even bedded clays and oozes deposited under sediment starved conditions. "Deposition in the fondo environment is slow," writes Rich (1951, p. 9), "and a long time would generally be represented by only a small thickness of sediment."

Trumpy (1955) proposed the term "leptogeosyncline" for deep, volcanic related geosynclinal troughs that accumulated only minor amounts of sediment.

The "starved basin" model was first proposed by Adams (1951) in his account of abrupt thinning of Pennsylvania sediments into the Midland Basin. Thick terrestrial clastics were deposited on the near shore shelf, but reef growth further out on the shelf prevented clastics from being transported to the basin interior. As the basin subsided, thin dark shales were deposited under increasingly stagnant, euxinic conditions.

The introduction of reef-building fauna in the middle Ordovician may have been a factor in the formation of sediment starved basins. Prior to their development, tidal flat processes added most carbonate material to shelves.

With the appearance of reef-building organisms, large masses of carbonate could be constructed in and around shelf areas, restricting basin circulation and cutting off terrigenous sediment supply to the deeper basin areas (Wilson, 1975).

Wilson (1975, pp. 335-354) summarized the lithologic characteristics of sediments deposited in deep, starved, mostly geosynclinal troughs, protected from major terrigenous input:

(1) Thin radiolarites.

(2) Red (ferruginous) biomicrites and nodular limestones.

(3) Light colored pelagic limestones.

(4) Dark basinal micrites and spiculitic limestones, commonly cherty, and containing the trace fossil *Chondrities.*

(5) Distal turbidites.

(6) Bioclastic grainstones and packstones:

  (a) containing small epiplanktonic bivalves.

  (b) Red to pink encrinites (echinoderms deposited in a non-reducing environment).

(7) Spiculites.

(8) Calcareous brecciated debris flows from nearby shelves and slopes.

(9) Ferruginous manganese crusts and nodules in limestone (slow sedimentation and concretionary growth in deep water).

Modern sedimentation rates in the deep sea are variable, but low, ranging from almost zero to nearly 400 mm/1,000 years. Controlling factors

include sediment supply, dissolution, and erosion. Deep sea clays accumulate at a rate of less than 2 mm/1,000 years, biogenic silica is deposited at relatively high rates that range from 4 to 400 mm/1,000 years, and pelagic carbonates accumulate at an average of 30 mm (uncompacted)/1,000 years (Scholle et al., 1983).

Sediment Starvation and Transgressions -- Breaks in sedimentation and associated lithologies related to transgressions are well documented. When base level is raised by a transgressive event, sediments deposited under near shore conditions at low sea level stand become stranded on the flooded shelf, and deposition of terrigenous clastics from exposed continental areas is restricted to near shore estuarine and deltaic environments, leaving the shelf sediment starved (Swift, 1968). Transgression-induced alluviation, as this is called, has been used to explain condensed sequence development in the Devonian of New York (McCave, 1973; Johnson and Freedman, 1969).

More recent developments in sequence stratigraphy (see volumes edited by Bally, 1985, and Wilgus et al., 1988) have included as a major element condensed sections that consist of thin pelagic or hemipelagic sediments deposited at slow rates developed during regional transgressions (van Wagoner et al., 1985, 1990).

More recent developments in sequence stratigraphy (see volumes edited by Bally, 1985, and Wilgus et al., 1988) have included as a major element condensed sections that consist of thin pelagic or hemipelagic sediments deposited at slow rates developed during regional transgressions (van Wagoner et al., 1985).

Post-Pleistocene shelf sedimentation has been largely restricted to near shore areas. Deposition in the northwest Gulf of Mexico consists of Mississippi Fluvio-deltaic clastics and almost negligible middle and outer shelf pelagic carbonates (Curray, 1960; Phelger, 1960). Emery (1968) estimated that 70% of the sediments exposed on today's shelves were deposited under near shore conditions prior to the Pleistocene rise in sea level, and these "relict" sediments are in disequilibrium with current shelf processes. Relict sediments deposited under near shore conditions and reworked by deeper shelf processes following a transgression are called "palimsest" (Swift, 1972).

High Energy Condensation

Condensed strata do not always form under conditions of low sediment input and low depositional energy. Where depositional energy and sediment input are considerable, reworking, sediment bypass and removal, and amalgamation by successive turbulence events can form exceptionally thin sedimentary packages. The relative effects of sluggish sedimentation versus these higher energy processes were considered in the earliest investigations into the genesis of condensed deposits.

Heim (1934, p. 372) introduced the term "stratigraphic condensation" to describe the combined processes of low sedimentation rate and occasional small-scale reworking events (see also Heim and Stitz, 1934). Rod (1946) considered minimal sediment input to be the most important process in sedimentary condensation, and regarded reworking as a process of "normal" sedimentation. Rod, however, failed to provide an alternative process for the

mixing of faunal zones, which he included as a basic element in his definition of condensed deposits.

Mixing of faunal zones by reworking has been considered an essential feature of condensed deposition (Shaub, 1948; Heim, 1958; Wendt, 1970). Jenkyns (1967, 1970), Jenkyns and Torrens (1969), and Bernoulli and Jenkyns (1974), emphasized the importance of turbulent reworking on submarine topographic highs rather than low energy "stagnant" sedimentation to the formation of condensed deposits. Deposition in an environment affected repeatedly by storms has been shown to result in considerable post-mortem bias (faunal mixing) in completely amalgamated shell beds (Seilacher, 1982; Kidwell and Aigner, 1985). Although physical reworking is usually cited as the cause of mixing, the effects of biogenic processes cannot be discounted.

Among the types of turbulence events that can result in sedimentary condensation are storms (tempestites), turbidity currents (turbidites), and floods (innundites) (Seilacher, 1982). These events involve an initial culmination of turbulence energy resulting in erosion, followed by waning energy conditions and deposition. The change in depositional conditions is recorded in vertical and horizontal sedimentary gradients. Also, normal ecological bottom conditions, and the biotic communities developed therein, are disrupted.

The erosional phase removes and reworks previously deposited sediments to a depth that depends on the strength of the event and cohesiveness of the substrate. This is usually recorded as casts or lay at the base of the overlying deposit. As the energy of the event wanes and sediment

begins to be deposited, a recognizable sequence of bed forms develops in response to changing flow regimes. Horizontal proximality trends that form in response to energy gradients have been described for storm events by Aigner (1982, 1985).

As an event brings in new sediment, its energy can resuspend previously deposited sediments. Finer sediment is carried into the basin and new, coarser sediment is mixed with older deposits. When the events are repeated, amalgamated deposits representing many events are formed in proximal situations, while finer grained bypassed sediment forms thin single event beds in distal situations (Aigner, 1982; 1985).

There is some evidence that carbonate mud surfaces buried under amalgamated lag beds are selectively cemented during early diagenesis. These surfaces may be repeatedly exposed and reburied, leading to the formation of hard grounds (Fursich, 1971, found a common association between hard grounds and tempestites).

Turbulence events of all types can condense and amalgamate sedimentary deposits. However, turbidity currents and floods are usually associated with volumes of sediment too great to form condensed deposits. Amalgamated and condensed deposits formed under conditions of turbulence, reworking, and bypass (low net rate of deposition) are most commonly associated with repeated storm events (Seilacher, 1982).

The formation of complex amalgamated shell beds by repeated "rare" storm events has been addressed by Gebhard (1982), Kidwell and Aigner

(1985), and Kidwell (1989). Models involving the concentration -- or condensation -- of shells, phosphate, glauconite, and durable accessory minerals have been presented by Seilacher (1982, 1985), Reif (1982), Aigner (1982, 1984), and Reineck (1982). Proximal amalgamated deposits might not be distinguishable from deposits formed from a single event because each event destroys evidence of previous events (Fursich, 1971; Bayer et al., 1985; Aigner, 1985). However, they may show faunal mixing and a concentration of more durable components that increases with each successive amalgamation (Seilacher, 1982).

Brett and Baird (1985, 1986) and Barid and Brett (1981) have incorporated these concepts in their interpretation of the Hamilton Group in New York. They suggest that repeated condensation horizons capping symmetrical shoaling packages were formed from shallow water storm amalgamation during regressive low sea level stands. McCave (1969, 1973) had reported these same horizons to be formed in deep water at times of transgressive alluviation.

Low energy and high energy condensation regimes are not necessarily restricted to separate systems; they may be genetically related. James (1980) noted that the base of shallowing-upward sequences can represent sedimentary hiatus, while their tops are marked by condensed, winnowed deposits. The possible coexistence of condensation regimes on transgressive shelves has been suggested by Kidwell (1989). The Miocene deposits Kidwell described consist of shoaling upward sequences underlain by condensed deep water bone beds and overlain by shallow water amalgamated shell beds. The concepts of dynamic stratigraphy, which incorporate concepts of proximality

trends and punctuated aggredational cycles, strongly suggest that different condensation regimes could -- in fact, should -- coexist in the same system.

The Brassfield Formation exhibits features indicative of all types of condensation described above. The condensed nature of the Brassfield can be related to the response of platform sedimentation to shifting depositional conditions related to relative changes in sea level.

REGIONAL GEOLOGY, PALEOGEOGRAPHY AND TECTONICS

MAJOR STRUCTURAL FEATURES

The major tectono-sedimentological features of the North American eastern midcontinent include the Cincinnati, Kankakee, Findley and Algonquin Arches, and the Illinois, Michigan and Appalachian Basins. These features were not fully developed in Lower Silurian time (Figures 1 and 2). The Lower Paleozoic Waverly Arch was roughly in the position of the Findley and Algonquin Arches, but was not active in the Lower Silurian (Woodward, 1961; Lukasik, 1988). The Cincinnati and Kankakee Arches were also poorly developed, and the Appalachian and Michigan Basins were partially open to one another. A broad stable area called the Wabash Platform (Droste and Shaver, 1983) occupied the area between the present day Appalachian, Michigan and Illinois Basins.

In the Late Ordovician, the Appalachian Basin became a major locus of terrigenous clastic deposition, receiving sediment from the Taconic Highlands to the east. The basin was largely filled in by latest Cincinnatian time, and deposition gave way to erosion when sea level dropped dramatically at the close of the Ordovician. Sedimentation began anew when the seas advanced in the Early Silurian (Smosna and Patchen, 1978).

The Illinois Basin had not yet developed into a structurally closed depositional center by Brassfield time. The proto-Illinois Basin (Vincennes

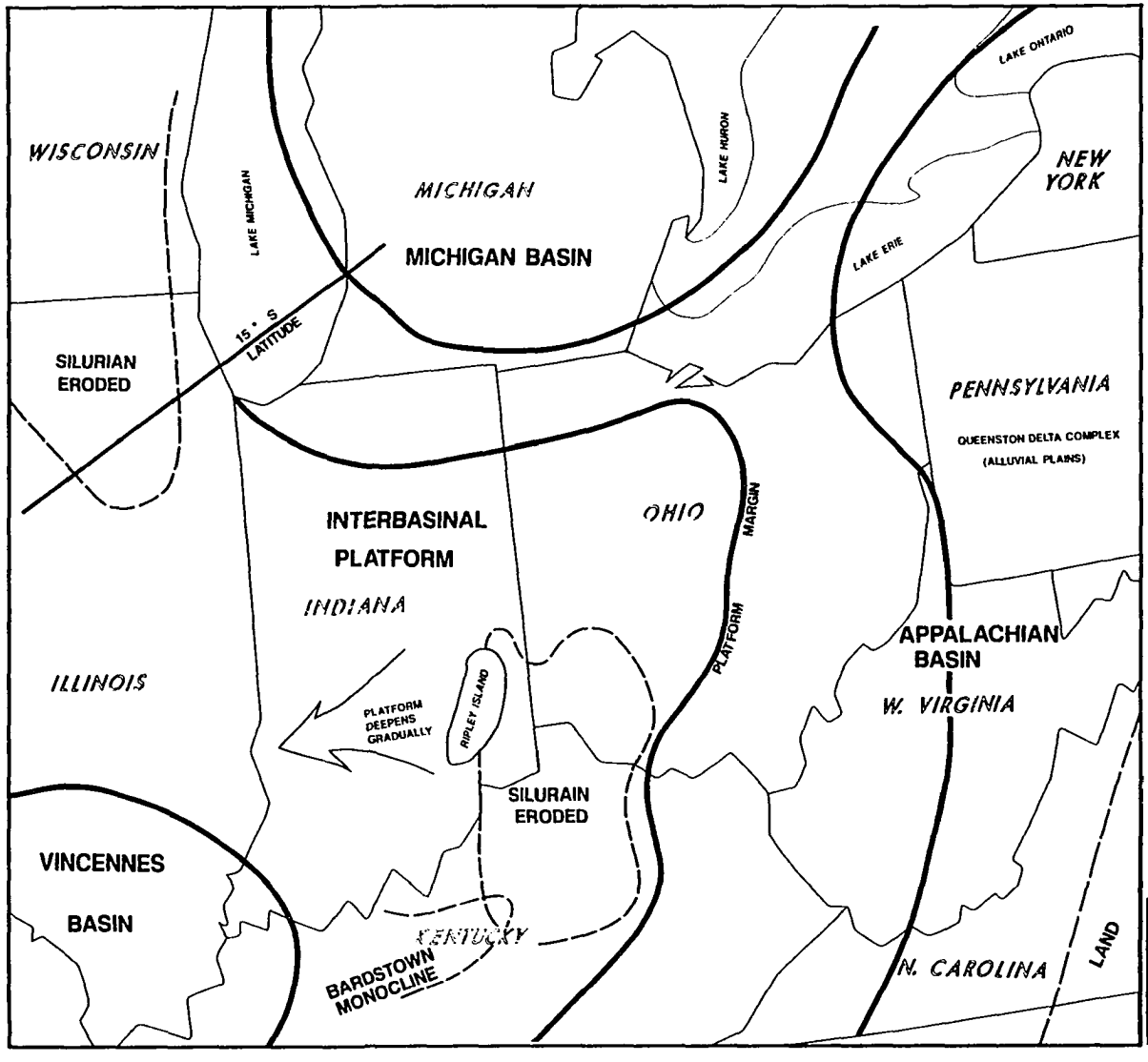

FIGURE 1
LOWER SILURAIN PALEOGEOGRAPHY OF THE EASTERN MIDCONTINENT

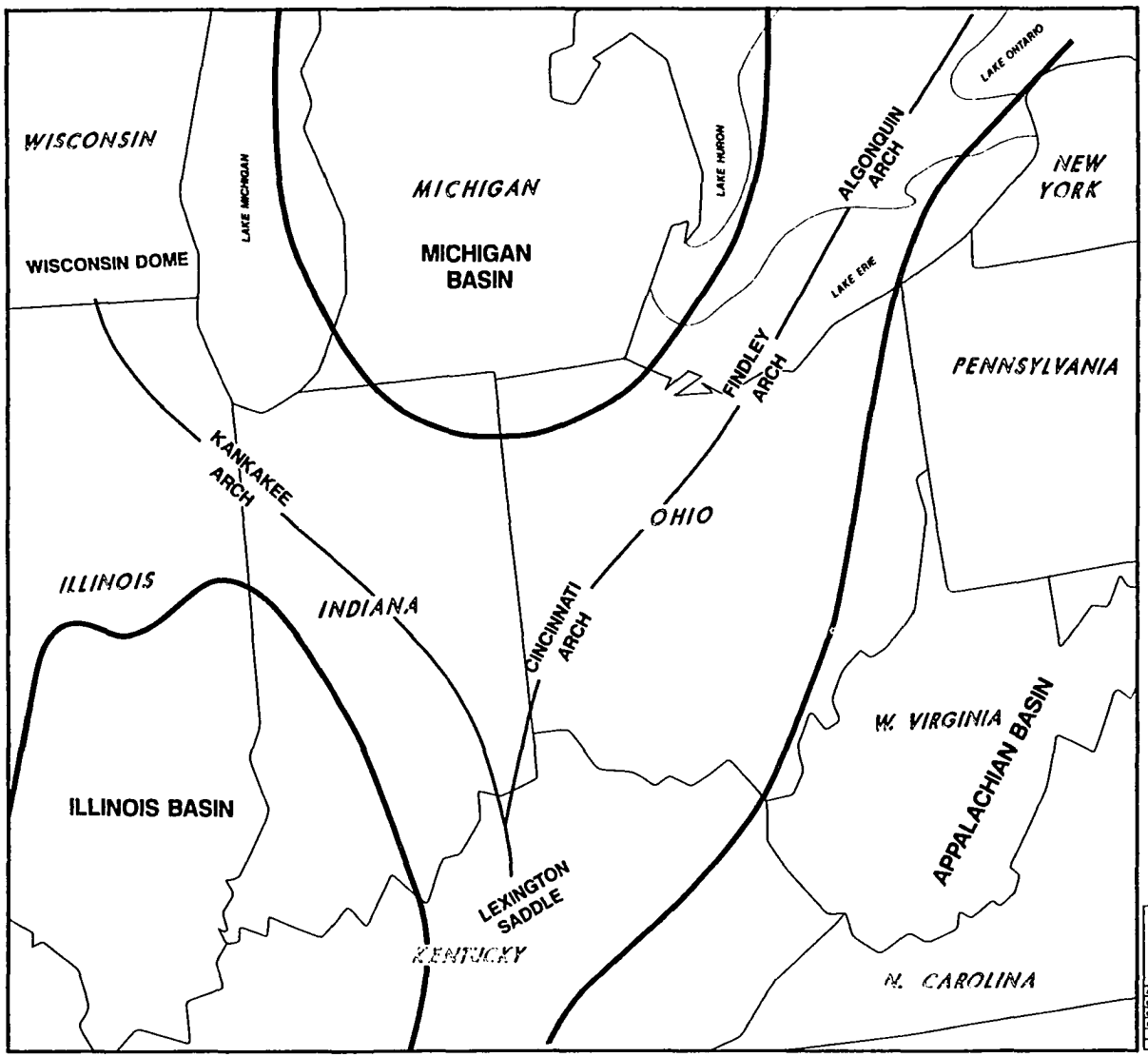

FIGURE 2
MAJOR REGIONAL FEATURES OF THE EASTERN MIDCONTINENT.
(MODIFIED FROM DROSTE AND SHAVER, 1983).

Basin of Droste and Shaver, 1983), was accumulating moderately thin Brassfield, Sexton Creek, and Kankakee sediments. The Michigan Basin was also receiving relatively thin Brassfield-equivalent strata (Manotoulin Dolomite and Cabot Head Shale), and did not begin to accumulate large volumes of sediment until Salina time. Over 3,000 feet of sediment -- the greatest thickness of Silurian strata on the central North American Craton -- were deposited in the Michigan Basin during the Salina (Ham and Wilson, 1967).

TECTONIC MOVEMENT IN BRASSFIELD TIME AND THE AGE OF THE CINCINNATI ARCH

The Cincinnati arch extends 600 kilometers north-northeast from the Nashville Dome in Tennessee and the Jessamine Dome in Kentucky to west-central Ohio, where it splits into the Kankakee and Findlay Arches. It separates the southern Appalachian Basin from the Illinois Basin, and northern Appalachian Basin from the Michigan Basin. Strata dip away from the crest of the arch in Cincinnati at $1/2^{o}$ to $1/4^{o}$. Green (1961) reports a dip of $1/3^{o}$ or less toward the Michigan and Illinois Basins. McDowell (1979) measured a dip of $1/2^{o}$ to the east of the Cincinnati Arch into the Appalachian Basin in Kentucky. Lukasik (1988) mapped a uniform dip of just over $1/2^{o}$ on the east side of the arch in Ohio, that increases slightly toward the axis of the Appalachian Basin.

The age of inception of the Cincinnati Arch remains unclear. However, lithologic evidence strongly indicates that it was not a significant barrier to sedimentation until post-Brassfield time.

Middle and Late Devonian strata (Boyle Dolomite, New Albany and Ohio-Chatanooga Shales) truncate progressively older Silurian strata toward the axis of the Cincinnati Arch, suggesting that the arch developed between the Early Silurian and Middle Devonian (McDowell, 1983). Scotford (1964) and Janssens (1967) provided other stratigraphic and mineralogical evidence supporting a post-Ordovician origin. Its initiation has also been placed in the Upper Ordovician, because some Upper Ordovician and Lower Silurian strata thin toward the arch from the east (Freeman, 1951; Gordon and Ettenschn, 1984).

Silurian strata thicken into the Appalachian Basin from the Cincinnati Arch at a rate that increases with progressively younger Silurian strata (Lukasik, 1988; Peterson, 1981; Becker, 1974). Lukasik (1988) suggested that this resulted from deposition off the eastern edge of the regionally broad Wabash Platform, and does not provide direct evidence for the development of a tectonic arch. The trend of increased rate of thickening in younger Silurian strata may have resulted from an increase in the rate of subsidence in the Appalachian Basin as the Silurian progressed, rather than tectonic uplift of the Cincinnati Arch (Lukasik, 1988). The eastern margin of the platform probably acted as a hinge line for subsidence in the Appalachian Basin that later served as the locus of structural movement (McDowell, 1983).

The Brassfield Formation was originally deposited over the Wabash Platform and was later eroded from the Cincinnati area when the arch developed. Foerste (1935), and Cressman (1981) described 6 m of Brassfield

at the Jeptha Knob cryptoexplosion structure near Shelbyville in Shelby County, Kentucky, over 20 km east of any other exposure. Foerste also described an outlier on Scrubgrass Creek near Mitchelsberg in Boyle County, Kentucky, between the southern most exposures on the east and west flanks of the arch. The outlier at Tri County Stone Quarry in Switzerland County, Indiana exposes 3 m of Brassfield, as compared to the western most exposures in Franklin, Decatur, Ripley and Jefferson Counties, Indiana that expose 1 m or less. Jilson (1945) reported Brassfield strata from Claxton Creek in southern Owne County, Kentucky, 50 km from the nearest outcrop to the west, though lithologic and faunal evidence were not presented. Other outliers have been recognized in Montgomery (Frost, 1989, personal communication) and Warren (Lowell and Baker, 1989, personal communication), counties Ohio. These provide the most compelling evidence against the presence of depositional barrier in the position of the Cincinnati Arch when the Lower Silurian was deposited.

MINOR LOCAL TECTONISM IN BRASSFIELD TIME

Peterson (1981) provided evidence for minor local tectonic movement during the Silurian on the west flank of the Cincinnati Arch in Kentucky. The Brassfield is uniformly thin throughout southwestern Indiana and northwestern Kentucky, but thickness abruptly south of Bardstown, Kentucky. Minor downwarping in this area (the Bardstown Monocline) during Brassfield time resulted in the development of thicker Brassfield strata, but this was restricted to a relatively small geographic area. Thinner Brassfield sediments deposited on

a more stable part of the platform are found just south and southwest of Bardstown.

Thickening of Brassfield strata north of Bardstown between Oldham and Shelby Counties, Kentucky, has been interpreted as deposition in a small structural depression known as the Lyndon Syncline (Kepferle, 1976; 1977).

REGIONAL GEOLOGY OF THE ORDOVICIAN AND SILURIAN EASTERN MIDCONTINENT

A vast epeiric sea, dominated by carbonate deposition, covered much of the eastern midcontinent in the Middle to Late Ordovician. On its eastern edge was a long and gently curving orogenic belt extending from southeast Canada into Georgia - the Taconic highlands - that formed as the Iapetus Ocean closed. The Taconic Highlands greatly influenced sedimentation in the eastern United Sates. Tectonics and sedimentation were concentrated in the southern part of the Taconics east of Tennessee during deposition of the Middle and lower Upper Ordovician (Rodgers, 1967).

Deposition of the upper third of the Upper Ordovician, was affected by tectonic activity and clastic sedimentation that had shifted north to Pennsylvania, New York and New England (Dennison, 1976; Dennison and Head, 1975; King, 1959). Coarse to fine clastics were spread westward from the eroding highlands into the seas covering the Eastern Interior. This system is recorded from New York to Ohio in the red sands and siltstones of the Queenston Delta Complex, and includes the Upper Ordovician and Lower Silurian fluvio-deltaic and shallow marine sands of the Juniata and Tuscarora

Sandstones. Queenston red sands, silts and muds were thought to have accumulated on a lower delta plane under subaerial conditions (Folk, 1960) or as prodeltaic sediments later oxidized as the seas retreated at the close of the Ordovician. The fluvio-deltaic sediments of the Queenston complex grade laterally into the shallow marine limestones and shales of the Preacherville Member of the Drakes Formation and the Whitewater Formation in the study area.

Tobin (1982) and Bretsky (1970) have interpreted the Cincinnati Series strata as representing deposition on the inner part of a shallow carbonate ramp which, by the close of the Ordovician, dipped gently to the east. The ramp developed on the western edge of the Appalachian basin in a position coinciding with the stable eastern edge of the Wabash Platform and records environments ranging from offshore to supratidal.

Cincinnatian strata are composed of at least three major shoaling-upward cycles ("mega-cycles" of Tobin, 1982), the bulk of which are composed of minor distal to proximal storm dominated shoaling cycles analogous to punctuated aggradational cycles (Jennette, 1986).

Lower Cincinnatian rocks in Kentucky and Ohio record a range of depositional conditions developed on a storm dominated carbonate ramp that dipped gently to the northwest (Jennette, 1986; Wier et al., 1984; Tobin, 1982; Cressman, 1973; Weiss and Sweet, 1962).

Lithofacies patterns through Cincinnati time record a rotation of the platform-ramp to the north and east. Uppermost Cincinnatian strata are suggestive of an eastward dipping ramp. Upper Cincinnatian Saluda sediments record deposition in deeper environments to the east and indicate an eastern supply of terrigenous clay and silt (Weir et al., 1984).

West of the present day Cincinnati arch, sediments of the Maquoketa group thin from 1000 feet in eastern Indiana west to 100 feet near Illinois. These sediments record shoaling conditions in the east and sluggish depositional conditions in the basin to the west (Gray, 1972; Cressman, 1973; Weir et al., 1984).

Following deposition of the Upper Ordovician sediments, seas retreated from much of the midcontinent. By this time, much of the Appalachian Basin and the Mississippi Embayment to the west had been filled (Cressman, 1973; Weir et al., 1984). Basin infilling was followed by a global eustatic lowering of sea level and a period of major erosion (Beuf et al., 1971; Dennison, 1970; Dennison and Head, 1975).

EVOLUTION OF THE LOWER SILURIAN MIDCONTINENTAL CARBONATE PLATFORM

Lower Silurian seas transgressed over the exposed Ordovician surface following the low stand at the Silurian-Ordovician boundary. Shallow shelf, peritidal, and supratidal carbonate deposition dominated the broad Wabash Platform between the Michigan, Appalachian and proto-Illinois basins (Droste

and Shaver, 1983). The eastern edge of the early Silurian platform roughly coincided with the eastern flank of the Cincinnati Arch. Again, this platform edge may have been a hinge line on the west side of the subsiding Appalachian Basin that later developed into the Cincinnati Arch. It also could have served as the eastern shallow limit of shoaling upward carbonates in the Upper Ordovician. The northern limit of the platform was somewhere in northern Ohio and northern Indiana. The platform dipped gently to the west, but significant westward downwarping did not occur until late or post-Brassfield time. Very shallow platform and terrestrial environments situated west of the present day Cincinnati Arch separated deeper platform and Appalachian Basin environments from peritidal and subtidal environments to the west (Droste and Shaver, 1983; Peterson, 1981).

Silurian strata become thicker and generally finer grained over a very short distance east of the platform edge. Peritidal sediments of the Belfast Member were deposited in an onlap configuration up the east edge of the platform. These are the oldest Brassfield or Brassfield-equivalent strata deposited on the platform (Rexroad et al., 1965; Rexroad, 1967). Following the deposition of the Brassfield Formation, accelerated downwarping of the Appalachian Basin resulted in progressive thickening of sediments toward its axis, and the orientation of the platform edge rotated from north-south to northeast-southwest (Lukasik, 1988; McDowell, 1983; Patchen and Smosna, 1975). This was probably related to the tectonic development of the Cincinnati Arch. Strata above the Brassfield thicken to the west of the arch, as well (Peterson, 1981; Pinsack and Shaver, 1964; Becker, 1974; Rago, 1952).

Early Silurian sediments thicken north of the study area in the subsurface. The platform extended into northern Indiana, and was stable relative to the adjacent subsiding Michigan and Appalachian Basins. It was broader than the present day Cincinnati Arch, and in a different position, although the northern edge of the platform corresponds roughly to the position of the northern flank of the Cincinnati Arch. As the seas transgressed, following the close of the Ordovician, sediments were deposited to the far north (now in subsurface) and later coarse and remarkably thin carbonate sands were deposited atop the shallow platform.

Dip of the platform to the north apparently increased in late or post Brassfield and Salomonie time (Kerr, 1976). Subsidence in the Michigan Basin began to accelerate, and Salomonie strata are considerably thicker in the Michigan Basin than in Indiana. However, the Brassfield equivalent Kankakee Dolomite in the Michigan Basin is thin, indicating that the basin was relatively quite and received very little sediment until latest or post Brassfield time.

The platform dipped gently to the west from its steeper eastern edge. Strata above the Brassfield, including the Osgood to the north and the Sexton Creek and Laurel to the north and west, probably started to accumulate before the close of Brassfield time. Subsidence to the west was not as great as to the north, however (Pinsak and Shaver, 1964), and Brassfield sediments are more uniformly thin in southern Indiana and northern Kentucky than in northern Indiana and Ohio. This may be partly because the Illinois Basin did not develop into a structurally closed depositional center until the Niagaran (Droste and

Shaver, 1983). The platform east of the basin remained relatively stable until then.

THE ORDOVICIAN - SILURIAN DISCONTINUITY

Studies of sea level change across the Ordovician - Silurian boundary and its effects on faunal development and sedimentation include those of Colville and Johnson (1982); Johnson et al., (1981); Sheehan (1972); Zeigler et al., (1968), McKerrow (1979); and Berry and Boucot (1973).

There is strong evidence of extensive Late Ordovician - Early Silurian glaciation of Gondwana (Beuf, et al., 1966; Berry and Boucot, 1972). The extent of glacial till and comparison of Early Silurian with Pleistocene data indicate sea level dropped about 100 meters (Sheehan, 1972). By Early Llandovery time sea level began to rise in response to the melting Gondwana ice cap and shallow epeiric seas quickly covered the continental land masses. At their peak, Lower Silurian seas were some of the most extensive in the Paleozoic, covering as much as 65% of the North American Craton. McKerrow (1979) described two short glacially related sea level pluses in the Early Silurian -- the first in the basal Llandovery and the second in the basal Upper Llandovery (C1-C2). These short transgressions are thought to have spanned 1 - 2 m.y. McKerrow also noted an overall sea level rise through the Llandovery, but it is not clear if this was a result of glacial melting, accelerated sea floor spreading, or both.

PALEOGEOGRAPHY

The position of the continental masses in the Paleozoic has been determined by several authors (e.g., Scoteese et al., 1979; Ziegler et al., 1977, 1979, 1984; Bambach et al., 1980). Ziegler, et al., (1977) published a detailed work on the paleogeography and climatology of the Early Silurian.

Laurentia, which included North America, Greenland, Scotland, and northwest Ireland was positioned over the equator and extended into the northern and southern tropics. Evaporites were deposited at Ellsemere Island to the north and at the Ontario - Quebec border to the south. Authigenic mineralization (e.g., hematite, chamosite, and phosphorite) occurred in the Appalachian Basin at about 30^{o} south. Shallow water carbonates were deposited over much of the continental interior, except where inundated by clastics, as in the eastern Appalachian Basin (Ziegler, et al., 1979).

PALEOCLIMATE AND OCEAN CIRCULATION

Atmosphere

Relative climatic uniformity prevailed in Early Silurian time because the northern hemisphere was almost entirely oceanic, and much of the land area in the southern hemisphere was flooded by epeiric seas (Ziegler, et al., 1977). The climate at the beginning of the Silurian was humid and comparatively cool (Seslavinski, 1978). Atmospheric circulation would have consisted of polar easterlies in the high latitudes, prevailing westerlies in the mid latitudes, and northeast and southeast trades in the tropics. Circulation patterns in the

southern hemisphere would have been more sharply defined, owing to the greater thermal gradients set up by the presence of land masses.

The Silurian Intertropical Convergence Zone (Ziegler et al., 1977) formed along the equator where warm moist air from the tropics met and rose (as it does today). As the rising air cooled, a belt of extensive cloudiness and precipitation would have formed. From here, storms tracked southwest in the southern hemisphere as they were deflected by the Coriolis force, and had a strong influence on deposition in the Ohio-Indiana-Kentucky area.

Ocean Circulation

The eperic seas covering the continental land masses in the Early Silurian were probably too shallow for the development of the types of current systems developed in today's deep ocean basins. Currents in the epeiric seas were driven by wind-wave systems and hurricanes. Storm systems greatly affected sedimentation and faunal community development. The literature addressing the effects of storms on shallow sea sedimentation is quite extensive; the reader is referred to Aigner (1985) and Jennette (1986).

STRATIGRAPHY

HISTORICAL DEVELOPMENT

The Brassfield Formation was first recognized as a distinct lithologic unit by Locke (1838). He described the sequence of limestones, dolomites and shales that constitute the Brassfield Formation as the "Flinty Limestone" in Adams County, Ohio and the "hard gray limestone" member of the Cliff Limestone in Preble County, Ohio.

Early studies of the Silurian in Ohio, Kentucky and Indiana followed stratigraphic nomenclature that was developed in the mid to late 1800's for the Silurian in New York. The New York terminology included, in ascending order, the Medina, Clinton, Niagara, Salina, and Waterline Groups. Currently accepted nomenclature recognizes the Medina, Clinton, Lockport and Salina Groups.

Owen (1985) assigned the oolitic ironstones and associated limestones and dolomites capping the Cincinnati Series in Kentucky to the Clinton, because their lithology closely resembled the Clinton in New York. Similarly,. Linney (1882) correlated the Lower Silurian and overlying shales in Kentucky with the New York Clinton and Rochester Shale.

In a series of Ohio Geological Survey reports, Orton (1869, 1870, 1873, 1878, 1884) reported Lower Silurian strata in Ohio as correlative with the

Clinton, and Meek (1872) described what he thought were Clinton age fossils from these strata.

Evidence for Clinton-equivalent strata in Indiana was provided by Bordon (1875), Linney (1882) and Thompson (1886). The term Clinton Limestone was at first very loosely applied in Indiana to a poorly defined interval that included strata above and below the Brassfield. Foerste (1896, 1897) mapped the Indiana Clinton in detail and described the Brassfield Formation as it is currently recognized.

Foerste (1904) recognized that the Clinton of Kentucky, Indiana and Ohio was not directly correlative in terms of fauna or lithology with the Clinton of New York, and in 1896 proposed that the name Clinton in Ohio be changed to the Montgomery Formation, for the exposures in Montgomery County, Ohio. The name was preoccupied, however, and use of the name Clinton continued. Foerste (1906) later proposed the name Brassfield Limestone for exposures along the now abandoned Louisville and Atlantic Railroad that extends between Brassfield and Panola in Madison County, Kentucky. The name was adopted and this has become the Brassfield type area.

The erroneous correlation of Brassfield strata with the New York Clinton was corrected shortly after Foerste proposed the name Brassfield Limestone. Schuchert (1913, 1914) reclassified the Medina in New York (stratigraphically above the Clinton) to include the Cataract Formation in Ontario. Characteristic fauna of the Cataract had previously been ascribed to the Clinton. He also

correlated the Brassfield to the Medina and Cataract, but recognized their faunal assemblages were not directly equivalent. Foerste (1923) confirmed Schuchert's correlation on the basis of similar faunal communities.

NOMENCLATURE

Brassfield Formation

The Brassfield Limestone was formally elevated to formation rank by Rexroad (1965), though it had for some time been informally referred to as a such (Butts, 1915; Warn, 1941; Bowman, 1956). The formation surname was preferred because the name "Brassfield Limestone" could not be properly applied to outcrops where dolomite or shale were the dominant constituents.

Calvert (1968) proposed the Brassfield be reduced in rank to a member of the Manitoulin Dolomite in southern Ohio and northern Kentucky. The Manitoulin is the basal Silurian unit in the Michigan basin, now recognized as a Brassfield equivalent. McDowell (1983) suggested that the Brassfield be reduced in rank to a member of the Drowning Creek Formation in Kentucky, because it is thin to the south and appears to be conformably overlain by Drowning Creek strata to the north.

Belfast Member

The "Belfast bed" was first described by Foerste (1896) as the massive weathering dolomite that marks the base of the Brassfield in the eastern outcrop area. Foerste described the Belfast as up to 2 m thick, silty, argillaceous, and generally lacking megafossils. Bowman (1956) and Rexroad (1965)

recognized the Belfast as a member of the Brassfield. McDowell did not include the Belfast as a member of the Brassfield in Kentucky, because it is thin and there has been disagreement over its identification and distribution.

Lee Creek Member

Nicoll and Rexroad (1968) described this upper member of the Brassfield found in limited areas on the west side of the Cincinnati Arch. The Lee Creek Member of the Brassfield is a thin, fine grained, red, brown or green dolomite. It contains sand sized glauconite pellets and coarse quartz silt, and, with few exceptions, is devoid of megafossils. The type section of the Lee Creek is near the head of a short tributary of Lee Creek in Jefferson County, Indiana.

This report follows Brassfield nomenclature used by Foerste (1931, 1935), Rexroad (1965, 1967), Nicoll and Rexroad (1968) and recently summarized by Lukasik (1988). The formal units recognized in this study, as described above, include the Brassfield Formation, which is subdivided into the Belfast Member, Lee Creek Member, and, what is herein called the Middle Member. Sediments between the Lee Creek and Belfast have not been previously recognized as a separate member. The Brassfield is recognized as a distinct lithologic unit in Ohio, Indiana and Kentucky and its status as a lithostratigraphic formation should be retained throughout the outcrop area. The Belfast and Lee Creek units have limited distribution, but where present, are always associated with the Middle Member. All three members are easily distinguishable on the basis of petrology (this report) and conodonts (Rexroad,

1967; Nicoll and Rexroad, 1968). Therefore, their status as members should be retained.

Brassfield Subdivisions

Several informal subunits have been applied to the Brassfield in Ohio and Northern Kentucky. Rexroad, et al., (1965) described two units south of Bath County, Kentucky and four in Ohio. O'Donell (1967) found five in Ohio and Northern Kentucky. McDowell (1983) reports six lithofacies on the east side of the arch in Kentucky, while Gordon and Ettensohn (1984) found five. Ehlers and Hoover (1961) recognized two subunits in Ohio.

The number of lithologic subdivisions described above reflects regional differences in Brassfield lithology around the Cincinnati Arch. The subdivision scheme used in this report is simple, and can be applied to all Brassfield exposures. This report recognizes four subdivisions of the Brassfield:

- the Belfast;
- the lower division of the Middle Member;
- the upper division of the Middle Member; and
- the Lee Creek.

These correspond to separate major phases in the depositional history of the formation. Further subdivision of the two Middle Member units varies along the outcrop belt. These divisions are summarized in Figure 3, and their significance is discussed in detail in the Results and Discussion sections of this report.

EHLERS & HOOVER 1961	BYRNE 1961	ODONELL 1967	FROST 1977	GORDON 1980	HENDRIX 1983	ADENUGA 1985	THIS REPORT (See Facies Description)		
SOUTHWEST OH NORTH/SOUTH	CENTRAL KY	CINCINNATI ARCH	WEST CENTRAL OH	CENTRAL KY	SOUTHWEST OH	WEST CENTRAL OH	WEST ARCH	NORTH ARCH	EAST ARCH
DAYTON FM.	PLUM CREEK SHALE	DAYTON, OSGOOD, CRAB ORCHARD	DAYTON FM.	PLUM CREEK SHALE	DAYTON LS	DAYTON	OSGOOD / LEE CK (VII)	DAYTON	PLUM CREEK
UPPER BRASSFIELD / PINK SHALEY	BIOCLAST ZONE	UPPER THIN BEDDED UNIT	UPPER ZONE (IRREGULAR BEDDED)	UPPER MASSIVE / UPPER SHALEY UNIT	MIXED CARBONATE SHALE UNIT	BEAD BED / UPPER THIN BEDDED UNIT	FACIES VI	FACIES V	FACIES III
			MIDDLE ZONE (THIN BEDDED)	MIDDLE THIN BEDDED UNIT					
LOWER BRASSFIELD / WHITE CHERTY	CHERT ZONE	UPPER MASSIVE UNIT	LOWER ZONE	LOWER MASSIVE UNIT	SKELETAL SAND UNIT	LOWER THICK BEDDED UNIT		FACIES IV	FACIES II B / FACIES II A
	GLAUCONITE ZONE	LOWER THIN BEDDED UNIT	SUGAR ROCK	BELFAST MBR.	(BELFAST) CARBONATE MUD UNIT	BELFAST MBR.			
BELFAST UNIT	HOWARDS CREEK BED	LOWER MASSIVE UNIT	BELFAST					BELFAST MBR.	
ELKHORN SHALE	WHITEWATER FM.	BELFAST MBR. / ORDO	ELKHORN	DRAKES FM.	RICHMOND GROUP		ORDO		

FIGURE 3 - DIVISION OF THE BRASSFIELD FORMATION INTO SUBUNITS.

EX-15-15-H-928

THICKNESS AND EXTENT

The Brassfield Formation is the most widely distributed unit of its age on the North American craton. It is recognized in Ohio, Indiana, Kentucky, Tennessee and Arkansas (Schwartz, 1942), and is coextensive with strata in the Illinois, Michigan and Appalachian Basins. Its exceptionally wide distribution and relative thinness have earned it distinction of one of the remarkable and distinctive sequences of all Paleozoic time (Ham and Wilson, 1967). Figure 4 illustrates the thickness and extent of Llandovery age sediments on the eastern midcontinent.

Belfast Member

Foerste (1896) recognized the Belfast as far south as Fleming County, Kentucky near Hillsboro. Rexroad et al. (1965) felt that the basal massive beds of the Brassfield Formation described by Foerste (1906, 1931) in the southern most outcrops in Kentucky, were equivalent to the Belfast that Foerste had described earlier in southern Ohio and Northern Kentucky. Gorden and Ettensohn (1984) recognized Belfast only as far south as Bath County, Kentucky.

Brassfield Formation Middle Member

The Middle Member is exposed at every outcrop of Brassfield, and it accounts for most changes in thickness of the formation as a whole. The Brassfield is thickest east of the Cincinnati Arch and thinnest to the west. Its greatest outcrop thickness is in Adams County, Ohio, where over 18 m are exposed. The Brassfield thickens to the east by the addition of thin carbonates

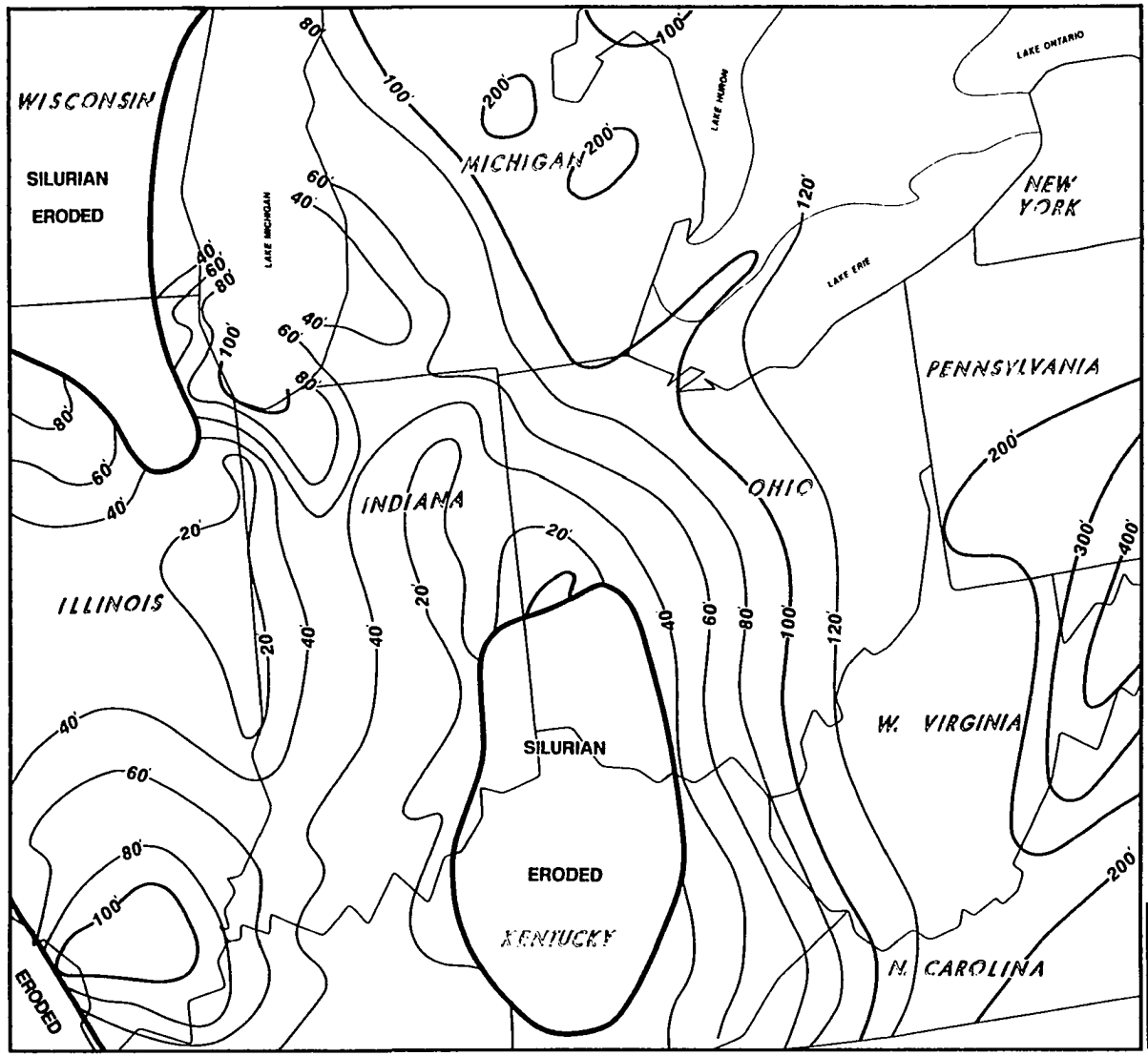

REFERENCES:
LUKASIK, 1986; DROSTE & SHAVER, 1983; REXROAD, 1980; SHELL STRATIGRAPHIC ATLAS 1975; BECKER, 1974; THIS REPORT

0 100 200 Mi
0 100 200 300 Km

CI = 20' EXCEPT WHERE INDICATED

FIGURE 4

THICKNESS OF LLANDOVERIAN AGE SEDIMENTS

and shale to its upper portion (Lukasik, 1988). In the subsurface, its maximum thickness (22 m) and greatest shale content is in Vinton County, Ohio. From here into West Virginia it becomes thinner and is progressively replaced by shales of the Cabot Head. The Cabot Head may represent a deeper water equivalent of the Brassfield in the subsurface.

The Brassfield thins north to the Dayton, Ohio area, where it averages about 5 m and contains very little shale. North of Dayton, the Brassfield gradually thickens into the subsurface. The northern most exposure of Brassfield is in Miami County, Ohio at the Armco Quarry. Here the Brassfield consists of nearly 8 m of shale-free limestone.

The Brassfield becomes progressively thinner to the west into Indiana and south around the west flank of the Cincinnati Arch. Near Richmond, Indiana it averages 4 m and thins southward to 1 m near Madison, Indiana. From here, the thickness averages 2 m south to Nelson County, Kentucky. South of Louisville, Kentucky the Brassfield is 6 to 7 m thick. The southern most outcrop on the west flank of the Cincinnati Arch is in Raywick, Kentucky, where the Brassfield measures 4.5 m.

The Brassfield extends north and west into the Indiana subsurface as a relatively thin unit (Shaver, 1970). Rago (1952) mapped the Brassfield in the southern Indiana subsurface and reported that it thickens to a maximum of 30 m in western Indiana, while Becker (1974) found the Brassfield difficult to map in subsurface in this area because it is so thin. Rago apparently included units

overlying the Brassfield in his correlation, which he erroneously based on chert content. His 30 m estimate is excessive by an order of magnitude.

The Brassfield is nearly 6 m thick at its southern most exposure on the east side of the arch near Crab Orchard, Kentucky, Lincoln County. From here northward, the unit gradually thickens and increases in shale content to its maximum outcrop thickness in southern Ohio.

The Brassfield is thinnest in Ripley County, Indiana, and is absent from parts of Decatur, Ripley, Jennings and Jefferson Counties, Indiana. At these locations, the Osgood Dolomite directly overlies Upper Ordovician Saluda and Whitewater Formations. Foerste (1891) thought this represented thinning of Brassfield sediments over an Upper Ordovician topographic remnant called Ripley Island. At location 20 the Brassfield laps onto an eroded Upper Ordovician surface. It thickens abruptly from this area toward the axis of the arch, suggesting Brassfield sediments were originally deposited over the arch (see discussion on the age of the Cincinnati Arch).

Lee Creek Member

The Lee Creek has limited, patchy distribution on the west side of the Cincinnati Arch. It is recognized from Bullit, Kentucky north to Decatur County, Indiana. Exposures in Indiana are thin and discontinuous. Its maximum thickness is over 1 m in Jefferson County, Indiana, but averages less than 0.25 m and is typically present as thin isolated lenses. Generally, the Lee Creek thins north and west of Bullit County, Kentucky (Nicole and Rexroad, 1968).

The contact between the Lee Creek and the Middle Member of the Brassfield is sharp and unconformable. Where the Lee Creek rests on Ordovician strata (Saluda or Whitewater Formations), the contact is also sharp. The Lee Creek is immediately overlain by the basal beds of the Osgood.

LITHOSTRATIGRAPHIC RELATIONS

The Lithostratigraphic relations in and adjacent to the study area are summarized in Figures 5 and 6 and discussed below.

The Brassfield is the basal Silurian formation in the study area and everywhere unconformably overlies Upper Ordovician strata. The underlying Upper Ordovician strata include the Drakes Formation (the Queenston Shale in subsurface) in the southeast, the Elkhorn Shale to the east and north, the Whitewater Formation to the northwest, and to the west and southwest, the Saluda Dolomite. The Brassfield overlies the Saluda from the southwestern most outcrop at Raywick, Kentucky to just north of Madison, Indiana. The Brassfield overlies progressively younger beds of the Whitewater Formation north of Madison to Richmond, Indiana, where it overlies the Elkhorn Formation.

The Brassfield is overlain by younger Silurian strata everywhere but in parts of Madison, Gerrard and Lincoln Counties, Kentucky. Here, Devonian strata progressively overstep Silurian, so that Devonian shale rests on

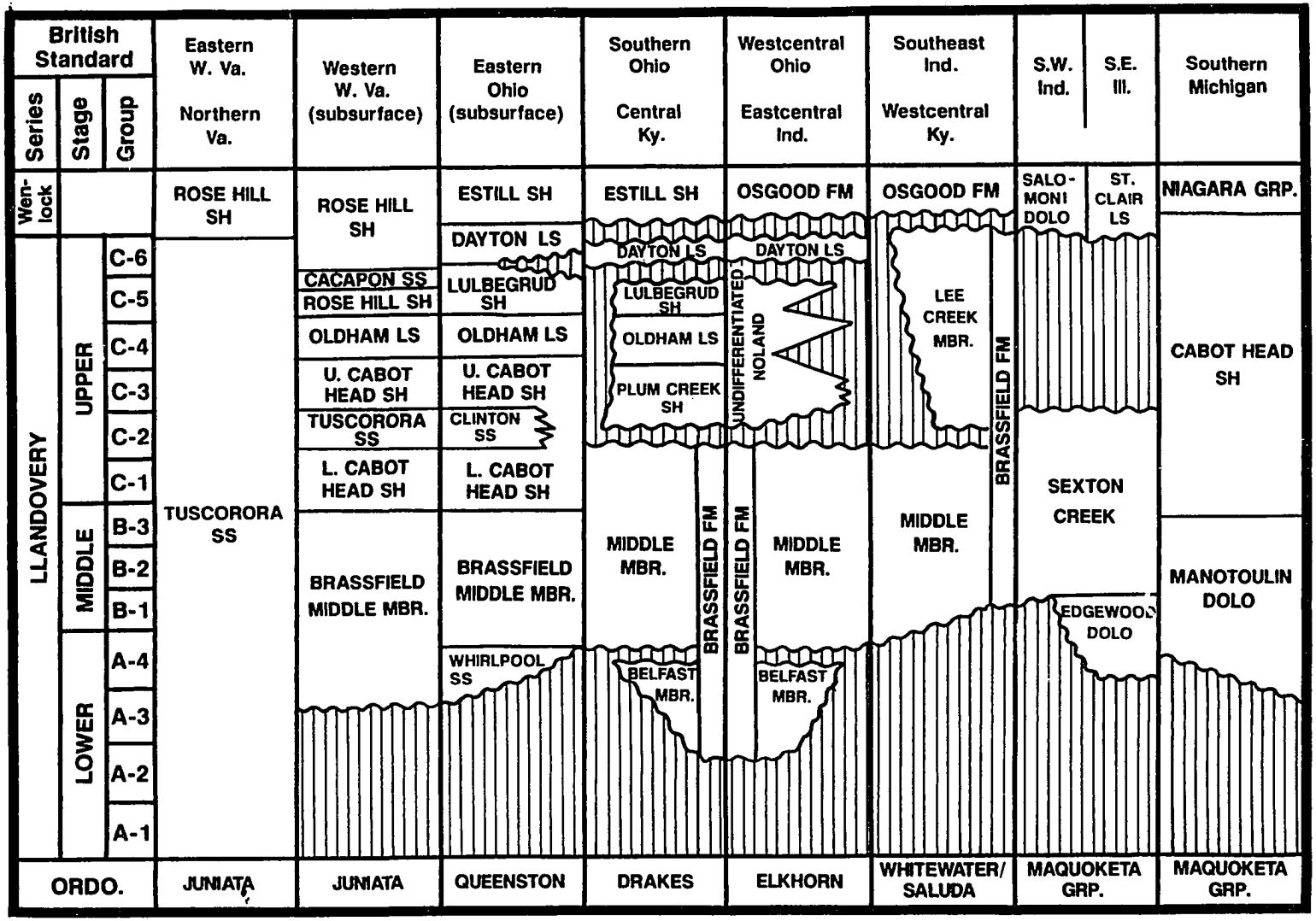

FIGURE 5: STRATIGRAPHIC RELATIONSHIPS OF LLANDOVERY AGE SEDIMENTS OF THE EASTERN MID-CONTINENT

EX-15-15-H-911

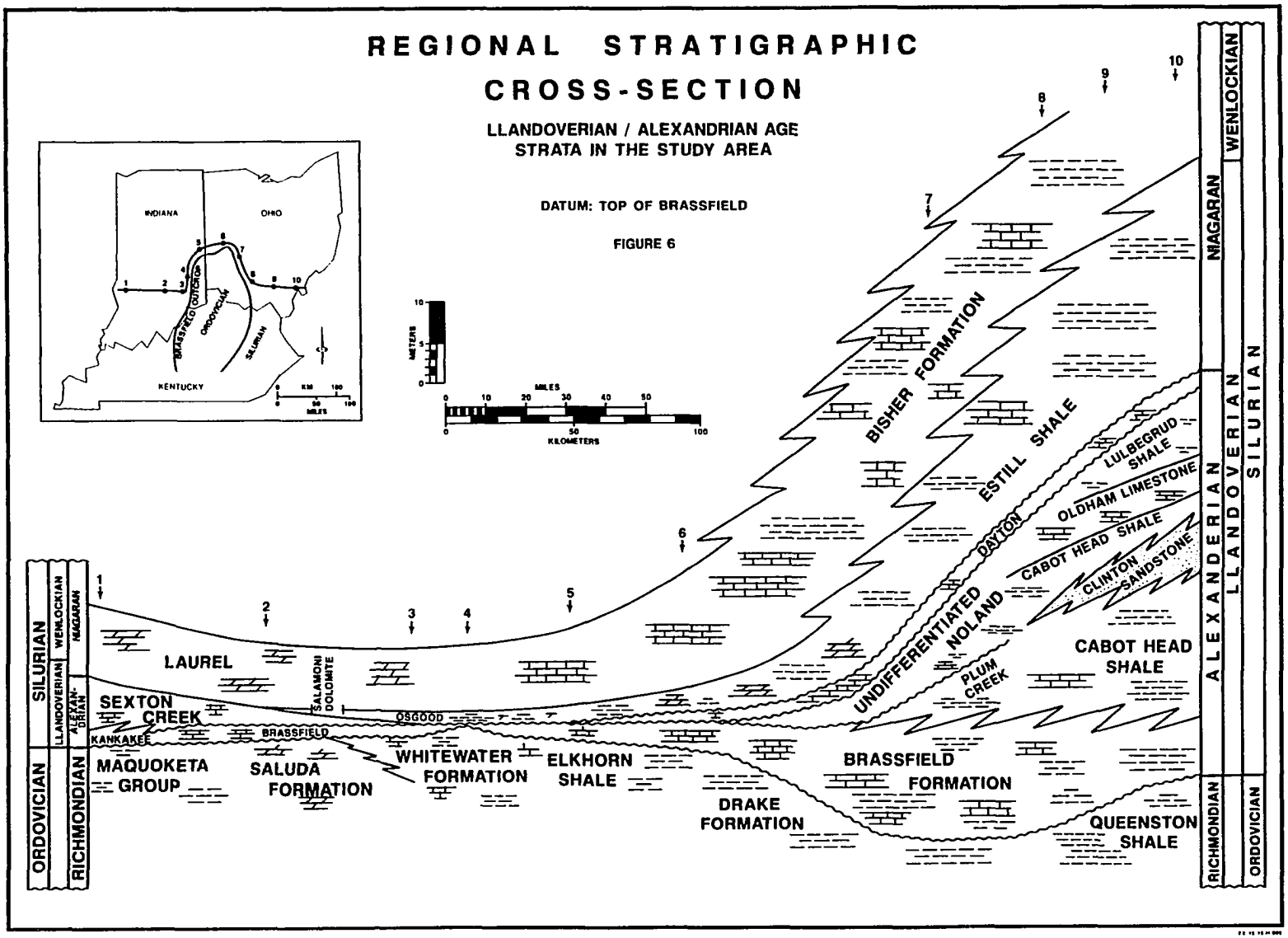

Brassfield near Farristown, Madison County, Kentucky, and rests directly on Upper Ordovician strata in parts of Lincoln and Boyle Counties, Kentucky.

On the east side of the Cincinnati Arch in Southern Ohio and Northern Kentucky the Brassfield is overlain with apparent conformity by the Plum Creek Shale in outcrop, (Noland Formation, Rexroad, 1965; Drowning Creek Formation, McDowell, 1983) and the Cabot Head Shale in subsurface (Rexroad, et al., 1965, Lukasik, 1988). The top of the Brassfield is difficult to define in this area because it appears to interfinger with the overlying shales.

Traditionally, the top of Brassfield has been placed above a distinct mega-rippled bed of large crenulate crinoid columnals, first described by Foerste as the "Bead Bed." However, the occurrence of the Bead Bed is not always limited to a single horizon, so its use as a marker for the top of the Brassfield is discouraged. Lukasik (1988) defined the top of the Brassfield as the point at which shale volume exceeds 50%. This scheme was formulated for electric logs, however, and is not recommend for use in outcrop. I suggest the top of the Brassfield be placed above the upper most beds that indicate sedimentary hiatus. This horizon almost always occurs above the Bead Bed. It is commonly recognized as one or more ironstone or hematitic beds in the east, and as the upper most ironstone, erosional surface, or deep basinal deposit (Lee Creek Member) to the west. These relationships will be discussed in detail in a subsequent section.

The Cabot Head and Plum Creek shales are progressively overstepped by the Dayton Formation in the north and northwest outcrops. The Dayton unconformably overlies the Brassfield north of Clinton County, Ohio to Preble County, Ohio were the Dayton pinches out under the Osgood Shale. The dolomites and shales of the Osgood overlie the Brassfield south of Clinton County, Ohio to the southern most extent of the study area (Peterson, 1981). However, Rexroad (1967) suggests that the strata overlying the Brassfield south of Bullit County, Kentucky might better be identified as Crab Orchard Shale. Rexroad (1967) found the Osgood to be progressively younger to the north.

AGE AND CORRELATION

Murchinson and Sedgwick laid the ground work for the Silurian System with their work in the British Isles in the mid-nineteenth century. Murchison's "formations" were subdivided into 11 graptolite zones by Lapworth (1879-1880). Elles and Wood (1901-1918) expanded Lapworth's 11 graptolite zones to 21, and Jones (1925) further redefined these. The three divisions proposed by Murchison include, in ascending order, Llandovery, Wenlock, and Ludlow. These, with the addition of Pridoli as the youngest, are the currently recognized British Silurian series.

The reference section for the North American Silurian is in New York. Chamberlin and Salisberg (1905) divided the New York Silurian into the Oswegan, Niagaran and Cayugan Series, in ascending order. Savage (1908) proposed the term Alexandrian to replace Oswegan. Alexandrian has been adopted as the preferred North American series name for the Lower Silurian in

the recent literature (e.g., Rexroad, 1965; COSUNA, 1985A, 1958B; Lukasik, 1988).

It is common to see North American and British nomenclature freely intermixed in North American literature. Berry and Boucot (1967) suggest adopting the British standard, contending that North American terminology is useful only in New York, where it was developed.

Correlation of the Brassfield has been based largely on brachiopods and conodonts. Brachiopod divisions have been worked out in detail by Berry and Boucot (1967) and their work was based on the following brachiopods:

(1) *Cryptothyrella* (synonm: *Whitfieldella*) ranges from Ordovician to C_1 or C_2 (Early to Late Llandovarian). This genus is found at or above the "Bead Bed."

(2) *Platymerella* has been placed within B_1 to C_2 and correlates with the Sexton Creek and lower Kankakee Dolomite of the Illinois Basin.

(3) *Microcardinalia* ranges from C_2 to C_3 and is commonly associated with *Triplesia*. Berry and Boucot (1970) report *Microcardinalia* from above the Brassfield only. Rexroad (1967) has found it in association with the Bead Bed at the top of the Brassfield near Dayton, Ohio. Rexroad also found the same species well above the Brassfield to the southeast, suggesting that the Brassfield is younger to the northwest (assuming the distribution is not facies related).

The most reliable and useful Brassfield biostratigraphy is based on the conodont studies of Rexroad (1965, 1967) and Nicole and Rexroad (1968). This work was conducted before multi-element conodont stratigraphy, but the correlations are still valid (Rexroad, 1988, personal communication). Correlations baed on conodonts are preferred over those based on brachiopods because conodonts are abundant in the Brassfield, less facies dependent, and provide better stratigraphic resolution.

There is some inconsistency between correlations based on conodonts and brachiopods, as well. For instance, O'Donnel (1967) points out that the age of the top of the Brassfield is younger based on brachiopods than it is based on conodonts (relative to graptolites).

The age of the Brassfield ranges from lower Lower Llandovery to Upper Llandovery C_2 (based on conodonts) or C_3 (based on brachiopods) (Rexroad, 1965). The Llandovery is dated from 438 to 428 MYBP (Harland et al., 1982). On this basis the Brassfield is estimated to represent roughly five to eight million years. Others estimate the Brassfield to represent 11 million years (Schutter and Todd, Exxon Prod. Res., personal communication, 1989). Glauconite pellets from the Brassfield Formation have yielded Rb-Sr and K-Ar dates that range from 355 to 370 MYBP (Devonian). However, the isotopes in the glaucontie were most likely "reset" in the Devonian (Grant et al., 1984).

Rexroad (1967) dates the Belfast Member of the Brassfield Formation, using conodonts, as lower Llandoverian. The Belfast contains the oldest

conodonts in the Brassfield and has been correlated with the Edgwood Dolomite in the Illinois Basin. The Lee Creek Member to the west, as described by Nicoll and Rexroad (1968), contains the youngest Brassfield conodonts. Rexroad (1988, personal communication) suspects that the conodonts in the Lee Creek correlate with the conodonts of the lower Waco on the east side of the arch.

The Waco has been correlated with the Dayton (Rexroad, 1970; McDowell, 1983; and Lukasik, 1988) which lies far above the Brassfield in southeastern Ohio and adjacent Kentucky. This relationship is also discussed by Rexroad (1980) and Nicoll and Rexroad (1968). In Southern Ohio, the Brassfield is overlain by 3 m of Cobot Head Shale, 3 m of Oldham Limestone, 2 to 3 m of Lulbegrud Shale, and 1 m Dayton Limestone. These strata expand east into the subsurface to a thickness of nearly 70 m (Lukasik, 1988). This relatively thick sedimentary package is condensed to 1 m, or less, of Brassfield and Lee Creek on the west side of the Cincinnati Arch.

METHODS AND STUDY AREA

This study is based on data collected through detailed field observations, hand sample descriptions, petrographic microscopy, and x-ray diffractometry.

Over 700 km of Brassfield Formation outcrop are exposed in a continuous open-down horse-shoe-shaped, belt around the flanks of the Cincinnati Arch in Ohio, Kentucky, and Indiana. Fifty-six outcrops and one core, representing the entire outcrop belt, were measured and described (Figure 7).

Vertical sections range in thickness from 1 cm to 16 m A total of 288 m sections were described and sampled. Outcrops were described in terms of thickness, texture (classification of Dunham, 1962), bedding type, bedding thickness, paleo current direction (where possible), physical and biogenic sedimentary structures, facies and formation contacts, fossils, color, and any unusual features. Sections were marked off in meters and described bed by bed. Outcrop locations are given in Appendix (1).

Over 600 hand samples were collected from the field. Most of these were slabbed and examined under a binocular microscope with reflected light. Many were treated with 5% HCl and alizarine red stain. These data were used to augment outcrop descriptions.

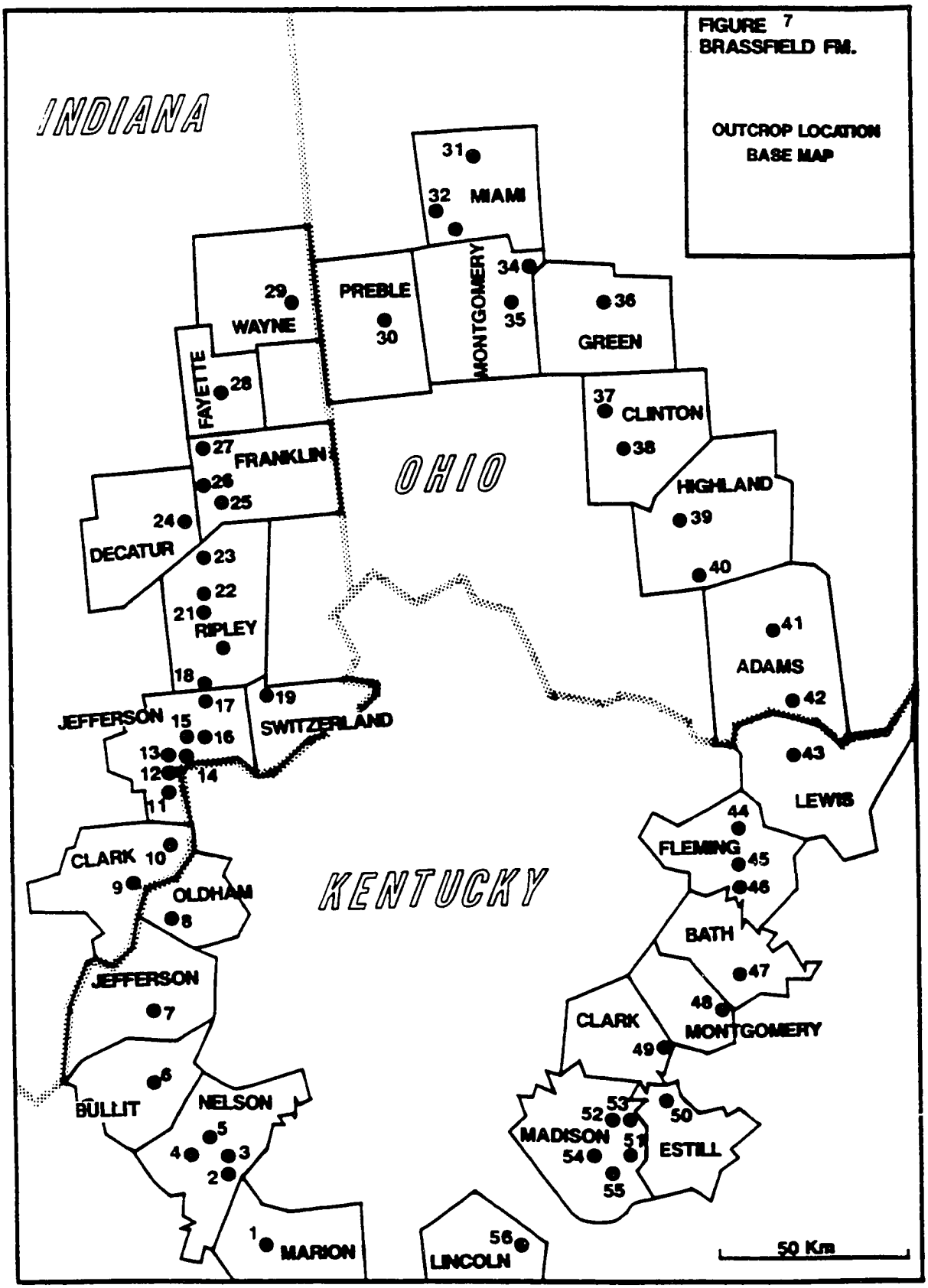

From these, 244 were chosen for thin section preparation. Thin sections were ground to a thickness of 25 to 30 microns and stained for calcite and ferroan carbonate in a solution consisting of 0.5% - 2.0% hydrochloric acid, 0.2% alizarine red S, and 0.5% potassium ferricyanide in distilled water for one to two minutes (acid strength and staining time were varied to achieve the best results with different rock types). Two hundred points were counted per sample using a standard petrographic microscope. The original fabric of some dolomitized samples was determined using flurorescence microscopy. Lithoclast type, biolcast type, and texture were described for 178 relatively non-dolomitized thin sections. Six dolomite samples (one sample from each major Brassfield dolomite type) were checked for fluid inclusions in hopes of determining dolomite origin, but no useful data were obtained. Dolomite morphology and noncarbonate constituents were described for 177 dolomite samples. All petrographic data are presented in Appendix 2.

X-ray diffraction analysis was conducted on 57 samples using a Siemens 500 x-ray diffractometer. Of these, 44 were analyzed for relative percents of limestone and dolomite, 13 for clay minerals (Appendix 4), and six for iron oxides. All XRD peak data is presented in Appendix 3. Clay mineraology is discussed in Appendix 4.

Carbonates were analyzed as power mounts composed of crystallites less than 5 microns in size. Ground samples were examined from 36^{o} to 46^{o} theta at a rate of 0.05^{o} 2 theta per second. A calibrated dolomite-limestone

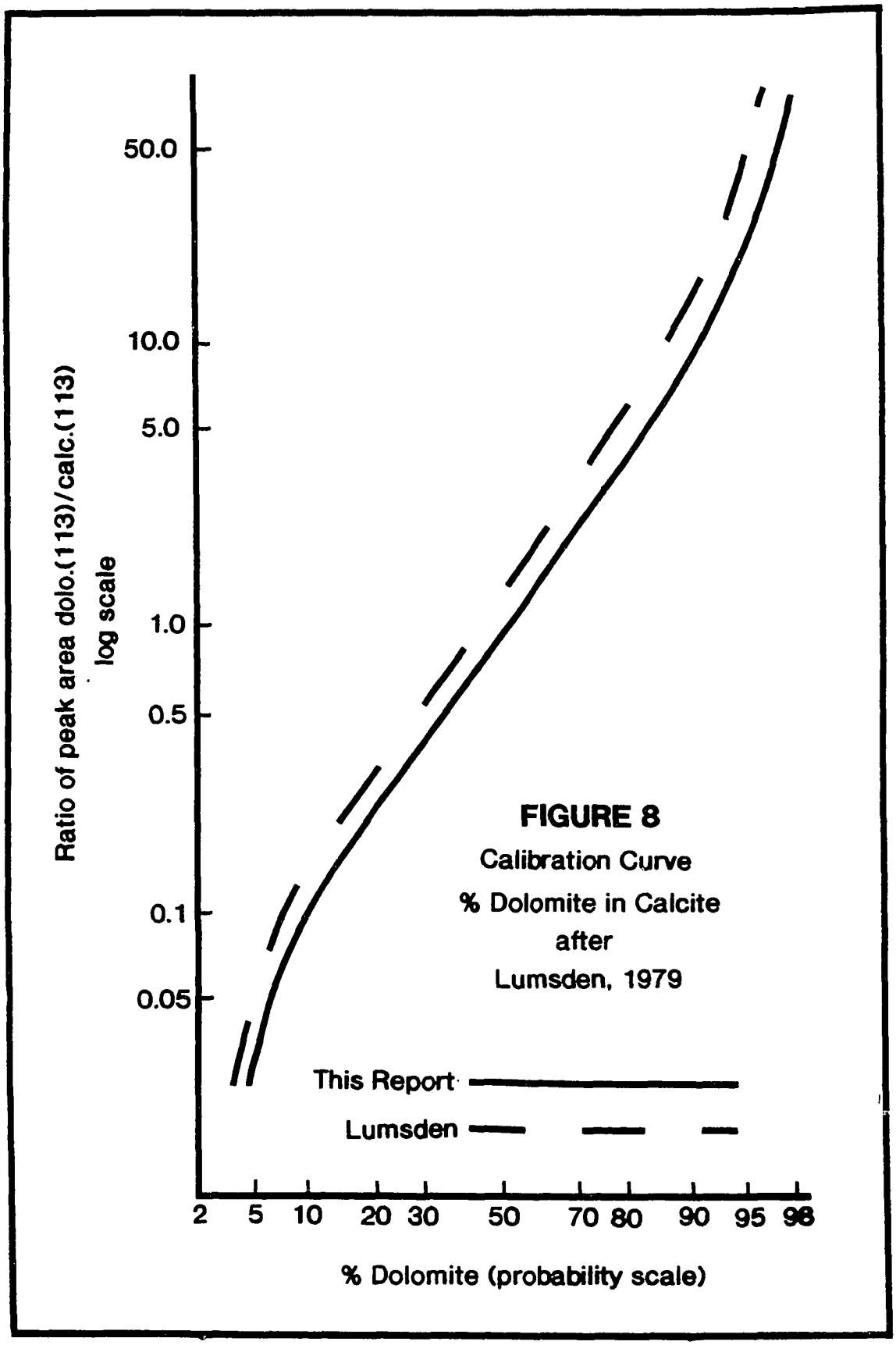

FIGURE 8
Calibration Curve
% Dolomite in Calcite
after
Lumsden, 1979

curve was constructed by analyzing mixtures of pure powdered calcite and dolomite in known ratios (Figure 8).

Limestone dolomite ratios were determined by dividing the integrated area of the dolomite 113 peak by the integrated area of the calcite 113 peak (Figure 9) and converting to percent dolomite with the calibrated ratio curve (see Lumsden, 1979; Hardie and Tucker, 1988 for further discussion on this method). These data were compared with the limestone dolomite curve published by Lumsden (1979). The standards analyzed for this study plotted consistently to the right of the Lumsden curve (see Figure 8). The Lumsden curve estimated between 0% and 9% less dolomite than the sample actually contained. A new curve was constructed to calculate dolomite calcite ratios in the Brassfield. As shown in Table 1, results from point counting and x-ray diffractometry are very comparable.

Clay samples were prepared using glass slide suspension mounts and measured from 2^{o} to 32^{o} theta. Iron oxides were analyzed using both powder and suspension mounts, and run from 20^{o} to 60^{o} theta.

TABLE 1

COMPARISON OF PERCENT DOLOMITE IN CARBONATE AS DETERMINED FROM POINT COUNTING AND XRD TECHNIQUES

LOCALITY	SAMPLE	FACIES	PERCENT DOLOMITE OF CARBONATE	
			XRD ANALYSIS %	PETROGRAPHIC ANALYSIS %
41	OBC 4	III (Fe rich)	0	0
34	EQT	V (Fe rich)	13	7
38	TF9C	V (Fe rich)	0	1
43	T	III	75	85
24	NPQ 2.3W	VI	0	Tr
24	NPQ 2.3B	VI Phosphatic	0	0
23	NQ Crust	VI Phosphatic	12	13
41	OBC 16T	III	4	2
29	EF 1.0	I	95	100
56	CO 2.3	III	94	100
56	CO 5.2	III	100	100
50	RR 3.1	I	93	100
50	RR 4.1	II B	100	100
43	T 2A	I	100	100
43	T 5	II B	100	100
43	T II	III	100	100
41	OCB 11-0	III	0	2
41	OBC 14	I	80	100
39	TC 1B	II A OR B	92	98
32	L6	V	0	1
36	AC 96	V	82	93
36	AC 107	V	23	28
32	LFLW	IV	12	14
29	EF 5.3	V	33	27
16	MN 2.2	VI	34	38
7	SR 2.8	VI	93	100
7	SR 3.3	VII	73	71
8	BR 2.65	VI	7	Tr
6	S2.1	VI	12	17
6	S3.0	VII	100	100
3	BGP9	VI	96	100
1	RWK 6.7	III	94	100

FACIES ANALYSIS

The Brassfield Formation displays wide lithologic variety in Ohio, Kentucky and Indiana. Rock types have been grouped into seven well defined lithofacies identified through field observations, petrography, and x-ray diffraction analyses. Brassfield lithofacies recognized in this report include:

- Facies I (The Belfast Member) is a thick bedded, finely laminated silty, glauconitic, and fine grained dolomite.
- Facies IIA (The Middle Member) contains coarsening-up thinly bedded carbonates and shales that are transitional with facies IIB.
- Facies IIB (The Middle Member) consists of wavey-bedded, coarsening-up, cherty massive grainstones to wackestones.
- Facies III (The Middle Member) consists of thin to thick interbedded and coarsening up carbonates and shales.
- Facies IV (The Middle Member) consists of thick cross bedded packstones and grainstones.
- Facies V (The Middle Member) consists of thin bedded grainstones to packstones with occasional clay laminae and small, well developed bioherms.
- Facies VI (The Middle Member) is a widely distributed salmon-colored, iron rich unit consisting of cross bedded grainstones and mud flasers.

- Facies VII (The Lee Creek Member) is a very thin, fine grained dolomite with abundant glauconite pellets, phosphate, fragments, and quartz clasts.

The following section presents a detailed description and interpretation of each facies, including aspects of dolomitization. Petrographic data, x-ray diffraction data, and clay mineral analysis are presented in Appendices 1, 2, and 3, respectively. Facies distribution, thickness, and dolomite content are illustrated in maps, and general sedimentologic features are shown in one or more composite sections for each facies. This will be followed by a summary of dolomitization and a depositional history overview of the Brassfield integrating individual facies interpretations.

FACIES I -- (BELFAST MEMBER)

Lithofacies description

Facies I (the Belfast Member) is a fine grained, silty dolomite. It is the oldest Brassfield unit (Rexroad, 1967), and where present, occurs at the base of the formation below facies II or facies IV. This report recognizes the Belfast from Nelson County, Kentucky, east and north through the southeast quadrant of the outcrop belt in Kentucky, north into Ohio, and west to Wayne County, Indiana. It is only locally present from Lincoln to Fleming Counties, Kentucky, and in Clinton County, Ohio. Its thickness ranges from a few cm. to 2 m. It is absent on the west side of the Cincinnati Arch from Wayne County, Indiana south to Nelson County, Kentucky. Figures 10 and 11 illustrate the thickness, distribution, and lithologic character of facies I.

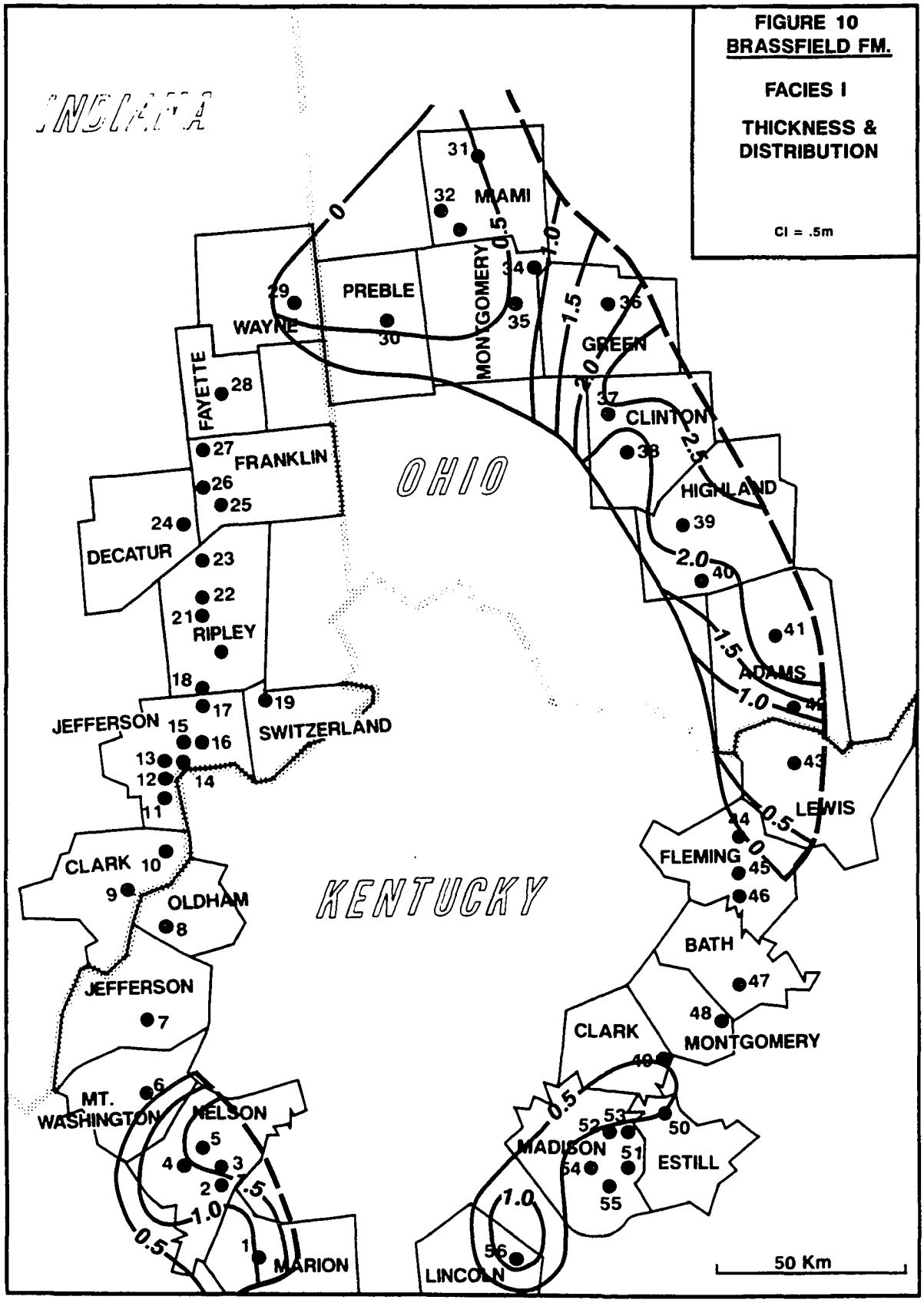

EXPLANATION OF SYMBOLS
USED IN COMPOSITE SECTIONS


CRINOIDS


CORAL


BRYOZOAN


TRILOBITES


BRACHIOPODS


GASTROPODS

STROMATOPOROIDS


FISH BONES


BIOTURBATION


STYOLITES


OOLITES


PELLETS


INTRACLASTS


CHERT NODULES


FLASER BEDS

Fe HEMATITIC OR IRON RICH

P PHOSPHATIC

EX-15-15-H-953

FACIES I COMPOSITE SECTIONS

FIGURE 11

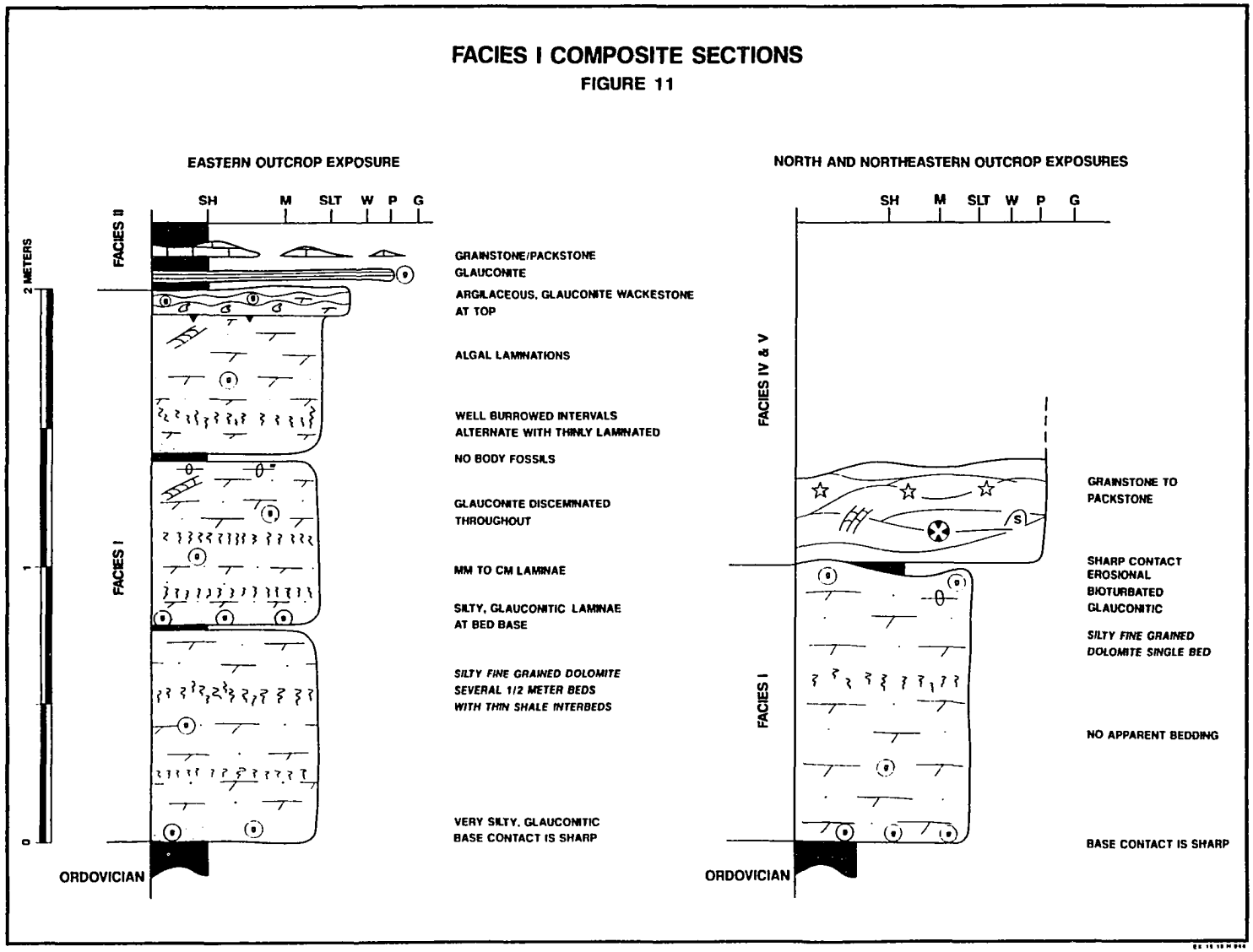

Facies I is a massive weathering, finely laminated to bioturbated, glauconitic, silty dolomite. Its average petrographic makeup is 93.4% dolomite, 2.3% late stage calcite cement, 1.6% angular quartz silt, 1.6% pyrite (much lower if location 29 is omitted), 0.5% pellets (usually glauconitic), 0.5% bioclasts (crinoids and few brachiopods), and 0.2% chert. Its color ranges from greenish yellow, to gray, to brownish gray. It is made up of one to four (rarely more) massive beds. Several beds are present at localities 37, 38, 41, and 42. The contacts between beds are always sharp and are commonly marked by bioturbated, glauconitic, and silty or sandy intervals (see Figures 12 and 13).

Other sedimentary features of the Belfast include desiccation cracks (Hendrix, 1983), gypsum casts (Harrison, 1982; and personal communication 1988), and birdseye voids parallel to laminations. Irregular algal laminae are also present, particularly at the base of the unit in eastern most outcrops. Thin (5-10 cm.) hummocky stratified silt beds are rare, but distinct where present.

Bioclasts and ghosts of bioclasts (usually small brachiopods or crinoids) are present, but rare, and occur as coarse, ferroan dolomite that is easily distinguishable from the finer grained surrounding matrix (Figure 14). The original sediment appears to have been silt or mud, and many thin sections reveal a pelletel texture under fluorescent illumination.

The carbonate in the Belfast is nearly 100% dolomite (Figure 15). A small percentage of calcite exists as late stage interrhombic cement.

FIGURE 12

HAND SAMPLE OF FACIES I SHOWING ALTERNATING BIOTURBATED AND LAMINATED INTERVALS

FIGURE 13

HAND SAMPLE OF FACIES I SHOWING TRACES OF GLAUCONITE (DARK SPECKS) AND MOTTLED TEXTURE

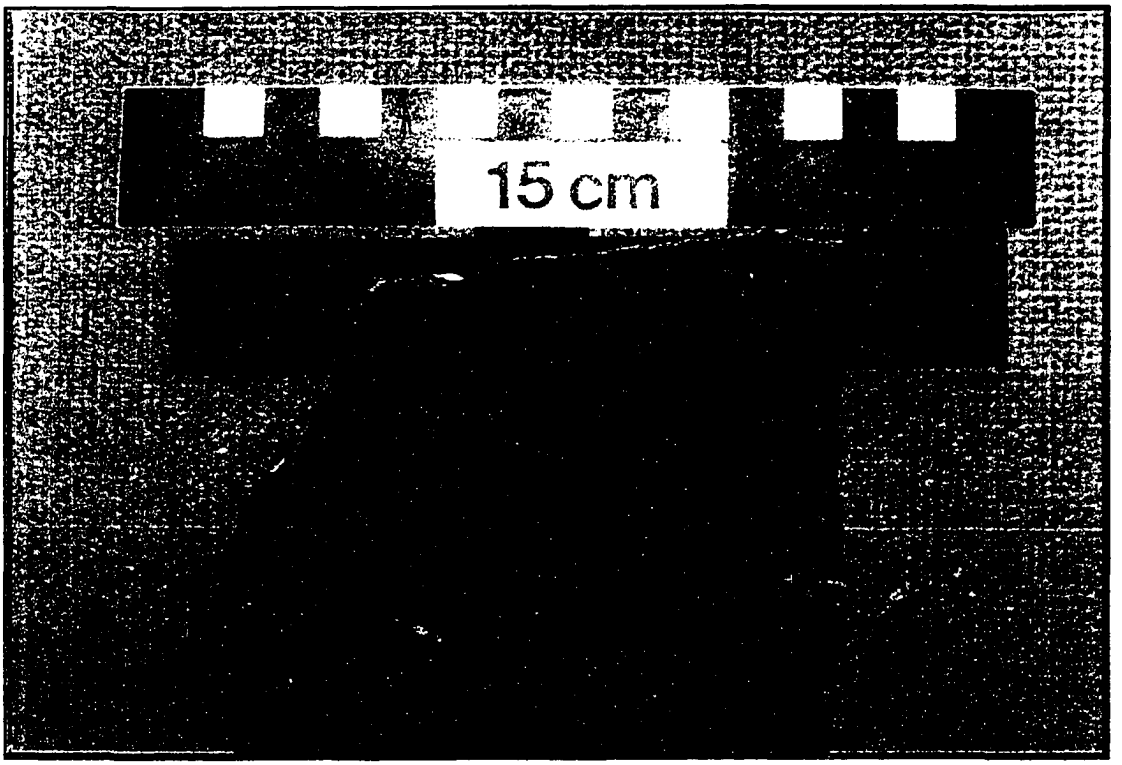

Location 41 Facies I

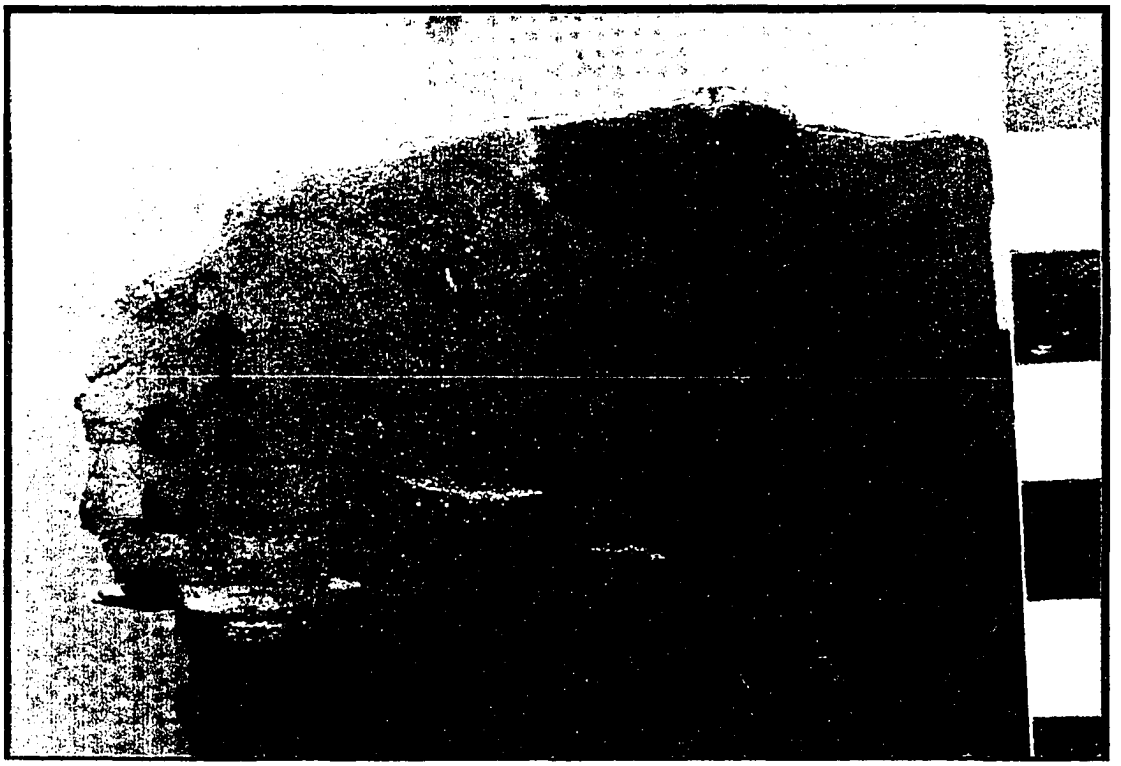

Location 56 Facies I

FIGURE 14

BIOCLASTS IN FACIES I THOUGH RARE, OCCUR ON COARSE CRINOID GHOSTS EASILY DISTINGUISHABLE FROM SURROUNDING FINER GRAINED MATRIX
ALSO NOTE COLLOPHANE FRAGMENT

FIGURE 15

FINE TEXTURED SILTY DOLOMITE TYPICAL OF FACIES I
(NOTE: XN = CROSS NICOLES
P = PLANE LIGHT
S = STAINED THIN SECTION)

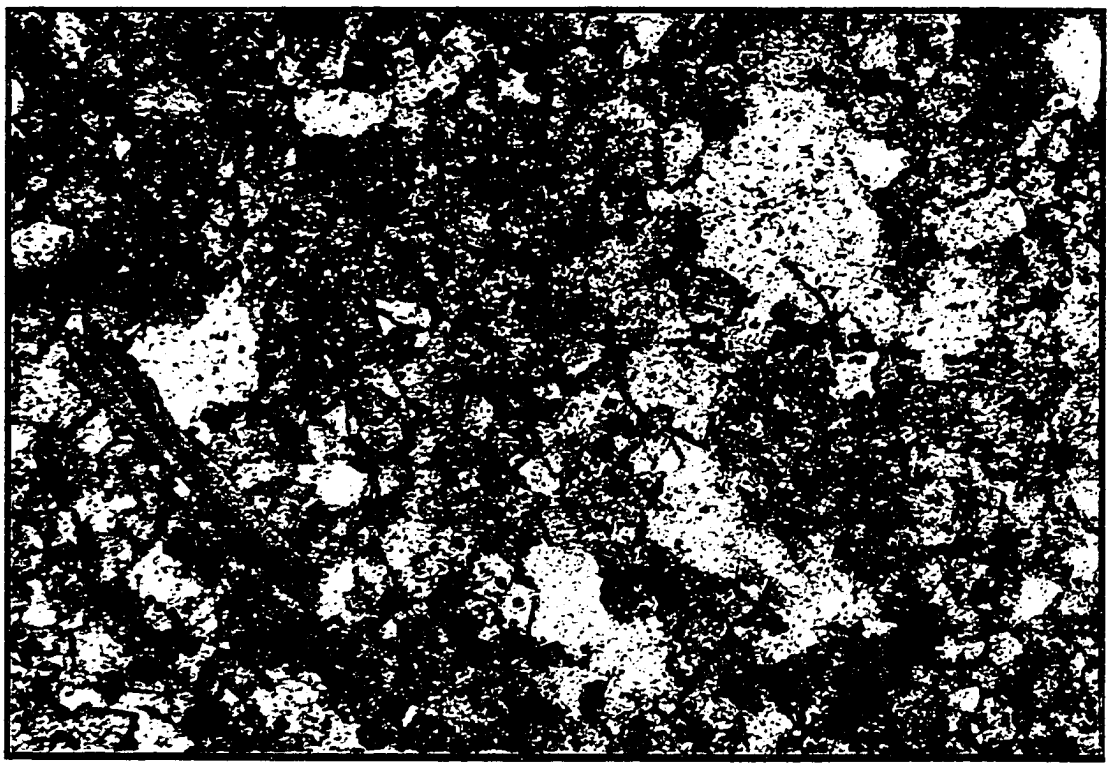

Location 4 Facies I P/S 200 microns

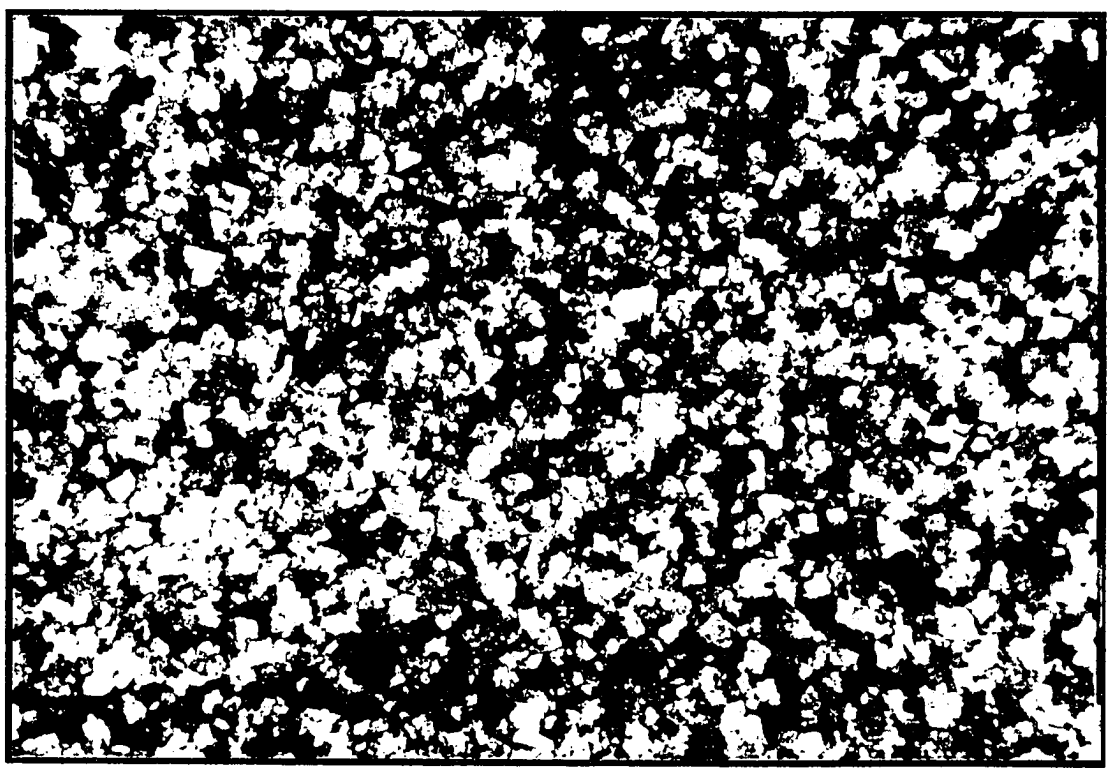

Location 34 Facies I XN/S 500 microns

The facies is much siltier than overlying Brassfield sediments, containing up to 9% angular quartz silt. The silt is evenly disseminated through out the unit, though it is sometimes concentrated in thin laminae or at bedding contacts.

Glauconite is a common element, and occurs as well-formed dark green pellets, in contrast to the glauconitized bioclasts found in overlying Brassfield strata. The concentration and stratigraphic distribution of glauconite in facies I varies between exposures. It is most often concentrated at the base and top of the unit, or between well-defined beds. In few localities it is disseminated throughout.

Bioturbation is moderate to intense in the Belfast. Chondrites is the most common (and often only) biogenic trace. Intensely bioturbated intervals, 12 to 5 cm. thick, have erosional contacts with overlying, non-bioturbated, horizontally laminated intervals of more or less equal thickness. In other cases, bioturbation is concentrated at bed tops.

Phosphatic collophane fragments (conodonts and fish bone) and pelloids are present in Nelson, Lincoln, and Estill Counties, Kentucky (localities 56, 50, and all exposures in Nelson County).

Lithofacies interpretation

A peritidal, possibly intertidal depositional setting for facies I is strongly supported by sedimentologic and biologic evidence.

The sediments in facies I were originally mud or silt with sparse macrofossils. Crinoids, large brachiopods, and gastropods occur both as unaltered clasts and as coarse ferroan dolomite ghosts, and are easily distinguished from the surrounding fine grained dolomite. The rarity of macrofossils reflects original diversity, rather than a loss through dolomitization. Shell bearing macroinvertebrates were not a major component of the facies I environment, presumably because of stressful restricted-marine conditions. Biogenic structures, most commonly Chondrites, provide the greatest evidence for organism activity. The presence of algal laminates also indicate shallow conditions. Gray and Boucot (1972) provided palynological evidence for an intertidal to marginal marine setting for the Belfast, in contrast to normal marine conditions for the overlying Brassfield sediments.

The sedimentary evidence for shallow, low energy, restricted marine conditions is abundant. Dolomite constitutes nearly 100% of carbonate in facies I (even where overlying facies of the Brassfield remain un-dolomitized). Quartz silt and glauconite pellets are relatively abundant, and are sometimes concentrated in discrete laminae. Thin parallel lamination intervals truncate highly bioturbated sediments. Hummocky cross stratification in facies I probably indicates deposition under high flow regime conditions, perhaps set up in very shallow water as flats drained following storm surge. Other less common evidence for subaerial exposure includes mudcracks, gypsum casts, calcite filled vugs, and birdseye-like voids parallel to lamination.

Thicker exposures comprising several beds are interpreted as representing stacked pritidal parasequences. The parasequences are separated by continuous flat surfaces marked by argillaceous laminae, high silt or glauconite content, or complete biogenic reworking.

Distribution and thickness of the Belfast was influenced by the topography of the eroded, Upper Ordovician surface. Relatively small topographic highs could have easily precluded deposition of shallow intertidal sediments, explaining the abrupt changes in thickness of facies I over short distances, and its absence in may localities. Facies I thins from east to west onto the platform. The western most exposures of facies I consist of relatively thin, single beds, and probably represent the final stages of facies I deposition. An anomalously thick exposure of Belfast near Bardstown, Kentucky (measuring 2 meters) was deposited in a structural low -- the Bardstown Monocline (Kepferly, 1976). The Belfast thins rapidly north and west of these exposures.

Dolomite Description

The dolomite in facies I and all other Brassfield facies is described in terms of the following characteristics:

(1) percent dolomite of total carbonate

(2) modal rhomb size

(3) rhomb morphology

(4) presence and number of rhomb zones

(5) relative iron content

(6) texture selective replacement

(7) dolomite related porosity

Percent Dolomite

The percent dolomite of total carbonate (calcite + dolomite) in individual samples was determined by thin section point counting and compared to results obtained by x-ray diffractometry. The discrepancy between the dolomite/ limestone ratio as determined by x-ray diffraction versus point counting has been addressed by Lumsden (1979) and Hardy and Tucker (1988).

The dolomite content of each facies has been mapped, except for facies I and VII, which are nearly 100% dolomite. Point count, rather than diffractometry data was used to construct the maps because the data set is more complete and the difference in results between the two methods is insignificant.

Modal Rhomb size

Each sample was checked for modal rhomb size. A unimodal size distribution is thought to indicate a single nucleation event on a unimodal substrate (e.g., a single dolomitization event on all silt or mud sized sediment). Polymodal distributions indicate more than one nucleation event on unimodal or polymodal substrates, or one nucleation event on polymodal substrates such as would occur with dolomitization of packstones or wackestones (Sibley and Gregg, 1987).

Rhomb Morphology

Rhombs are described as having planar or nonplanar crystal boundaries. Planar crystals are subdivided into euhedral and subhedral forms. Planar dolomite crystals are thought to form at relatively low supersaturation and/or temperatures. At high supersaturations (critical saturation), or above some temperature (critical roughening temperature is estimated at between 50° and 100° C) crystal growth occurs as random addition of atoms to the crystal face and results in nonplanar crystals (Sibley and Gregg, 1987). All dolomite in the Brassfield is planar, and therefore thought to occur at relatively low temperatures and saturations.

Selectivity

Dolomitization is described as partial and texture selective, or whole-rock. It was usually possible to determine what part of the original texture was dolomitized with partially dolomitized samples.

Zoning

Where present, the number of growth zones in rhombs has bee noted.

Iron Content

Staining for iron provided a qualitative estimate of ferroan content. Stages of ferroan growth (ferroan zones) have also been recorded.

Porosity

Porosity is commonly related to type and degree of dolomitization. Interrhombic and dolomoldic porosity are the most common types of dolomite

related porosity in the Brassfield. Interrhombic porosity is generally associated with completely dolomitized samples, whereas partially dolomitized samples exhibit dolomoldic porosity.

Original Texture

The original texture of dolomitized samples were described where possible. Florescence microscopy was helpful in determining this, particularly with fine grained, completely dolomitized samples.

Facies I is nearly 100% dolomite and has two petrographic expressions in Ohio. The first has unimodal rhomb size distribution (30 to 80 microns), is planar-subhedral, nonzoned, and nonferroan to slightly ferroan. Porosity is mostly interrhombic, ranging from 1% to 18% and averaging under 8%. The second type, similar to Facies I dolomite in Kentucky, is polymodal (80 and 250 microns), planar-euhedral, commonly shows one well developed zone, and is nonferroan, except for occasional ferroan zones. interrhombic porosity is most common, ranging from 7% to 40%, and averaging under 19% (see Figures 16 and 17).

Dolomite Interpretation

Unimodal dolomite of facies I in Ohio is suggestive of a single nucleation event on a unimodal surface under low temperature and low temperature and low saturation conditions. Polymodal sized dolomites in both Ohio and Kentucky are interpreted as having formed during two nucleation events on

FIGURE 16

FACIES I DOLOMITE

FIGURE 17

FACIES I DOLOMITE

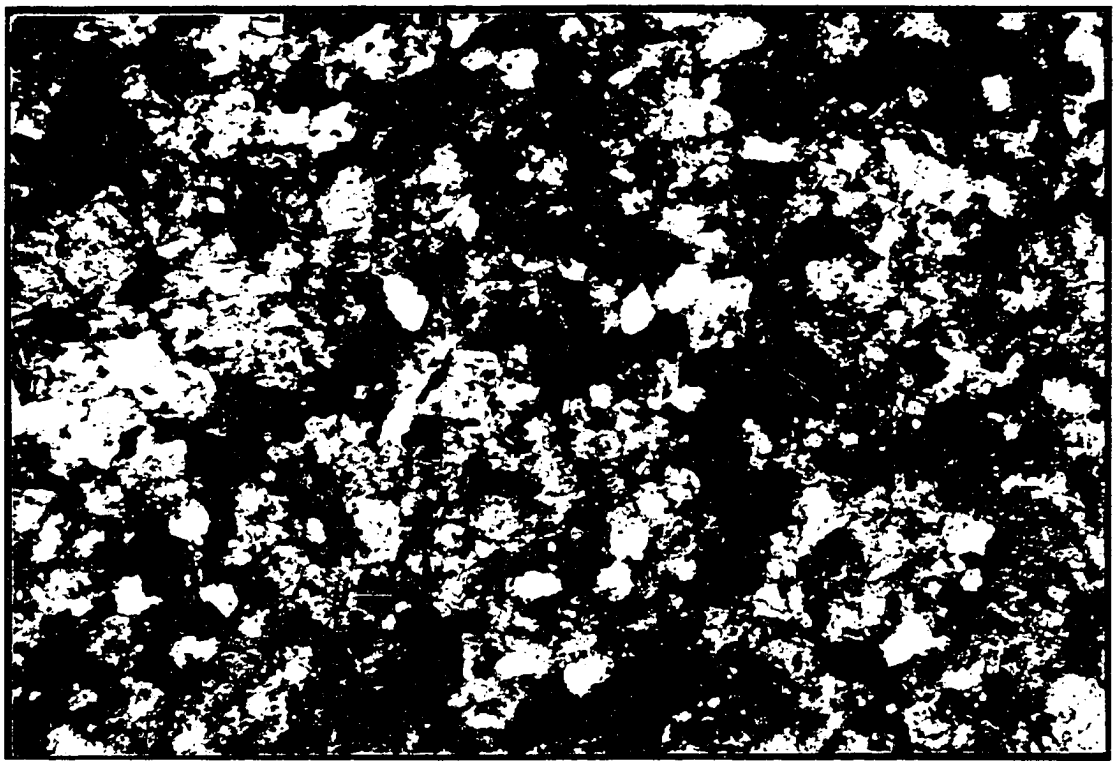

Location 41 Facies I XN/S 200 microns

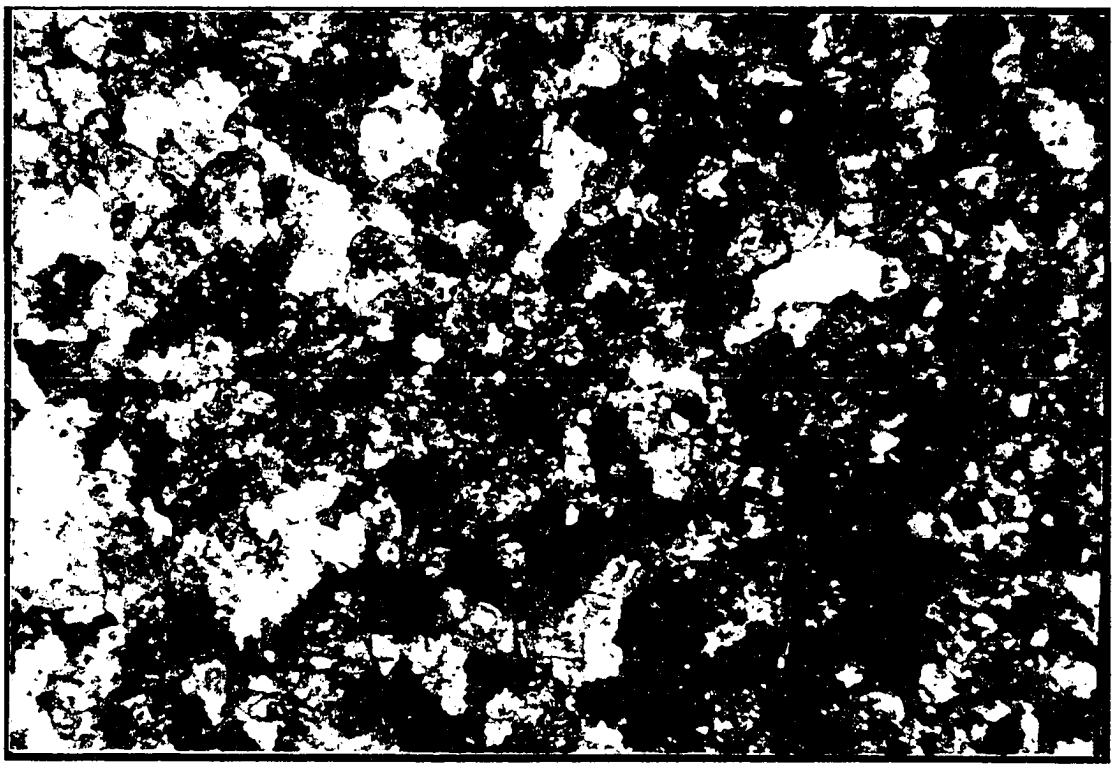

Location 43 Facies I P/S 200 microns

unimodal substrates. Dolomite in facies I characterized by fine, uniomdal sized rhombs, occurs below dolomite-poor Brassfield facies, whereas polymodal dolomite, indicative of two nucleaton events, occurs below intensely dolomitized Brassfield strata. Facies I was originally fine grained (silt or mud) and some samples reveal a pelletal texture under fluorescent illumination.

FACIES II

Facies II is separated into two subfacies that are easily distinguished in outcrop on the basis of shale content and bedding.

Lithofacies Description - IIA

Facies IIA is composed of coarsening-upward, thinly bedded, carbonates and shales. It is present on the east side of the Cincinnati Arch from northern Clinton County, Ohio to Bath County, Kentucky, and is always found below facies IIB. It is 2 meters thick in Adams County, Ohio and thins to less than 0.25 meters at its northern and southern limits. Figures 18 and Figure 19 illustrate the thickness, distribution, and lithologic character of facies II in the study area. Figure 20 shows a typical outcrop exposure of facies I and II.

Where best developed, facies IIA consists of 1 - 10 cm. thick limestone or dolomite beds interbedded with gray shale beds of approximately equal thickness. Its average petrographic composition is 35.0% dolomite, 32.0% bioclasts, 17.0% calcite cement, 14.0% micrite, 1.3% glauconite pellets, 0.3%

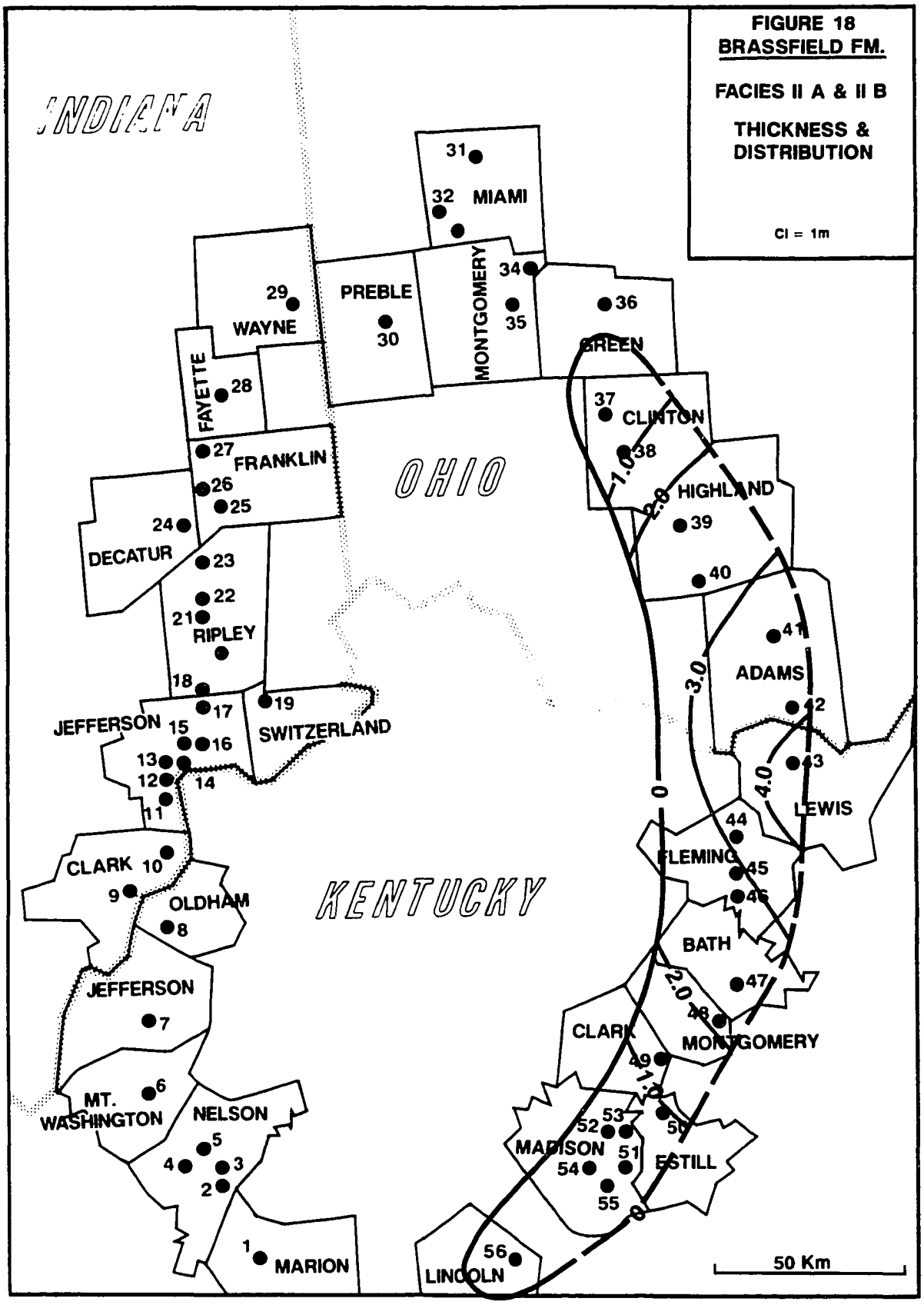

FACIES II-A AND II-B COMPOSITE SECTIONS

FIGURE 19

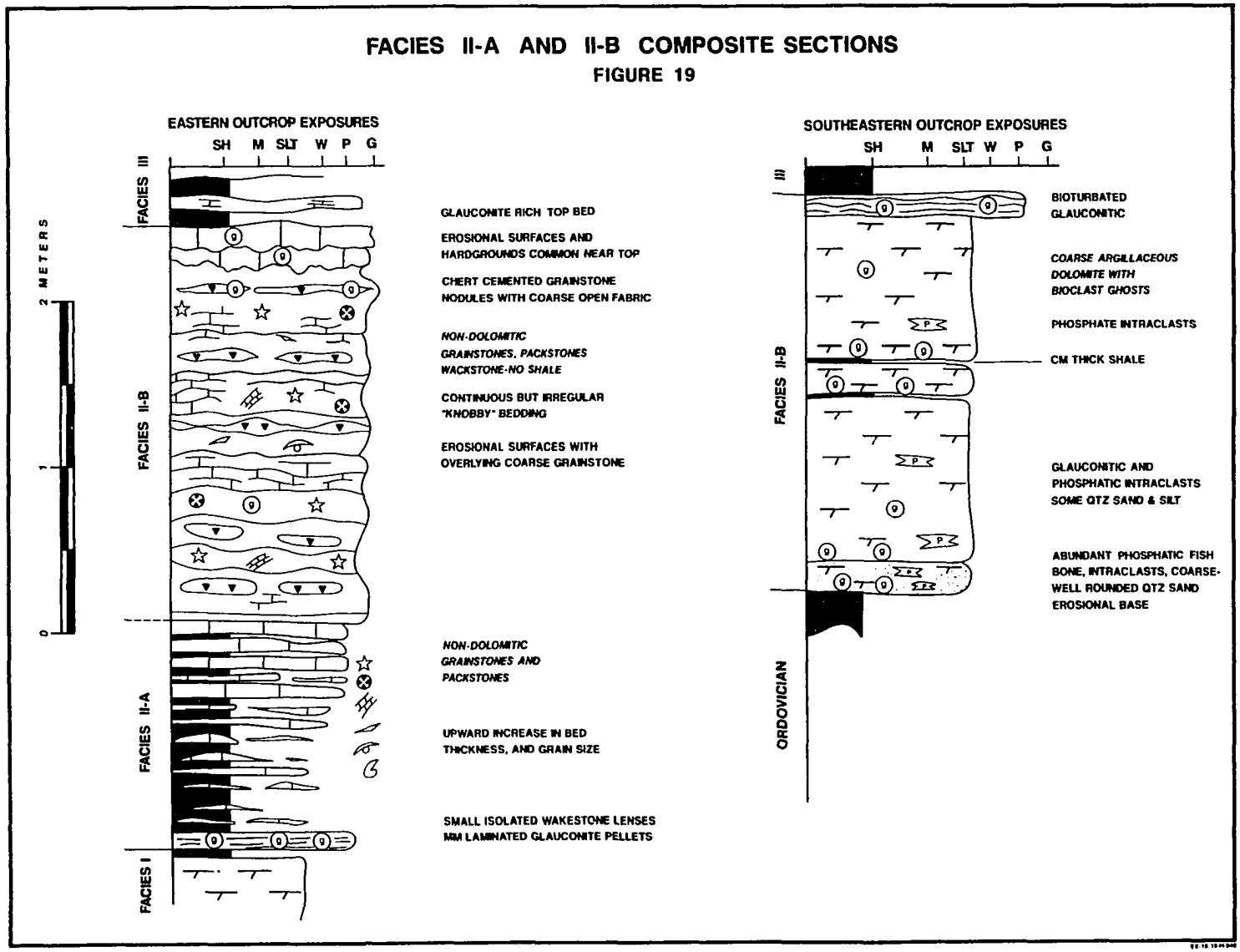

FIGURE 20

FACIES I, IIA, AND IIB (COMPLETELY DOLOMITIZED IN THIS CASE)

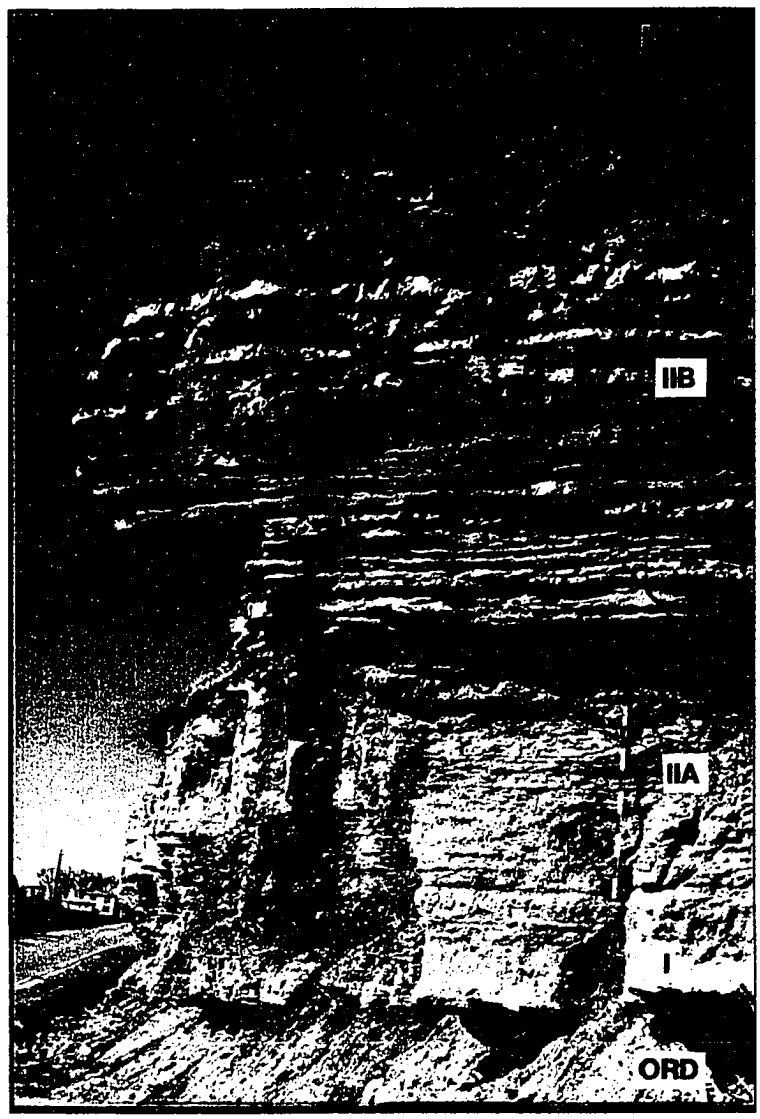

Location 43 Facies I, IIA and IIB

quartz sand and silt, and 0.3 pyrite. Average bioclast composition for all of facies II is 74.0% crinoid, 12.0% brachiopod, 4.5% coral, 3.0% trilobite, 2.5% unknown, 2% bryozoan, and 2% ostracode.

Bedding thickness, continuity, and grain size increase up section. Textures range from thinly laminated fine grainstones, siltstones, and bioturbated wackestones (Figures 21 and 22) to normal graded wackestones and packstones (Figure 23). Horizontal lamination, cross laminated and bioturbated beds are common. Grain size ranges from silt to centimeter sized bioclasts. Beds with erosional bases and internal surfaces are common (Figures 23 and 24).

Glauconite, in the form of partially to wholly glauconitized echinoderm fragments and pellets, is a common constituent of facies IIA. Glauconite is more concentrated at the base, but is present throughout the unit (Figure 25). Where facies I is not present and facies IIA is the basal Brassfield unit, its base is marked by a 5 to 10 cm. thick, mottled, and very glauconite rich bed.

Lithofacies Description, IIB

Facies IIB is a shale-free wavy bedded, cherty, coarsening-upward unit that is transitional with facies IIA. It is present from northern Highland County, Ohio south to Maidson County, Kentucky. It occurs above facies IIA on the east side of the Cincinnati Arch, north of Montgomery County, Kentucky, and is either the basal Brassfield facies or lies above facies I from here southwest to Marion,

FIGURE 21

HORIZONTALLY LAMINATED FINE GRAINSTONE WITH EROSIONAL BASE

FIGURE 22

BIOTURBATED, GLAUCONITE RICH BED AT THE BASE OF FACIES IIA (THIS LITHOLOGY IS TYPICAL OF THE BASE OF FACIES IIA WHERE IT MARKS THE BASE OF THE BRASSFIELD)

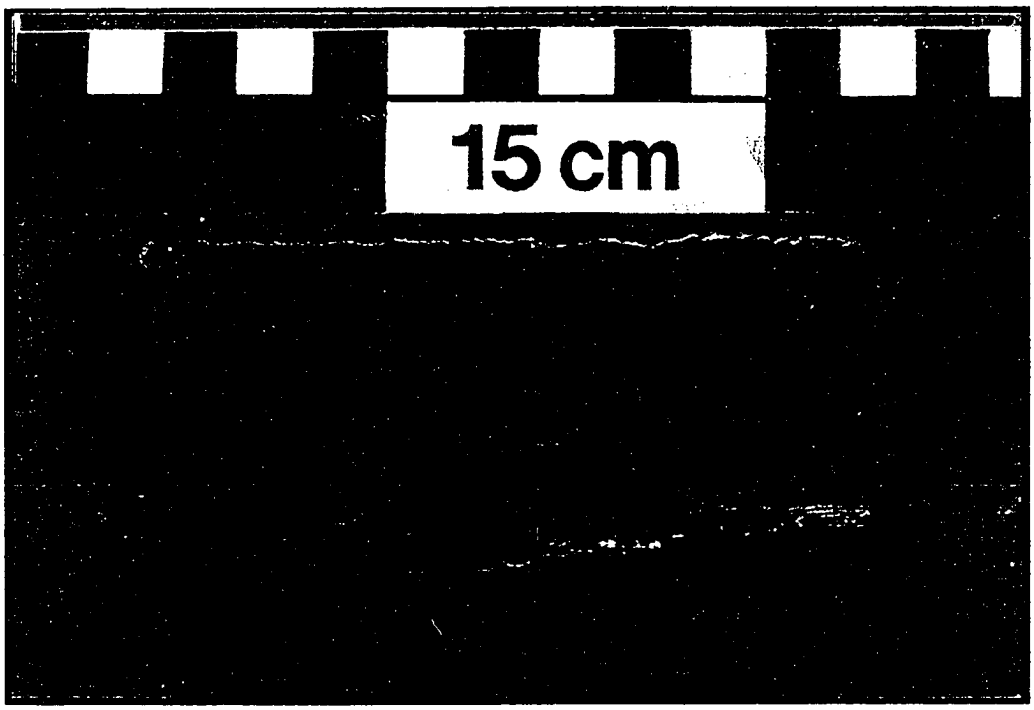

Location 41 **Facies IIA**

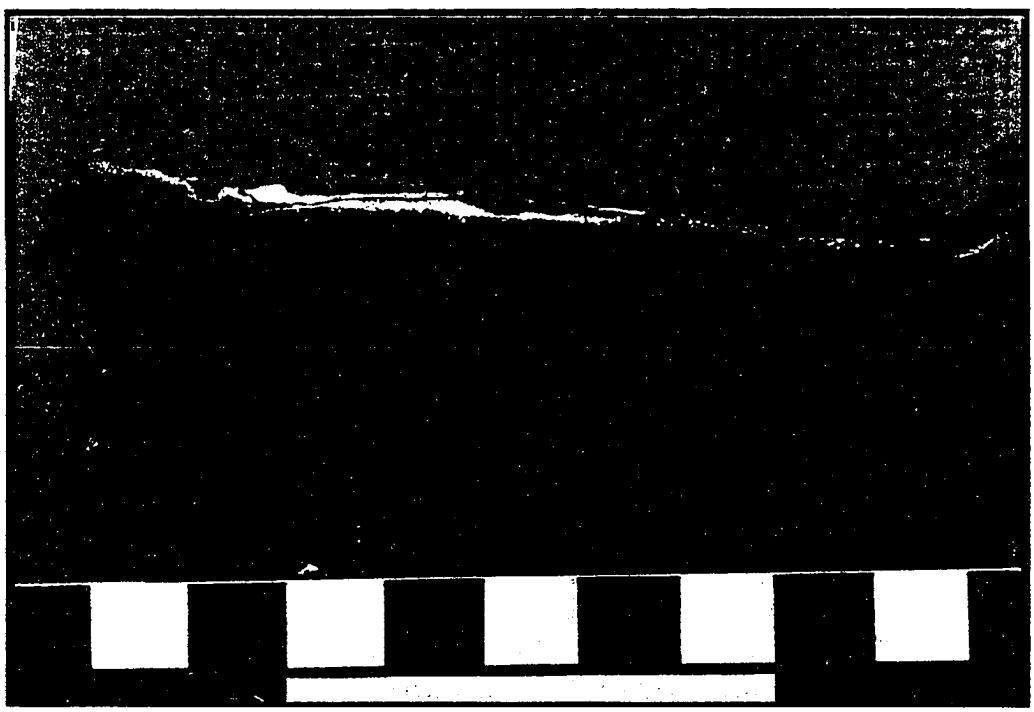

Location 45 **Facies IIA**

FIGURE 23

NORMALLY GRADED COARSE WACKESTONE OF FACIES II-A WITH SHARP EROSIONAL BASE

FIGURE 24

FACIES IIA BED WITH INTERNAL EROSIONAL SURFACE

Location 41 Facies IIA

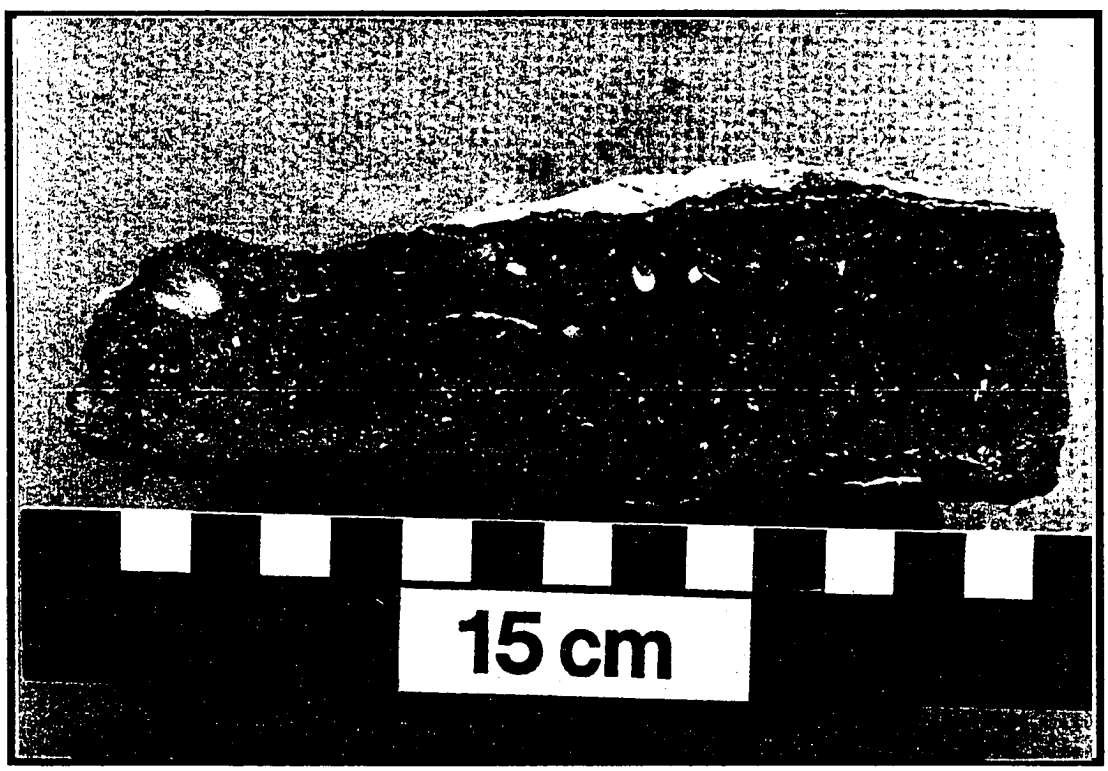

Location 41 Facies IIA

FIGURE 25

THIN SECTION SHOWING ECHINODERM FRAGMENTS WITH VARYING STAGES OF GLAUCONITE REPLACEMENT

FIGURE 26

CROSS LAMINATED, GLAUCONITE RICH GRAINSTONE

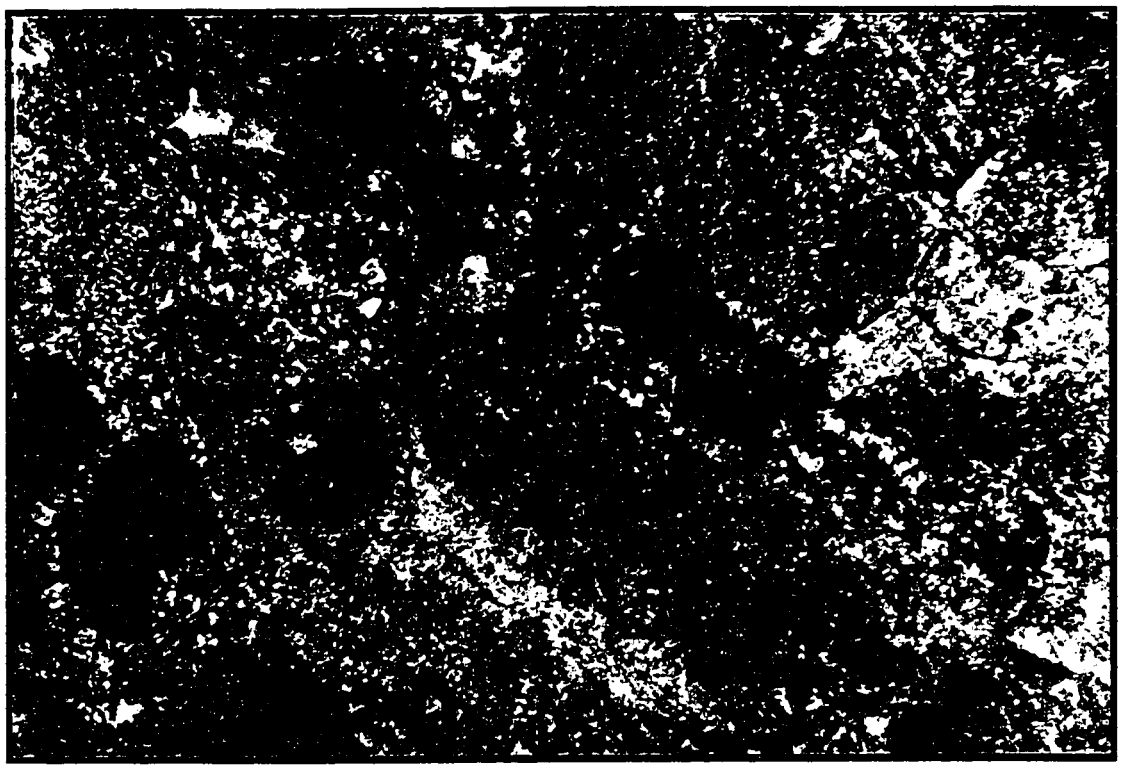

Location 41 Facies IIA P/S 200 microns

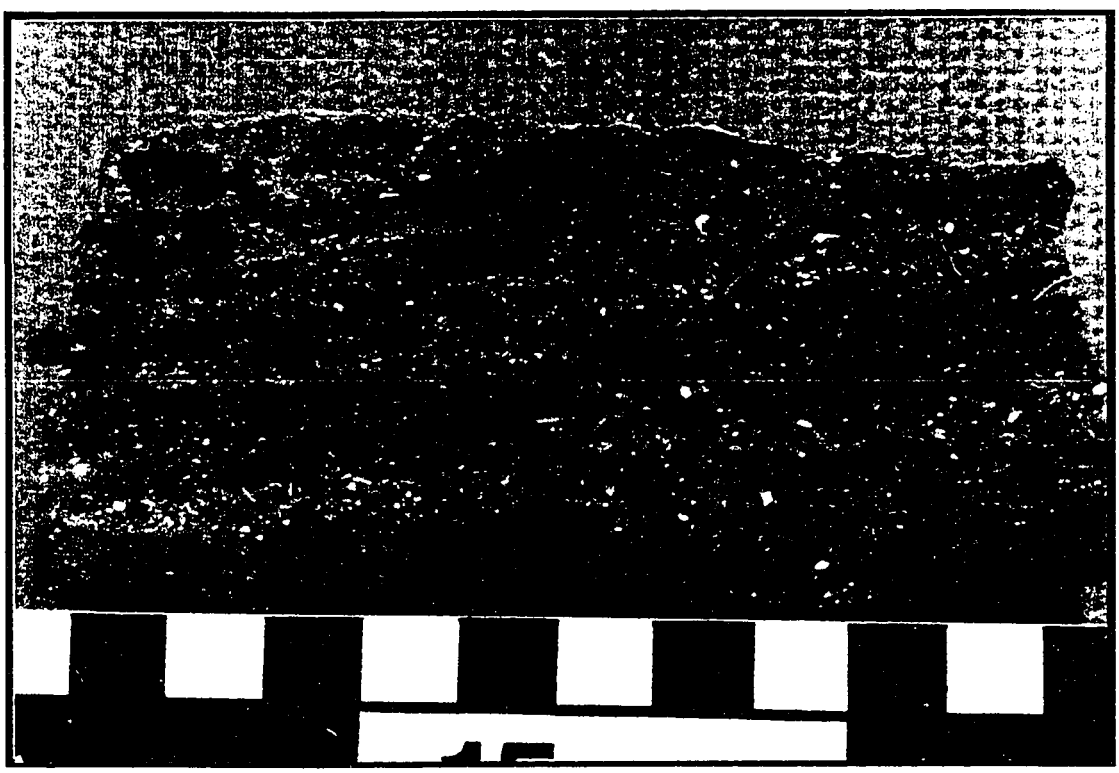

Location 41 Facies IIB

County, Kentucky. Its thickness is nearly always 2 meters, although it is less well-developed and thinner at its northern and southern limits.

Bedding thickness of Facies IIB ranges from 2 to 20 cm. Bedding surfaces are irregular or knobby, but are laterally continuous along outcrops. Some surfaces are rippled, and thin shaley or argillaceous partings are present, but rare.

Rock types range from wackestones to coarse open grainstones, and normally graded beds are common. Horizontal and cross laminated beds alternate with unstructured or mottled wackestones (Figures 26, 27, and 28). Grain size is highly variable, ranging from silt to centimeter sized clasts, and most beds contain at least some very coarse material. The average petrographic composition of IIB is 37.5% bioclasts, 27.5% cement, 17.5% micrite, 15.0% chert, 2.0% dolomite, 1.3% glauconite pellets, and 0.5% quartz.

Most exposure of facies IIB contain chert in nodular, but moderately continuous, horizons. The silicification process does not appear to have been texture selective; all rock types have been altered. Chert cemented coarse open grainstones exhibit remarkably preserved original (early) cement fabric, and provide a view of early cementation in Brassfield sediments that is usually obliterated by syntaxial crinoid overgrowths. Syntaxial crinoid overgrowths in the form of broad bladed, isopachous, optically continuous, ferroan and nonferroan calcite are common (Figure 29).

FIGURE 27

MOTTLED WACKESTONE

FIGURE 28

COARSE CRINOID PACKSTONE WITH ABUNDANT GLAUCONITE

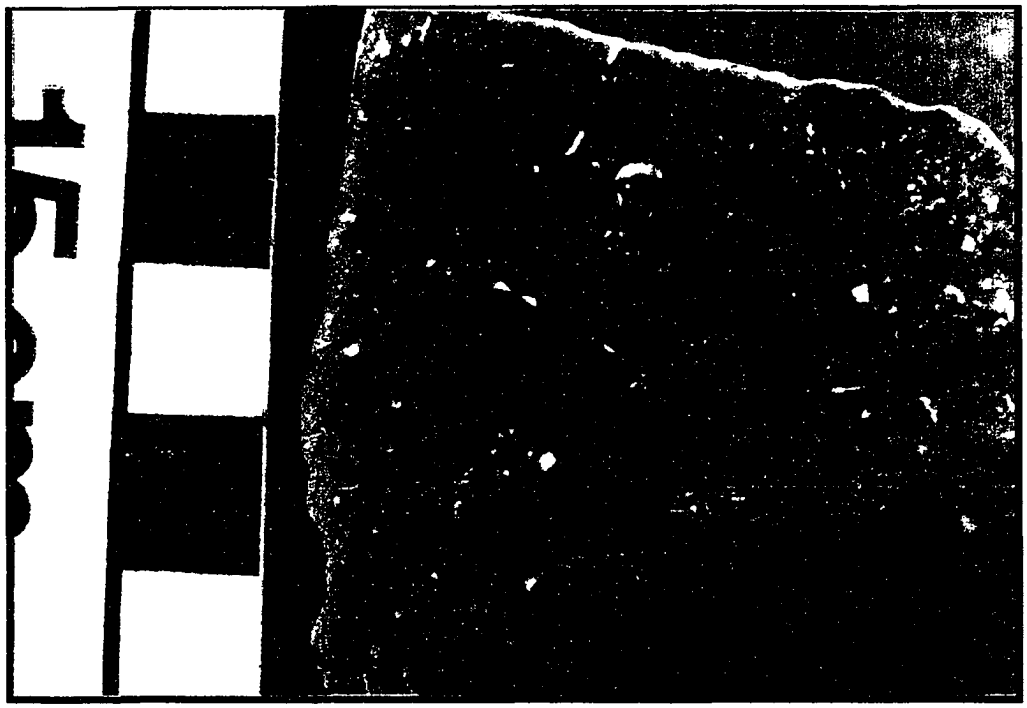

Location 41 Facies IIB

Location 41 Facies IIB

FIGURE 29

CRINOID FRAGMENT WITH FERROAN SYNTAXIAL OVERGROWTH, ENCASED IN CHERT CEMENT

FIGURE 30

FIBROUS AND SPHERICAL ARAGONITIC CEMENT TEXTURES ENCASED IN CHERT CEMENT

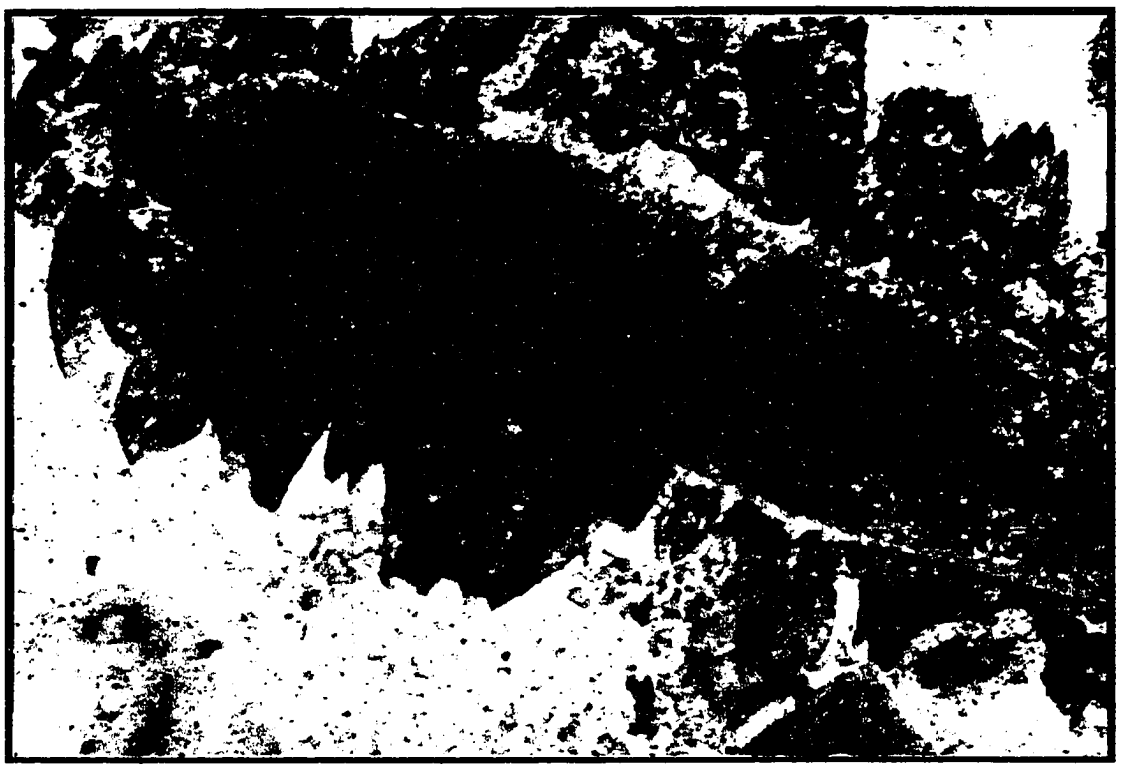

Location 41 Facies IIB P/S 200 microns

Location 41 Facies IIB P/S 200 microns

Bladed high Mg-calite cements occur as several aragonitic cement textures, including fibrous, isopachous fibrous, and an unusual spherical form found on aragonite fibers, syntaxial over growths, and as floating spheres in chert (Figure 30).

Glauconite constitutes up to 1% of this unit and is present most commonly as glauconitized crinoid bioclasts, where the glauconite is concentrated in the micro pores of the stereome structure. Glauconite is found throughout of facies IIB, but is more concentrated at the top of the unit in Adams and Highland Counties, Ohio.

Erosional hardground surfaces occur in the upper part of the facies IIA at 41 and 40. The surfaces are irregular and have several cm. of relief. Fine pyrite is concentrated along the eroded surface. A coarse packstone was deposited above the contact at both localities (Figures 31 and 32).

An interval rich in quartz sand, chertified and pyritized lithoclasts, glauconite pellets, and phosphatized lithoclasts and fish bones, (the Howards Creek Bed of Byrne, 1961), occurs at the base of facies in IIB from northern Estill and Madison Counties, through Clark, Montgomery, and Bath Counties, Kentucky. It is only developed where facies IIB is the basal Brassfield unit. Byrne reported the lithology to be limited to a single bed, up to 0.5 m. thick, at the base of the Belfast, but the non-carbonate clasts characteristic of the basal bed are present in lesser concentrations throughout the facies in this area (Figures 33 and 34). Slightly more concentrated lags are formed at the base of individual beds.

FIGURE 31

HARDGROUND SURFACE AT THE TOP OF FACIES IIB ("UP" IS TO THE LEFT)

FIGURE 32

HARDGROUND SURFACE AT THE TOP OF FACIES IIB, SIMILAR TO THAT SHOWN ABOVE ("UP" IS TO THE LEFT)

Location 40 Facies IIB

Location 41 Facies IIB

FIGURE 33

COARSE LAG AT THE BASE OF FACIES IIB CONSISTING OF QUARTZ SAND, PYRITIZED LITHOCLASTS, GLUACONITE PELLETS AND PHOSPHATIC FRAGMENTS

FIGURE 34

THIN SECTION OF BED SHOWN ABOVE.
FISH BONES, GLAUCONITE PELLETS AND QUARTZ GRAINS ARE IN ABUNDANCE

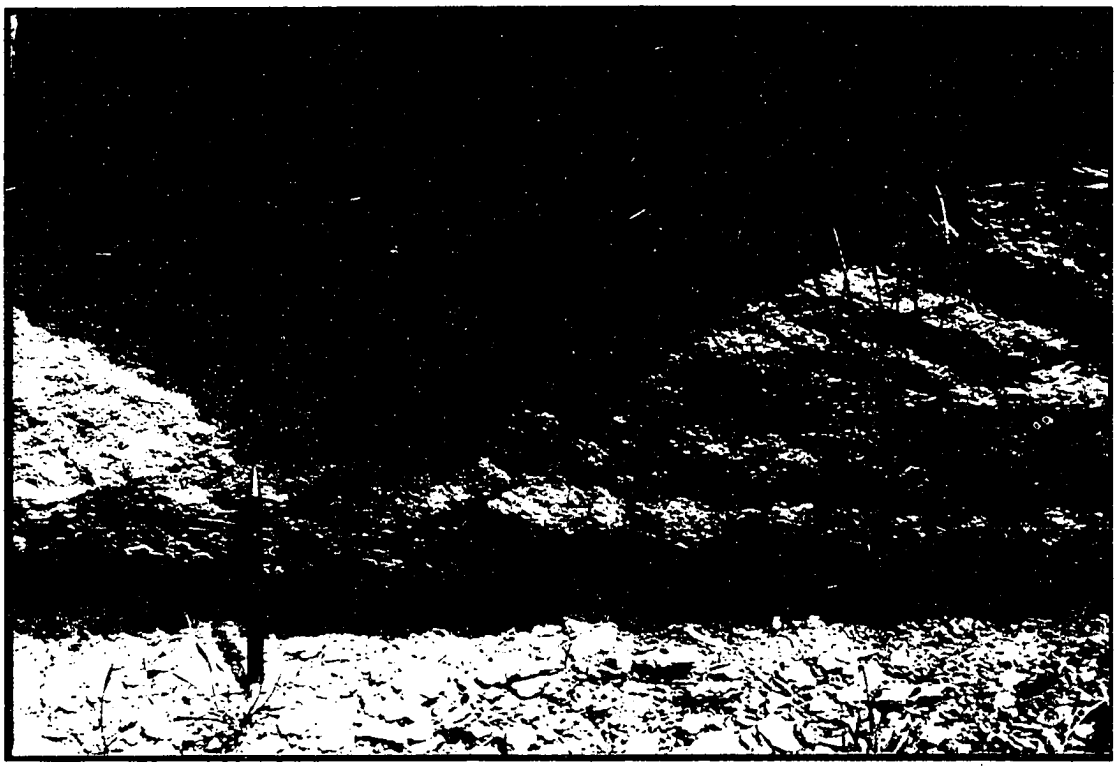

Location 48 Facies IIB

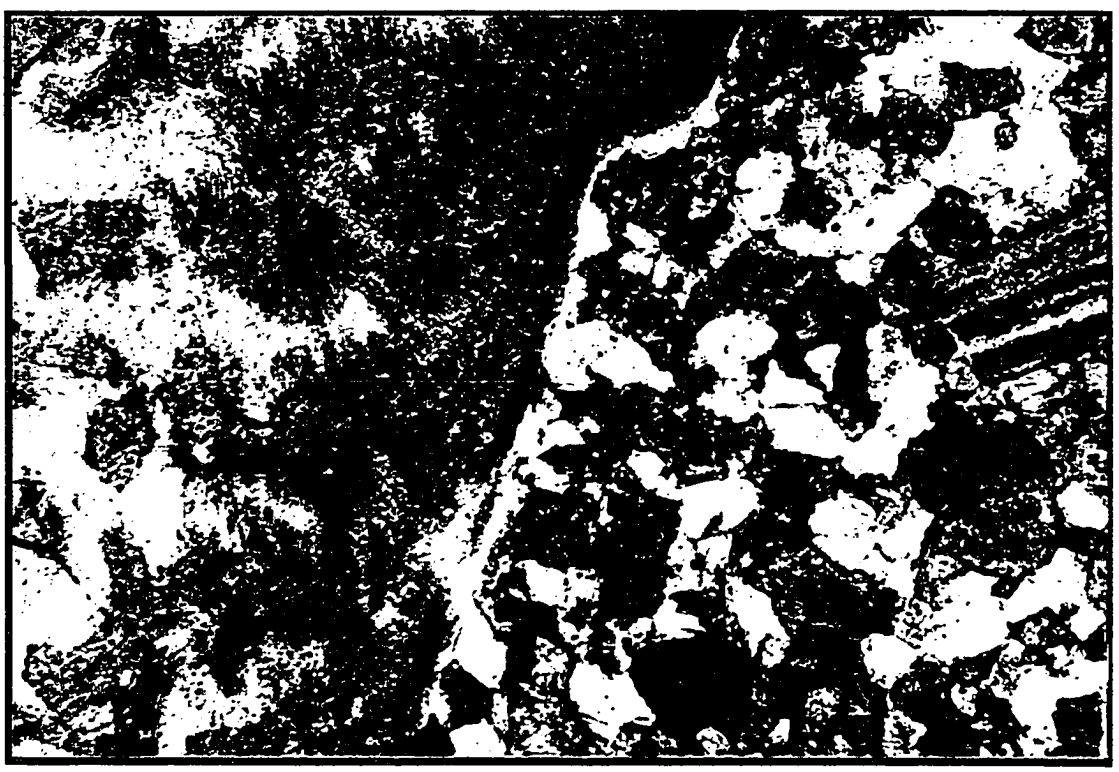

Location 48 Facies IIB P/S 500 microns

Coarse well rounded quartz sand grains and collophane fragments are found in facies IIB as far south as southern Madison County, Kentucky (locations 51 and 53) which suggests that the "Howards Creek Bed" has a wider distribution than described by Byrne (1961). Again, these clasts are only found where facies IIB marks the base of the Brassfield.

Lithofacies Interpretation - IIA

The contact between subfacies IIA and IIB is gradational. Together, they represent a shallowing-upward transition, probably from below, to at or above normal wave base, as indicted by an upward increase in bed thickness, grain size, and decrease in shale content.

Thin (1 to 5 cm.), non-continuous beds at the base of facies IIA grade into more continuous and somewhat thicker (5 to 10 cm.) beds near its top. These represent relatively distal tempestites and are characterized by moderately thin beds with sub-parallel laminations and erosional bases, starved ripples, fining up wackestones and packstones, some of which have large clasts at their base, or less commonly thin sub-parallel laminated grainstones. The thickness of shale intervals decreases up section from over 25 cm. to mm. partings near the transition with IIB.

Facies IIA represents renewed deposition following a transgression-induced hiatus in deposition. At many localities, its base is marked by a concentration of glauconitized bioclasts that probably formed when sedimentation slowed after the deposition of facies I.

Facies IIA contains a far more diverse fauna than in facies I. Crinoids, brachiopods, corals, trilobites, bryozoans, and ostacods are well represented, and indicate open, normal-marine conditions.

Lithofacies Interpretation - IIB

The alternating coarse wackestones, packstones and cross-bedded grainstones in facies IIB represent a shallowing-upward accumulation of proximal tempestites. Graded, cross bedded, and rippled grainstones and packstones, the amount of coarse material, and lack of shale indicate deposition at or above wave base.

The fauna of facies IIB, is slightly less diverse than that of IIA, consisting predominantly of crinoids, with lesser amounts of coral and brachiopod material. Many of the crinoids in facies IIB are large, robust forms that may have thrived in the higher energy environment.

Pitted and eroded ferruginous hardgrounds near the top of facies IIB at localities 41 and 40 are overlain by coarse packstones and grainstones that contain clasts eroded from the crust (See Figures 31 and 32) and suggest a period of low sedimentation coupled with erosion. Although the hardground surfaces do not appear to be bio-encrusted, they are highly scoured and probably formed in a high energy, shallow water environment. As sedimentation resumed after hardground formation, coarse bioclasts, intraclasts eroded from the crusts, and glauconitized bioclasts altered during depositional

hiatus, were deposited over the hardgrounds. This type of hardground is restricted to the top of facies IIB.

Very coarse, open, chert cemented grainstones with relatively unabraded bioclasts near the top of IIB provide additional evidence for shallow conditions. Aragonite and high Mg-calcite cements (indicative of normal marine phreatic conditions) pre- and post-date syntaxial echinoderm overgrowths (commonly formed in a mixed marine-fresh water zone). The aragonite cements occur as fibrous needles and as unusual spheres (aragonitic framboids) that are between 10 and 50 microns in diameter (Figure 30). High Mg calcite forms small bladed rim cements. All forms of calcite cement are entombed by pore filling botryoidal chert. This suggests shifting between normal marine phreatic and very shallow marine to mixing zone or nonmarine conditions. The very open packed nature of the sediment fabric and "stunted" crinoid overgrowths indicates the chert, which was the final cement phase, was formed relatively early -- before compaction.

It should be noted that though previous workers have suggested the chert is packstone selective (Hendrix, 1982) or whole rock replacive (O'Donell, 1967), the chert in facies IIB is both primary pore filling and replacive. In grainstones, it replaces and maintains fine details of bioclasts (usually brachiopods or corals and less commonly crinoids) and grows as banded botryoidal chalcedony into pore space. This habit invariably preserves very open packing and indicates early, perhaps synsedimentary silicification. In packstones and wackestones, fine grained chert replaces micrite and bioclasts without retaining shell structure. In still other cases well preserved, chertified

bioclasts are present in otherwise non-chertified packstones. It is possible that these isolated chertified bioclasts were selectively altered, but it seems more likely that they were eroded from previously chertified sediments and redeposited. The importance of the chert to this study, particularly the chert found at the top of facies IIB, lies in the evidence it provides for the shifting, albeit shallow, marine to marginal marine conditions that mark the top of the Facies II shallowing-upward sequence.

Facies IIB marks the base of the Silurian in the southeast quadrant of the outcrop belt in north central Kentucky. Complete dolomitization of the Brassfield south of Ohio has made identification of bioclasts difficult. However, the unit is rich in coarse, well rounded quartz grains, fish bones and other collophane fragments, well formed glauconite pellets, and ferruginous intraclasts several cm in dimension that may have been eroded from a ferruginous hardground. These constituents indicate a high degree of condensation brought about by a combination of low sedimentary input and repeated reworking under shallow marine conditions, which would tend to concentrate durable clasts while weeding out the less durable or chemically unstable constituents. This process has been employed to explain the selective preservation of certain shell types and resultant shift in the faunal spectrum in progressively "cannibalized" shelly tempestites (Seilacher, 1982). Aragonite shells are removed first, followed by calcite shells, high magnesium calcite echinoderm fragments, and finally, apatitic remains. The final product of this process is a bone bed. Other concentrated clasts in facies IIB include glauconite pellets and quartz grains.

Quartz grains in facies IIB are well rounded and many appear to be sandstone rock fragments with concavo-convex grain to grain contacts. The degree of rounding and type of grain contact could hardly be attributed to Brassfield depositional and diagenetic conditions. They were probably derived from eroded Ordovician sediments to the east.

Dolomite Description -- Facies IIA, IIB, and III

Dolomite content of facies II and III increases dramatically between localities 41 and 43 (facies II contains 6% dolomite at 41 and 90% at 43). Facies III contains 7% at 41 and 92% at 43 (See Figure 35). No petrographic data was collected from locality 42 (between localities 41 and 43), but hand samples stained well for calcite and showed little evidence of dolomitization. The transition between dolomite and limestone in this area is very abrupt and occurs somewhere in the 15 km stretch between localities 42 and 43. Dolomite content of the Brassfield in the southern part of the outcrop belt averages 97%. Virtually all calcite in this area is a late stage cement that postdates the dolomite.

In Lewis, Fleming, and Bath Counties, Kentucky facies II and III show polymodal, euhedral, and lesser subhedral, rhomb morphologies. Dolomitization is "whole rock" in this area. The coarsest dolomite has replaced crinoid bioclasts, smaller 150 micron rhombs replace cement, and 50 to 70 micron rhombs replace micrite (Figure 36). Locality 41 exhibits the most distinctly zoned dolomite of all Brassfield exposures (between two and four zones, Figure 37). Zones commonly alternate from nonferroan to ferroan.

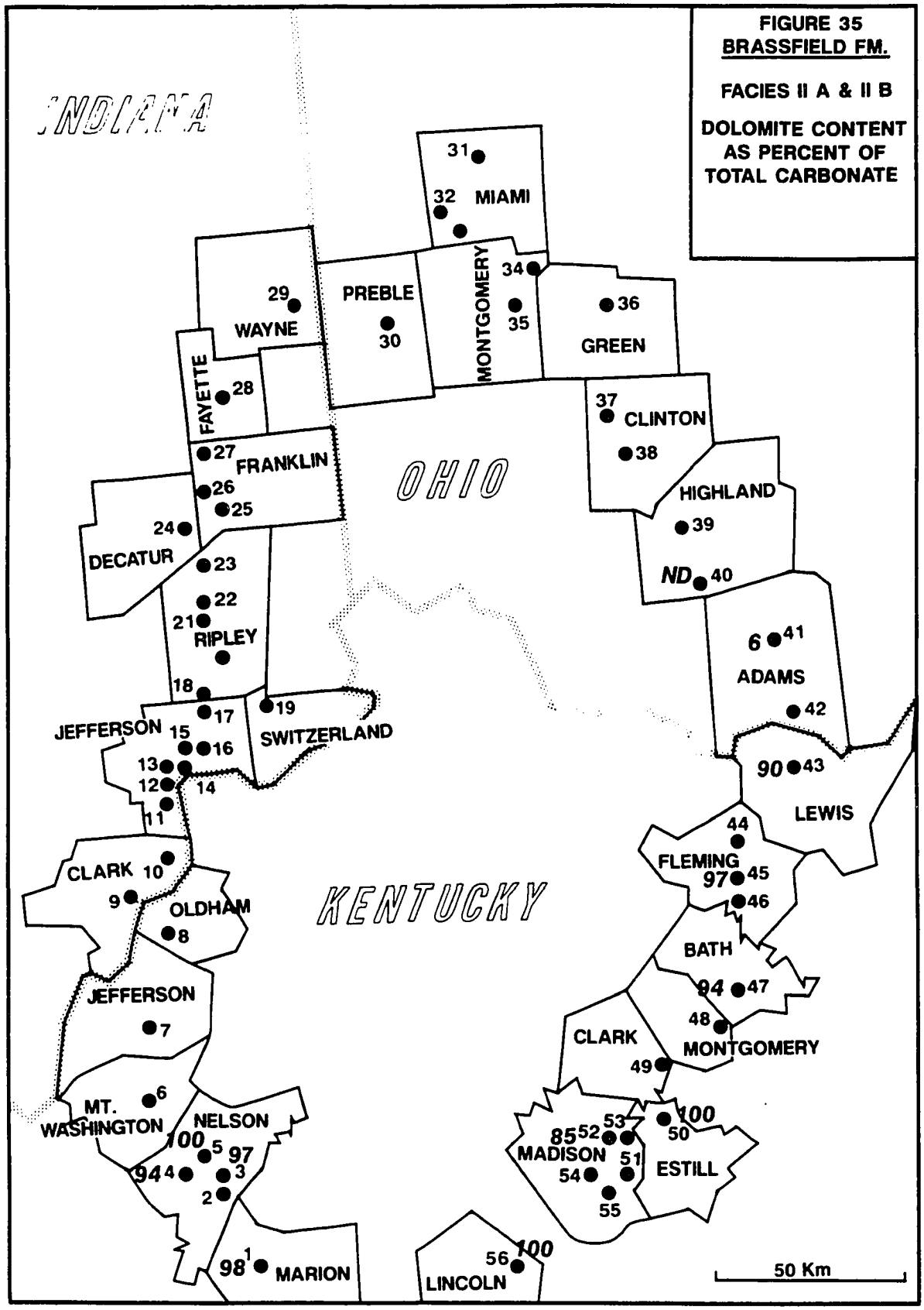

FIGURE 36

DOLOMITIZATION OF FINE AND COARSE MATERIAL

FIGURE 37

WELL ZONED DOLOMITE OF FACIES III

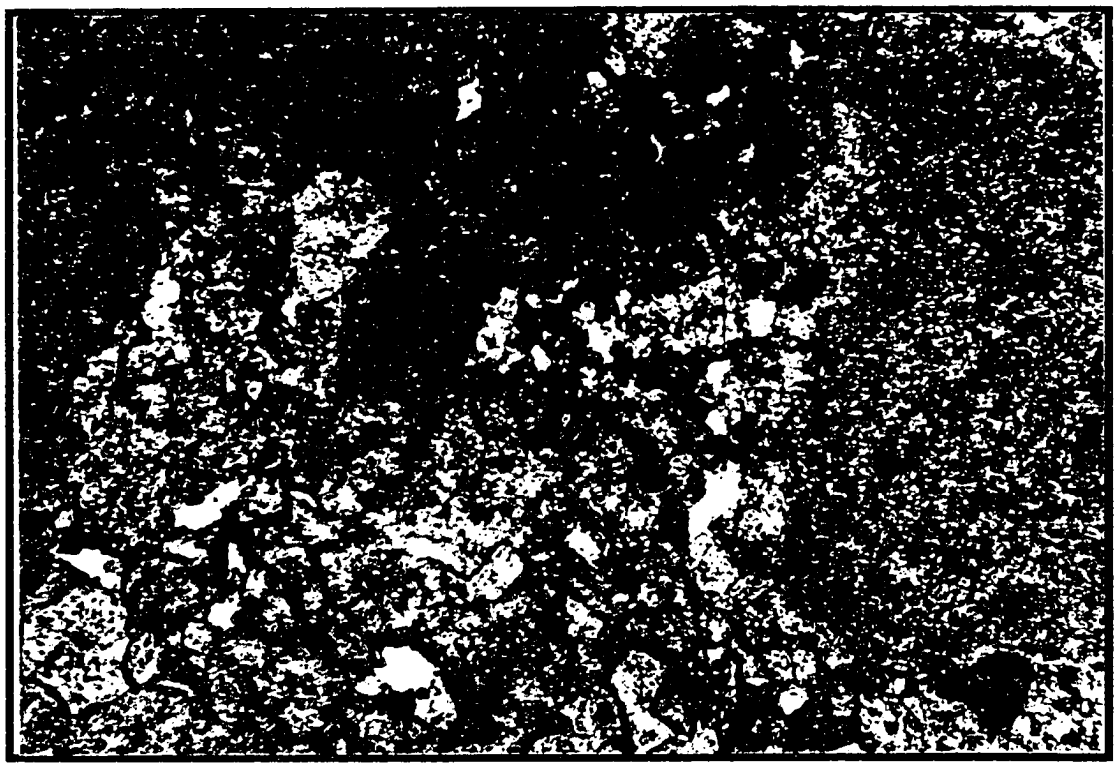

Location 56 Facies III P/S 500 microns

Location 43 Facies III P/S 500 microns

Nonzoned rhombs are ferroan. Syntaxial calcite overgrowths mimic rhomb growth in many samples where coarse ferroan dolomite has replaced large bioclasts (Figure 38). Most dolomite in facies II and III is ferroan to slightly ferroan. Porosity is mostly interrhombic, ranging from 0% to 22% and averages 4%. Dolomoldic porosity is common only in facies II where chert and carbonate are in contact (Figure 39). The dissolution of dolomite rhombs was enhanced possibly because pore fluids collected along the impermeable chert-carbonate contact.

Dolomite Interpretation - Facies IIA, IIB, and III

Dolomite textures in facies II and III are indicative of one or more nucleation events on polymodal substrates. Crystal growth conditions included low temperature and low to moderate saturations with respect to dolomite. Dolomite has replaced most calcite in facies II and III in Kentucky, and the polymodal nature of the rhombs is clearly related to variations in original texture. North of the Ohio River facies II and III are dolomite poor, indicating the dolomitization process that affected facies II and III in Kentucky was unrelated to depositional conditions or lithofacies.

Dolomitization was much more intense to the south than to the north. The unusual, sharply zoned dolomite textures (as at locality 43) are found only in the transition area between dolomite and limestone. Most ferroan dolomite in the Brassfield occurs as outermost zones on nonferroan or slightly ferroan rhombs, suggesting an association with the waning stages of dolomitization (perhaps a relative increase in iron content of the dolomitizing fluids

FIGURE 38

COARSE FERROAN DOLOMITE REPLACEMENT OF BIOCLASTS AND SYNTAXIAL CALCITE OVERGROWTHS ON DOLOMITE RHOMBS

FIGURE 39

DOLOMOLDIC POROSITY AT THE CONTACT BETWEEN CARBONATE (IN THIS CASE, A WACKESTONE) AND CHERT

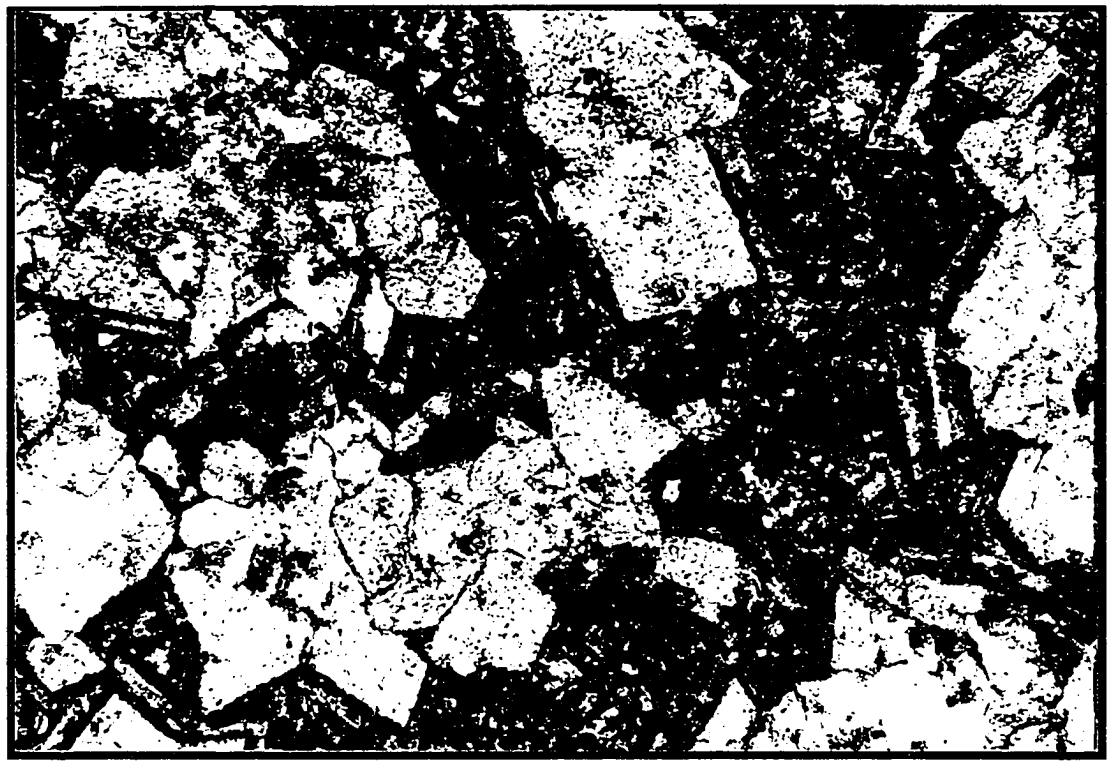

Location 43 Facies III P/S 500 microns

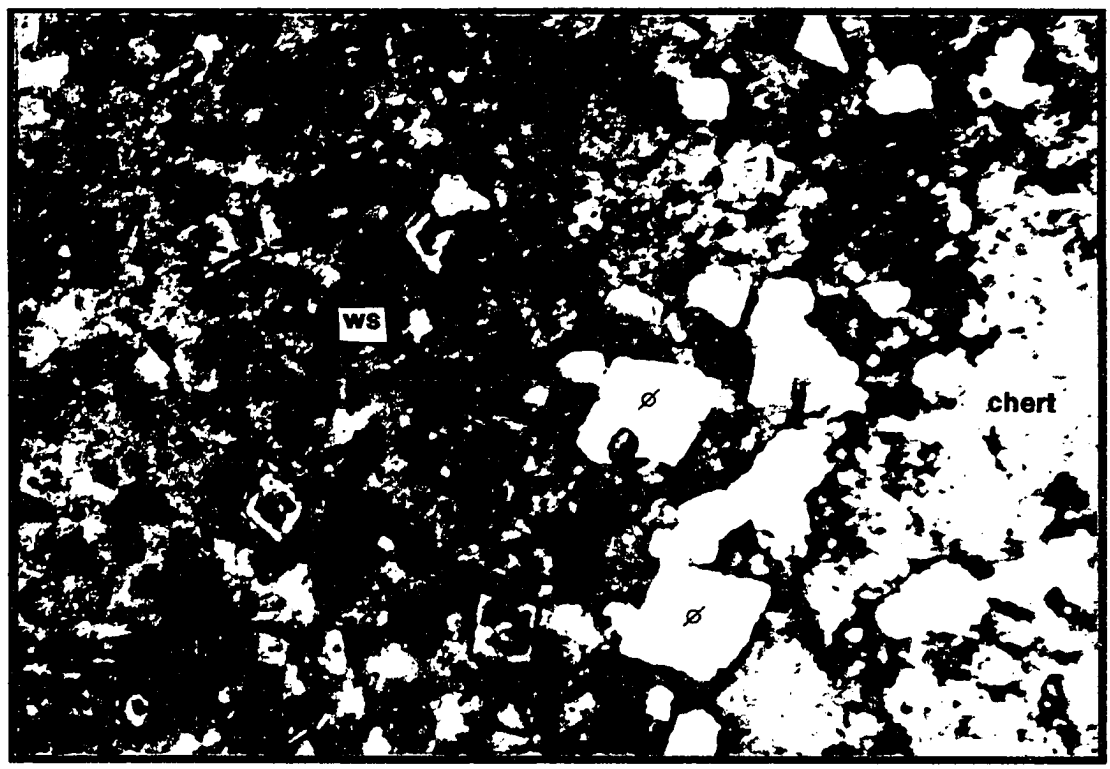

Location 41 Facies IIB P/S 500 microns

accompanies a drop in dolomite saturation). Because locality 43 is located between the transition from dolomite to limestone, conditions could have vacillated between strongly dolomitizing (nonferroan) and waning stage dolomitization (ferroan) resulting in rhombs with alternating ferroan - nonferroan zones.

Some samples from locality 43 have dolomite rhombs with late stage calcite overgrowths or dolomite zones that have been partially to completely replaced by calcite (Figure 38). Theirault and Hutcheon (1987) and Zenger (1973) attributed this feature to late stage calcite replacement of dissolved dolomite zones, which occurs when the dolomitizing fluids, originally over saturated with respect to dolomite, approach saturation with respect to both calcite and dolomite, theoretically after the precipitation of ferroan dolomite zones.

FACIES III

Lithofacies Description

Facies III is a coarsening-upward unit composed of interbedded carbonates and shales. It is between 3 and 10 m. thick and is exposed from southern Highland County, Ohio south to Lincoln County, Kentucky. It consists of wackestone, packstone, and grainstone beds that range in thickness from a few cm. to 0.5 m. (most beds range between 10 and 30 cm.) interbedded with varying amounts of gray shale. Shale content of the facies is greatest in Adams County, Ohio and northern Lewis County, Kentucky where the facies is thickest. Figures 40, and 41 illustrate distribution, thickness, and lithologic

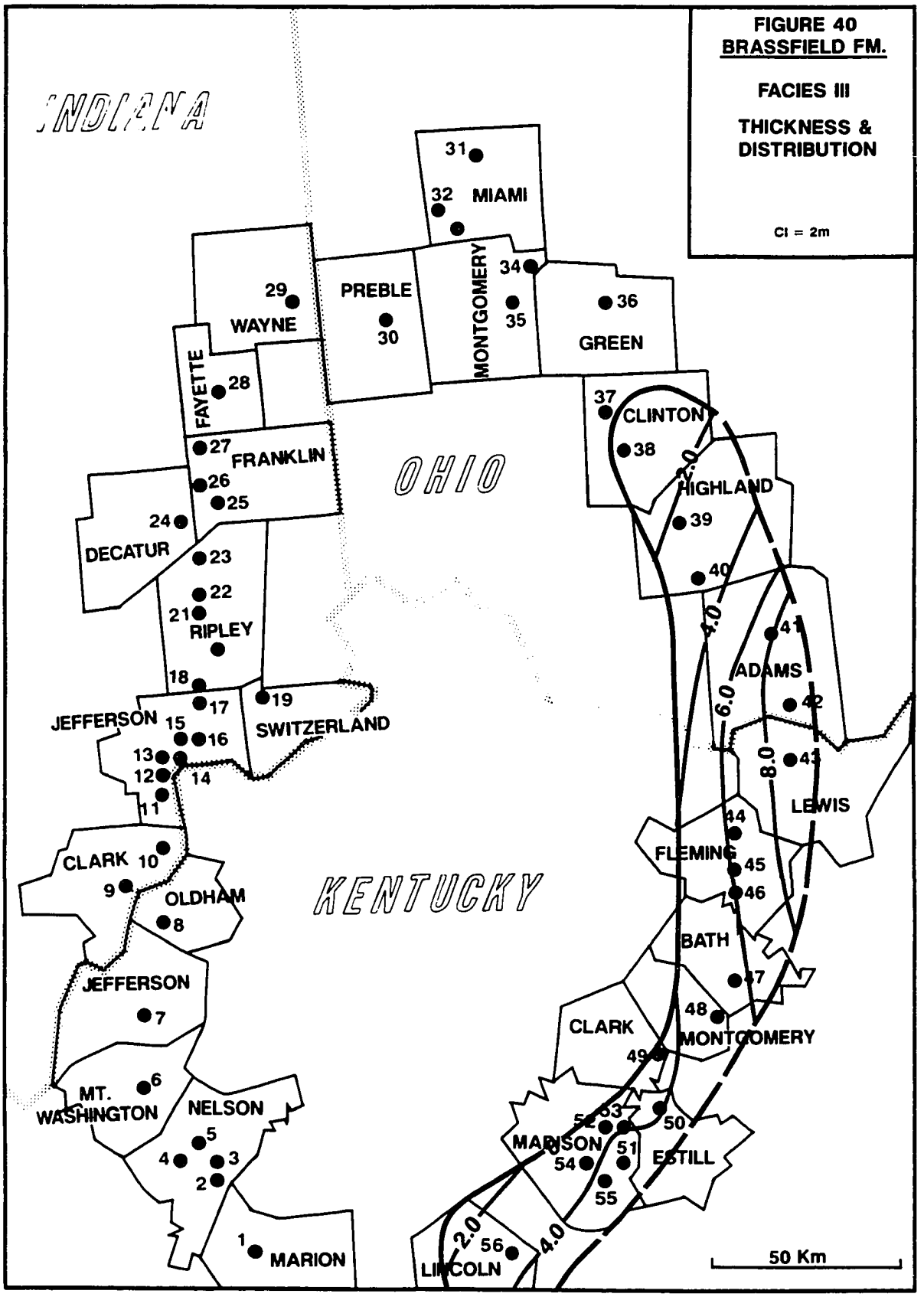

FACIES III COMPOSITE SECTION

FIGURE 41

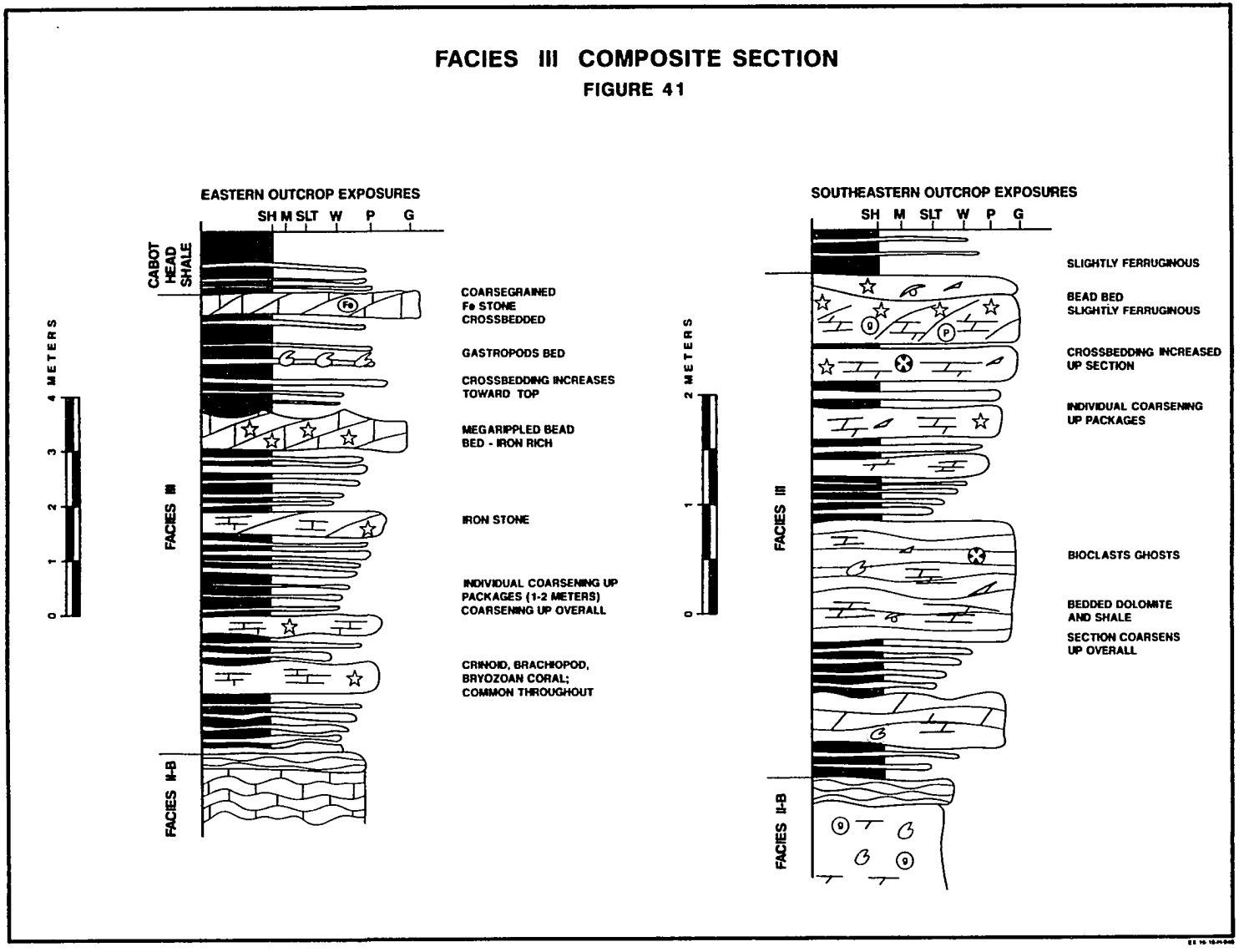

character of facies III in the study area. Figures 42 and 43 show some variation in outcrop exposures of facies III.

Bedding thickness and grain size increase up-section, and smaller coarsening-up packages can be identified at many outcrops. Petrographic analysis indicates an increase in modal grain size from 200 microns near the bottom of facies III to over 750 microns at the top. The number of large intraclasts also increases markedly near the top. Average petrographic composition of facies III is 41.7% bioclasts, 31.2% cement, 9.8% hematitic ooids, 7.5% dolomite, 4.2% intraclasts, 4.0% mud, and 1.7% glauconite pellets. Average bioclast content is 72.4% crinoid, 11.4% bryozoan, 4.3% coral, 4.3% brachiopod, 4.1% unidentified, 1.9% trilobite, 1.1% ostracod, and 0.6% gastropod.

Horizontal and low angle cross bedded (HCS) fine grained grainstones and non-laminated wackestones are characteristic of beds near the base of the unit. Some scour and channel features are present. The upper beds in facies III are mega-rippled and cross-bedding is high angle (Figures 44, 45, 46, and 47). Bioturbation throughout is low to moderate with horizontal traces more common than vertical. Local occurrences of hardground surfaces are characteristic of the facies.

Thin (1 centimeter to 0.25 meter) ironstone beds with hematitic bioclasts and cement occur near the top of facies III from Estill County, Kentucky north to Clinton County, Ohio (Figures 48 and 49). They are discontinuously present

FIGURE 42

FACIES I, IIA AND IIB, AND III

FIGURE 43

FACIES IIB AND III LOCALITY 51
NOTE THE DIVISION OF DEPOSITIONAL PACKAGES (6TH ORDER SEQUENCES) IN FACIES III

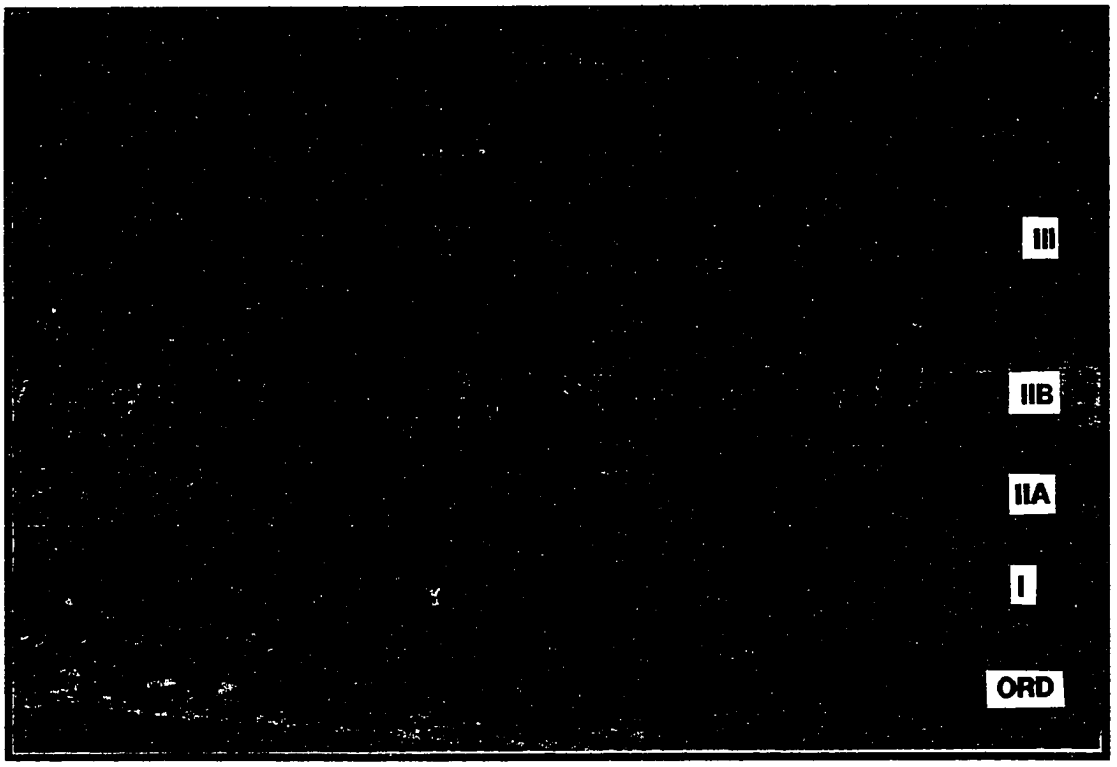

Location 41 Facies I, IIA, IIB and III

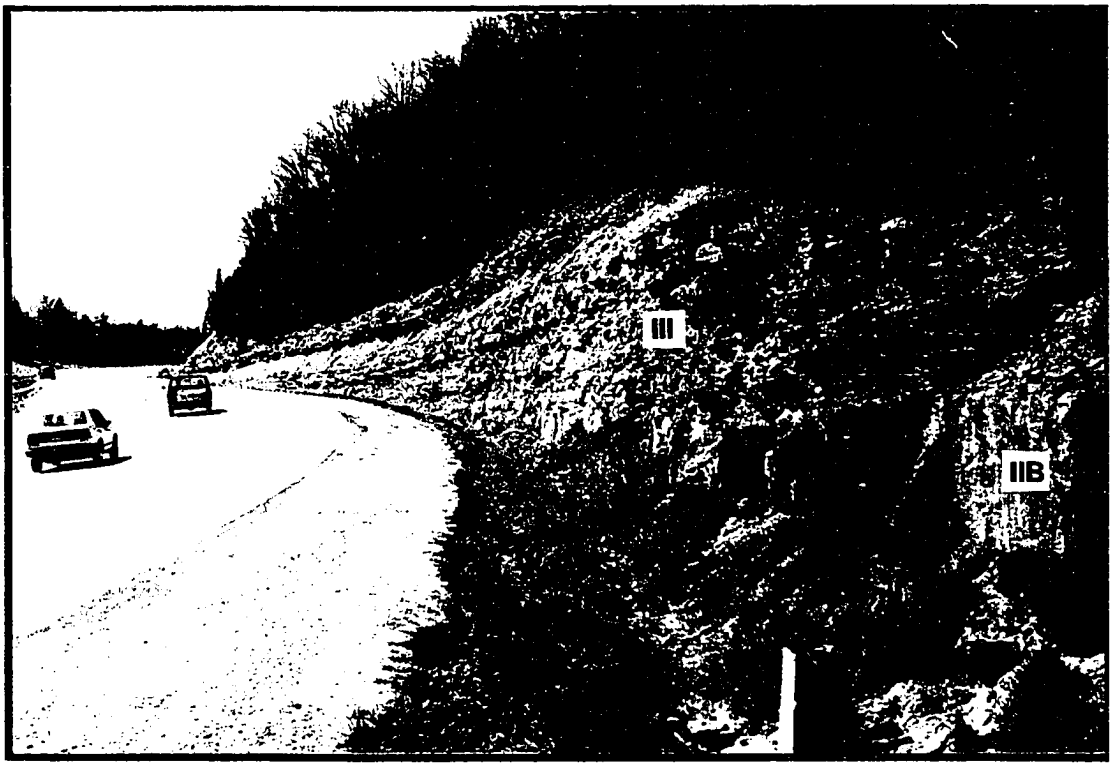

Location 51 Facies IIB and III

FIGURE 44

MEGA-RIPPLED CRINOID SANDS NEAR THE TOP OF FACIES III

FIGURE 45
A COARSE PACKSTONE WITH SHALE INTRACLASTS NEAR THE BASE OF FACIES III

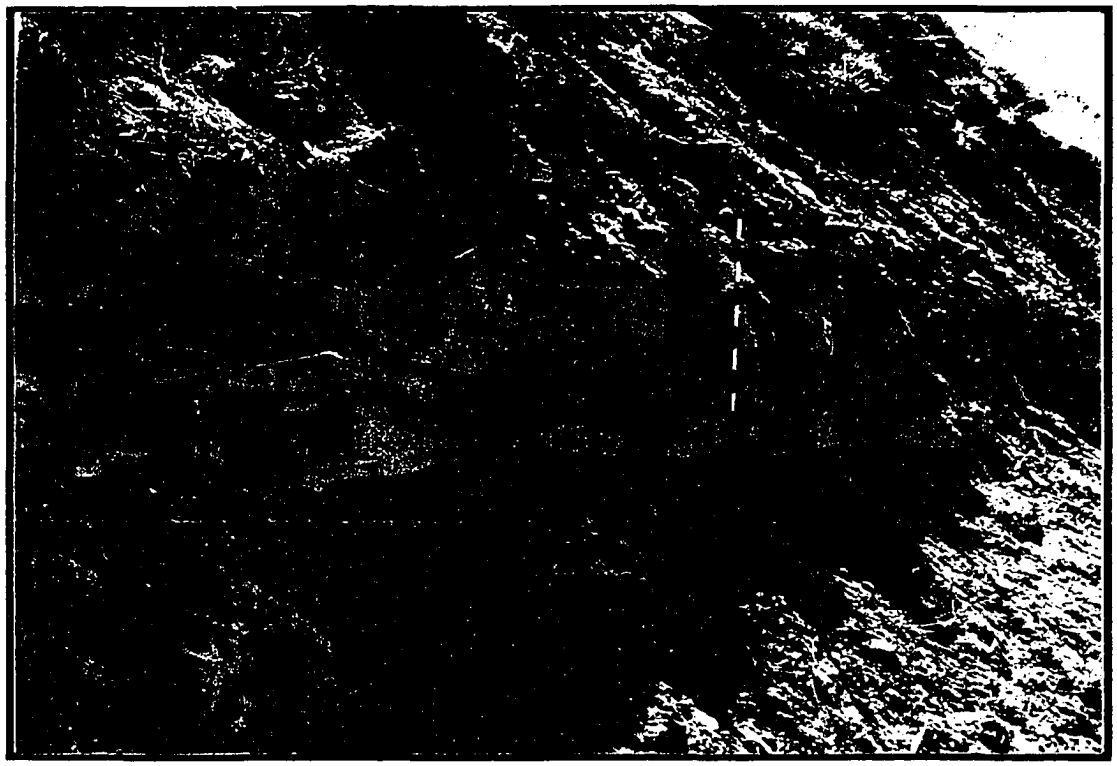

Location 44 Facies III

Location 41 Facies III

FIGURE 46

HORIZONTALLY LAMINATED FINE GRAINSTONE OF FACIES III

FIGURE 47

COARSE, POORLY SORTED GRAINSTONE NEAR THE TOP OF FACIES III

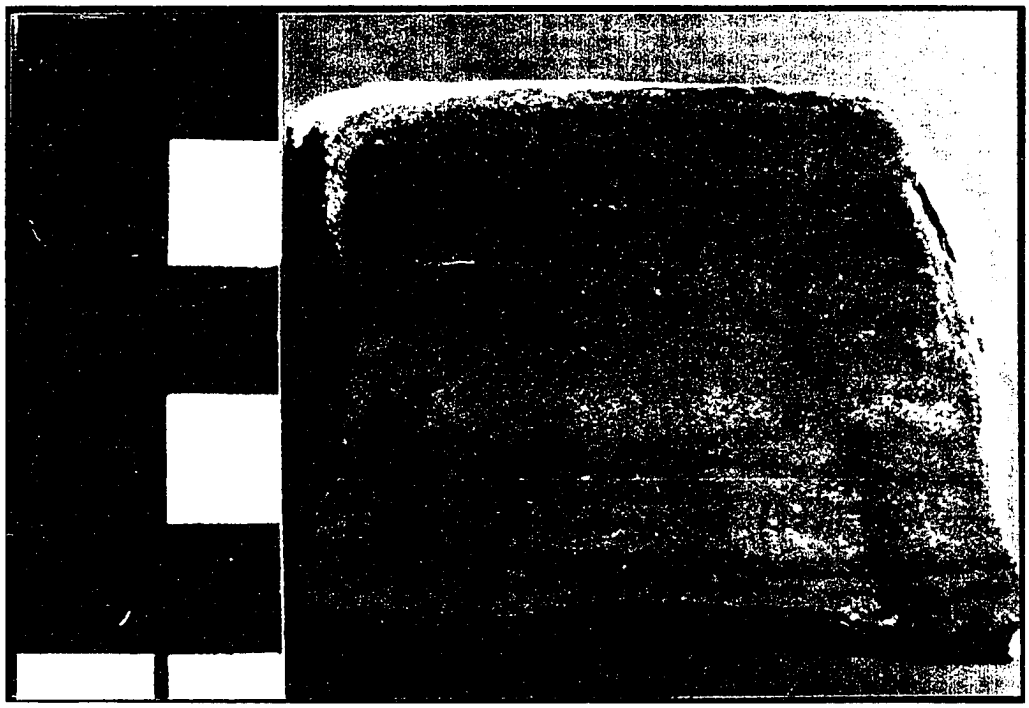

Location 41 Facies III

Location 41 Facies III

FIGURE 48

IRONSTONE NEAR THE TOP OF FACIES III

FIGURE 49

HEMATITIC BIOCLASTS AND WEATHERED GLAUCONITIC BIOCLASTS FROM AN IRONSTONE IN FACIES III

Location 41 Facies III P/S 100 microns

Location 41 Facies III P/S 500 microns

north of Clinton County to Montgomery County, Ohio. Hematitic intervals are typically represented by more than one ironstone horizon.

Lithofacies Interpretation

An overall upward increase in bedding thickness, decrease in shale content, increase in high energy sedimentary structures, and occurrence of hematitic ironstones at the top of the unit indicate progressive shallowing-upward conditions. The fauna, composed mostly of crinoids, bryozoans, corals, brachiopods, trilobites, and ostacods, indicate normal marine conditions. There is a sudden increase in grastropod content toward the top of the facies, indicative of slightly more restricted conditions brought on by shallowing. As with facies II, the carbonate beds in facies III represent distal to proximal tempestites. In Ohio, facies III is composed of beds that appear to represent isolated events. The upper most beds, including thick, coarse grained, and mega rippled crinoid grainstones (the "Bead Bed"), and coarse grained ironstones, represent proximal storm depositional conditions, but do not appear as amalgamated as facies III exposures to the southeast. Beds of facies III in the southeast are thicker, less shaley, and more indicative of deposition under proximal storm conditions.

Facies III can locally be divided into several minor coarsening-upward packages. The shalier, most distal shallowing upward tempestite cycles of facies III are composed of, in ascending order, thin parallel laminated and fine grained packstones or fine grainstones, well bioturbated packstones and wackestones with erosional bases and shale intraclasts, and cross-bedded

grainstones. The upper cycles are capped by very coarse megaripled grainstones, oolitic ironstones, or less commonly glauconite rich dolomitic grainstones. Four such cycles can be identified at location 41, while three are found at 52 and 51. Individual cycles are obscured by amalgamation in exposures that represent more proximal conditions and contain less shale (e.g., locality 56).

Dolomite Description and Interpretation

The dolomite content of facies III is illustrated in Figure 50. A discussion of its character and interpretation has been presented in the Facies II discussion.

FACIES IV

Lithofacies Description

Facies IV is a relatively thick, cross-bedded, packstone to grainstone unit. It is present from Northern Highland County, Ohio north and west to Wayne County, Indiana, and in Bullit and Nelson Counties, Kentucky, in the southwest quadrant of the outcrop belt. It ranges from 1 to 8 m. thick, or more. Local quarry operators refer to this facies as "Lower White Brassfield," named for its chalky white appearance, which is unusual for the Brassfield. It is commonly found above the Belfast (facies I) and below the biohermal facies (facies VI). Figures 51 and 52 illustrate the distribution, thickness and lithologic character of facies IV. Figure 53 shows facies IV in outcrop.

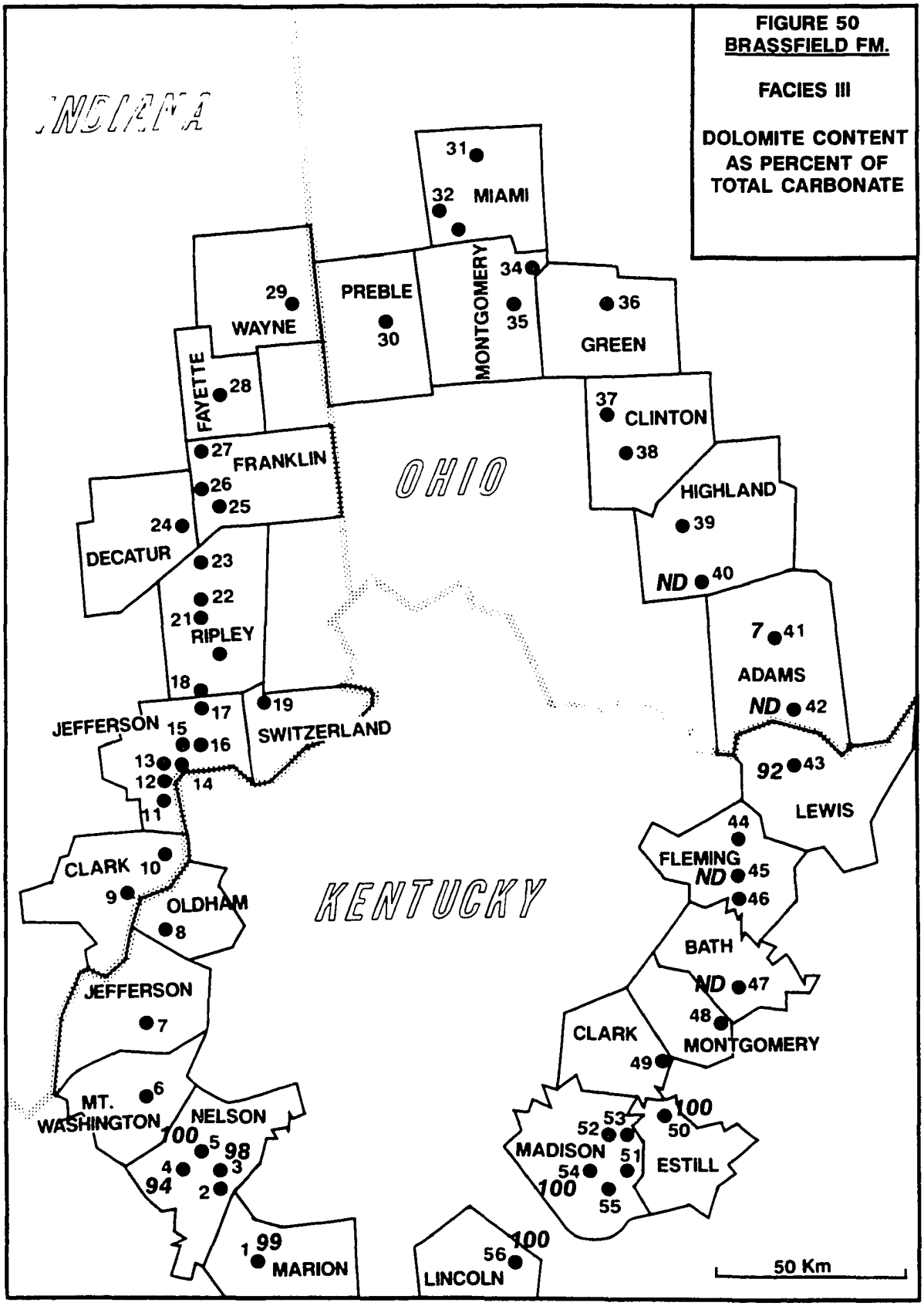

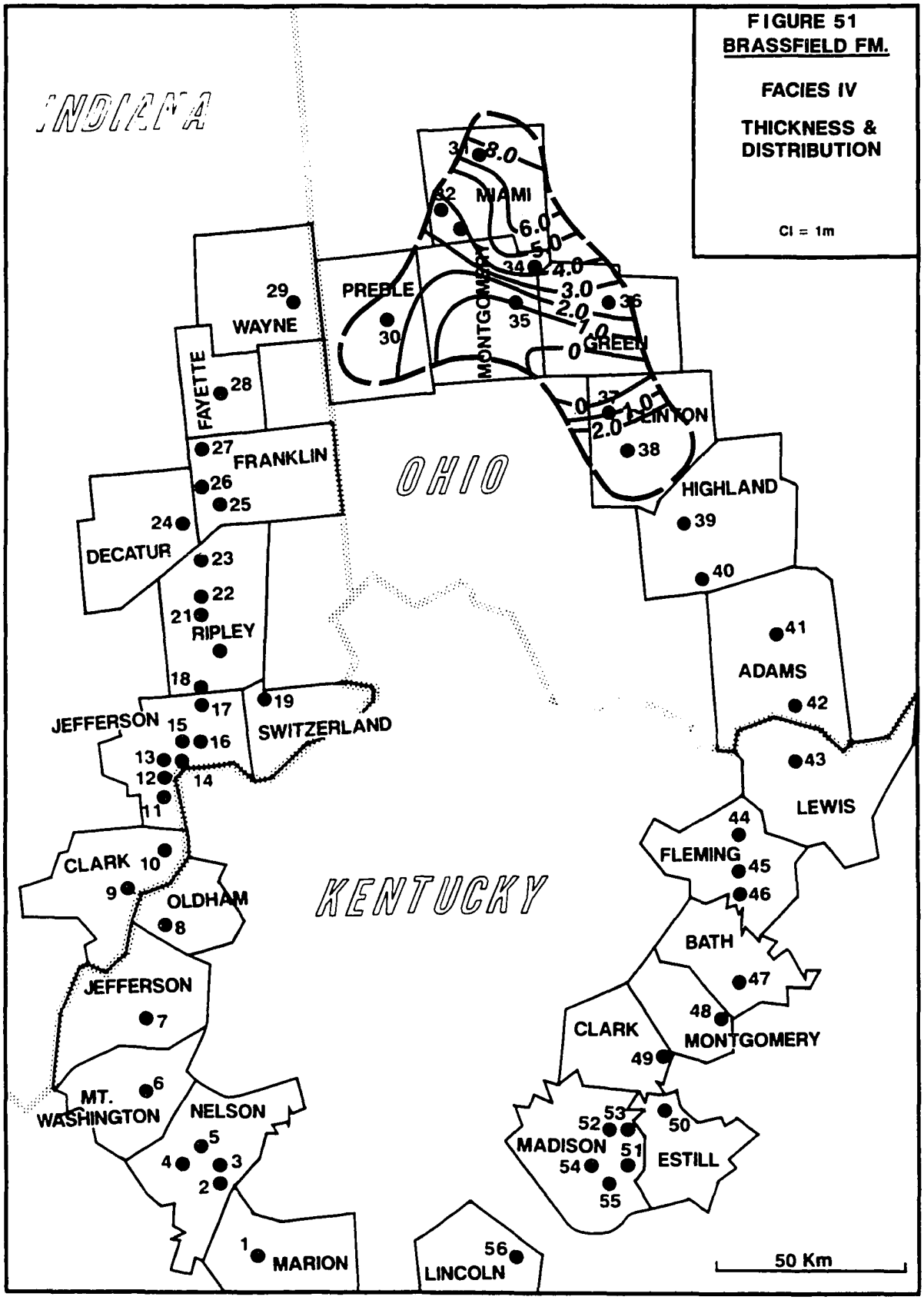

FACIES IV COMPOSITE SECTION

FIGURE 52

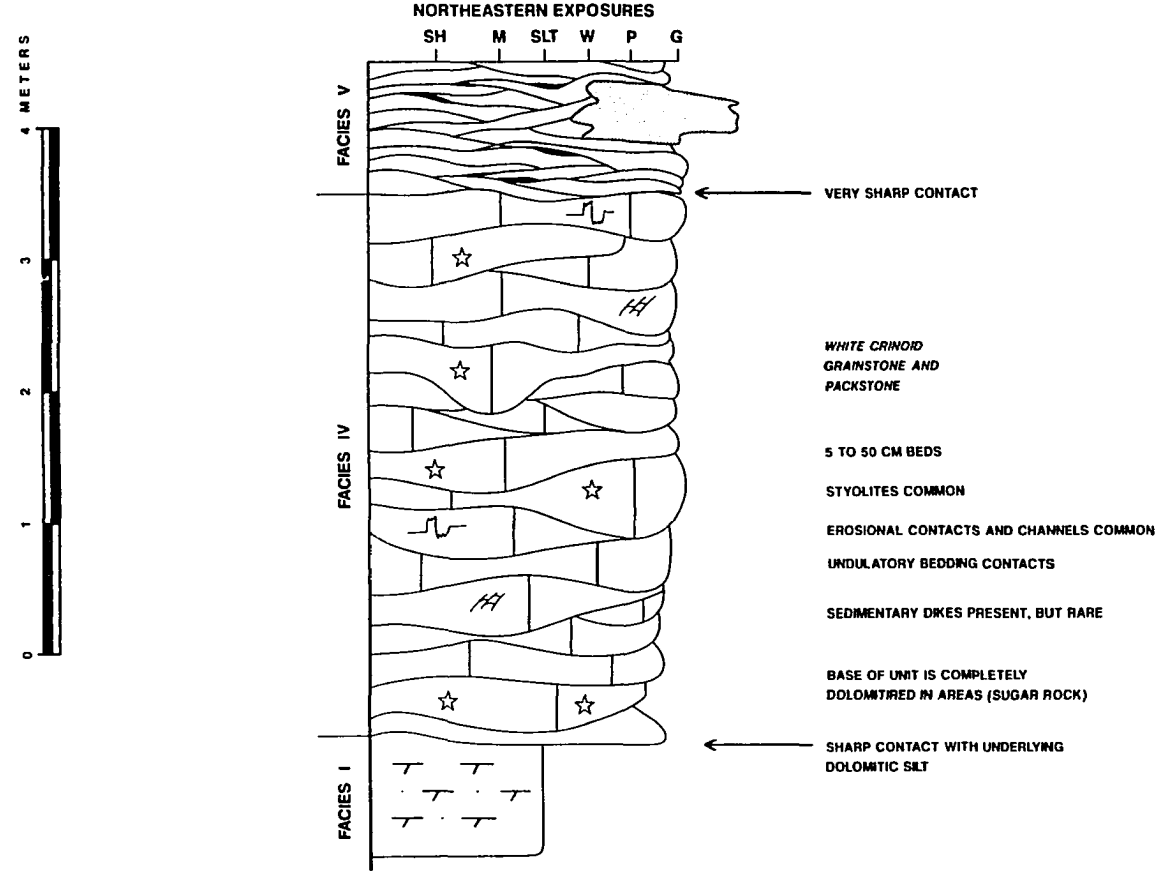

FIGURE 53

FACIES IV, V, AND OVERLYING DAYTON FORMATION

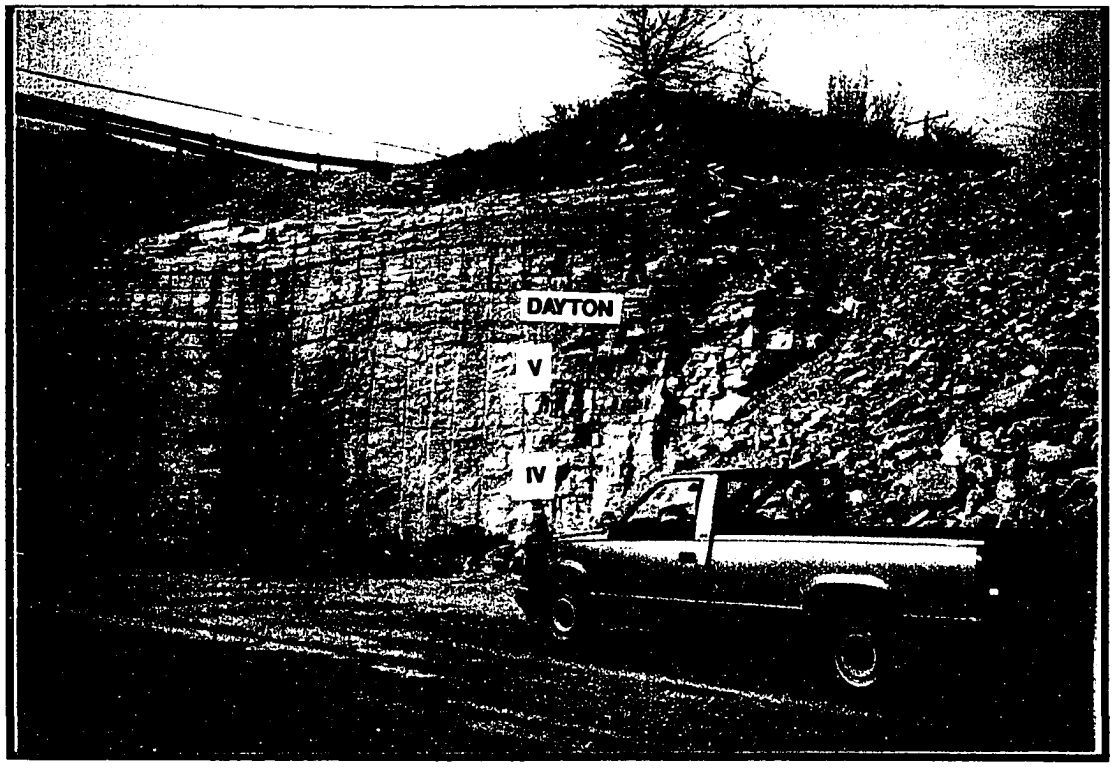

Location 31 **Facies IV**

At locality 39, facies IV is separated from the Belfast by a thin shale and overlain by the Plum Creek Shale (localities 37, 38, 39). Where facies IV is overlain by the biohermal unit, the contact between them is sharp and erosional.

Bedding thickness ranges from 5 to 50 centimeters. Contacts are sharp, and rarely horizontal; erosional contacts and channel like features are common. Most of the unit is cross bedded. Styolites, with up to 30 centimeters of displacement are present throughout the unit.

Packstones and grainstones are the predominant rock types. As elsewhere in the Brassfield, crinoids are the most common type of bioclast, but facies IV has a content of bryozoan, and to a lesser extent, solitary coral fragments that is high relative to other facies in the Brassfield (Figures 54 and 55). Brachiopods and trilobites are also common in facies IV. Average petrographic composition of the facies is 46.2% bioclasts, 26.4% dolomite, 18.8% calcite cement, 4.7% micrite, 3.7% pellets, 0.5% intraclasts, and 0.1% pyrite. Average bioclast composition is 87.3% crinoid, 11.6% bryozoan, 0.6% unidentified, 0.3% brachiopod, and 0.2% trilobite.

Dolomite rhombs that have replaced micrite constitute about 11% of this unit, though dolomitization in parts of the facies is complete (see following "Dolomite" section).

FIGURE 54

BRECCIATED PIECES OF FACIES IV NEAR THE EDGE OF A SEDIMENTARY INJECTION DIKE RICH IN GLAUCONITE PELLETS

FIGURE 55

THIN SECTION OF A GRAINSTONE FROM FACIES IV (MICORITIZED GRAINS ARE ACTUALLY BRYOZOAN FRAGMENTS WITH MUD IN THE ZOEECIA)

Location 32 Facies IV

Location 32 Facies IV P/S 500 microns

Lithofacies Interpretation

The thick cross-bedded grainstones and packstones, channel like features, and erosional contacts that typify facies IV were formed as a complex of skeletal blankets and shoals that accumulated relatively rapidly on the shallow platform, well above normal wave base. Faunal diversity is relatively low, but still indicative of normal marine conditions, where crinoids and bryozoans communities thrived.

Facies IV is not greatly condensed and exhibits little evidence of internal paraconformable surfaces. The high percentages of well preserved fenestrate bryozoans (relative to the rest of the Brassfield) suggest that these sediments accumulated more or less in situ, and were not transported far or subjected to intense repeated reworking. The bryozoans were probably protected from abrasion when buried by successive rapidly deposited sand sheets in a relatively high energy environment (Newell, 1940).

The glauconite rich injection dike at locality 32 (Figure 54) formed when the loading pressure of the rapidly deposited skeletal sand sheet became great enough to force muddly sediments up from below. The glauconite was originally deposited over facies I, which directly underlies facies IV at this locality. The glauconite formed during the hiatus in sedimentation that accompanied the transgression following the deposition of facies I.

Dolomite Description

Dolomite content of facies IV ranges from 4% to 100% and averages 32%. Most exposures of facies IV average about 11% dolomite, but part of facies IV in Montgomery and Greene Counties, Ohio are intensely dolomitized and elevate the total average (Figure 56). Less dolomitized examples typically contain isolated, unimodal, (100 to 300 microns), planar-euhedral rhombs. Dolomite in this facies selectively replaces micrite, which is present as packstone or wackestone matrix, or more commonly as pellets. Many of the pellets are actually rounded fragments of bryozoa whose zooecia are filled with micrite. Only fragments of the actual skeleton remain (Figure 57).

Intensely dolomitized samples consist of rhombs that have a polymodal size distribution (150 microns to mm sized rhombs) and planar-euhedral to subhedral crystal boundaries (Frost, 1977, labeled this lithology "sugar rock" for its coarse, sucrosic texture). Replacement in these samples is not selective. Only some large crinoid clasts and their over growths have escaped total replacement (Figure 58). At most localities, the "sugar rock" occurs as a continuous unit at the base of facies IV. At locality 34, however, replacement across the face of the quarry wall is patchy. Dolomitized zones measuring a meter across are found in otherwise unaltered limestone (Figure 59).

All rhombs are generally nonzoned and nonferroan. However, there are rare examples of late stage ferroan zoning in samples with a high percentage of dolomite. These same samples usually have traces of post dolomite calcite cement. Dolomite-related porosity is mostly interrhombic, but some is

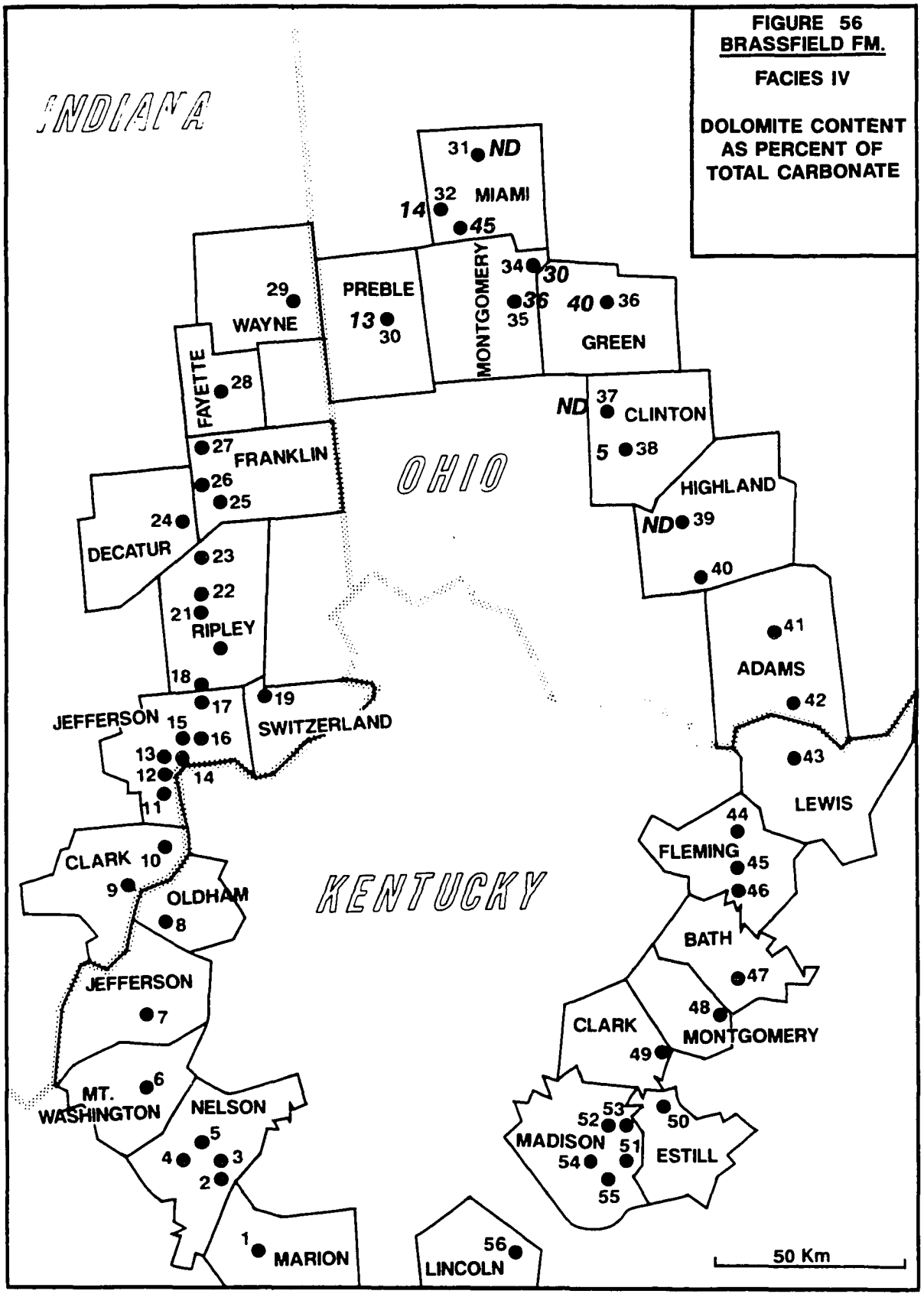

FIGURE 57

DOLOMITE REPLACING FINE GRAINED CARBONATE (IN THIS CASE, MICRITIZED BRYOZOAN FRAGMENTS)

FIGURE 58

NON-SELECTIVE OR NEARLY "WHOLE ROCK" DOLOMITIZATION

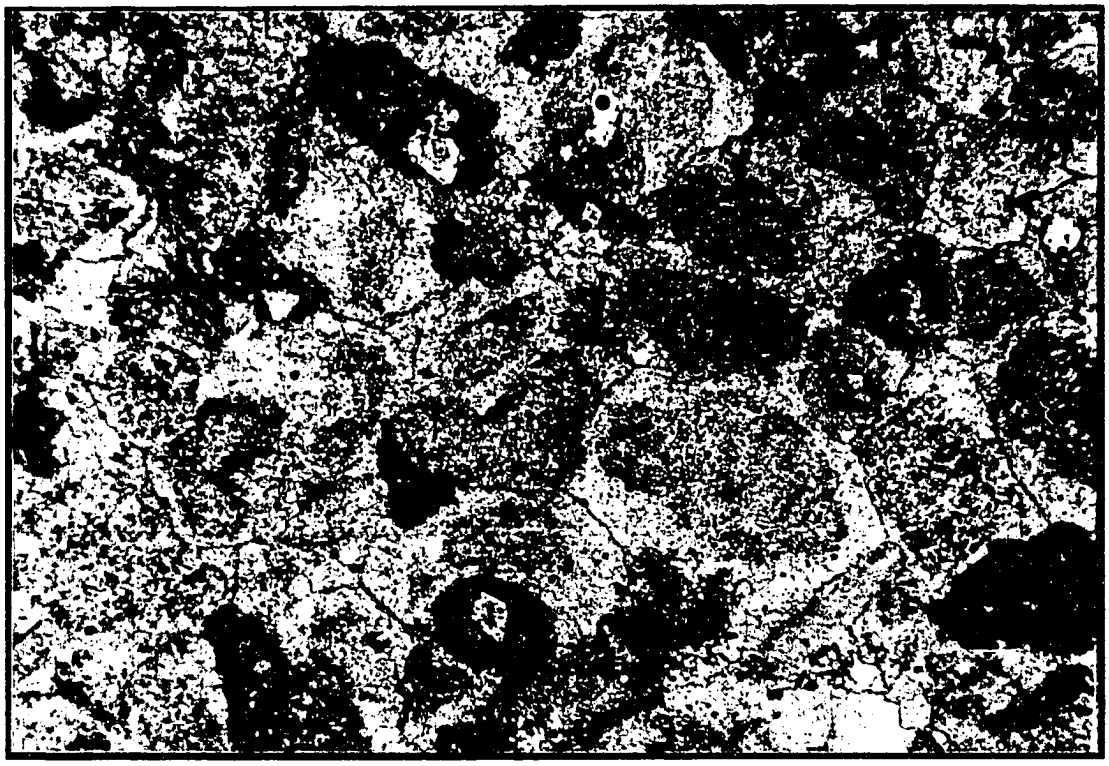

Location 34 Facies IV P/S 500 microns

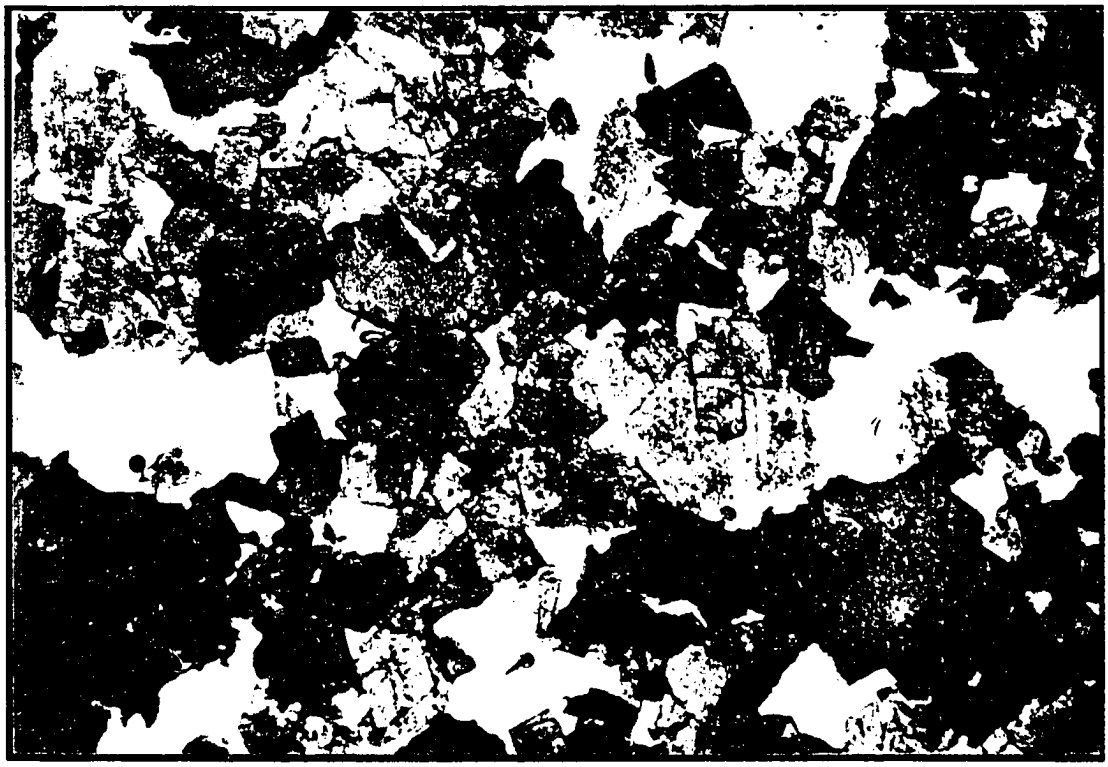

Location 34 Facies IV P/S 500 microns

FIGURE 59

ISOLATED ZONES OF DOLOMITE ARE VISIBLE ON THIS LIMESTONE QUARRY WALL AS BROWN PATCHES

FIGURE 60

FERROAN DOLOMITE RIMS ARE POST DATED BY LATE STAGE CALCITE CEMENT

Location 34 Facies IV

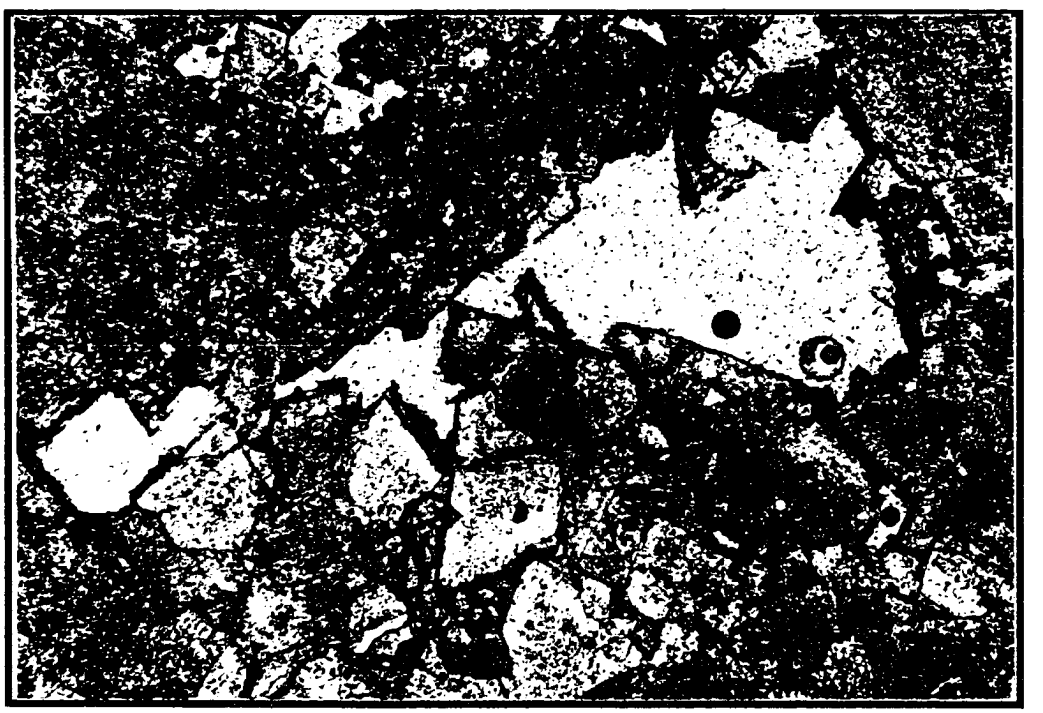

Location 31 Facies IV P/S 500 microns

dolomoldic. Porosity ranges from a trace to 29% and averages 6%. Porosity increases with intensity of dolomitization.

Dolomite Interpretation Facies IV

The range in dolomite content of Facies IV is not related to differences in depositional texture. Samples with a low relatively percentage of dolomite have a size mode and morphology indicative of a single nucleation event on a unimodal substrate, and growth under low temperature and low saturation conditions. The intensely dolomitized samples indicate a single nucleation event on a polymodal substrate and growth conditions of low temperature but somewhat higher saturation (but still below the critical saturation for nonplanar rhombs) and/or residence time of dolomitizing fluids than the partially dolomitized samples. The consistent position of the "sugar rock" lithology at the base of the facies may have resulted from internal stratification of formation waters, with more saturated dolomitizing fluids below less saturated fluids.

This dolomite is highly porous and forms an excellent aquifer (Frost, 1977). Once the dolomitization process began to pick up, pore space would have increased and fluid communication improved. Patchy dolomitization at locality 34 may represent an intermediate phase. The latest stage of dolomitization formed ferroan zones on rhombs that terminate into large pores. More recently, some rhombs have been partially dissolved, increasing the percent of dolomoldic porosity (Figures 58 and 59). Some late diagenetic stage calcite was precipitated over ferroan dolomite rims (Figure 60).

FACIES V

Lithofacies Description

Facies V is a cross-bedded grainstone unit in which small bioherms and discontinuous clay lenses are developed. It occurs in parts of Clinton, Green, Montgomery, Miami, and Preeble Counties, Ohio, usually above facies IV. The unit is referred to by quarry operators as the "Upper Brassfield." Its thickness ranges from 1 to 4 meters, and isopach mapping of facies V and VI using data from locally 31 indicates that facies V thins over the thicker parts of facies IV. Figures 61 and 62 illustrate its thickness, distribution, and lithology in the study area. Figures 63 and 64 show bedding characteristics visible in outcrop.

Bed thickness is generally less than that in facies V averaging between 5 and 10 centimeters, and individual beds are traceable for only a few meters. Cross-bedding is characteristic of most of the bedded unit. Beds adjacent to bioherms dip away from the bioherms at angles that approach 25^{o}.

Facies V can be distinguished from facies IV on the basis of bedding thickness and color (facies V is darker and thinner bedded than facies IV, compare Figure 65 with Figures 54 and 55) even though bioherms themselves are not always present.

The bioherms are small (Figure 66) -- generally 1 or 2 meters in diameter -- though larger ones have been reported (Sheely, 1981). They have boundstone cores with coarse packstone and grainstone flanking beds. The cores consist of stromatoporoids and a variety of corals, including Halysites,

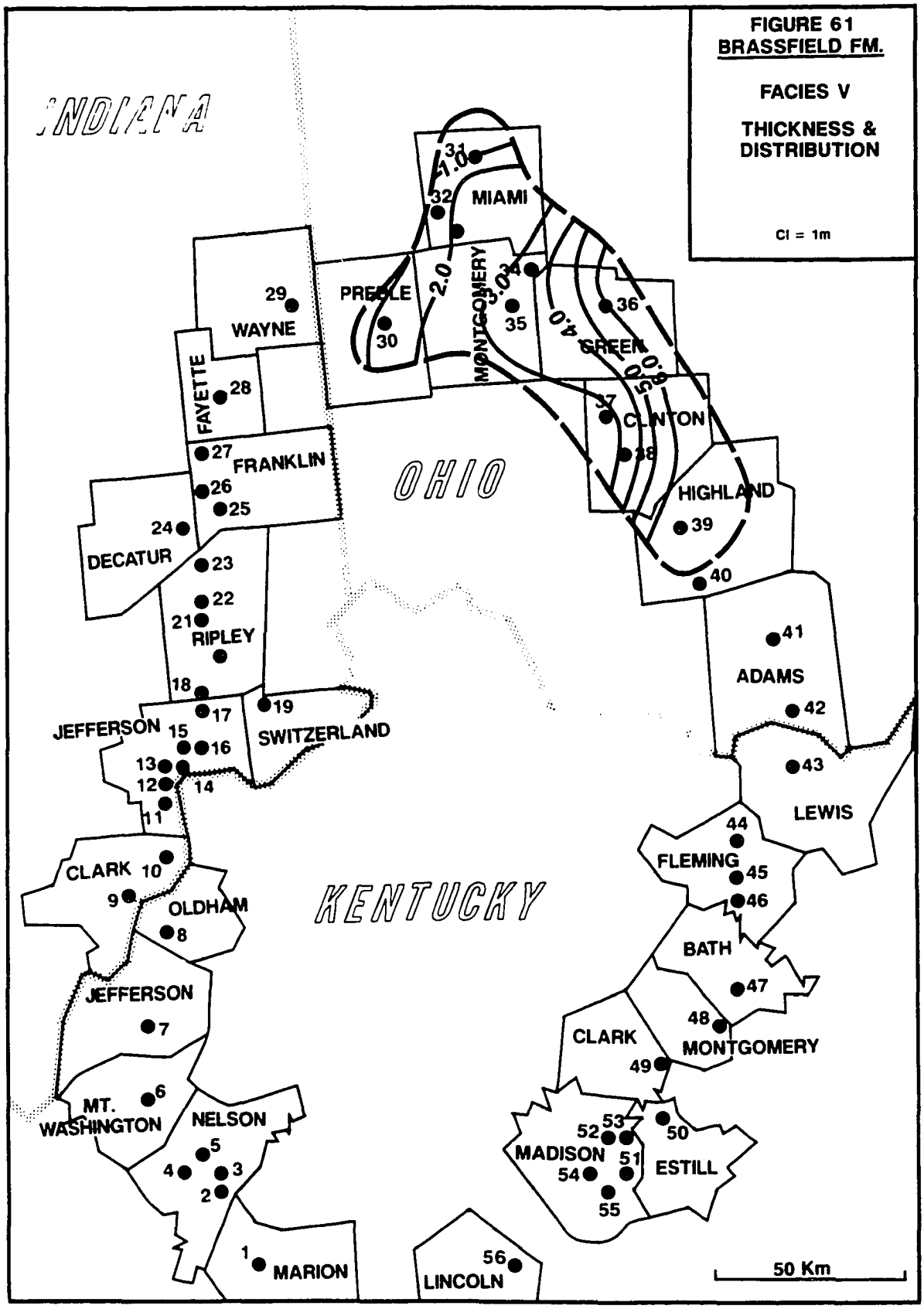

FACIES V (BIOHERM) COMPOSITE SECTION

FIGURE 62

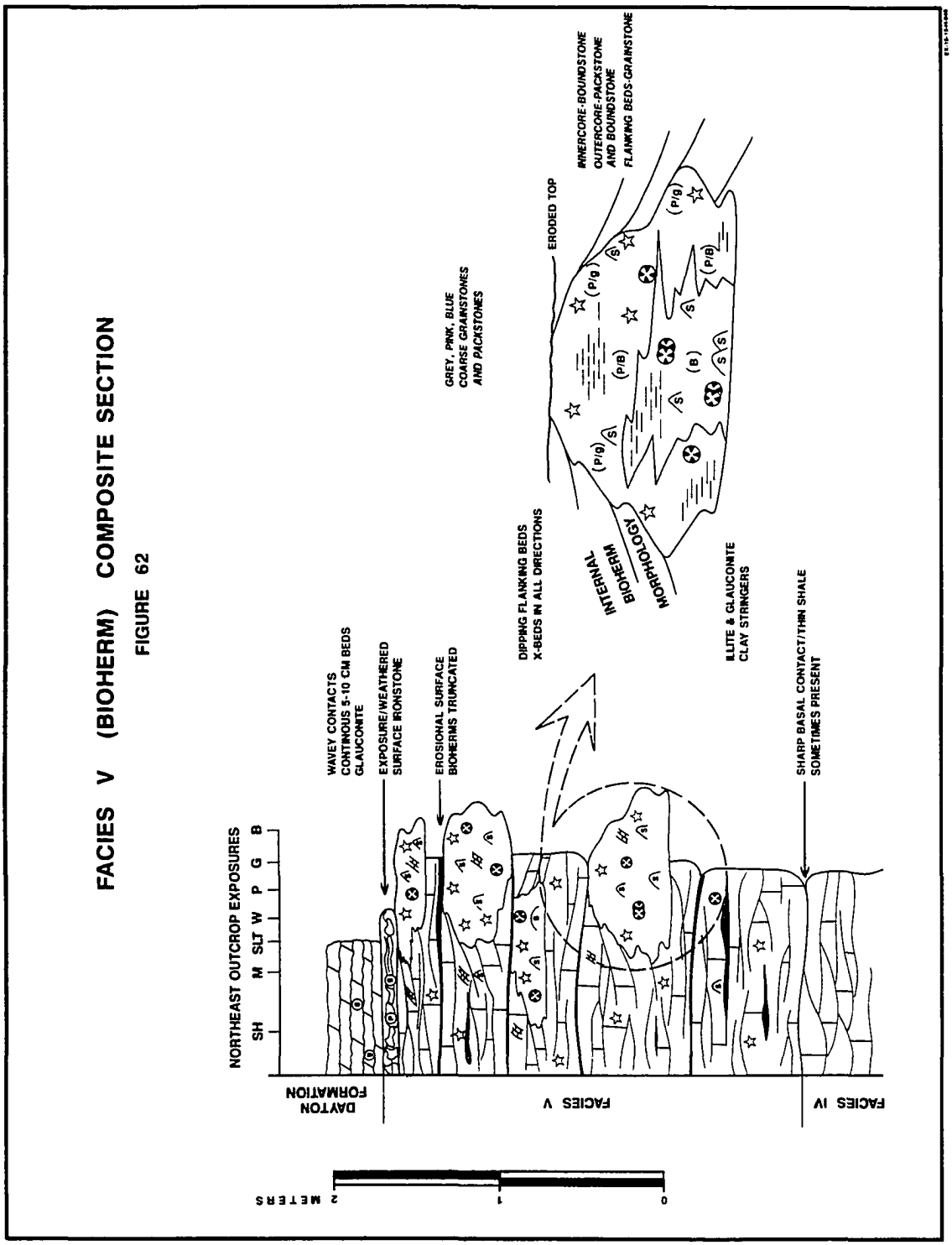

FIGURE 63

STACKED SIXTH ORDER DEPOSITIONAL PARASEQUENCES IN FACIES V (FOUR ARE VISIBLE HERE, BUT THE NUMBER OF RECOGNIZED SIXTH ORDER SEQUENCES VARIES BETWEEN OUTCROPS)

FIGURE 64

WEATHERING ENHANCED CROSSBEDDED CRINOID GRAINSTONES OF FACIES V

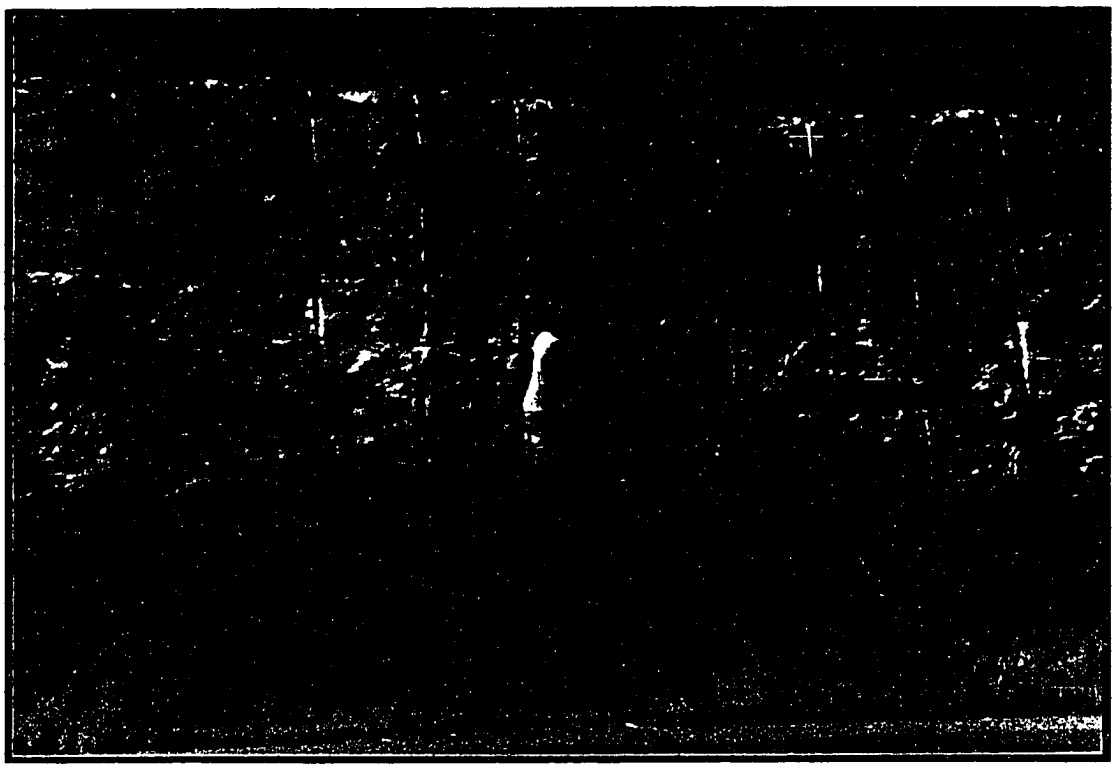

Location 33 Facies V

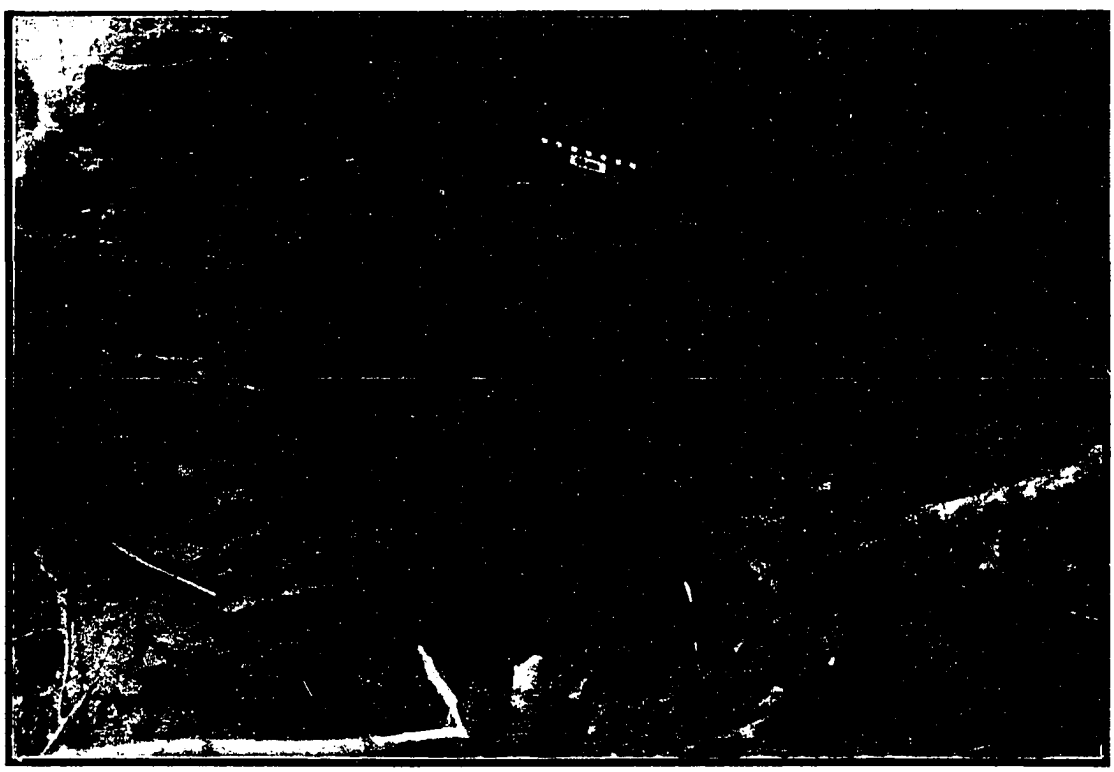

Location 38 Facies V

FIGURE 65

PINK GRAINSTONES WITH CRINOID FRAGMENTS, STROMATOPOROID CLASTS, AND TRACES OF GREEN CLAY TYPICAL OF FACIES V

FIGURE 66

SMALL BIOHERM (1.5 M ACROSS) IN FACIES V TRUNCATED BY OVERLYING DAYTON FM.
(CONTACT MARKED BY HAND)

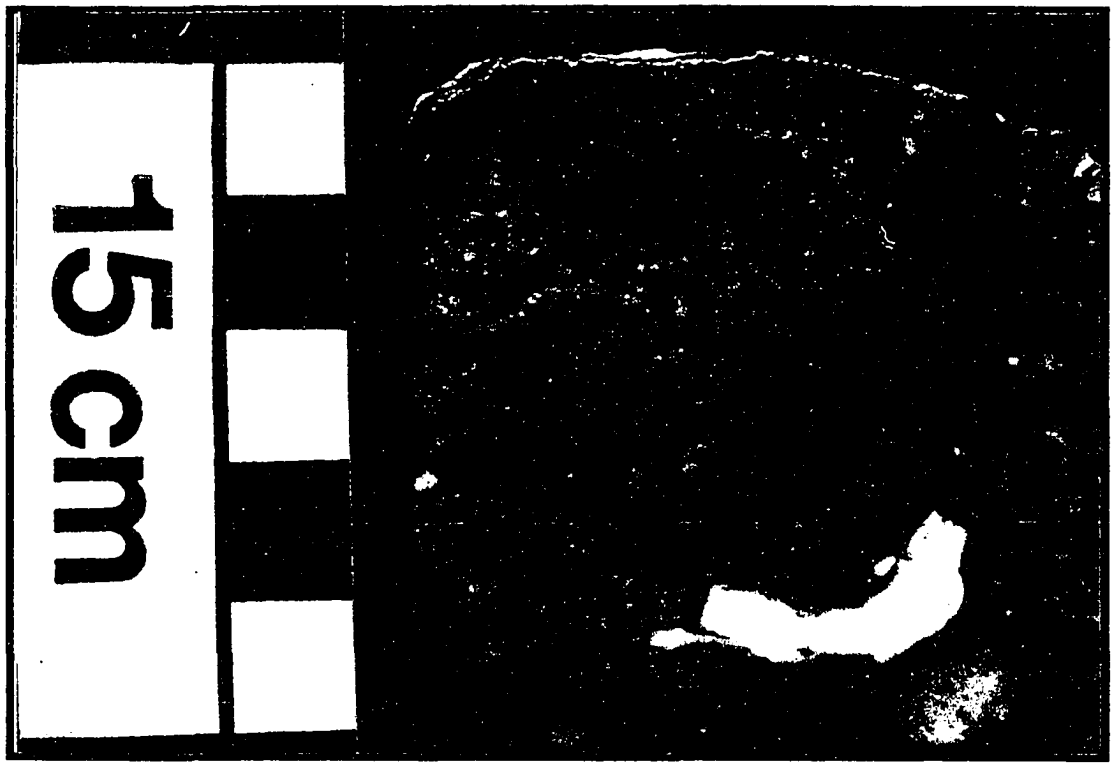

Location 32 Facies V

Location 33 Facies V

Favosites, and Rugosa. Crinoid holdfasts also occur in the bioherms. The flanking beds of the bioherms include coarse fragments of those organisms mentioned above, as well as abundant brachiopods, bryozoa, and trilobites. The average composition of facies V is 50.8% bioclasts, 24.7% calcite cement, 12.7% dolomite, 6.7% micrite, 2.9% pellets, 2.0% hematitic ooids, .2% unidentified, and traces of intraclasts, clay, chert, and pyrite. Average bioclast composition is 70.0% crinoid, 13.1% bryozoan, 10.1% coral, 2.7% brachiopod, 1.2% stromatoporoid, 0.6% unidentified, 0.7% trilobite, and traces of gastropod.

The bioherms are developed within several stacked, well defined units, 1 to 2 meters thick, that are bound by very laterally continuous surfaces. At least six such units are evident at locality 33. They are separated by erosional surfaces, and less commonly, thin shale or clay rich partings. The bioherms never cross the contact surfaces, and in some cases their tops have been eroded by the overlying contact (Figure 66).

The contact between facies V and the overlying Dayton Formation is erosional, and contains glauconite and hematite.

Lithofacies Interpretation

The stacked skeletal sand sheets and small muddy bioherms were deposited in shallow water, above wave base. The fauna is relatively diverse and indicative of normal marine conditions. The 1 m. thick sand packages are separated by erosional surfaces or thin clays that truncate bioherm tops and provided the substrate on which overlying bioherms developed. These

paraconformable surfaces formed during slowed sedimentation associated with small scale or localized rises in sea level.

Bioherm development began with colonization of the substrate by stromatoporoids, Halysites, Favosites, and rugose corals. Crinoids and bryozoans are present outside the core of the bioherms and, crinoid hold fasts are common. The small bioherms served to baffle and collect mud. Bioherm growth was arrested with a relative rise in sea level. During the hiatus, glauconite rich illite accumulated on the sea floor and was incorporated into the overlying skeletal sheet when carbonate sedimentation resumed.

In short, these units are small scale shallowing-upward sequences, separated from one another by small scale transgression induced hiatus surfaces. Shallowest conditions in the upper most beds of the facies resulted in the deposition of ironstones and very coarse grained sand waves, indicating an overall upward shoaling trend.

Six upward-shoaling sequences are recognizable at location 33, while some localities only one or two are identifiable, and the bioherms themselves are not always present. In such cases, the paraconformities may simply be unrecognizable. Variation in the number of packages, and difficulty in accurately correlating them from outcrop to outcrop suggest the factors affecting their formation -- assumed to be relative rises in sea level -- were at least in part controlled by local, rather than basin wide processes. Such processes might include differences in autochthonous sediment production, effects of pre-

existing topography, or local tectonic adjustments. Detailed isopach mapping of facies IV and V using core data collected at locality 31 shows that facies V thins over thicker accumulations of facies IV. If the thickness of facies V is limited by topographic high areas of facies IV, then the number of recognizable shoaling packages developed in facies V could have been similarly limited.

The top bed of facies V, and commonly the upper meter of the facies, contains hematitic oolites and cement. These ironstones are identical to those found at the top of facies III (see Figures 67 and 68). The top of facies V at location 32 contains a fine grained, bioturbated, glauconite and pyrite rich bed that probably formed under quieter, less oxygenated conditions in a position laterally equivalent to the ironstones found at the top of nearby sections.

Dolomite Description

Facies V contains from 0% to 94% dolomite and averages 7% (Figure 69). Dolomite in this facies has characteristics very similar to the dolomite-poor samples in facies IV. Rhombs are unimodal (average 100 microns), planar-euhedral, and are generally non-zoned and non-ferroan, though a few ferroan zones were noted. Dolomite related porosity ranges from 0% to 10% and averages under 2%. Porosity is most commonly dolomoldic.

Dolomite Interpretation

Modal rhomb size and morphology indicate a single nucleation event on a unimodal substrate and growth conditions of relatively low temperature and

FIGURE 67

IRONSTONE AT THE TOP OF FACIES V

FIGURE 68

THIN SECTION OF IRONSTONE AT THE TOP OF FACIES V

Location 38 Facies V

Location 34 Facies V P/S 500 microns

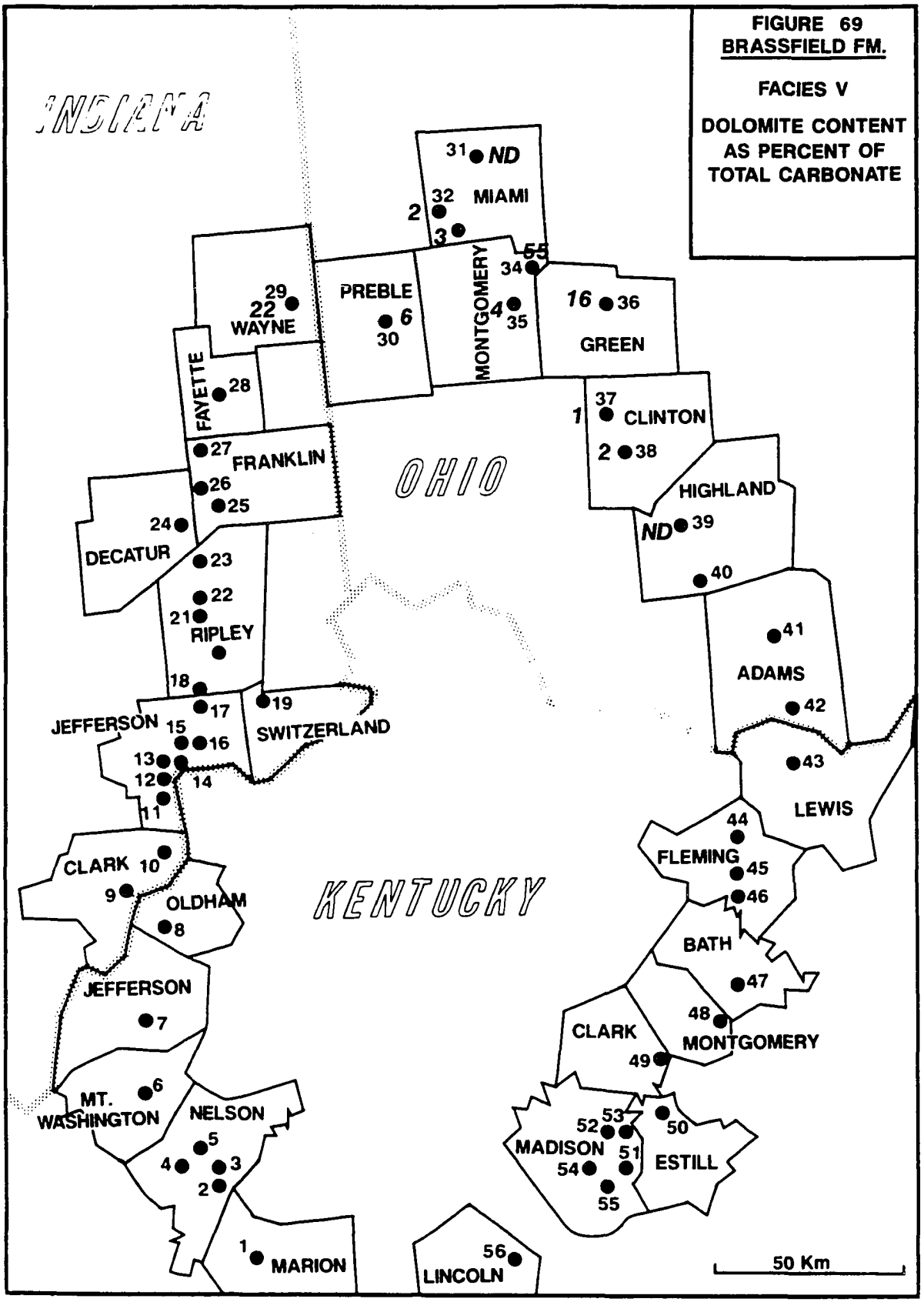

low degree of supersaturation. It is clear from Figure 70 that the dolomite has selectively replaced micrite. Dolomitization of facies V is interpreted to have occurred contemporaneously with the dolomitization of facies IV.

FACIES VI

Lithofacies Description

Facies VI is a relatively thin and widespread, cross bedded, iron-stained, crinoid grainstone. It crops out from Fayette County, Indiana south to Bullit County, Kentucky, where the Brassfield thickness and changes facies. Most Brassfield on the west side of the Cincinnati Arch consists of facies VI. The Lee Creek Member of the Brassfield (facies VII) is the only other lithology present in Indiana and northwestern Kentucky.

The thickness of the unit ranges from 2 centimeters in parts of Ripley County, Indiana (locality 20) to 2 meters in Switzerland County, Indiana (locality 19) and Oldham County, Kentucky (locality 8). The facies thickens to the east, as evidenced by the outlier at location 19. It is missing entirely from parts of Ripley and Jefferson Counties, Indiana. Figures 71 and 72 illustrate the thickness, distribution, and lithologic character of facies VI in the study area.

Facies VI is underlain by the Upper Ordovician Whitewater Formation in and north of Jefferson County, Indiana and correlative Saluda Formation to the south. The contact between the Upper Ordovician strata and facies VI is sharp and erosional (Figure 73).

FIGURE 70

DOLOMITIZATION OF GEOPETAL MICRITE IN A GASTROPOD FROM FACIES V

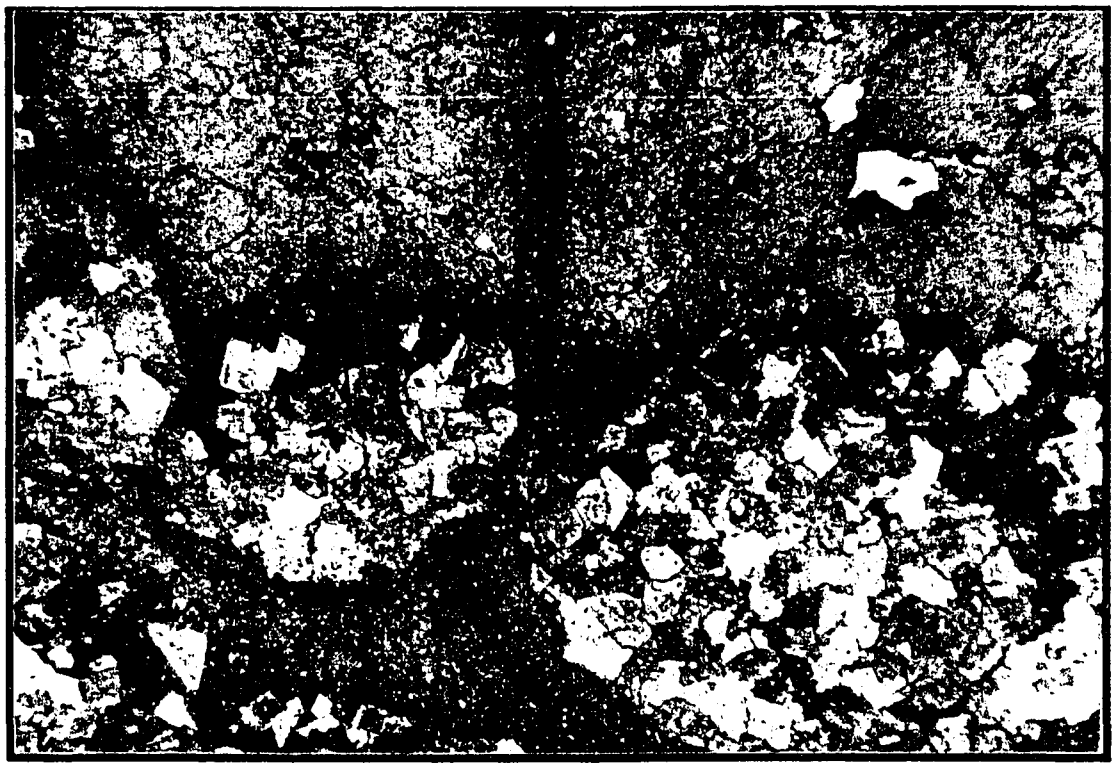

Location 36 Facies V P/S 500 microns

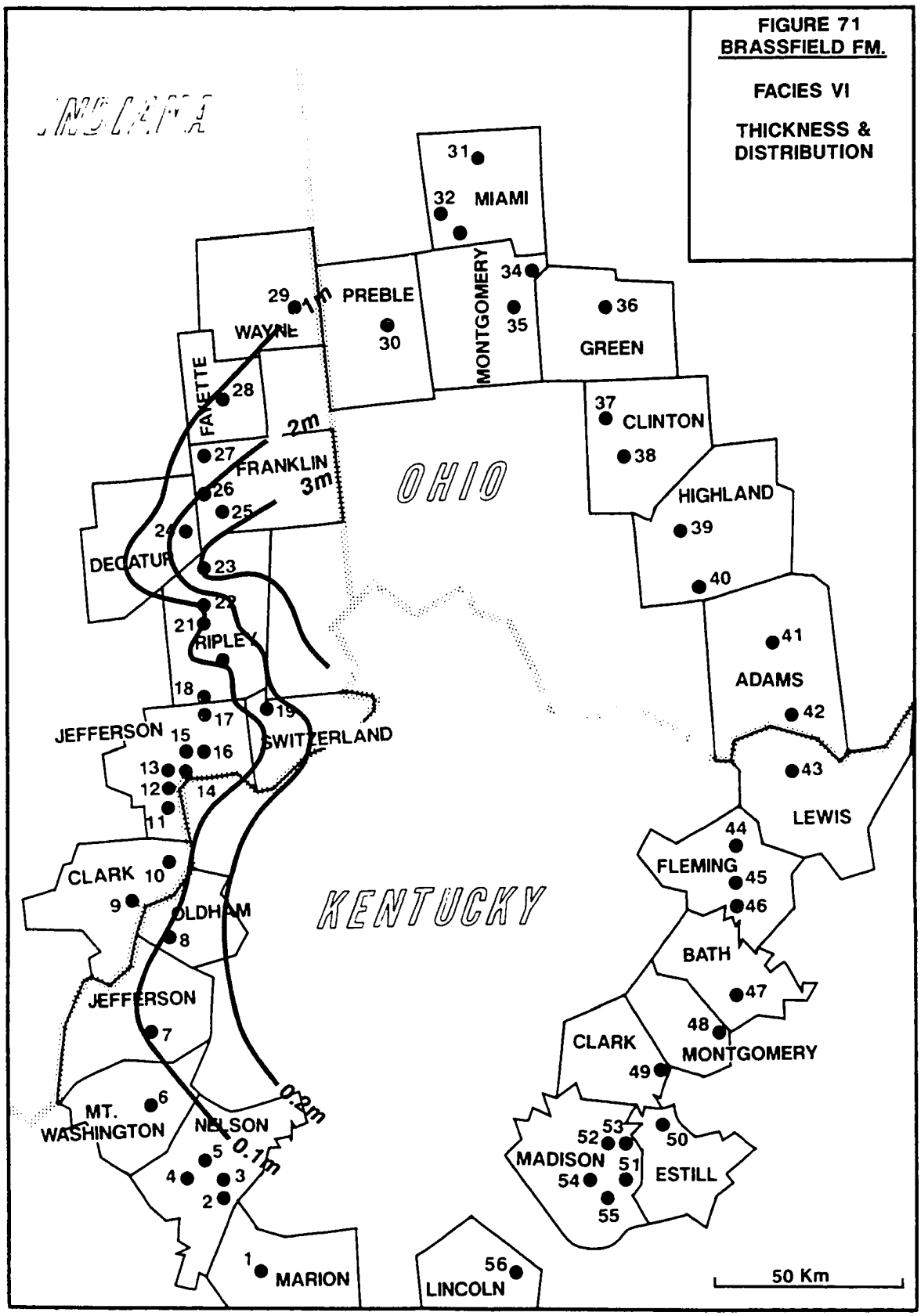

FACIES VI COMPOSITE SECTIONS

FIGURE 72

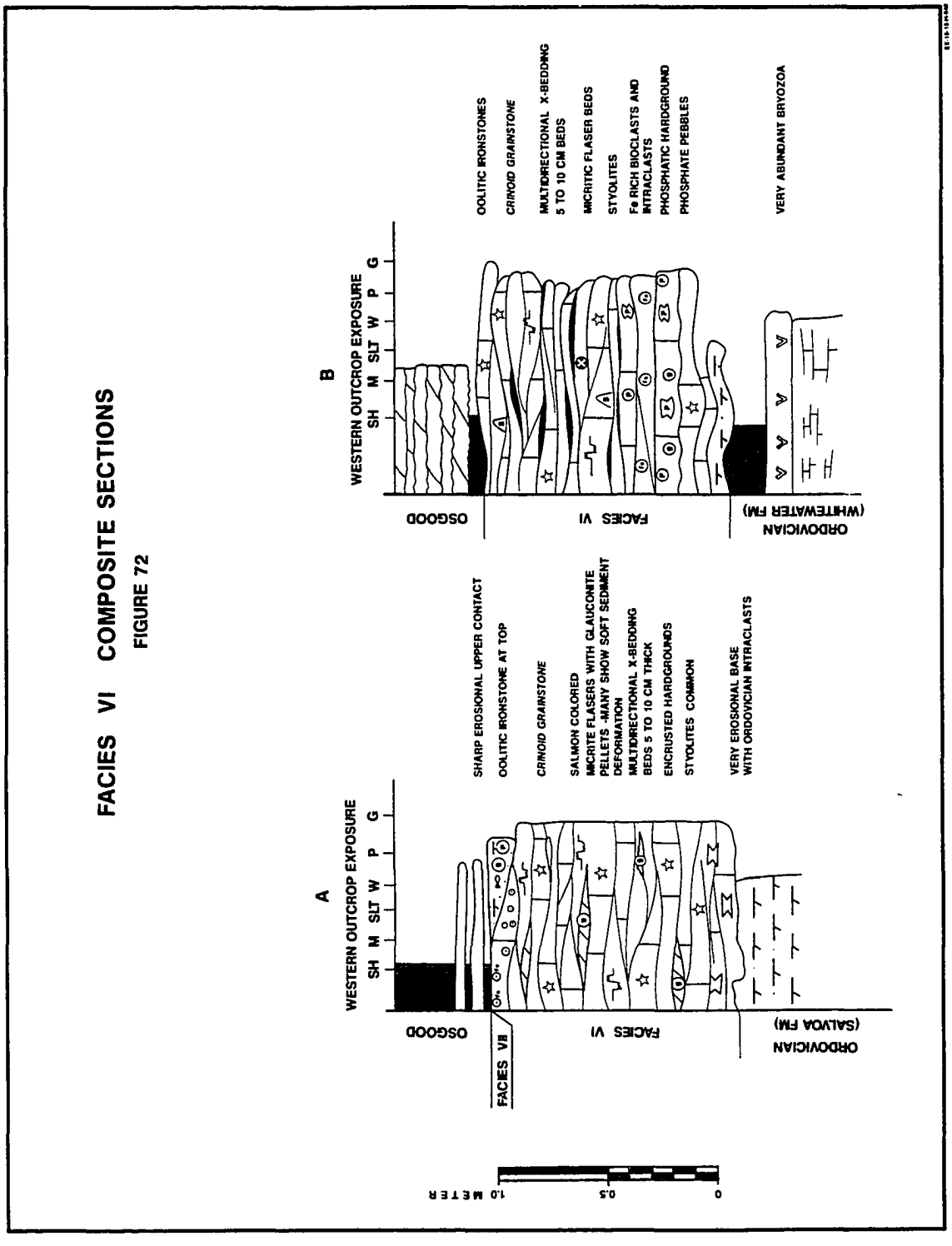

FIGURE 73

EROSIONAL BASE OF BRASSFIELD FACIES VI OVER THE UPPER ORDOVICIAN SALUDA FORMATION

FIGURE 74

POLISHED SLAB OF FACIES VI TAKEN DIRECTLY BELOW THE OVERLYING OSGOOD FORMATION
(NOTE: THE EROSIONAL BORED SURFACE AND MULTIPLE PHOSPHATIC AND IRON RICH LAMINATIONS)

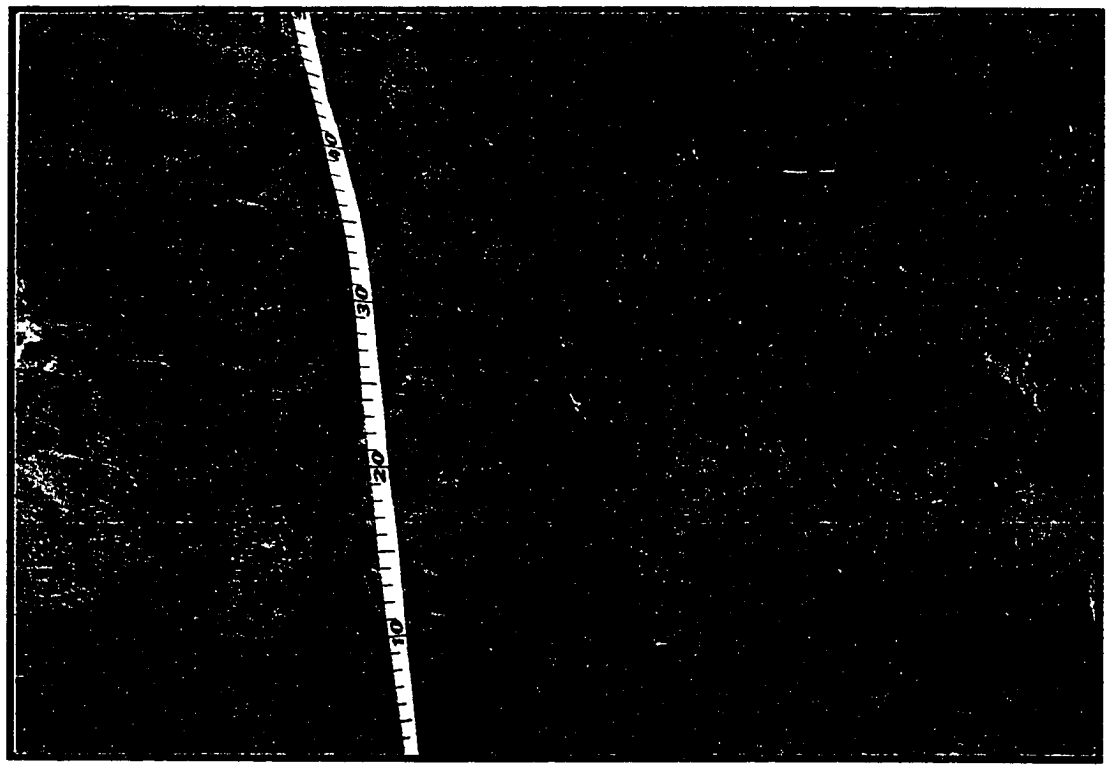

Location 16 Facies VI

Location 23 Facies VI

Relief of the Upper Ordovician surface approaches 0.5 meters at localities 13, 16, and 23 in Jefferson and Ripley Counties, Indiana. The surface topography appears to have been the result of high energy erosion and solution. Encrusting bryozoans and stromatoporoid borings up to 4 centimeters deep, and phosphatic crusts are common features of the Ordovician surface. Lafferrier, et al., (1986) recognized three separate phosphatization events at the Ordovician -- Silurian contact, manifested as separate thin phosphatic laminations. The laminations are formed in borings and pits in the Ordovician surface. The crusts, and phosphatic pebbles associated with them, are composed of fluorapatite, carbonate fluorapatite, and calcite (Laferrier et al., 1986). Angular to slightly rounded Ordovician lithoclasts with dimensions up to several centimeters occur at the base of facies VI, just above the Ordovician surface.

Facies VI is overlain by the interbedded dolostones and shales of the Osgood Formation, or by the Lee Creek Member of the Brassfield Formation (facies VII). The contact between the Brassfield and the dolostones of the Osgood is very erosional, and phosphatic crusts, hardgrounds, and ironstones mark the contact (Figures 74, 75, and 76). The contact between the Lee Creek and facies VI is also sharp with local relief of up to 0.5 meter (Figure 77).

Beds in Facies VI are generally less than 15 centimeters thick, are cross bedded, and are discontinuous. Dolomitized mud and silt flaser beds are common and many show soft sediment deformation. Glauconite is commonly found concentrated in the flasers. Some flaser beds are wackestones with

FIGURE 75

PHOTOMICROGRAPH OF FERRUGINOUS HARDGROUND AT THE TOP OF FACIES VI

FIGURE 76

ERODED AND BORED UPPER SURFACE OF FACIES VI

Location 23 Facies VI P/S 500 microns

Location 24 Facies VI

FIGURE 77

UNEVEN EROSIONAL CONTACT BETWEEN FACIES VI (MIDDLE MEMBER) AND FACIES VII (LEE CREEK MEMBER)

FIGURE 78

HARDGROUND SURFACE WITH LARGE CEMENTED BIOCLASTS AND SMALL PHOSPHATIC CLASTS FACIES VI

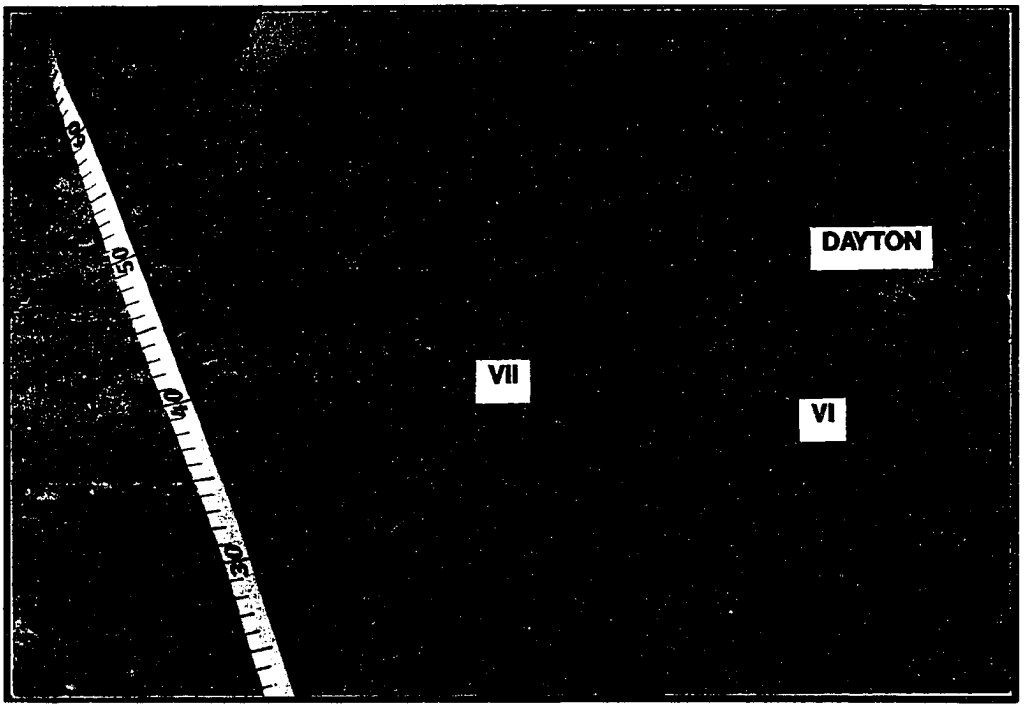

Location 16 Facies VI and VIII

Location 24 Facies VI

ostracod and trilobite bioclasts as large as 750 x 100 microns. Many bedding surfaces are rippled. Encrusted hardgrounds or firm grounds and phosphate pebbles (see description below) are present on some bedding surfaces. Average composition of facies VI is 42.5% bioclasts, 22.9% calcite cement, 15.7% micrite, 12.1% dolomite, 2.7% intraclasts, 2.2% pellets, 0.7% pebbles (commonly phosphatic), 0.5% hematitic ooids, 0.2% chert, 0.2% pyrite, and 0.2% quartz silt. Average bioclast composition is 74.3% crinoid, 8.3% bryozoan, 7.4% brachiopod, 3.3% stromatoporoid 5% coral, 2.1% unidentified, 1.1% trilobite, 0.8% ostracode, and 0.3% gastropod.

Phosphatic pebbles and bioclasts are common at many exposures of facies VI from Fayette County, south to Jefferson County, Indiana (e.g., localities 25, 24, 23, 18, 20, 16, and 15). At locality 24 the pebbles are dispersed in a packstone and are associated with a hardground surface (Figure 78). A well formed phosphate pebble hardground occurs at locality 18 in southern Ripley County, where pebbles up to several centimeters long have been cemented and eroded to a very flat surface. Many of these pebbles have been truncated. Individual pebbles and the hardground surface are bored. Deposited above the hardground are several crinoid grainstone beds rich in smaller phosphatic pebbles and hematitic ooids (Figures 79, 80, and 81).

Lithofacies Interpretation

The lithology of facies VI can be summarized as predominantly coarse grained, cross bedded, slightly ferruginous grainstones with small, silty, glauconitic, and dolomitic flaser beds. Dolomite ironstones and associated

FIGURE 79

UPPER SURFACE OF PHOSPHATIC PEBBLE HARDGROUND IN FACIES VI

FIGURE 80

VERTICAL POLISHED SLAB OF SAMPLE SHOWN ABOVE
(NOTE: THE BORED PEBBLES AND SHARP EROSIONAL UPPER SURFACE)

Location 18 Facies VI

Location 18 Facies VI

FIGURE 81

PHOSPHATE AND IRON RICH BED DEPOSITED ABOVE THE PHOSPHATIC PEBBLE HARDGOUND IN FACIES VI AT LOCATION 18
(SEE FIGURES 79 AND 80)

FIGURE 82

THIS FRACTURE IN MICRITE IS INTERPRETED AS A DESICCATION CRACK IN SEMICOMPACTED MUD IN AN INTERTIDAL ENVIRONMENT OF FACIES VI

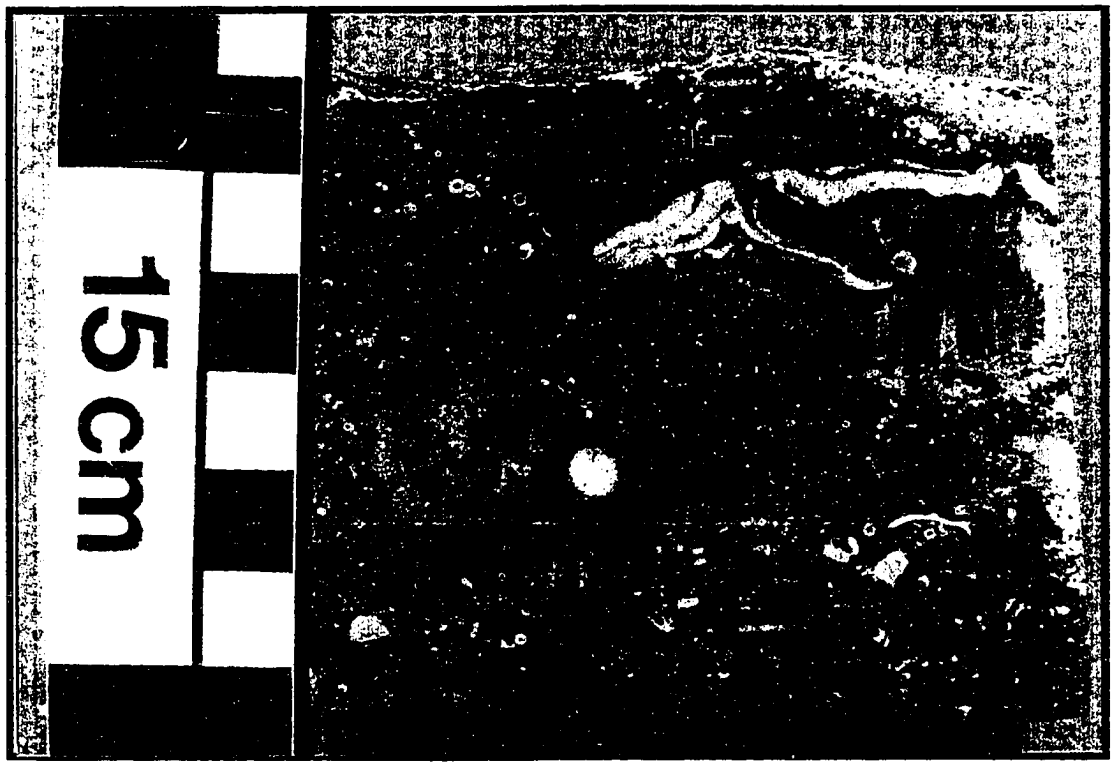

Location 18 Facies VI

Location 24 Facies VI P/S 500 microns

phosphatic pebbles and crusts are also common. The base of the facies is erosional and Ordovician clasts up to several centimeters in dimension occur just above the contact. Most exposures of the Brassfield Formation on the west side of the Cincinnati Arch are composed of 1 meter or less of facies VI.

Facies VI represent very low net sedimentation in shallow, well agitated waters. It records a complex history of repeated rapid depositional events, depositional hiatus, reworking, and sedimentary bypass. The relatively diverse fauna indicate normal marine conditions. The mineralogy records geochemical environments that shifted, at least locally, from slightly reducing conditions (favorable for the formation of glauconite and phosphate) to oxidizing conditions (favorable for the chemical weathering of glauconite and the formation of hematitic ironstones).

Evidence for shallow water origin includes:

- Cross-bedding;
- Lack of fine grained material (except for flaser beds and a few atypically muddy accumulations interpreted to be intertidal (see Figure 82);
- Coarse grain size;
- Highly abraded grains;
- Presence of cemented desiccation cracks;
- Erosional contact with underlying Ordovician;
- Abundance of oxidized iron as hematitic bioclasts (which lends the characteristic salmon brown color to this facies) and ironstones; and

- Cementation present almost exclusively as syntaxial echinoderm overgrowths.

The most compelling evidence for condensation in facies VI is found in the abundance of lithologies that generally require slow sedimentation rates for their formation. These lithologies, which are commonly found together, include oolitic ironstones and hematitic bioclasts, phosphatized crusts, bioclasts, and pebbles, and glauconite. Cemented, bored, phosphatic, and bio-encrusted hardgrounds and clasts also indicate slow sediment input.

Individual shoaling cycles are well developed and easy to recognize in facies II, III, and V, but difficult to identify in facies VI. Shallowing-upward conditions, most likely related to those that formed the shoaling cycles in facies II, III, (IV), and V, presumably effected the deposition of facies VI as well, but individual cycles are obscured by the over-print, or amalgamation, of subsequent dispositional events that reworked previously deposited sediments and bypassed fine sediment to deeper parts of the platform. Several examples of phosphatic deposits and associated ironstones, typical of deposition at the top of shoaling cycles (Van Houten, 1982) are exposed in facies VI. True oolitic ironstones are present at different stratigraphic horizons in facies VI (see localities 23, 18, 20 and 24), which may indicate a continual lateral and temporal shift of conditions favorable for ironstone formation on this part of the platform, through the depositional history of the facies.

The entire facies is slightly iron rich and could be thought of as a early stage ironstone. The facies consists mostly of crinoid bioclasts which have red-

brown staining in the micro-pores of the stereom structure lending the characteristic brown or salmon color (Figures 83 and 86). The concentration of the staining mineral is too low for identification by XRD (in most cases, hematite was detected rarely), but has the appearance of weathered glauconite or hematite in thin section.

These bioclasts were probably slightly glauconitized during times of relative sedimentary quiescence (phosphorites also formed at around this time), and later oxidized when the waters became shallower and conditions favoring the formation of ironstones returned. These ironstones are stratigraphically equivalent to the ironstones that cap the shoaling-upward cycle tops in facies II, III, IV, and V.

Crinoid bioclasts with glauconite and weathered glauconite in their stereom structure are variously altered to hematitic oolites (Figure 84). Smaller, well-formed glauconite pellets accumulated with fine grained material during these times of quiescence, and were reworked into flaser beds (glauconite pellets are commonly found in the flaser beds in this facies) or bypassed to deeper parts of the platform with other sediments. Also, during the less active times of sedimentation, hardgrounds encrusted by bryozoan and stromatoporoids were formed.

Facies VI thins over topographic highs on the paleo-Ordovician surface. This is clearly illustrated at locality 20, where the facies pinches out completely from 0.5 meters over a distance of only 20 meters. Ordovician carbonate beds are truncated beneath facies VI, indicating the Brassfield thins over an

FIGURE 83

PHOTOMICROGRAPH OF A SLIGHTLY DOLOMITIZED CRINOID GRAISTONE SYNTAXIAL OVERGROWTH ARE CLEAR, WHILE THE BIOCLASTS THEMSELVES APPEAR CLOUDY BROWN, MOST LIKELY FROM IRON ENRICHMENT IN THE STEREOME PORE STRUCTURE

FIGURE 84

GLAUCONITIZED CRINOID FRAGMENTS, PARTIALLY AND COMPLETELY ALTERED TO HEMATITE

Location 7 Facies VI P/S 500 microns

Location 23 Facies VI P/S 500 microns

Ordovician topographic high, and does not represent an area where facies VI was not deposited, or was eroded from above.

The Brassfield was not deposited in parts of Decatur, Rippley, Jennings, and Jefferson Counties, Indiana, which has been attributed to the presence of a broad Ordovician high area on the platform (Ripley Island of Foerste, 1891). Location 20 represents the edge of this feature. Facies VI thins considerably at location 24, as well (from 2.25 meters to 0.5 meters over a distance of 200 meters). Unlike locality 20, where the thinning lithology is all grainstone, the lithology of the thin deposit at location 24 includes a significant amount of fine carbonate, which may represent accumulation on incipient intertidal flats developed at the edge of the "Ripley Island" positive.

Cementation of facies VI is almost exclusively in the form of syntaxial echinoderm over growths. Repeated reworking of the sediments concentrated the crinoid fraction and repeated exposure to shallow conditions would explain the dominance of crinoid over growths.

A possible scenario for the accumulation of any facies VI deposit might be:

(1) Shallow water, high energy deposition of carbonate sands which eroded the Ordovician surface;

(2) Sallow water conditions persist, but sediments do not accumulate -- in situ carbonate production is minimal predominant processes include abrasion [resistant crinoid bioclasts are concentrated], reworking and sedimentary bypass (of fines and coarse material);

(3) Water depth increases, conditions become quieter, a limited amount of fine grained carbonate accumulates, glauconite forms as small pellets and in the stereome pores of crinoid bioclasts, phosphatic hardgrounds and intraclasts are formed concomitant with glauconite where conditions are favorable;

(4) Water shallows and depositional energy increases, fines are reworked into flaser beds but not completely bypassed, bioclasts that had become glauconitized in previous stage are partially to fully oxidized -- this imparts the salmon color to the facies, oxidizing environment favors development of oolitic ironstones, mixing zone cementation conditions quickly cement crinoid rich sediments that are subsequently eroded;

(5) Depositional energy increases still more, hematitic oolites are reworked and mixed with coarser, less abraded bioclasts into a coarse grainstone;

(6) Process returns to some previous stage and results in stacked oolitic ironstones with glauconitized bioclasts, phosphatic pellets and hardgrounds, "rusted" crinoid rich carbonate sands with glauconite rich flaser beds, erosional surfaces, and encrusted hardgrounds.

Dolomite Description

Dolomite content of facies VI sample ranges from a trace to 100% and averages 9%. In general, dolomite content of the facies increases greatly to the south (Figure 85). Two types of dolomite are found in facies VI. The first is unimodal (25 to 50 microns), planar-subhedral, nonzoned, ferroan to slightly ferroan, and nonporous. The second is unimodal (75 to 150 micron), planar-euhedral, nonzoned, nonferroan, and has only a trace of interrhombic porosity.

Dolomite Interpretation

The finer grained dolomite has selectively replaced mud, completely replacing mud flasers in grainstones, micritic pellets, and micritic matrix. As with the other mud replaced textures, the morphology of this dolomite indicates a single nucleation event on a unimodal substrate under conditions of relatively low saturation and temperature.

The second type of dolomite in facies VI has nucleated at the interface between syntaxial crinoid overgrowths and has replaced both cement and bioclasts, suggesting somewhat higher dolomitizing fluid saturations or longer exposure to dolomitizing fluids than samples with only micrite selective dolomite (Figure 86). The micrite selective dolomite is present throughout facies VI. It is interpreted here as having formed contemporaneous with partially dolomitized sediments of facies II, III, IV, and V.

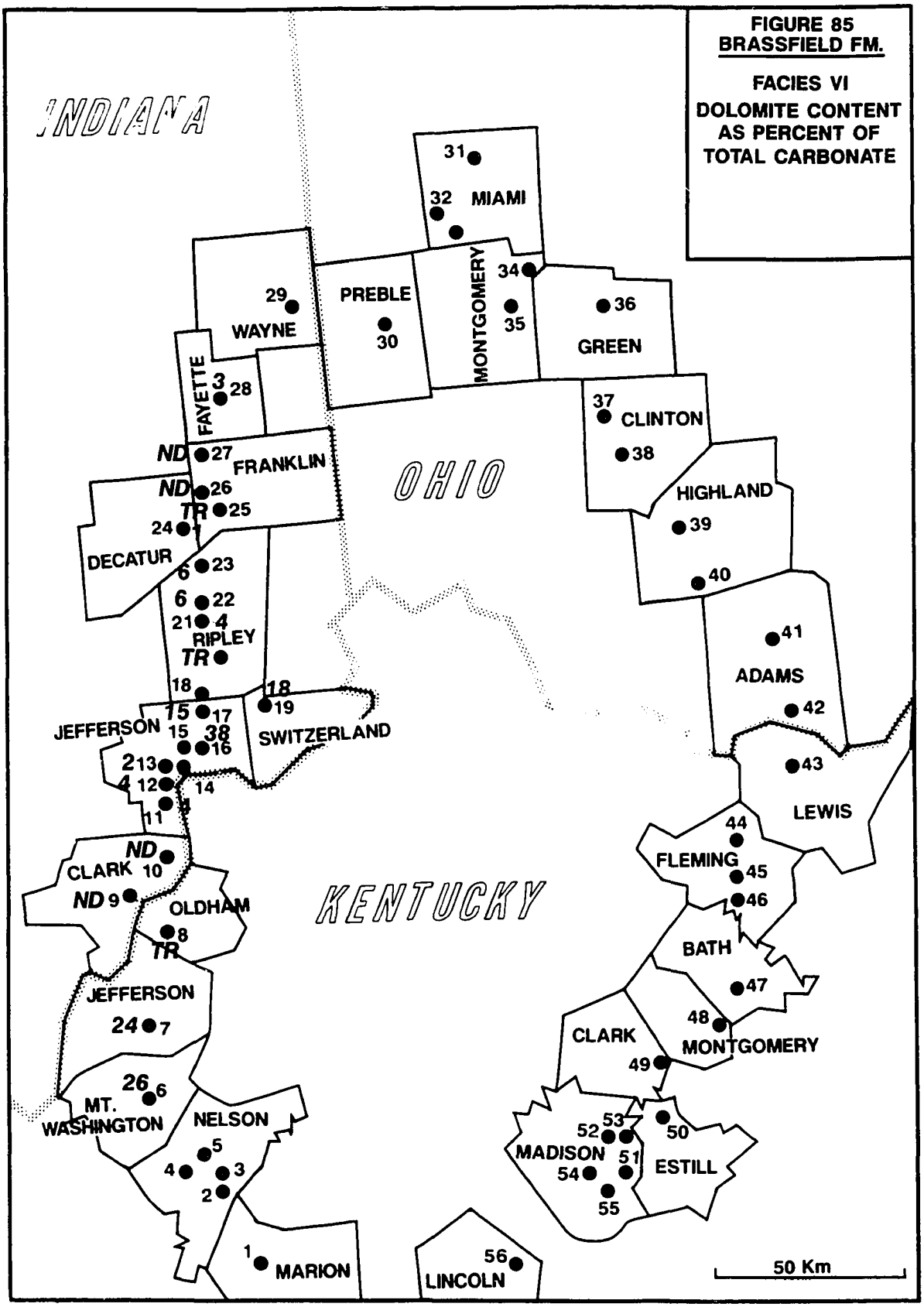

FIGURE 86

DOLOMITE REPLACING CRINOID OVERGROWTHS

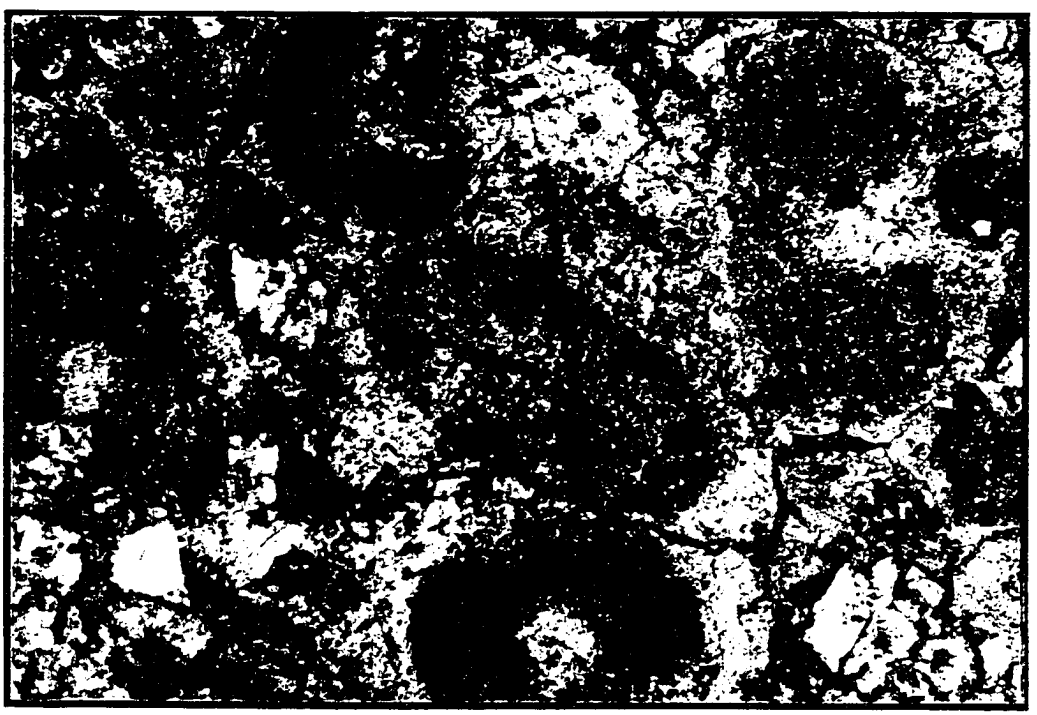

Location 16 Facies VI P/S 500 microns

The cement and bioclast replacive dolomite is limited to southern Madison County, Indiana south to Bullit County, Kentucky, becoming more abundant to the south (localities 7 and 6, in particular, showed a marked increase). South of Bullit County, Brassfield sediments (facies I, II, and III) are completely dolomitized. The increase in this type of dolomite toward the south, independent of the micrite selective dolomite, suggest two possible scenarios. Either dolomitization occurred as a single event, and was more intense to the south, or a separate, more intense dolomitizing event occurred in the souther part of the study area.

FACIES VII (LEE CREEK MEMBER)

Lithofacies Description

Facies VII is a thin, fine grained, dolomite rich in glauconite and collophane. It is present from Clark County, Indiana south to Bullit County, Kentucky. Here, the Brassfield thickens abruptly into the Bardstown Monocline and the Lee Creek is no longer recognized. Facies VII is discontinuously present in Decatur and Switzerland Counties, Indiana. It ranges between 1 centimeter and 1.2 meters thick, and is typically less than 0.25 meters thick, and occurs as a moderately continuous bed to very discontinuous lenses. The Lee Creek rests unconformably on facies VI, or, where this lithology is missing, on the Upper Ordovician Whitewater or Saluda Formations. Its upper contact with the Osgood Formation is also unconformable (Nicole and Rexroad, 1968). Figures 87 and 88 illustrate the thickness, distribution, and lithologic character of facies VII in the study area.

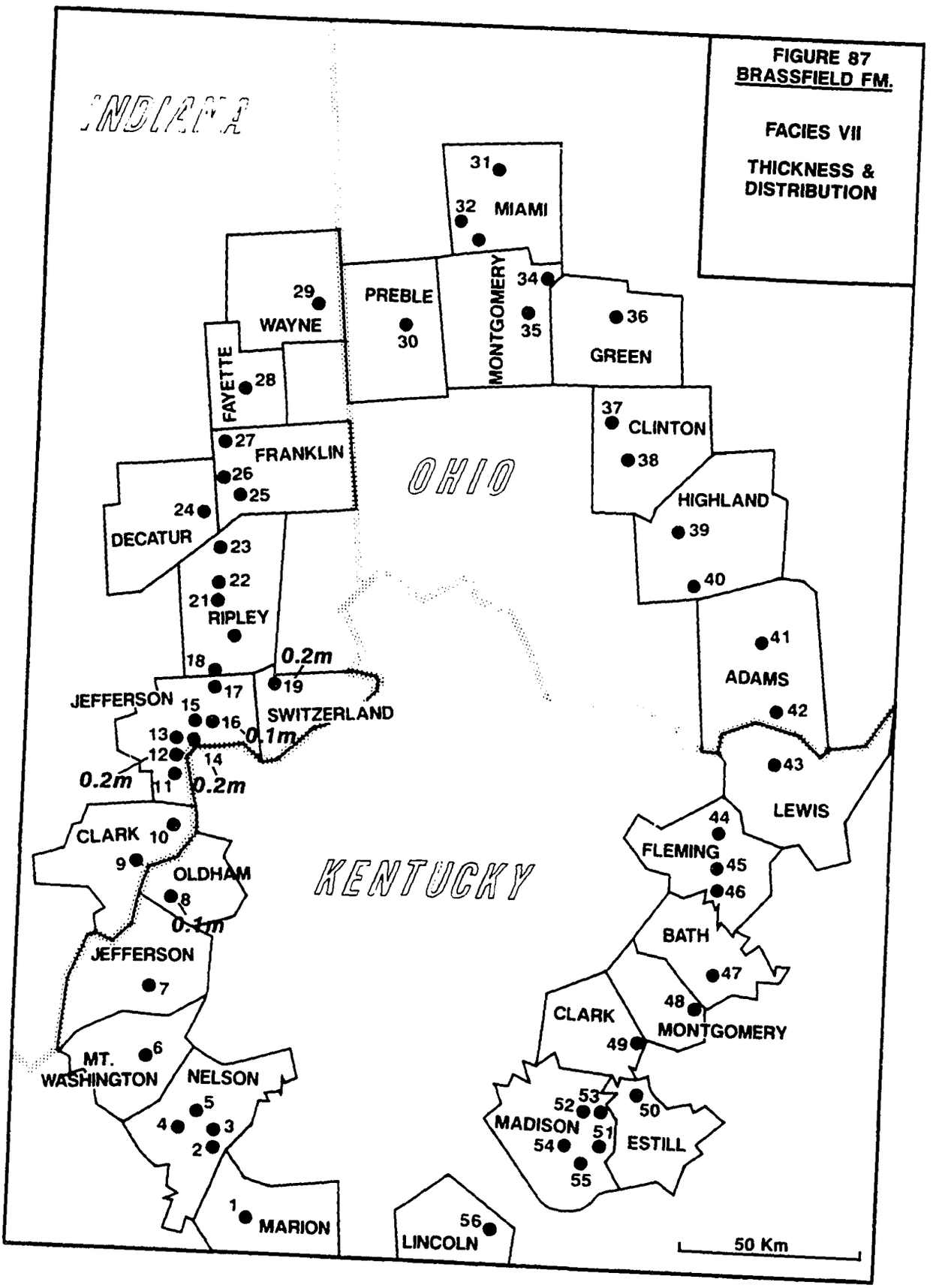

FACIES VII COMPOSITE SECTION

FIGURE 88

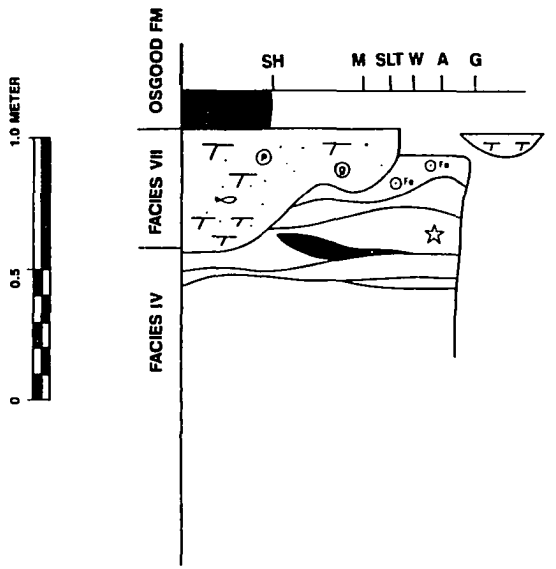

SILTY DOLOMITE

CONDENSATION LITHOLOGIES INCLUDE
GLAUCONTE, PHOSPHATE CLASTS, FISH BONES

EROSIONAL CONTACTS ABOVE AND BELOW

COLOR YELLOW, GREEN, BROWN

THIN DISCONTINOUS LENSES

The Lee Creek is a fine-grained tan, brown, or green dolomite. Sand-sized glauconite pellets are abundant. Also mixed in the Lee Creek are quartz silt and rounded sand grains, chert replaced bioclasts, phosphatized pellets, and lithoclasts and collophane bone fragments. Ripple lamination, mottling, and soft sediment deformation of laminae are common sedimentary features (Figures 89 and 90).

Lithofacies Interpretation

The Lee Creek is a highly condensed deposit that formed under quiet water, sediment starved conditions. The fauna of faces VII appears to be very restricted, and most fossils are altered in some way (e.g., glauconitized, chertified, or phosphatized). It averages about 0.25 m. thick and is stratigraphically equivalent to sediments with thickness a hundred times greater, or more, on the east side of the Cincinnati Arch.

Facies VII is a fine grained dolomite that contains glauconite pellets, chertified bioclasts and pellets, quartz silt and well rounded sand, and phosphatic pellets and collophane bone fragments. Unaltered carbonate bioclasts are not present. The mostly fine grained nature and complete lack of unaltered bioclasts in this facies sets it apart from the high energy condensed sediments in facies VI. The coarser clasts and occasional ripple lamination indicate at least some influence of currents, but on the whole, represents relatively deep conditions, below storm wave base and far from a sediment source. The change from the shallow depositional regime of facies VI to deep water indicated by facies VII has implications for changing overall

FIGURE 89

PHOTOMICROGRAPH OF FACIES VII (THE LEE CREEK)
HAND SAMPLE SHOWN BELOW RIGHT

FIGURE 90

POLISHED HAND SAMPLE OF FACIES VII - THE LEE CREEK MEMBER
QUARTZ AND CHERT GRAINS ARE LIGHTER TAN, WHILE GLAUCONITE
PELLETS STAND OUT AS DARK GREEN

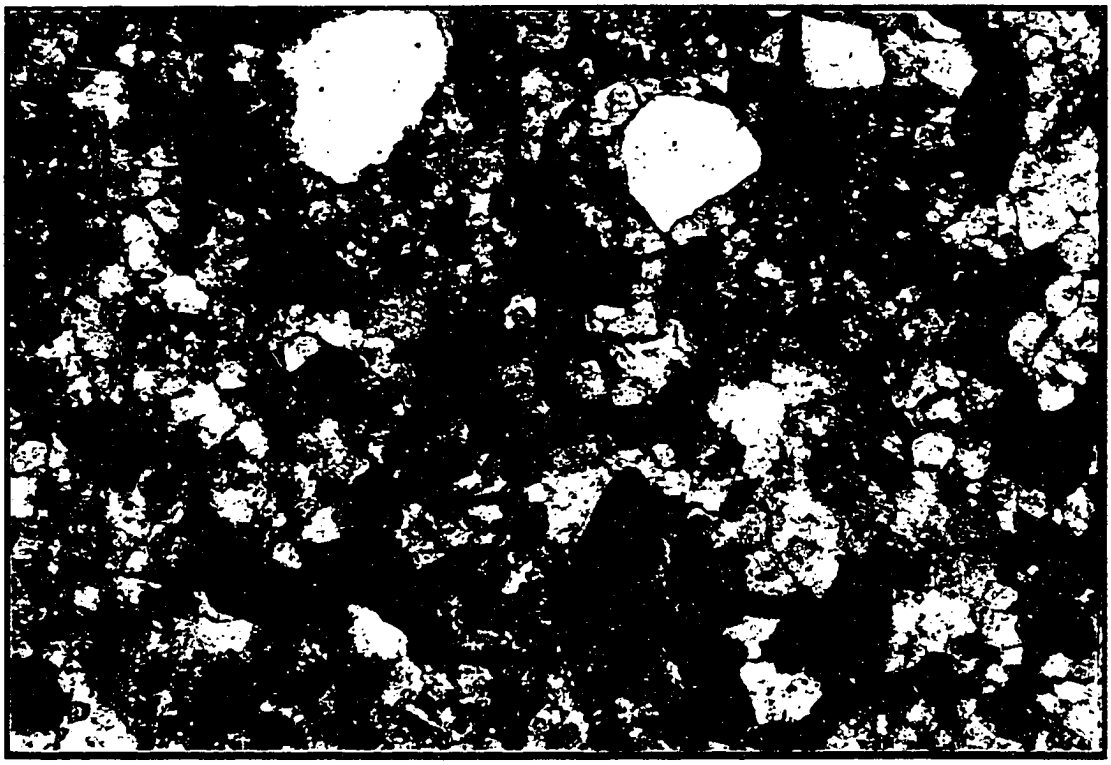

Location 14 Facies VII XN/S 500 microns

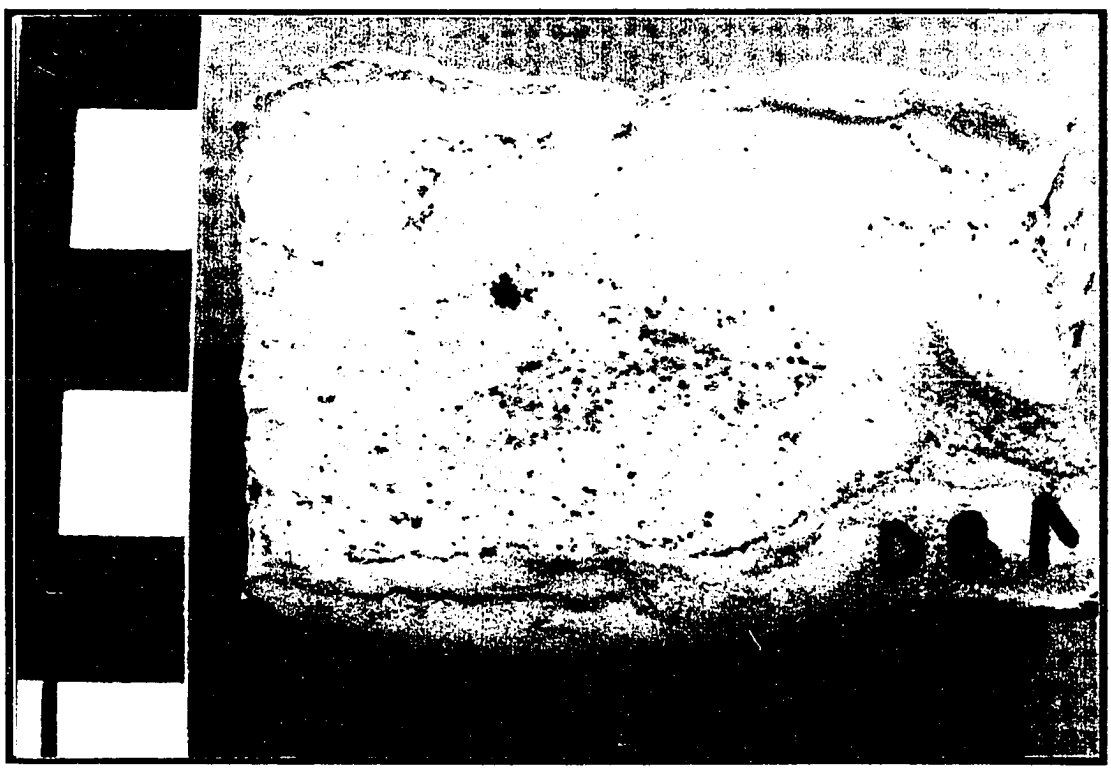

Location 14 Facies VII

platform conditions near the end of Llandovery. This will be discussed in a subsequent section.

Dolomite Description

The carbonate in facies VII is 100% dolomite at all exposures. Rhombs are unimodal in size (50 to 150 microns), though there are few polymodal examples, planar-subherdal to euhedral, nonzoned (rare ferroan zones were found), non- to slightly ferroan, and nonporous (Figure 90).

Dolomite Interpretation

Dolomite has replaced all carbonate in this facies. The original texture appears to have been mud or silt (hand samples that show inclined lamination and interspersed coarse noncarbonate clasts suggest silt, rather than mud, was more likely the original carbonate texture). Rhomb size and morphology suggest a single nucleation event under low temperature, low saturation conditions.

SUMMARY OF DOLOMITE IN THE BRASSFIELD

This report recognizes seven dolofacies in the Brassfield which are:

(1) uniformly fine grained dolomite; facies I; Ohio

(2) mixed fine to coarse grained dolomite; facies I; Ohio

(3) mixed coarse to fine grained dolomite; facies I; Kentucky;

(4) micrite selective dolomite; facies II, III, IV, V, VI, and VII; Ohio and Indiana

(5) completely dolomitized zone in facies IV; Ohio (sugar rock in northeast quadrant of outcrop belt)

(6) completely dolomitized sediments of facies II and III; Kentucky

(7) bioclasts and coarse calcite cement selective dolomite; facies VI; southern Indiana and northwest Kentucky.

The distribution and diagnetic character of these dolofacies indicate at least two, possibly more, dolomitizing events effected the Brassfield.

Facies I exhibits features associated with penecontemporaneous supratidal dolomite. Evidence for this includes presence of finely laminated microcrystalline texture, a general absence of fossils, indications of subaerial exposure (mud cracks, birds eye voids, and salt casts), detrital quartz silt, and laminated low angle cross-bedded intervals alternated with bioturbated intervals. The origin of intertidal or supratidal dolomites is usually attributed to some variation of the reflux model (see Morrow, 1982a and 1982b, and Hardie, 1987 for review).

Whether facies I represents true dolomitization by evaporative reflux is unclear. Aside from rare salt casts, evidence for gypsum precipitation is lacking, and this is a common association with sabkha dolomites. It is clear, however, that facies I dolomite predates other Brassfield dolomite, and depositional conditions were favorable for penecontemporaneous dolomitization of the pelletal muds and silts.

Dolofacies 4 through 7 can be attributed to one or more late stages of dolomitization independent of lithofacies. Dolofacies 2 and 3 represent facies I dolomite that has been dolomitized a second time. There is a sharp difference between dolomite north and south of the Ohio River that is not facies dependent.

Dolomitization in Ohio and Indiana either occurred as a separate less intense event than that in Kentucky, or occurred as a less intense extension of the same dolomitization event. The transition from completely to partially dolomitized sediments is abrupt, and suggests a separate event to the south, possibly related to the erosion and exposure of Silurian sediment in the Devonian, which was more intense in southern areas. However, the evidence presented herein is not unequivocal and the number of late dolomitizing events remains an open question.

Previous studies of Brassfield dolomites (Hendrix, 1982; Gordon, 1980) have invoked the brackish-water mixing zone model as the mechanism of dolomitization in the Brassfield Middle Member ("Dorag" model of Badiozamani, 1973; "schizohaline" model of Folk and Land, 1975). The "Dorag model is not necessarily the best scenario to account for Brassfield dolomitization, particularly given its extended depositional history, and position as a carbonate platform. Hardie (1986) suggests that, given enough time, marine meteoric waters will become major dolomitizing fluids where stable circulation systems drive the waters through carbonate platforms for thousands or millions of years. The Brassfield may represent such a system.

PALEOCURRENTS, FACIES ORIENTATIONS AND PLATFORM PALEOGEOGRAPHY

Figures 10, 18, 40, 51, 61, 71 and 87 illustrate a consistent north northeast - south southwest orientation of Brassfield facies paralleling both depositional strike and the inferred position of the eastern platform edge (see also Figure 2). This interpretation is consistent with subsurface trends in Silurian strata described by Lukasik (1988).

Orientation and direction of ripple and megaripple cross-bedded intervals recorded at several localities in the Brassfield Middle Member are illustrated in Figure 91. Random to slightly eastward directed paleocurrents are present in the western study area (facies VI). Data in the northern study area indicates a moderate north and east direction (facies IV and V). Southeastern outcrops show consistent southeast directed paleocurrents, particularly in facies III.

Paleocurrents to the west and north indicate reworking by multi-directional currents. The lack of well defined current directions suggest if undirectional storm currents were involved in the formation of the sedimentary structures, the effects were erased by fair weather, multi-directional current processes. Paleocurrents in facies IV and V show slight indications of transport toward the paltform edge. Data from facies III in the southeast are indicative of offshore directed currents probably related to storms. On-shore directed storm winds typically produce wind drift surface currents that pile up water near or on-shore (coastal set up) and result in a gravity driven on-shore-offshore pressure gradient. Consequently, surface currents are directed on-shore, whereas bottom currents flow off-shore to

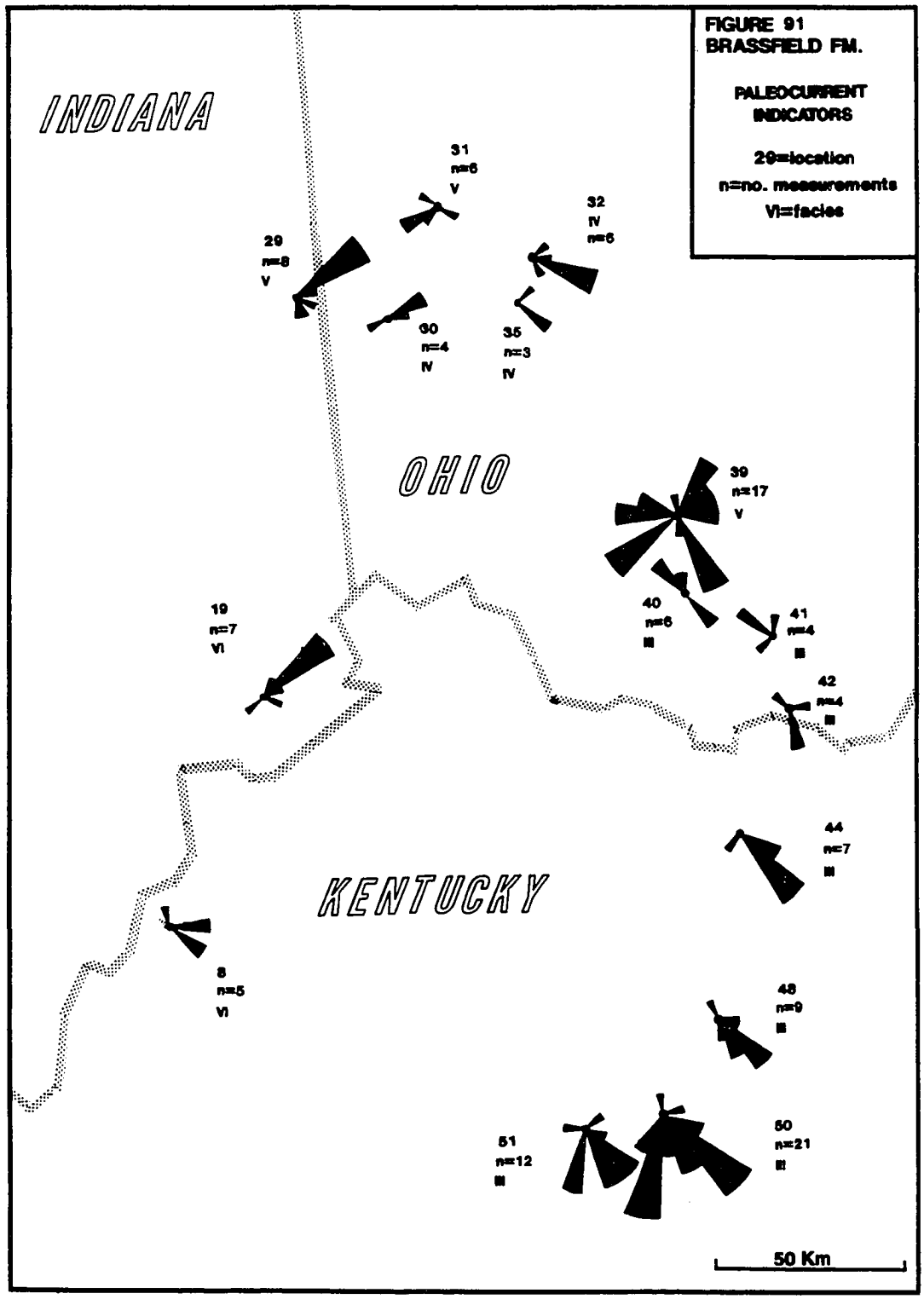

compensate for coastal set up (see review by Walker, 1984). However, it is unlikely that this process caused the off-shore directed currents recorded in facies III in the southeast.

First, there was no extensive land area where water accumulated by coastal set up processes, with the exception of the Ripley positive area, which was very limited in extent and probably would not have affected return currents in the southeast. The entire platform was probably flooded, and wind, rather than gravity driven currents would have been effective in moving sediment.

Second, storms would probably not have approached the eastern margin of the platform from the east. The study area was positioned 15^{o} to 20^{o} south of the Lower Silurian paleoequator (Ziegler, et al., 1977), well within latitudes most often affected by tropical storms (Marsaglia and Klein, 1982). Storms would have originated in the equatorial regions, tracked west and south as they were deflected by the Coriolis force, and approached the study area from the present-day northwest to northeast, sweeping over shallow parts of the platform, reworking and eventually transporting sediments to deeper areas of the platform to the east and southeast.

Offshore bottom currents set up by return storm flow, as described above, would require storm approach nearly 180^{o} from their most likely path. Therefore, the consistent current indicators to the southeast probably indicate sediment transport by tractive wind driven currents in the direction of storm travel.

SUMMARY OF THE BRASSFIELD DEPOSITIONAL MODEL

This section briefly summarizes the Brassfield Formation depositional model. A detailed discussion of the model will follow.

The Brassfield Formation was deposited on a carbonate platform west of the Appalachian Basin. It is a remarkably thin and widespread unit whose depositional history began with the Lower Silurian transgression and continued through most of the Llandovarian. It records a mosaic of depositional and condensation regimes that developed in response to oscillations of the Lower Silurian transgression.

Seven facies have been identified in the Brassfield: These are:

Facies I - Peritidal flats.

Facies II - Shoaling-upward sequence; distal tempestites through shore face sands.

Facies III - Composite shoaling-upward sequences; distal to proximal tempestites and hematitic oolite sands,

Facies IV - Shallow platform sand sheets/shoals.

Facies V - Shallow platform sand sheets/shoals with bioherms.

Facies VI - Shallow platform amalgamated ferruginous sand sheets.

Facies VII - Deep starved basin muds and silts.

The depositional history of these facies can be explained in terms of a hierarchy of sea level fluctuations that correspond to third (Vail, et al., 1977) fourth, fifth, and sixth order sequences (Busch and Rollins, 1984; Brett and Baird, 1986).

BRASSFIELD SEQUENCES

Sixth order sequences are the building blocks of facies. Coeval sixth order sequences are genetically related, but not directly correlative over significant lateral distances. This suggests their development is controlled at least in part by localized processes, for instance, local tectonic adjustment, variations in local production of carbonate sediment, variations in clastic input, or simply irregularities in sea floor topography.

Fifth order Brassfield sequences are equivalent to facies tracts, which are correlative groups of facies. Facies tracts in the Brassfield record the sedimentologic response of the platform to fifth order sea level oscillations. Fifth order sequences are allocyclic and the facies tracts they compose are basin wide. Their bounding surfaces are unconformable and correlative across, and probably away from the study area. Facies tracts in the Brassfield include the following facies:

Tract (1)	Facies I.
Tract (2)	Facies II, IV, and possibly part of VI.
Tract (3)	Facies III, V, and VI.
Tract (4)	Facies VII.

Facies tract 1, 2, and 3 (facies I through VI) constitute one fourth order sequence. Facies tract 4 (facies VII) constitutes another. Fifth and sixth order sequences in facies VII are obscured by intense condensation. Bounding surfaces of third and fourth order sequences are very unconformable and widely correlative.

DEPOSITIONAL CONDITIONS

Facies tract 1 was deposited as on-lapping peritidal flat packages during the initial Lower Silurian transgression. Facies tract 2 records distal storm to shallow platform shoaling conditions developed as sea level began to rise more rapidly. Facies tract 3 records shoaling-upward conditions that prevailed during a third fifth order oscillation. Local perturbations resulted in varied sixth order cycles within facies tract 3. Following the deposition of facies tract 3, a dramatic change to deep sediment starved conditions occurred in Indiana, while the Upper Cabbot Head Shale, Oldham Limestone, Lulbegrud Shale, and Dayton Limestone were deposited to the east.

Following the deposition of facies tract 3 (facies III, V, and VI) clastic sedimentation increased intermittently in central and eastern Ohio, and the Appalachian Basin, resulting in the deposition of the Cabot Head and Lulbegrud Shales, which contain normal marine fauna that accumulated under preitidal to subtidal conditions. Thick shales of the Rose Hill Formation were deposited further to the east. Minor regressive intervals accounted for the deposition of the regionally persistent Oldham and Dayton Limestones and their equivalents, whose lithologic and faunal characteristics are indicative of

shallow, moderately agitated peritidal conditions (Lukasik, 1988; Droste and Shaver, 1983). Equivalent regressive facies of the Rose Hill included carbonates at its western edge (but east of Ohio) and ferruginous sandstones to the east, nearer to the clastic source (Hunter, 1970).

The deposition of the Oldham and Dayton Limestones were facilitated by conditions of low clastic input and shallow well-agitated water on the eastern edge of the study area. The environment of deposition for the Lee Creek to the west, however, had to be deep enough to preclude autocthonus carbonate production.

A change in regional paleogeography followed the deposition of Brassfield tract 3 that lessened the influence of the eastern platform edge, and put the western study area in a deeper setting. Brassfield through Dayton sediments on the east side of the Cincinnati Arch record a transgression followed by conditions that vacillated between subtidal clastic dominated deposition and shallower peritidal carbonate dominated conditions. Strata on the west side of the arch suggest a different scenario that progressed from subaerial exposure at the base of the Brassfield, to shallow platform, to deep, subtidal, sediment starved conditions.

DISCUSSION OF DEPOSITIONAL MODEL

CORRELATION OF FACIES AND DEPOSITIONAL PHASES

The seven facies that comprise the Brassfield Formation in Ohio, Indiana, and Kentucky have been correlated into four distinct groups, or facies tracts (Figures 92 through 97). A facies tract is a system of different but genetically interconnected sedimentary facies of the same age (Teichert, 1958). Identification of each facies tract has been based on detailed description of the vertical and lateral juxtaposition of facies in 56 outcrops around the outcrop belt. The large number of closely spaced outcrops was the key to the correlation process.

Particular attention was paid to correlation of surfaces that separate vertically stacked facies. For instance, facies IIB and III are easily distinguished in outcrop on the basis of bedding character and shale content (see composite section descriptions, Figures 19 and 41) and their contact can be traced north to the surface separating facies IV and V, which is typically erosional (see composite section for facies IV and V, Figures 51 and 62). This same contact can be traced into Indiana to the highly erosional contact at the base of facies VI, which is coincident with the base of the Brassfield and the Silurian-Ordovician unconformity. Similar criteria are given for all other facies and contacts in the composite section illustrations shown in each facies description, and the facies correlation illustrations shown in Figure 92 through 96.

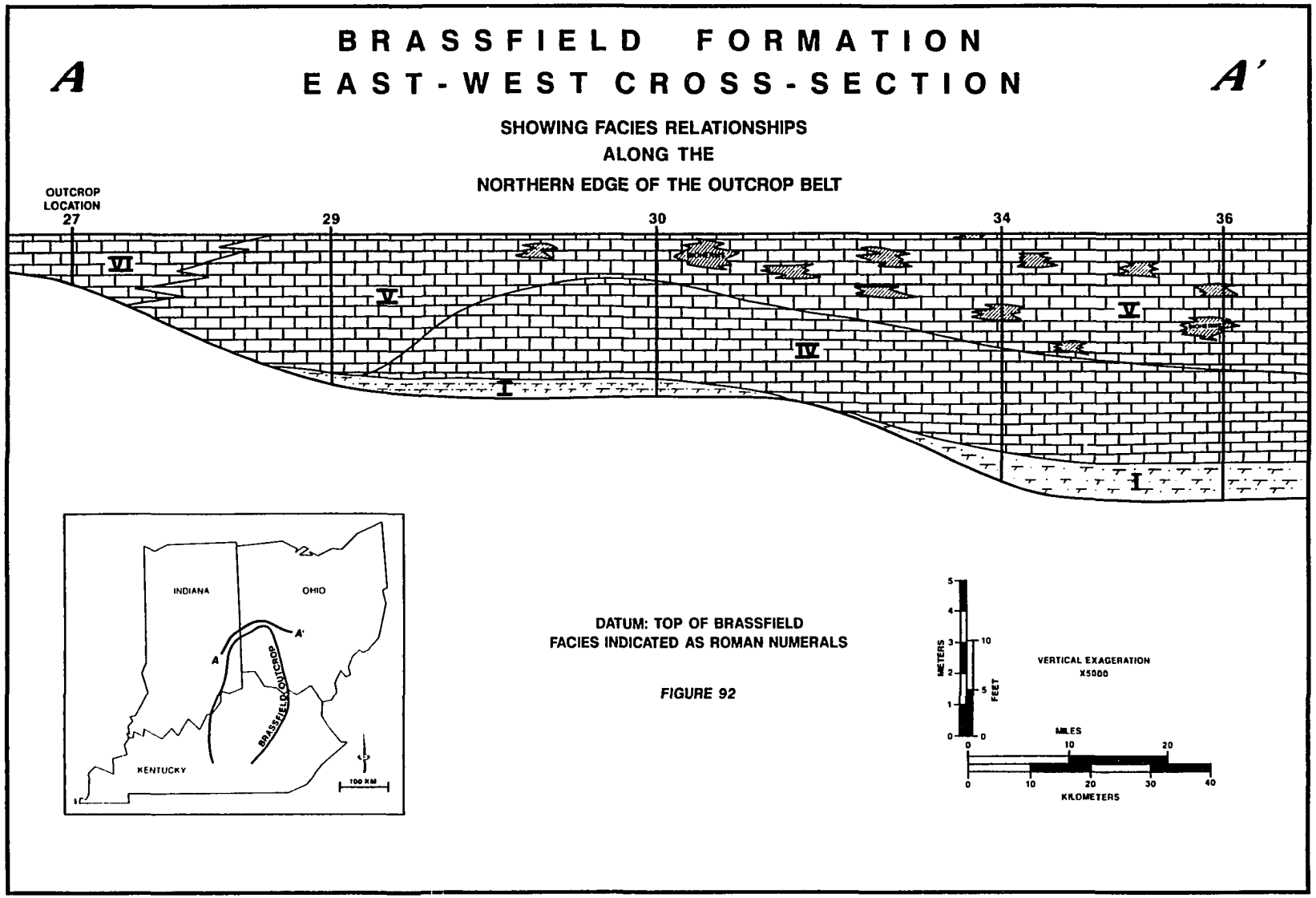

FIGURE 92

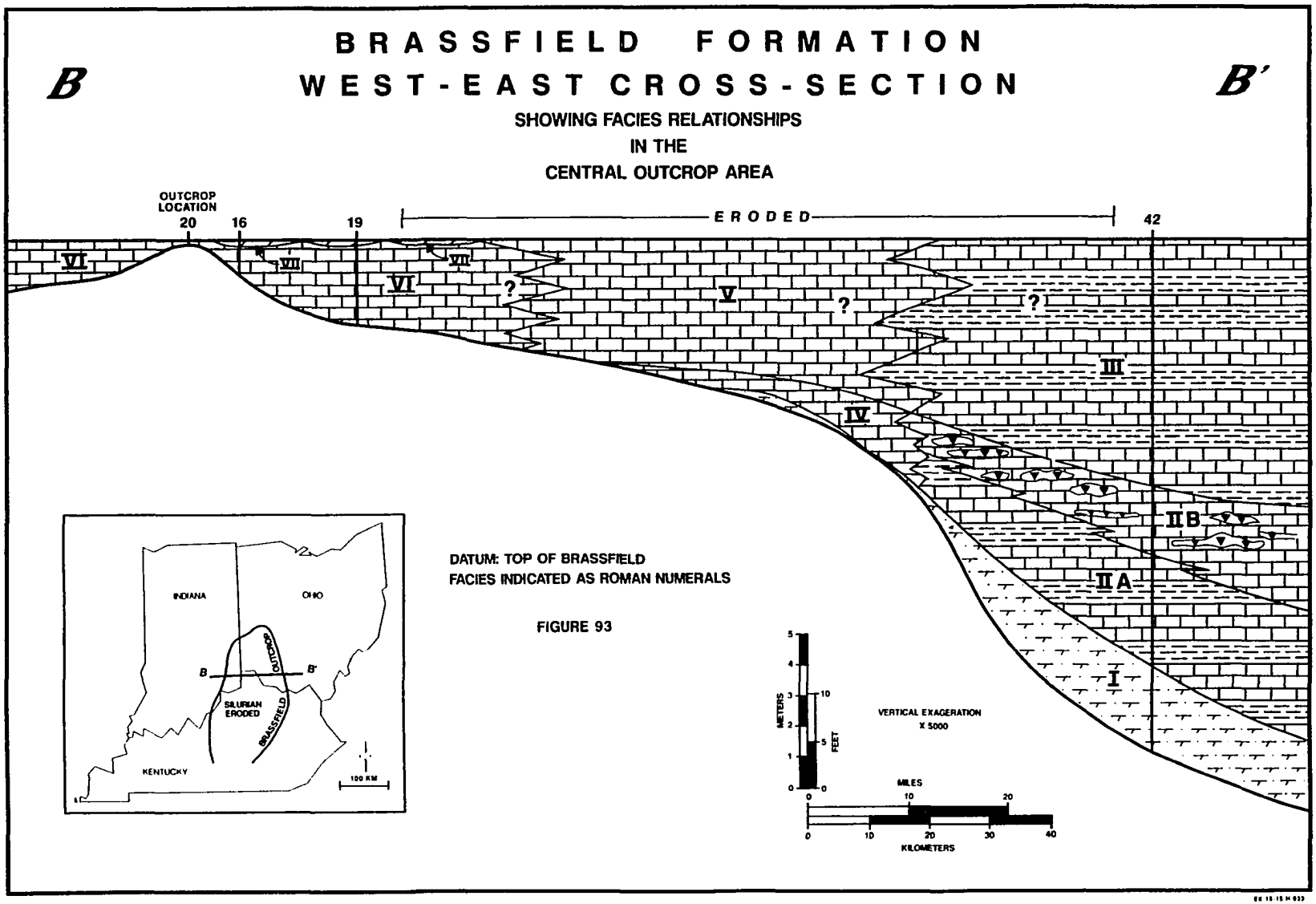

FIGURE 93

BRASSFIELD FORMATION
WEST-EAST CROSS-SECTION

C C′

SHOWING FACIES RELATIONSHIPS
IN THE
SOUTHERN OUTCROP AREA

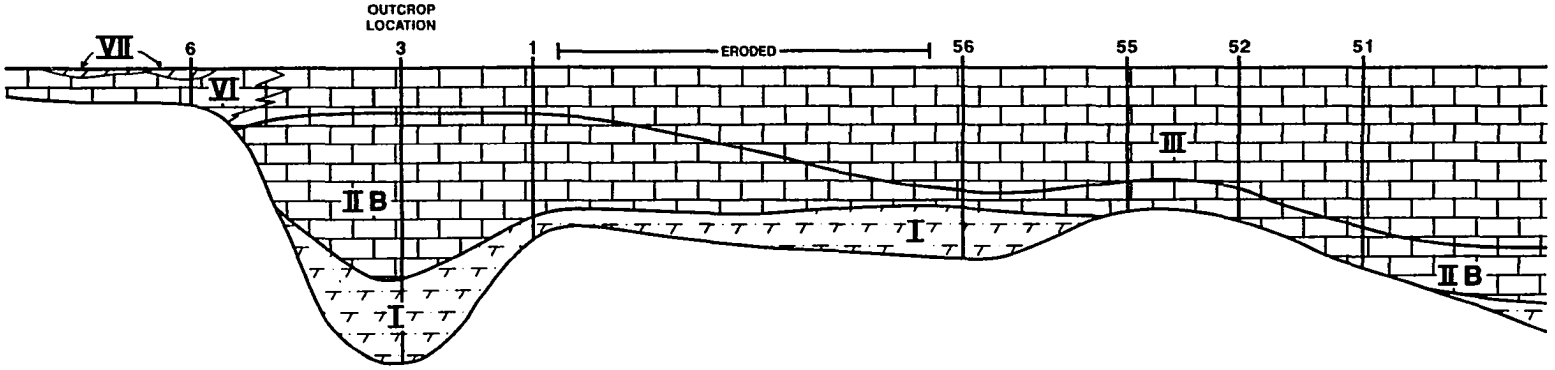

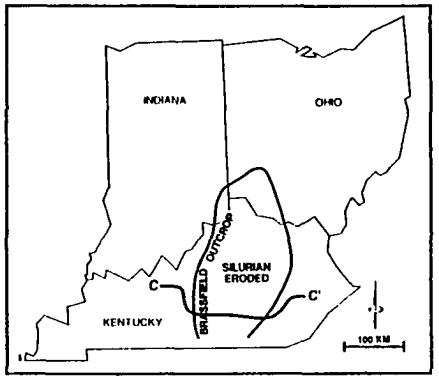

DATUM: TOP OF BRASSFIELD

FIGURE 94

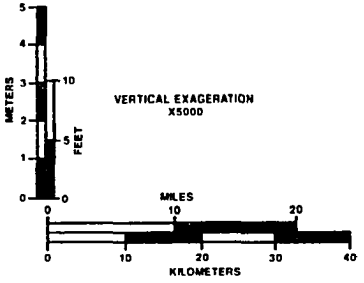

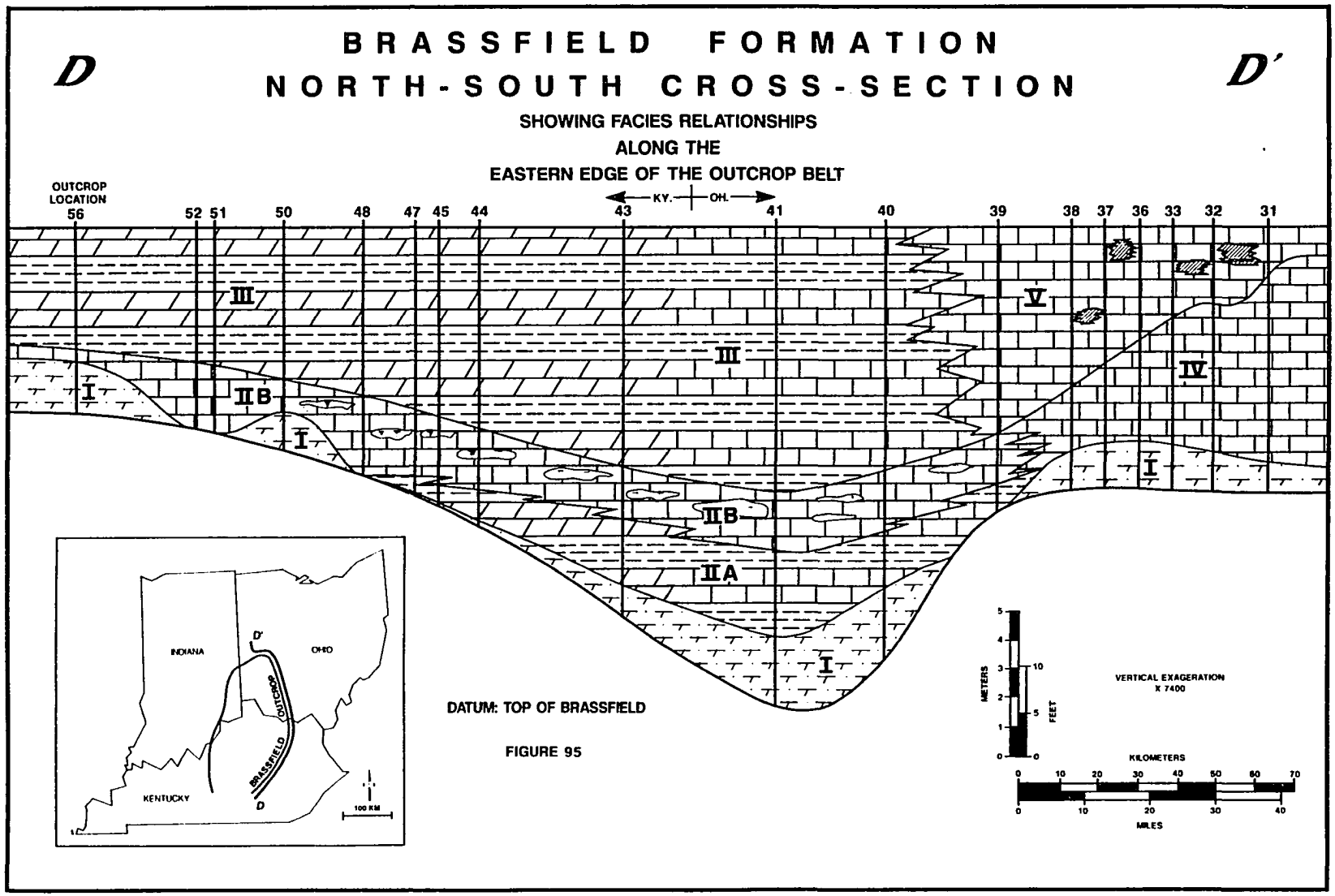

FIGURE 95

BRASSFIELD FORMATION
NORTH-SOUTH CROSS-SECTION

E E'

SHOWING FACIES RELATIONSHIPS
ALONG THE
WESTERN EDGE OF THE OUTCROP BELT

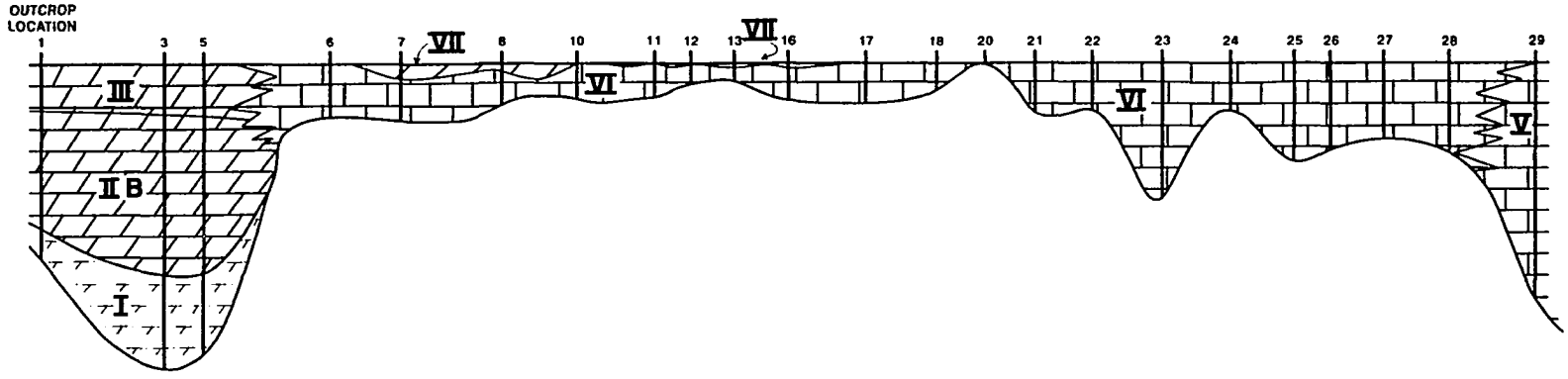

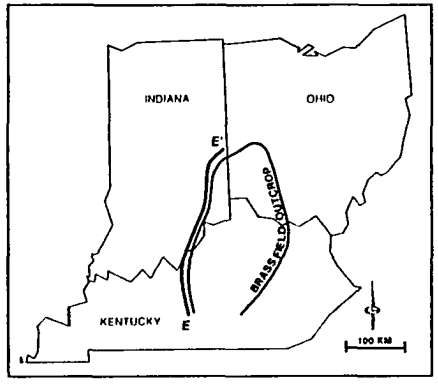

DATUM: TOP OF BRASSFIELD

FIGURE 96

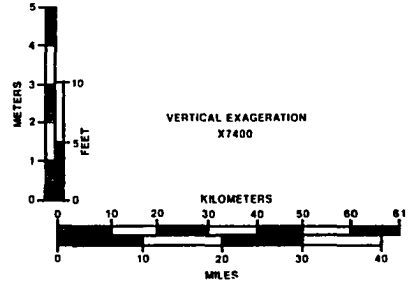

Conodont biostratigraphy of Rexroad (1967) and Nicoll and Rexroad (1968) have also been applied, but can only be used to help separate the three Brassfield members. It cannot be used to further subdivide the members.

Laterally correlative facies are grouped as follows:

Tract	Facies	
1	I	Belfast Member
2	IIA, IIB, IV, (VI?)	Middle Member
3	III, V, VI	Middle Member
4	VII	Lee Creek Member

Figures 92 through 96 illustrate the correlation of facies along the outcrop belt. Cross-sections A, B, and C are perpendicular to depositional strike. Cross-section D is along depositional strike and parallels the eastern edge of the Eastern Midcontinent interbasin platform. Cross-section E is also parallel to depositional strike, but is positioned far west of the platform edge.

Each facies tract formed during a different phase of Brassfield deposition and is bound by unconformable or paraconformable surfaces that are correlative throughout the outcrop area. Together, the four phases record overall transgressive conditions which continued through most of the Llandovery.

The interpretation of each facies tact, or depositional phase, incorporates interpretations of the individual correlative facies they contain. These are reviewed below.

Facies I is the only unit that records the first phase of deposition. It is a series of stacked peritidal flats deposited during the initial transgression of the Silurian sea over the Ordovician surface.

Phase 2 includes facies IIA to IIB, IV, and possibly part of VI. The shoaling-upward nature of each of these facies has been demonstrated. This facies tract represents deposition under very shallow platform conditions, where thin, amalgamated, carbonate sand sheets were developed under conditions of dynamic sedimentary bypass (facies VI to the west), submarine dunes accumulated rapidly on slightly deeper parts of the platform (facies IV in the northeast study area), and proximal to distal tempestites were deposited to the east (facies IIA to IIB).

Phase 3 comprises facies III, V, and all or most of VI. Like phase 2, it records overall shoaling conditions, but can be broken into several subordinate shoaling sequences. This facies tract formed under very shallow platform conditions when the dominant process was sediment bypass (facies VI), slightly deeper conditions where bioherms and cross-bedded sand sheets (facies V) developed in the northeast, and storm dominated platform environments where moderately proximal to distal tempestites were deposited (facies III).

Phase 4 is made up entirely of facies VII. It is a highly condensed deposit that formed under starved, relatively deeper basin conditions. Several relative changes in sea level occurred during phase 4, resulting in at least four time equivalent formations to the east (Cabot Head through Dayton interval). However, these sea level changes are not resolved in this thin and highly condensed facies.

TRANSGRESSIVE-REGRESSIVE SHALLOWING UPWARD SEQUENCES

The Brassfield Formation is composed of a series of transgressive-regressive depositional packages that record a hierarchy of shallowing-upward conditions. This arrangement has implications for correlation both within and away from the study area. For instance, facies tracts identified in the Brassfield are bound by unconformable surfaces that are traceable throughout and away from the study area, yet the shallowing-upward packages and associated paraconformable surfaces that comprise the facies tracts themselves are far less ubiquitous.

The shallowing-upward motif is inexorably linked to relative changes in sea level (see the discussion on sedimentary cycles in the "Background" section of this report), and it is clear that sea level fluctuations played an important role in the depositional history of the Brassfield. However, because some levels of the hierarchy are widely correlative, while others can only be traced over short distances, the magnitude and extent of the processes involved in their deposition must have been quite variable.

TRANSGRESSIVE CYCLE ORDERS

Vail, et al. (1977) defined three major orders of transgressive-regressive depositional sequences that are correlative across the continental shelves of the world. Two first order sequences of 225 - 300 m.y. duration are identified in the Phanerozoic. The second order sequences identified in the Phanerozoic represent intervals of 10-80 m.y. and are delineated by major unconformities. Third order cycles are deposited over intervals of about 1-10 m.y.

Busch and Rollins (1984) further subdivide third order sequences into fourth order (0.8 - 1.5 m.y.), fifth order (400,000 - 450,000 yr.), and sixth order units (100,000 - 250,000 yr.). Sixth order cycles approximate the punctuated aggradational cycles described by Goodwin and Anderson (1980) and Anderson, et al. (1985).

The time limits given above for cycle orders are based on specific examples where strata of known age are divided by the number of cycles they contain. The number, thickness, or even presence of minor cycles can be greatly affected by local factors. Therefore, estimations of their periodicity may vary a great deal.

For instance, the small (on the order of meters) shoaling-upward cycles in the Upper Ordovician Cincinnatian have periods estimated at about 50,000 years (Tobin, 1982). These are possibly small sixth order cycles that represent about half the duration of the sixth order cycles described by Bush and Rollins (1984). Major cycles are probably not affected by local perturbations, so yield more consistent periods.

This study recognizes third through sixth order cycles in the Brassfield. Figure 97 illustrates the relationships between facies and facies tracts, third, fourth, fifth, and sixth order depositional units, and correlative and non-correlative unconformable surfaces. Note the ranking and coincidence of unconformable surfaces.

Second and Third Order Cycles

The unconformity at the base of the Silurian -- the base of facies I of the Brassfield Formation -- marks a major regression in the middle of a second order cycle that began with the Ordovician and continued through the end of the Silurian. The Brassfield Formation is a third order depositional sequence that represents an amount of time well within the limits given by Vail, et al. (1977). Because it is condensed, its thickness is more typical of fifth or sixth order cycles (see Goodwin and Anderson, 1980; Anderson et al., 1985; Busch and Rollins, 1984; and Brett and Baird, 1986 for discussions on cycle thickness).

In general, unconformities separating higher order sequences are of more significant duration than those separating lower order sequences. Therefore, the third order bounding surfaces below facies I (Belfast Member) and above facies VII (the Lee Creek Member) probably represent more time than the bounding surfaces separating facies tracts (fifth order) or smaller units within the Brassfield, and are more widely correlative. Rexroad (1967) has correlated the Dayton Formation in Ohio with facies VII of the Brassfield (the Lee Creek Member) on the basis of conodonts, effectively extending the

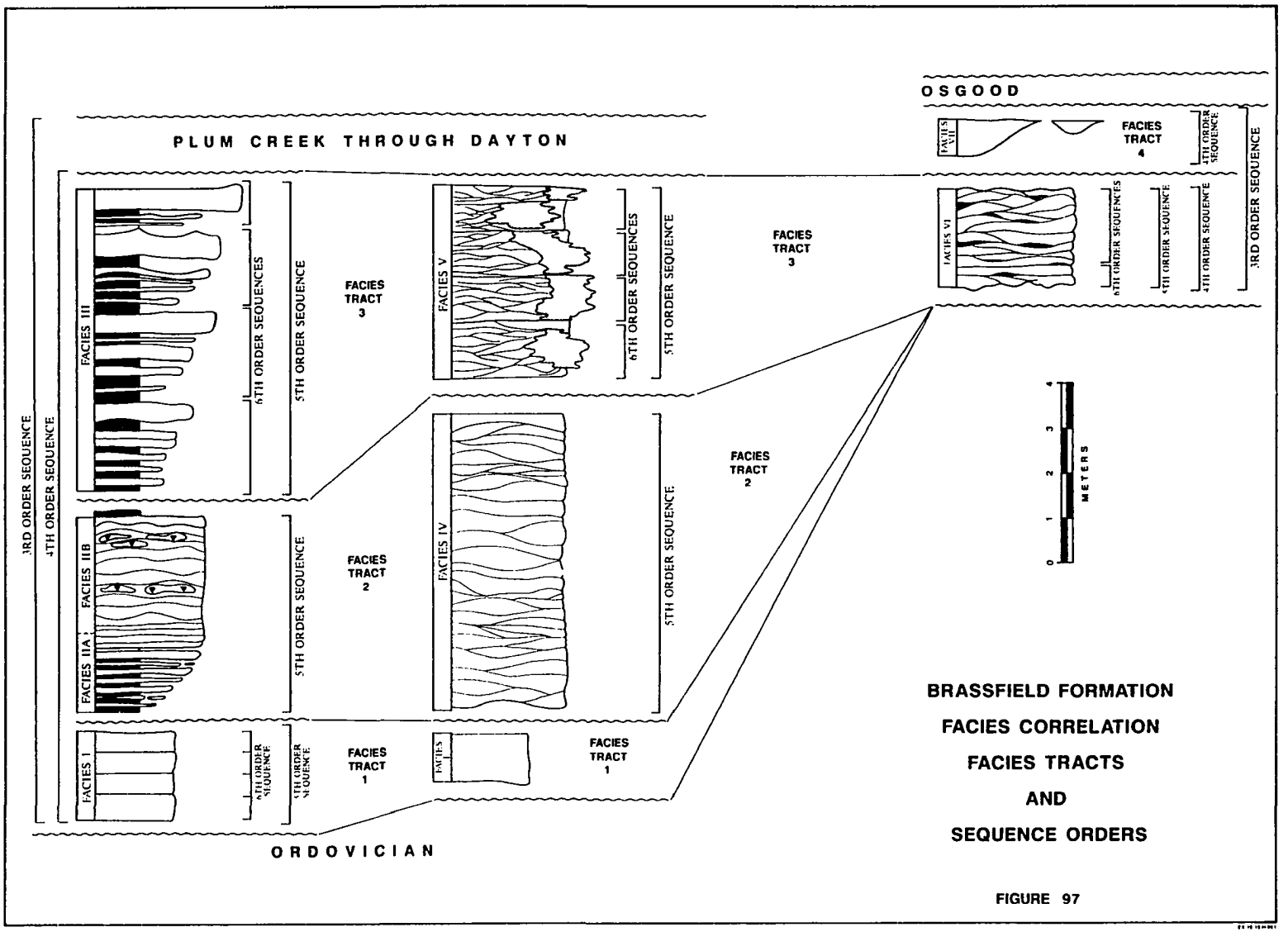

FIGURE 97

unconformity above facies VII from western Indiana eastward to the unconformity over the Dayton Formation in the Appalachian Basin.

Superimposed on the Brassfield third order cycles are fourth, fifth, and sixth order cycles. Third, fourth, and fifth order cycles are traceable across the study area, and possibly into neighboring basins. Sixth order cycles within facies tracts are only roughly correlative. The number, thickness, and petrology of sixth order cycles varies on an outcrop to outcrop scale.

Fourth Order Cycles

Facies traces 1 through 3, as a whole, represent a single fourth order cycle that begins with the initial stages of the basal Silurian transgression (it rests above the systemic boundary at the base of the Silurian), moves to somewhat deeper marine, distal to proximal tempestites, and is capped by sediments deposited under very shallow, shoaling conditions. The ironstones and associated unconformity at the top of this fourth order cycle can be correlated in outcrop from facies VI (below the Lee Creek) in eastern Indiana, to Ohio, above facies III and V, and south to central Kentucky above facies III. Facies tract 4 probably represents an entire fourth order cycle.

Fifth Order Cycles

Facies tracts 1, 2, and 3 are themselves fifth order cycles. Fifth order cycles cannot be identified in facies tract 4 (the Lee Creek) because it is too condensed. Fifth order Brassfield units consist of laterally correlative facies and unconformable bounding surfaces that are traceable throughout the study area.

They are usually shallowing-upward, as in faces tracts II-IV-VI and III-V-VI (with the exception of facies I, which represents only shallow water conditions, and facies VII, which represents deeper and quieter depositional conditions and is too condensed to determine changes in environment). Shallowing upward fifth order cycles range in thickness from less than 0.25 meters (facies I and VI) to over 8 meters (facies III).

Sixth Order Cycles

All fifth order Brassfield units are composed of sixth order units. Sixth order Brassfield units shoal - upward and range from a few cm to over four m in thickness. They are bound by unconformable and correlative conformable surfaces. Bundles of sixth order units are similar (for instance six units at locality 16, two at 37, three at 41, 51, and 52, and one at 5), but in most cases individual units can only be traced for short lateral distances.

SEA LEVEL CURVES

Figure 98 compares some published sea level curves from several that have been constructed for the Brassfield in this report. All curves show a significant drop in sea level at the Ordovician - Silurian boundary. All but Vail's (1977) global second order curve show a regression at the end of the Llandovery.

The Dennison and Head (1975) curve shows very little detail, illustrating an overall transgression through the Llandovery, followed by a drop in sea level

COMPARISON OF SEA LEVEL CURVES

FIGURE 98

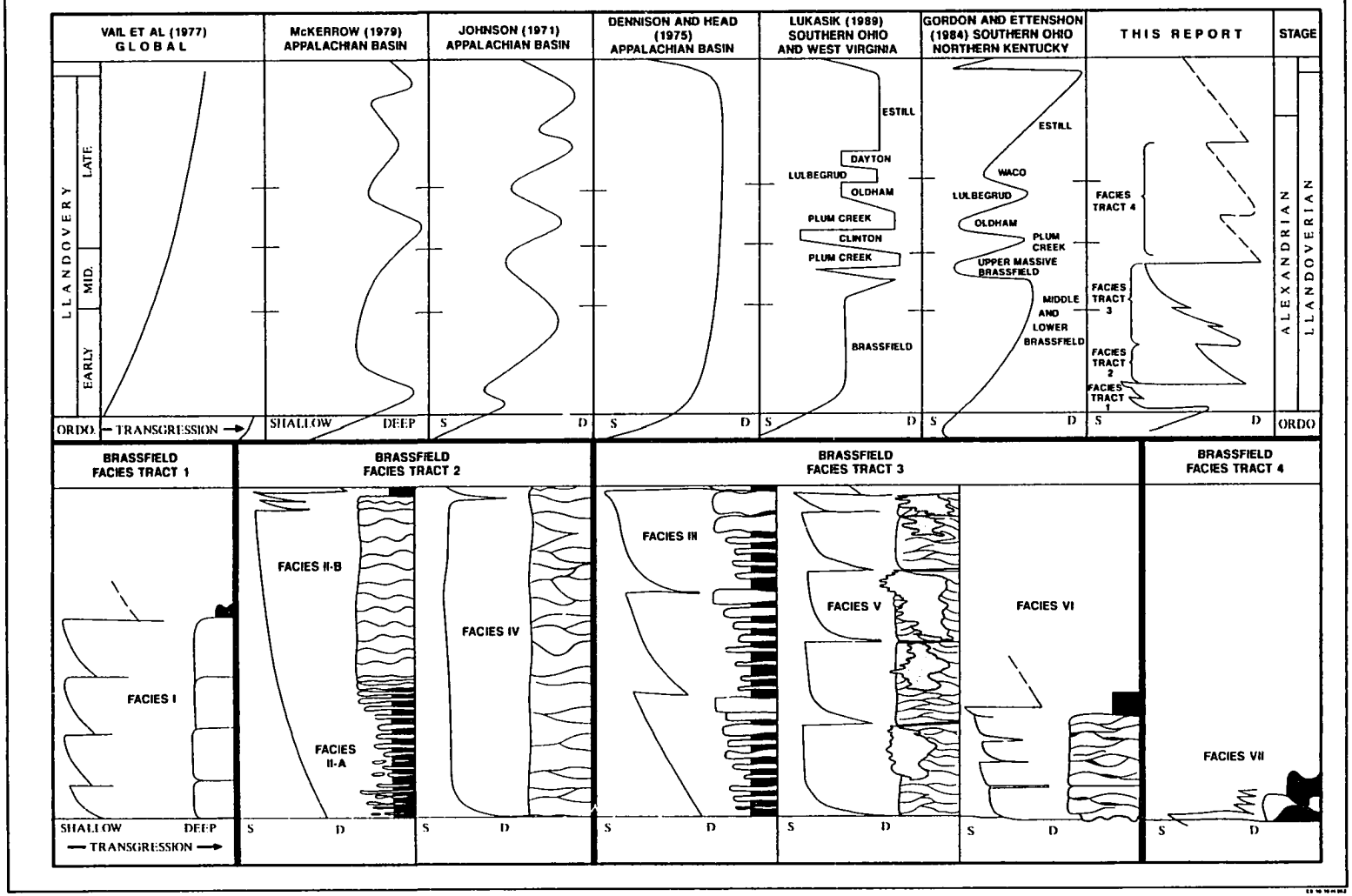

between the Llandovery and Wenlock Series. McKerrow (1979) and Johnson et al. (1981) include a transgression at the base of the basal Llandovery and basal Upper Llandovery, two small regressions in the Upper Llandovery, and a regression at the close of Llandovery. These curves correlate remarkably well with the Brassfield curves.

Third order curves are not easily seen on this scale, but the transgression illustrated on all curves at the base of the Llandovery is a third order boundary. Fourth order curves are at least roughly correlative. Particularly well illustrated is the correlation of the transgression at the top of facies tract 3 -- a fourth order boundary between Middle and Late Llandovery. Fifth and sixth order cycles are only illustrated on the curve from this report.

CONDENSATION OF THE BRASSFIELD FORMATION

The Brassfield Formation is a condensed sedimentary sequence. Its depositional history spans the Llandovery -- nearly 10 million years -- yet it is remarkably thin. Figure 99 illustrates the Brassfield and equivalent Lower Silurian strata, as well as periods of non-deposition, as they occur in time. The previous discussion has focused on the processes involved in the deposition of Brassfield sediments. The following discussion addresses Brassfield condensation processes in terms of four variables:

(1) condensation process;

(2) depositional sequence "orders";

(3) depositional environments represented by the various facies of the Brassfield Formation; and

(4) the lithology of condensed intervals in the Brassfield.

Types of Condensation Processes

Three modes of sedimentary condensation were outlined in the "Background" section of this report, all of which have affected condensation in the Brassfield. These include:

(1) frequent periods of rapid deposition combined with reworking, amalgamation of successive depositional events, and removal of sediments to deeper parts of the system (dynamic by-pass);

(2) moderate to rapid accumulations of sediment punctuated by extended periods of non-deposition or erosion (punctuated deposition);

LOWER SILURIAN STRATIGRAPHIC UNITS IN GEOLOGIC TIME

FIGURE 99

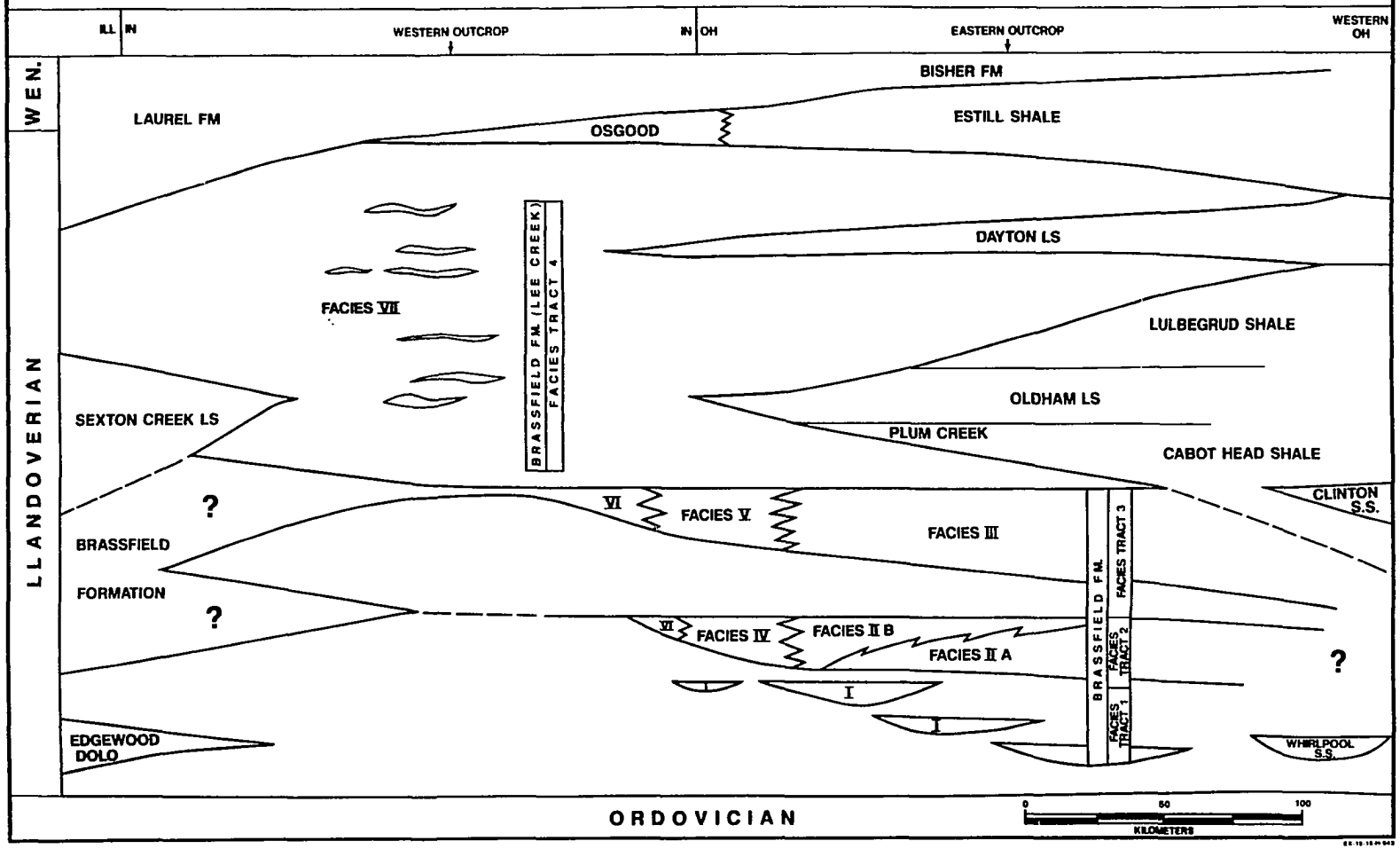

(3) persistence of very low sedimentation rates over extended periods (sediment starvation).

Some previous studies have addressed the effects of condensation on ecological and evolutionary information. In their discussion of postmortem bias of complexly amalgamated shell beds, Kidwell and Aigner (1985) present three shallow water condensation "pathways." The processes are similar to those described above, but they differ in scale. Kidwell and Aigner use two condensed sequences as examples: a Miocene section composed of six, 5 to 10 m condensed cycles that encompass a total of 2.5 m.y., and an Eocene section composed of seven, 3 to 8 m thick condensed cycles that encompass a total of 1.5 m.y. Their condensation regimes developed during transgressive cycles where shell gravel habitats were maintained over evolutionarily significant periods. However, the deposits encompass far less time, and are less intensely condensed than the Brassfield.

Depositional Sequence "Orders"

The Brassfield is composed of a hierarchy of third to sixth order depositional sequences. The type of condensation process and degree of condensation can be related to the order of the sequence in which the condensation occurs. Sequence order is related to the magnitude of relative sea level fluctuation. Larger order sequences, by definition, encompass longer periods of time than their constituent minor orders. Therefore, in a given depositional system, the condensed intervals associated with, for instance, third or fourth order sequences, potentially represent more time than fifth or sixth order sequences within the same system.

This hierarchy of condensation should not be used to compare condensation in neighboring basins. For instance, it would be incorrect to assume that a condensed interval associated with a fourth order cycle necessarily represents more time than a condensed interval associated with a fifth order cycle in a neighboring basin. The relationship also becomes less applicable to minor cycles. The difference between condensed intervals associated with fourth and fifth order sequences are not as great as between third and fourth or third and fifth order cycles.

Specific Depositional History of the Brassfield Formation

The Brassfield has a complex depositional history involving condensation by sediment saturation, punctuated deposition, and dynamic by-pass. Previous studies of condensation have made distinctions between two general types of condensed deposits deep water starved basin condensed deposits that accompany major sequences and changes in sea level, and short-term condensation associated with the shallow water phases of relatively minor (fifth or sixth order) cycles (Brett and Baird, 1986; Kidwell, 1989; Ensele and Seilacher, 1982; and Bayer and Seilacher, 1985). The Brassfield Formation provides an example of a significantly condensed deposit formed by processes usually limited to the formation of relatively small condensed intervals.

Lithology of Specific Condensed Intervals in the Brassfield

The lithologies of condensed intervals in the Brassfield vary according to condensation process, cycle order, and depositional environment. They can potentially be applied to other depositional systems.

PUNCTUATED DEPOSITION

Description

Rapid accumulations punctuated by periods of non-deposition or erosion are characteristic of distal tempestite sequences. Siliciclastic terrigenous input, or "background sedimentation", and autocthonus carbonate production is negligible. Frequency of storm-generated currents and availability of sediment determine the ratio of accumulated sediment thickness to time. Assuming that stronger storms generate currents that can carry sediment into deeper water, and that the effects of more common weaker storms are limited to shallower parts of the system, the frequency and intensity of storm influence at any given point on the shelf would increase with decreasing water depth. Given stable tectonic and eustatic conditions, sedimentation rate would be lowest at the base of a shallowing-upward sequence and increase up, simply by virtue of the decrease in water depth.

Thus, the base of shallowing-upward sequences can potentially be condensed, particularly where the depositional regime is dominated by infrequent periods of rapid deposition, punctuated by periods of low or non-deposition. However, if the system receives a continuous supply of fine terrigenous clastics, condensation will not occur. For instance, many of the cycles described by Tobin (1982) and Jennette (1986) in the Cincinnatian do not show condensation in their bases for this reason. Incidence and intensity of storm influence, and the amount (and thickness) of sediment deposited generally increases up, toward the middle of the sequence. Sequence tops may be dominated by by-pass condensation conditions (discussed below).

Occurrence in Cycle Orders

Condensation that accompanies punctuated deposition most commonly represents the base of fifth or sixth order shallowing-upward carbonate sequences. Where the base of the sequence coincides with a fourth, third or second order cycle boundary, the degree of condensation will likely be greater. Again if clastic input is high, this will not hold true.

Brassfield Examples and Lithology

Two types of condensation related to punctuated deposition occur in the Brassfield. Distal tempestites occur at the base of shoaling-upward storm dominated cycles, the base of Brassfield facies
IIA, the base of facies III, and the base of the minor shoaling cycles in facies III.

Glauconite accumulated during depositional hiatuses and was reworked into thin, horizontally laminated beds. Very fine, low angle laminated, normally graded, grainstones and packstones form discontinuous beds, beds with erosional bases, and features similar to gutter casts. Hardgrounds formed on more continuous beds or on upper surfaces of previously deposited shoaling cycles that lay exposed during sedimentary hiatus. Gordon (1980) describes in detail a hardground which occurs in his "thin-bedded unit." This would mark the base of a sixth order shoaling cycle in facies III in this report.

A second type of condensation related to punctuated deposition occurs at the base of thick, rapidly deposited packages that overlie surfaces formed

during periods of sedimentary hiatus. In this case, a period where the sea floor surface is exposed and sedimentation rate is low (following a fifth or sixth order sea level change) is followed by relatively rapid deposition of thick sands. Facies IV represents rapidly deposited shallow water carbonate sand shoals or subaqueous dunes. It is underlain by facies I and separated from it by a fourth order cycle boundary. This contact is glauconitic and very erosional. Also, at locality I, glauconite had apparently collected with fine grained sediments above facies I before the deposition of facies IV, as evidenced by the glauconite rich sedimentary injection dike that cuts up through facies IV.

The contacts between individual sixth order bioherm packages in facies V represent similar conditions. Small relative rises in sea level are followed by periods of non-deposition, accompanied by the formation of glauconite rich clay. Bioherm "core" organisms (stromatoporoids, rugose, Favosites and Halysities corals, and crinoids) colonized the exposed substrate, followed by further colonization by crinoids and rapid aggradation to very shallow conditions.

A minor sea level rise temporarily arrested sediment production and the process began anew. Contacts are erosional and glauconitic. The base of facies V is a composite fifth and sixth order cycle boundary, and is more obviously erosional than the strictly sixth order boundaries above.

Sixth order parasequences in facies I are separated by short intervals of sedimentary hiatus marked by erosional contacts, glauconite, omission

surfaces, and intense bioturbation. The glauconite in facies I formed during times of low sedimentation rate and was incorporated into overlying beds when sedimentation resumed. High silt content, characteristic of the facies I, seems to be typical of all basal Brassfield facies, and was probably eroded and concentrated from the underlying Ordovician.

DYNAMIC BY-PASS

Description

Reworking, amalgamation, and sediment by-pass are characteristic of shallow water, very proximal tempestite and upper shoreface conditions associated with the tops of shallowing-upward sequences. Short term gross sedimentation rate is high, but reworking and by-pass of sediments is great enough to significantly lower the overall net rate of accumulation.

More durable or survivable sedimentary components are concentrated under conditions of continuous reworking, amalgamation, and by-pass. These components include glauconite pellets and bioclasts, bone, teeth and other collophane fragments, phosphatized clasts, siliciclastic silt and sand, chert clasts, and hematitic bioclasts and oolites. Seilacher (1982) discussed the early phases of this type of condensation for carbonates, which begins with the "cannibalizing" of aragonitic shell fragments, followed by poly- or microcrystalline calcite shells, and finally echinoderm fragments, whose single crystal high-Mg composition is particularly durable.

Collophane fragments are the most resistant form of carbonate and tend to gain durability upon burial in phosphate rich sediments (Seilacher, 1982). These components are concentrated with each successive reworking, but are diluted with the addition of new material. Thus, a condensation lithology is developed slowly through successive amalgamation events.

Occurrence in Cycle Orders

Condensation through reworking, amalgamation, and by-pass is most commonly associated with the tops of shallowing upward packages, usually expressed as sixth, fifth, or fourth order cycles, though more major cycles could also be condensed in this way. Condensation under these conditions can be considerable, particularly in stable, topographically high areas where by-pass condensation conditions are maintained through several shallowing cycles, without development of deeper water non-bypass conditions. Condensation is intensified where an amalgamated deposit coincides with the upper boundary of a major sequence, because shallow conditions can presumably be maintained over longer periods.

Condensed oolitic ironstones are commonly formed at the tops of shallowing-upward sequences, many of which result from fifth or sixth order sea level changes, and can represent more than one shallow-upward cycle (Van Houten and Bhattacharyya, 1982; Hallman and Bradshaw, 1979). Ferric oxide and chamosite ooids are found in association with normal marine fauna characteristics of open, shallow littoral environments, and depauperate fauna characteristic of microtidal mudflats or brackish lagoons (Huner, 1970; Van

Houton and Bhattacharyya, 1982). Reduced detrital influx and moderately high energy are necessary conditions for their formation. Interruptions in accumulation permit precipitation of ferric oxide cement or phosphate, formation of hardgrounds, and accumulation of collophane fragments, marine mud, and glauconite (Van Houton and Bhattacharyya, 1982; Gygi, 1981). These associations have all been identified in the Brassfield Formation.

Brassfield Examples and Lithology

Amalgamated deposits are usually found at the tops of fully developed shoaling cycles in the Brassfield. The top of facies II is marked by coarse grainstones composed of a combination of newly deposited clasts (large unaltered and unabraided bioclasts) and indications of sedimentary hiatus (e.g., smaller abraded and glauconitized bioclasts, and hardgrounds), indicating amalgamation.

Facies III and V (fifth order cycles), and some sixth order cycles in facies III, are capped by one or more oolitic ironstone beds. These contain a mixture of condensed and non-condensed sediment that includes well developed hematitic ooliths, proto-oolith hematitic rims, hematitic intraclasts, non-hematitic glauconitic bioclasts that show varying degrees of glauconitization, abraded bioclasts, and large unbraided bioclasts (including originally aragonitic grains). This mixture would be expected in an amalgamation of condensed and newly deposited sediment.

Facies VI was deposited on a stable shallow part of the platform. It represents considerable condensation by reworking, amalgamation, and sedimentary by-pass through several sixth order cycles and possibly a fifth order cycle. It is unclear whether deposition of facies VI started coeval with facies II and IV, or facies III and V. Phosphatic horizons occur at the base, middle, and top of facies VI.

The variety of combinations of ironstone, glauconite, and phosphatic horizons in facies VI suggest a shifting mosaic of conditions favorable for their formation on the platform through time. The stratigraphy of phosphatic deposits within the iron rich sediments of facies VI should not be used as correlative markers for this reason. The close, but variable association of glauconite, phosphorite, and ironstones has been noted by Odin and Letolle (1980) and Van Houten and Bhattacharyya (1982). A possible scenario for the deposition of facies VI is as follows:

(1) Erosion of the Ordovician surface and formation of a conglomerate accompanied the initial transgression.

(2) Thin carbonate sands were deposited over much of the shallow platform.

(3) Shallow platform conditions prevail and less durable carbonate clasts are "weeded out," while the more durable single crystal crinoid bioclasts are concentrated both by amalgamation and autochthonous production.. Sedimentation is sporadic, and low enough at times to allow for colonization of the substrate by stromatoporoids.

(4) Minor (sixth order) rise in sea level temporarily halts deposition. Crinoid clasts are glauconitized in some areas and phosphatic pebbles and hardgrounds form in others. Fine material deposited in the late part of this stage is later resuspended and by-passed to deeper parts of the platform. Well formed glaucontie pellets (which may have originated as gluaconitized bioclasts) are mixed in with the fine material.

(5) Glauconitized bioclasts are reworked. Most are oxidized to a weathered brown rust color. Others are formed into actual oolitic ironstones. Many of these sediments are by-passed to deeper parts of the basin (to the east). Most non-crinoid components are removed by the ironstone stage. The ironstones in facies VI consist of nearly all hematitic crinoid bioclasts, while ironstones at the tops of facies III and V contain a wider variety of bioclasts.

Shifts in sea level return this cycle to a former stage and continued amalgamation of cycles yields facies VI.

SEDIMENT STARVATION

Description

Continuous low sedimentation rates are usually associated with moderate to major transgressions and deep, "starved basin" conditions. The deposits formed under these conditions are typically fine-grained pelagic to hemipelagic sediments (Van Wagoner, 1985; Wilson, 1975), bone beds (Reif, 1982), and glauconite rich bone sands with poorly preserved macroinvertebrate

shells (Kidwell, 1989). They are devoid of terrigenous sedimentation, as the rise in base level results in coastal alluviation of sediment and starvation of the shelf (Swift, 1968).

Occurrence In Cycle Orders

Formation of condensed sequences by sediment starvation is restricted to maximum transgressive conditions that result in a broad basin wide rise in base level. Local relative rises in sea level, such as those that formed the sixth order cycles in the Brassfield, may not be sufficient to form basin wide starved conditions. Starved basin conditions have only been identified in one fourth order Brassfield cycles .

However, minor (fifth or sixth order) cycles have been reported associated with starved basin type condensed deposits (Kidwell, 1989; Brett and Baird, 1986; Kidwell and Aigner, 1985). Minor-cycle sediment starved deposits should coalesce basinward into a more significantly condensed deposit that encompasses progressively larger scale cycles.

Brassfield Examples and Lithology

In the Brassfield, deep sediment starved conditions are represented by facies VII, a fourth order cycle deposit. It is a fine grained dolomite, with glauconite, collophane fragments, silt, and uncommonly, poorly preserved chertified bioclasts. Complete mottling is common, but some examples of lamination indicate at least occasional influence of currents.

Facies VII is correlative to the Cabot Head through Dayton Formation interval on the east side of the Cincinnati Arch (Nicolle and Rexroad, 1968; Rexroad, 1980). The transgressive and regressive events recorded in these strata should be traceable to individual condensed intervals on the east or north side of the Arch (if all evidence has not been eroded over the Cincinnati Arch) that coalesce westward into the Lee Creek.

REFERENCES CITED

Adams, J.E., H.N. Frenzel, M.L. Rhoads, and D.P. Johnson, 1951, Starved Pennsylvanian Midland Basin: American Association of Petroleum Geologists, v. 35, p. 2600-2607.

Adenuga, O.S., 1985, The petrology of the Brassfield Formation (Lower Silurian) between Richmond Indiana and Dayton, Ohio: unpublished MS thesis, Miami University, Oxford, Ohio, 63 pp.

Ager, D.V., 1981, *The Nature of the Stratigraphic Record* (ed.2): Halsted Press, New York, 122 pp.

Aigner, T., 1982, Calcareous tempestites: storm dominated stratification in Upper Muschelkalk limestones (Middle Triassic, SW-Germany), in U. Bayer, U. and A. Seilacher, eds., Sedimentary and Evolutionary Cycles: Berlin, Springer-Verlag, p. 180-198.

Aigner, T., 1984, Dynamic stratigraphy of epicontinental carbonates, Upper Muschelkalk (M. Triassic), South-German Basin: N. Jb. Geol. Palaont, Abh., v. 169, p. 127-159.

Aigner, T., 1985, Strom Depositional Systems: Heidelberg, Springer-Verlag, 174 pp.

Anderson, E.J., P.W. Goodwin, and T.H. Sobieski, 1984, Episodic accumulations and the origin of formation boundaries in the Helderberg Group of New York State: Geology, v. 12, p. 120-123.

Ausich, W.I., 1984a, Calyeocrinids from the Early Silurian (Llandoverian) Brassfield Formation of southern Ohio: Journal of Paleontology, v. 58, p. 1167-1185.

Ausich, W.I., 1984b, The genus Clidochirus from the Early Silurian of Ohio (Crinoidea; Llandoverian): Journal of Paleontology, v. 58, p. 1341-1346.

Ausich, W.I., 1985, New crinoids, and revisions of the superfamily Glypocrinacea (Early Silurian, Ohio): Journal of Paleontology, v. 59, p. 793-808.

Ausich, W.I., 1986a, Early Silurian Rhodocrinitcanean crinoids (Brassfield Formation, Ohio): Journal of Paleontology, v. 60, p. 84-106.

Ausich, W.I., 1986b, Early Silurian inadunate crinoids (Brassfield Formation, Ohio): Journal of Paleontology, v. 60, p. 719-735.

Ausich, W.I., 1986c, New camerate crinoids of the suborder Glyptocrinia from the Lower Silurian Brassfield Formation: Journal of Paleontology, v. 60, p. 887-897.

Badiozamani, K., 1973, The dorag dolomitization model - application to the Middle Ordovician of the Wisconsin: Journal of Sedimentary Petrology, v. 43, p. 965-984.

Baird, G.C., and C.E. Brett, 1981, Submarine discontinuities and sedimentary condensation in the upper Hamilton Group (Middle Devonian): Examination of marine shelf and paleoslope deposits in the Cayuga Valley, in Enos, P., ed, Guidebooks for Field Trips in South-Central New York: New York State Geological Association, 53rd Annual Meeting, p. 115-145.

Baker, A.A., J.W. Huddle, and D.M. Kinney, 1949, Palezonic geology of the north and west sides of Uinta Basin, Utah: American Association of Petroleum Geologists Bulletin, v. 33, p. 1161-1197.

Bally, A.W., ed., 1987, Atlas of Seismic Stratigraphy: American Association of Petroleum Geologists, Studies in Geology, no. 27, v. 1, 127 pp.

Bambach, R.K., C.R. Scoteese, and A.M. Ziegler, 1980, Before Pangea: the geographies of the Paleozoic world: American Scientist, v. 68, p. 26-38.

Barrell, J., 1917, Rythems and the measurements of geologic time: Bulletin of the Geological Society of America, v. 28, p. 745-904.

Bayer, U., E. Altheimer, and W. Deutschle, 1985, Environmental evolution in shallow epicontinental seas: sedimentary cycles and bed formation, in U. Bayer and A. Seilacher, eds., Sedimentary and Evolutionary Cycles: New York: Springer-Verlag, p. 347-381.

Bayer, U., and A. Seilacher, eds., 1985, Sedimentary and Evolutionary Cycles: New York, Springer-Verlag, 465 pp.

Becker, L.E., 1974, Silurian and Devonian rocks in Indiana southwest of the Cincinnati Arch: Indiana Geological Survey Bulletin 50, 83 pp.

Bernoulli, D., and H.C. Jenkyns, 1974, Alpine, Mediterranean, and central Atlantic Mesozoic facies in the relation to the early evolution of the Tethys: Society of Economic Paleontologists and Mineralogists Special Publication 19, p. 129-160.

Berry W.B.N., and A.J. Boucot, 1967, Pelecepod - graptolite association in the Old World Silurian: Geologic Society of America Bulletin, v. 78, p. 1515-1521.

Berry, W.B.N., 1970, Correlation of the North American Silurian Rocks: Geologic Society of America Special Paper 102, 289 pp.

Berry, W.B.N., 1972, Correlation of the South American Silurian rocks: Geological Society of America Special Paper 133, 59 pp.

Berry, W.B.N., 1973, Late Ordovician - Early Silurian platform sedimentation: Geologic Society of American Bulletin, v. 84, p. 275-284.

Beuf, S., B. Biju-Duval, J. Servaux, and G. Kulbicki, 1966, Ampeur des glaciations, Siluriennes au Sahara: leurs infruencset leurs consequences suer la sedimentation: Rev. Inst. Fr. Pet., p. 363-381.

Beuf, S., B. Biju-Duval, O. Decharpal, R. Rogon, O. Gariel, and A. Bennacef, 1971, Les gres du Paleozoique Inferieur Sahara-sedimentation et discontinuities; evolution structural d'un craton: Inst. Fr. Pet. Sci. Tech. Petrol., v. 18, 464 p.

Borden, W.W., 1875, (Geology of) Jefferson County, Indiana: Indiana Geological Survey, 6th Annual Report, p. 135-186.

Bowman, R.S., 1956, Stratigraphy and paleontology of the Niagaran section in Highland County, Ohio: unpublished Ph.D. dissertation, Ohio State University, Columbus, Ohio, 349 p.

Bretsky, P.W., 1970, Upper Ordovician Ecology of the Central Appalachians: Peabody Museum of Natural History Bulletin 34, Yale University, New Haven, 150 p.

Brett, C.E., and G.C. Baird, 1985, Carbonate-shale cycles in the Middle Devonian of New York: An evaluation of models for the origin of limestones in terrigenous shelf sequences: Geology, v. 13, p. 324-327.

Brett, C.E., and G.C. Baird, 1986, Symmetrical and upward shallowing cycles in the Middle Devoninan of New York state and their implications for the punctuated aggradational cycle hypothesis: Paleoceanography, v. 1, no. 4, p. 431-445.

Buckland, W., 1837, Geology and mineralogy considered with reference to natural theology, 2 v.: Philadelphia, Carey, Lea, and Blanchard, 443, 131p.

Burst, J.F., 1958, "Glauconite" pellets: their mineral nature and applications to stratigraphic interpretations: American Association of Petroleum Geologists Bulletin, v. 42, p. 310-327.

Busch, R.M., and H.B. Rollins, 1984, Correlation of Carboniferous strata using a hierarchy of transgressive-regressive units: Geology, v. 12, p. 471-474.

Butts, C., 1915, Geology and mineral resources of Jefferson County, Kentucky: Kentucky Geological Survey Series 4, v. 3, pt. 2, p. 59-70.

Byrne, R.M., 1961, The Ordovician-Silurian contact and related formations in Clark, Montgomery and Bath Counties: unpublished MS thesis, University of Kentucky, Lexington, Kentucky, 66 pp.

Calvert, W.L., 1968, Detailed discussion of outcrops observed at Ohio field stops, in Geological aspects of the Maysville-Portsmouth region, southern Ohio and northeastern Kentucky: Joint field conference, Ohio Geological Survey -Geological Society of Kentucky, guidbook, p. 21-37.

Colville, V.R., and M.E. Johnson, 1982, Correlation of sea-level curves for the Lower Silurian of the Bruce Peninsula and Lake Timiskaming District (Ontario): Canadian Journal of Earth Science, v. 19, p. 962-974.

COSUNA, 1985a, Midwestern basin and arches region, Correlation of stratigraphic units of North America project: American Association of Petroleum Geologists.

COSUNA, 1985b, Northern Appalachian region, Correlation of stratigraphic units of North America project: American Association of Petroleum Geologists.

Cressman, E.R., 1973, Lithostratigraphy and depositional environments of the Lexington Limestone (Ordovician) of Central Kentucky: United States Geological Survey Professional Paper 768, 61 pp.

Curray, J.R., 1960, Sediments and history of Holocene transgression, continental shelf, northwest Gulf of Mexico, in F.P. Shepard, F.B. Phleger, and T.H. van Andel, eds., Recent Sediments, Northwest Gulf of Mexico (API 51): published by the American Association of Petroleum Geologists, Collegate Press, Menasha, Wisconsin, p. 221-266.

Cuvier, G., 1817, Discours sur les Revolutions du Globe (ed. by F. Hoefer): Paris, Didot, 1867.

Darwin, C., 1859, *The Origin of Species*, London: John Murray (Facsimile edition, E. Mayr, ed.), Harvard University Press, 1964.

Dennison, J.M., 1976, Appalachian Queenston Delta related to eustatic sea-level drop accompanying Late Ordivician glaciation centered in Africa, in M.G. Basset, ed., The Ordovician System: Cardiff, Wales Press and National Museum of Wales, p. 107-120.

Dennison, J.M., and J.W. Head, 1975, Sea level variations interpreted from the Appalachian basin Silurian and Devonian: American Journal of Science: v. 275, p. 1089-1120.

Dott, R.H., Jr., 1983, Episodic sedimentation--How normal is average? How rare is rare? Does it matter?: Journal of Sedimentary Petrology, v. 53, p. 5-24.

Droste, J.B., R.H. Shaver, 1983, Atlas of Early and Middle Paleozoic paleogeography of the southern Great Lakes area: Indiana Geological Survey Special Report 32, 32 pp.

Dunham, R.J., 1962, Classification of carbonate rocks according to depositional texture, in W.E. Ham, ed., Classification of Carbonate Rocks: American Association of Petroleum Geologist Memoir, no. 1, p. 108-121.

Ehlers, E.G., and K.V. Hoover, 1961, The clay mineralogy of the shaly portions of the Brassfield Limestone: The Ohio Journal of Science, v. 61, p. 227-234.

Elles, G.L., and E.M.S. Wood, 1901-1918, Monograph of British graptolites, pts. I-XI: Paleontological Society of London, 539 pp.

Emery, K.O., 1968, Relict sediments on the continental shelves of the world: American Association of Petroleum Geologists Bulletin, v. 52, pp. 445-464.

Ensele, G., and A. Seilacher, eds., 1982, Cyclic and Event Stratification: New York, Springer-Verlag, 536 pp.

Folk, R.L., 1960, Petrology and origin if the Tuscarora, Rose Hill, and Keefer Formations, Lower and Middle Sillurian of eastern West Virginia: Journal of Sedimentary Petrology, v. 30, p. 1-58.

Folk, R.L., and L.S. Land, Mg/Ca ratio and salinity: two controls over crystalization of dolomite: American Association of Petroleum Geologists, v. 59, p. 60-68.

Foerste, A.F., 1891, On the Clinton oolitic iron ores: American Journal of Science, 3rd ser., v. 41, p. 28-29.

Foerste, A.F., 1896, An account of the Middle Silurian rocks of Ohio and Indiana: Cincinnati Society of Natural History Journal, v. 18, p. 161-190.

Foerste, A.F., 1897, A report on the geology of the Middle and Upper Silurian rocks of Clark, Jefferson, Ripley, Jennings, and southern Decatur Counties, Indiana: Indiana Department of Geology and Natural Resources, 21st Annual Report, p. 213-288.

Foerste, A.F., 1906, The Silurian, Devonian, and Irvine formations of east central Kentucky: Kentucky Geological Survey Bulletin, v. 7, 369 p.

Foerste, A.F., 1923, Notes on Medinan, Niagaran, and Chester fossils: Dension University Sci. Lab. Bulletin, v. 20, p. 37-120.

Foerste, A.F., 1931, Silurian fauna of Kentucky: Kentucky Geological Survey, Series VI, v. 36, p. 169-213.

Foerste, A.F., 1935, Correlation of Silurian formations in southwestern Ohio, southeastern Indiana, Kentucky, and western Tennessee: Dension University Sci. Lab. Bulletin, v. 14, p. 119-205.

Freeman, L.B., 1951, Regional aspects of Silurian and Devonian stratigraphy in Kentucky: Kentucky Geological Survey, Series 9, Bulletin 6, 565 pp.

Frost, J.P., 1977, A geologic study of the Brassfield Formation in portions of Green and Clark Counties, Ohio: unpublished MS thesis, Wright State University, Dayton, Ohio, 124 pp.

Fursich, F.T., 1971, Hartgrunde and Kondensation in Dogger von Calvados: Neus. Jahrb. Geol. Palaont. Abh., v. 138, p. 313-342.

Fursich, F.T., 1978, The influence of faunal condensation and mixing on the preservation of fossil benthic communities: Lethaia, v. 11, p. 243-250.

Fursich, F.T., 1979, Genesis, environments, and ecology of Jurassic Hardgrounds: Neues Jahrbuch Geol. Palaont. Abh. 158, p. 1-63.

Galliher, E.W., 1935, Geology of glauconite: American Association of Petroleum Geologists Bulletin, v. 19, p. 1569-1601.

Gebhard, G., 1982, Glauconitic condensation through high-energy events in the Albian near Clars (Escragnolles, Var, SE-France), in Bayer, U. and A. Seilacher, eds., Sedimentary and Evolutionary Cycles: Berlin, Springer-Verlag, p. 286-298.

Grant, N.K., T.E. Laskowski, and K.A. Foland, 1984, Rb-Sr and K-Ar ages of Paleozoic glauconites from Ohio - Indiana and Missouri, U.S.A.: Isotope Geoscience, v. 2, p. 217-239.

Gretener, P.E., 1967, Significance of the rare event in geology: The American Association of Petroleum Geologists Bulletin, v. 51, p. 2197-2206.

Goodwin, P.W., and E.J. Anderson, 1980, Punctuated aggredational cycles: A general hypothesis of stratigraphic accumulation: Geological Society of American Abstracts with Programs, v. 12, p. 436.

Gordon, L.A., and F. R. Ettensohn, 1984, Stratigraphy depositional environment and regional dolomitization of the Brassfield Formation (Llandovarian) in east-central Kentucky: Southeastern Geology, v. 25, p. 101-115.

Gould, S.J., 1965, Is uniformitarianisim necessary?: American Journal of Science, v. 263, p. 223-228.

Gray, H.H., 1972, Lithostratigraphy of the Maquoketa Group (Ordovician) in Indiana: Indiana Department of Natural Resources and Geological Survey Special Report 7, 31 pp.

Gray, J., and A.J. Boucot, 1972, Palynologycal evidence bearing on the Ordovician-Silurian paraconformity in Ohio: Geologic Society of American Bulletin, v. 83, p. 1299-1314.

Green, D.A., 1961, Cincinnati Arch Geologic Provence: Geologic Society of America 1961 Annual Meetings Abstracts with Programs, p. 60A.

Gygi, R.A., 1981, Oolitic iron formations: marine or not marine?: Eclogae geol. Hel., v. 74, p. 233-254.

Hallam, A., and M.J. Bradshaw, 1979, Bituninous shales and oolitic ironstones as indicators of transgressions and regressions: Journal of the Geologic Society of London, v. 136, p. 157-164.

Ham, W.E., and J.L. Wilson, 1967, Paleozoic epeirogeny and orogeny in the Central United States: American Journal of Science, v. 265, p. 332-407.

Hardie, L.A., 1987, Perspectives: Dolomitization: A critical view of some current views: Journal of Sedimentary Petrology, v. 57, p. 168-173.

Hardie, L.A., and M. Tucker, 1988, Chapter 7. X-ray powder diffraction of sediments, in M. Tucker, ed., Techniques in Sedimentology: Oxford; Boston, Blackwell Scientific Publications, p. 191-228.

Harland, W.B., A.V. Cox, P.G. Liewellyn, C.A.G. Pickton, A.G. Smith, and R. Walters, 1982, A Geologic Time Scales Cambridge University Press, Cambridge, 131 pp.

Harrison, W.B., 1974, Bivalvia of the Brassfield Formation of Kentucky, Indiana, and Ohio: unpublished Ph.D. dissertation, University of Cincinnati, Ohio.

Hayes, J.D., J. Imbrie, and J.J. Shackleton, 1976, Variations in the Earth's orbit: packmaker of the Ice Ages: Science, v. 914, p. 1121-1132.

Heim, A., 1934, Stratigraphische Kondensation: Ecolg. Geol. Helv., v. 27, p. 327-383.

Heim, A., 1958, Oceanic sedimentation and submarine discontinuities: Ecolg. Geol. Helv., v. 51, p. 642-649.

Heim, A., and O. Seitz, 1934, Die Mittlere Kreide in den helvetischen Alpen von Rheintal und Voralberg und das Problem der Kondensation: Denkschr. Schweiz. Naturf. Ges, v. 69, p. 185-310.

Hein, J.R., A.O. Allwardt, and G.B. Griggs, 1974, The occurrence of glauconite in Monterey Bay, California. Diversity, origins and sedimentary environmental significance: Journal of Sedimentary Petrology, v. 44, p. 562-571.

Hendrix, C.E., 1983, *Sedimentation and diagenesis of the Lower Silurian* Brassfield Formation Southwestern Ohio: unpublished MS thesis, University of Cincinnati, Cincinnati, Ohio, 201 pp.

Holbrook, C.E., 1964, Stratigraphic relationships of the Silurian and Devonian in Clark, Powell, Montgomery, and Bath Counties: unpublished MS thesis, University of Kentucky, Lexington, Kentucky, 79 pp.

Hsu, K.J., 1983, Actualistic catastrophism: Address of the retiring president of the International Association of Sedimentologists: Sedimentology, v. 30, p. 3-9.

Hunter, R.E., 1970, Facies of iron sedimentation in the Clinton Group, in G.W. fisher, F.J. Pettijohn, J.C. Reed, Jr., and K.N. Weaver, eds., Studies of Appalachian Geology: New York, Interscience Publishers, p. 101-124.

Hutton, J., 1788, Theory of Earth: Transactions of the Royal Society of Edinburough, v. 1, p. 208-304.

James, N.P., 1984, Shallowing-upward sequences in carbonates, in Walker, R.G., ed., Facies Models, 2nd ed.: Geoscience Canada Reprint Series 1, p. 213-228.

Janssens, A., 1967, Analysis of the Paleozoic movement of the Cincinnati Arch (abs.): Dissert. Abst., sect. B. Sci. and Eng., v. 28, p. 2481b-2482b.

Jenkyns, H.C., 1967, Fossil manganese nodules from Sicily: Nature, v. 216, p. 673-674.

Jenkyns, H.C., 1970, Fossil manganese nodules from the Sicilian Jurassic: Ecolg. Geol. Helv., v. 63, p. 741-774.

Jenkyns, H.C., 1971, The genesis of condensed sequences in the Tethyan Jurassic: Lethaia, v. 4, p. 372-352.

Jenkyns, H.C., and H.S. Torrens, 1969, Paleogeographic evolution of Jurassic seamounts in western Sicily: Preprint, Coll. Med. Jurassic Stratigr., Budapest, Sept. 1969, 19 pp.

Jennette, D.C., 1986, Storm dominated cyclic ramp deposits of the Kope-Fairview transition (Upper Ordovician) southwestern Ohio and northeastern Kentucky: unpublished MS thesis, University of Cincinnati, Cincinnati, Ohio, 210 pp.

Johnson, K.G. and G.M. Friedman, 1969, The Tully clastic correlatives (Upper Devonian) of New York State: A model for the recognition alluvial, dune (?), tidal, nearshore (bar and lagoon), and offshore sedimentary environments in a tectonic delta complex: Journal of Sedimentary Petrology, v. 39, p. 451-485.

Johnson, M.E., L.R.M. Cocks, and P. Copper, 1981, Late Ordovician - Early Silurian fluctuations in sea level from eastern Anticosti Island, Quebec: Lethaia, v. 4, p. 73-82.

Jones, O.T., 1925, On the geology of the Llandovery district, pt. 1: Geol. Soc. of London Quart. Jour., v. 81, p. 344-388.

Kallio, T.A., 1976, The stratigraphy of the Lower and Middle Silurian, Medina, Clinton, and Lockport Groups along Ohio Brush Creek in Adams County, Ohio: unpublished MS thesis, Miami University, Oxford, Ohio, 159 pp.

Kepferle, R.C., 1976, Gelogic map of the Crestwood Quadrangle, north-central Kentucky: United States Geological Survey Geologic Quadrangle Map GQ-1342, scale 1:24,000.

Kepferle, R.C., 1977, Geologic map of the Ballardsville Quadrangle, north-central Kentucky: United States Geological Survey Geologic Quadrangle Map GQ-1389, scale 1:24,000.

Kerr, J.W., 1976, Stratigraphy of central and eastern Ellsemere Island, Arctic Canada; pt. III, Upper Ordovician (Richmondian), Silurian and Devonian: Canadian Geological Survey Bulletin 260, 55 pp.

Kidwell, S.M., 1989, Stratigraphic condensation of marine transgressive records: origin of major shell deposits in the Miocene of Maryland: The Journal of Geology, v. 97, n.1, p. 1-24.

Kidwell, S.M., and T Aigner, 1985, Sedimentary dynamics of complex shell beds: implications for ecologic and evolutionary patterns, in Bayer, U. and A. Seilacher, eds., *Sedimentary and Evolutionary Cycles*: Berlin, Springer-Verlag, p. 383-395.

Kidwell, S.M., and D. Jablonski, 1983, Taphonomic feedback: ecological consequences of shell accumulation, in M.J. Tevesz and P.L. McAll, eds., *Biotic Interactions in Recent and Fossil Benthic Communities*: New York, Plenum Press, p. 195-248.

King, P.B., 1959, The Evolution of North America: Princeton University Press, Princeton, New Jersey, 189 pp.

Laferriere, A.P., D.E. Hattin, C.J. Foell, and T.F. Abdulkareem, 1986, The Ordovician - Silurian unconformity in southeastern Indiana: Indiana Department of Natural Resources and Geological Survey Occasional Paper 53, 12 pp.

Lapworth, C., 1879-1880, On the geological distribution of the Rhabdophora: Nat. Hist. Mag., Ser. 5, v. 3, p. 245-257, 449-445; v. 4, p. 333-341, 423-431; v. 5, p. 45-62, 273-285, 359-369; v. 6, p. 16-29, 185-207.

Laub, R.S., 1979, The corals of the Brassfield Formation (Mid-Llandovery; Lower Silurian) in the Cincinnati Arch region: American Paleontology Bulletin, v. 75, 457 pp.

Linney, W.M., 1882, Notes on the rocks of central Kentucky, with lists of fossils: Kentucky Geological Survey, 19 pp.

Locke, J., 1838, Geological Report: Ohio Geological Survey, 2nd Annual Report, 1859, p. 201-274.

Lukasik, D.M., 1988, Lithostratigraphy of Silurian rocks in southern Ohio and adjacent Kentucky and West Virginia: unpublished Ph.D. dissertation, University of Cincinnati, Cincinnati, Ohio, 314 pp.

Lumsden, D.N., 1979, Discrepancy between thin section and x-ray estimates of dolomite in limestone: Journal of Sedimentary Petrology, v. 49, p. 429-436.

Lyell, C., 1833, *Principles of Geology*, 1st ed.: London, Murray, v. 3, 389 p.

Marsiglia, K.M., and G.V. Klein, 1983, The paleogeography of Paleozoic and Mesozoic storm depositional systems: Journal of Geology, v. 91, p. 117-142.

McCave, I.N., 1969, Correlation using a sedimentological model of part of the Hamilton Group (Middle Devonian) of New York: American Journal of Science, v. 267, p. 567-591.

McCave, I.N., 1973, The sedimentology of a transgression: Portland Point and Cooksberg members (Middle Devonian), New York State: Journal of Sedimentary Petrology, v. 43, pp. 484-504.

McDowell, R.C., 1979, Lithostratigraphy of the Silurian outcrop belt on the east side of the Cincinnati Arch in Kentucky (abs.): Kentucky Geologic Mapping Project Symposium: Lexington, Kentucky, p. 18.

McDowell, R.C., 1983, Stratigraphy of the Silurian outcrop belt on the east side of the Cincinnati Arch in Kentucky with revisions in the nomenclature: United States Geological Survey Professional Paper 1151-F, 27 pp.

McKerrow, W.S., 1979, Ordovician and Silurian changes in sea level: Journal of the Geological Society of London, v. 136, p. 137-145.

Milankovitch, M., 1941, Konon der Eerbestrahlung und seine Anwendung auf das Eiszeitenproblem: Belgrade, Academie Royal serbe., 633 pp.

Morrow, D.W., 1982a, Diagenesis 1. Domomite - part 1: The chemistry of dolomitization and dolomite precipitation: Geoscience Canada, v. 9, p. 5-13.

Morrow, D.W., 1982b, Diagenesis 2. Dolomite - part 2: Dolomitization models and ancient dolostones: Geoscience Canada: v. 9, p. 95-107.

Newell, N.D., 1967, Paraconformities, in Teichert, C. and E. L. Yochelson, eds., Essays in Paleontology and Stratigraphy; R.C. Moore Commemerative Volume: University of Kansas Press, University of Kansas Special Publication no. 2, p. 349-367.

Nicoll, R.S. and C.B. Rexroad, 1968, Stratigraphy and conodont paleontology of the Salomonie Dolomite and Lee Creek Member of the Brassfield Limestone (Silurian) in southeastern Indiana and adjacent Kentucky: Indiana Geological Survey Bulletin 40, 73 pp.

Odin, G.S., and R. Letolle, 1980, Glauconitization and phosphatization environments: a tentative comparison: Society of Economic Paleontologists and Mineralogists Special Publication 29, p. 227-237.

Odin, G.S., and A. Matter, 1981, De glauconiarum origine: Sedimentology, v. 28, p. 611-641.

O'Donell, E., 1967, The Lithostratigraphy of the Brassfield Formation (Lower Silurian) in the Cincinnati Arch area: unpublished Ph.D. dissertation, University of Cincinnati, Cincinnati, Ohio, 143 pp.

Orton, E., 1869, Report of progress: Ohio Geological Survey, p. 268-290.

Orton, E., 1870, Report of progress: Ohio Geological Survey, p. 268-290.

Orton, E., 1873, Report on the third geological district: Geological Society of Ohio, v. 1, p. 416-463.

Orton, E., 1878, Geologic Survey of Ohio, v. 3, pp. 5, 384.

Orton, E., 1884, Geologic Survey of Ohio, v. 7, p. 11-13.

Owen, D.D., 1856, Geological Survey of Kentucky, 2nd Annual Report, p. 390.

Patchen, D.G., and R.A. Smosna, 1975, Stratigraphy and petrology of Middle Silurian McKenzie Formation in West Virginia: American Association of Petroleum Geologists Bulletin, v. 59, p. 2266-2287.

Peterson, L., 1981, Lithostratigraphy of the Silurian rocks exposed on the west side of the Cincinnati Arch in Kentucky: United States Geological Survey Professional Paper 1151-C, 29 pp.

Phleger, F.B., 1960a, Sedimentary patterns of microfaunas in northwest Gulf of Mexico, in F.P. Shepard, F.B. Phleger, and T.H. van Andel, eds., Recent Sediments, Northwest Gulf of Mexico (API 51): published by the American Association of Petroleum Geologists, Collegate Press, Menasha, Wisconsin, p. 267-301.

Phleger, F.B., 1960b, Recent sedimentology, northwest Gulf of Mexico; retrospect and prospect, in F.P. Shepard, F.B. Phleger, and T.H. van Andel, eds., Recent Sediments, Northwest Gulf of Mexico (API 51): published by the American Association of Petroleum Geologists, Collegiate Press, Menasha, Wisconsin, p. 365-367.

Pinsa, A.D., and R.H. Shaver, 1964, The Silurian formations of Indiana: Indiana Geological Survey Bulletin 32, 87 pp.

Rago, F.T., 1952, The Brassfield Formation of southern Indiana: unpublished MS thesis, Indiana University, Bloomington, Indiana, 41 pp.

Read, J.F., J.P. Grotzinger, J.A. Bova, and W.F. Koerschner, 1986, Models for generation of carbonate cycles: Geology, v. 14, p. 107-110.

Reif, W.E., 1985, Muschelkalk/Keuper bone-beds (Middle Triassic, SW-Germany) - storm condensation in a regressive cycle: in U. Bayer and A. Seilacher, eds., *Sedimentary and Evolutionary Cycles*: New York, Springer-Verlag, pl 299-325.

Rexroad, C.B., 1967, Stratigraphy and conodont paleontology of the Brassfield (Silurian) in the Cincinnati Arch area: Indiana Geological Survey Bulletin 36, 64 pp.

Rexroad, C.B., E.R. Branson, M.O. Smith, C. Summerson, and A.J. Boucot, 1965, The Silurian formations of east-central Kentucy and adjacent Ohio: Kentucky Geological Survey Bulletin, series X, v. 2, 34 pp.

Rich. J.L., 1951, Three critical environments of deposition, and criteria for recognition of rocks deposited in each of them: Bulletin of the Geological Society of America, v. 62, p. 1-20.

Rod, E., 1946, Uber ein Fossillager im oberen Malm der Melchtaieralpen: Ecolg. Geol. Hel., v. 39, p. 177-198.

Rodgers, J., 1967, Chronology of tectonic movements in the Appalachian region of eastern North America: American Journal of Science, v. 265, p. 408-427.

Sadler, P.M., 1981, Sediment accumulation rates and the completeness of stratigraphic sections: Journal of Geology, v. 89, p. 569-584.

Salop, L. J., 1977, Precambrian of the Northern Hemisphere: New York, Elsevier, 378 pp.

Savage, T.E., 1908, On the Lower Paleozoic stratigraphy of southwestern Illinois: American Journal of Science, 4th ser., v. 25, p. 431-443.

Schaub, H.P., 1948, Uber Aufarbeitung and Kondensation: Ecolg. Geol. Hel., v. 41, p. 89-94.

Schlager, W., 1981, The paradox of drowned reefs and carbonate platforms: Geological Society of America Bulletin, v. 92, p. 197-211.

Scholle, P.A., M.A. Arthur, A.A. Ekdate, 1983, Pelagic Environment, in P.A. Sholle, D.G. Bebout, and C.H. Moore, eds., *Carbonate Depositional Environments*: American Association of Petroleum Geologists Memoir, 33, p. 619-691.

Schuchert, C., 1913, The Cataract; a new formation at the base of the Siluric in Ontario and New York: Geologic Society of America Bulletin, v. 24, p. 107.

Schuchert, C., 1914, Medina and Cataract formations of the Siluric of New York and Ontario: Geologic Society of America Bulletin, v. 25, p. 277-320.

Scoteese, C.R., R.K. Bambach, C. Barton, R. Van der Voo, and A.M. Ziegler, 1979, Paleozoic base maps: Journal of Geology, v. 87, p. 217-277.

Scotford, D.M., 1964, The Cincinnati Arch: mineralogical-statistical evidence of a post-Ordovician origin: American Association of Petroleum Geologists Bulletin, v. 48, p. 427-436.

Seilacher, A., 1982, General remarks about event deposits, in G. Ensele and A. Seilacher, eds., Cyclic and Event Stratification: Springer-Verlag, New York, p. 161-174.

Seilacher, A., 1985, The Jeram Model: Event condensation in a modern intertidal environment: in U. Bayer and A. Seilacher, eds., Sedimentary and Evolutionary Cycles: New York, Springer-Verlag, p. 336-341.

Seslavinski, K.B., 1978, Ordovician and Silurian climates and global climate belts: International Geology Review, v. 21, p. 140-152.

Shaver, R.H., A.M. Burger, G.R. Gates, H.H. Gray, C.H. Hutchison, S.J. Keller, J.B. Patton, C.B. Rexroad, N.M. Smith, W.J. Wayne, and C.E. Wier, 1970, Compendium of rock unit stratigraphy in Indiana: Indiana Geological Survey Bulletin, v. 43, 229 pp.

Sheehan, P.M., 1972, The relation of Late Ordovician glaciation to the change over in North American brachiopod fauna: Lethaia, v. 6, p. 147-154.

Sheehy, T.J., 1981, Carbonate petrology of a carbonate buildup in the Brassfield Formation near Fairborn, Ohio: unpublished MS thesis, Wright State University, Dayton, Ohio, 51 pp.

Shell Oil Company, 1975, Stratigraphic Atlas -- North and Central America: Shell Oil Exploration Department, Houston, Texas.

Sibley, D.F., and J.M. Gregg, 1987, Classification of dolomite rock textures: Journal of Sedimentary Petrology, v. 57, p. 967-975.

Sloss, L.L., 1963, Sequences in the cratonic interior of North America: Geological Society of America Bulletin, v. 74, p. 93-113.

Smosna, R.A., and D.G. Patchen, 1978, Silurian evolution of central Appalachian Basin: American Association of Petroleum Geologists Bulletin, v. 62, p. 2308-2328.

Stith, D.A., and R.D. Stieglitz, 1979, An evaluation of "Newberry" analysis on the Brassfield Formation (Silurian) southwestern Ohio: Ohio Geological Survey Report of Investigations, v. 108, 25 pp.

Swanson, R.G., 1981, Sample Examination Manual: Publication of the American Association of Petroleum Geologists, Methods in Exploration Series, p. IVI-IV45.

Swartz, C.K. (chairman) et al., 1942, Correlation of the Silurian formations of North America: Geologic Society of America Bulletin, v. 53, p. 533-538.

Swift, D.J.P., 1968, Coastal erosion and transgressive stratigraphy: Journal of Geology, v. 76, p. 444-456.

Takahashi, J.I., 1939, Synopsis of glauconitization, in P.D. Trask, ed., Recent Marine Sediments. A symposium: Publication of the American Association of Petroleum Geologists, p. 502-512.

Teichert, C., 1958, Concept of facies: American Association of Petroleum Geologists Bulletin, v. 42, p. 2718-2744.

Theriault, F., and I. Hutcheon, 1987, Dolomitization and calcitization of the Devonian Grosmont Formation, Northern Alberta: Journal of Sedimentary Petrology, v. 57, p. 955-966.

Thompson, M.A., 1886, A sketch of the Silurian rocks of Indiana: Indiana Geology and Natural History, 15th Annual Report, p. 13-16.

Tobin, R.C., 1982, A model for cyclic deposition in the Cincinnatian Series of southwestern Ohio, northern Kentucky, and southeastern Indiana: unpublished Ph.D. dissertation, University of Cincinnati, Cincinnati, Ohio, 483 pp.

Trumpy, R., 1955, Wechselbeziehungen zwischen Palaogenographie und Deckenbau: Naturforschende Gesellschaft in Zurich, Vierteljahrsch ift, pt. C, p. 217-231.

Vail, P.R., R.M. Mitchum, and S. Thompson, III, 1977, Seismic stratigraphy and global changes of sea level, part 3: Relative changes in sea level from coastal onlap, in C.E. Payton, ed., Seismic Stratigraphy-Applications to Hydrocarbon Exploration: American Association of Petroleum Geologists Memoir 26, p. 63-97.

Van Andel, T.H., 1981, Consider the incompleteness of the geologic record: Nature, v. 294, p. 397-398.

Van Houton, F.B., and D.P. Bhattacharyya, 1982, Phanerozoic oolitic ironstones - geologic record and facies model: Annual Review of Earth and Planetary Science, v. 10, p. 441-457.

Van Wagoner, J.C.R.M. Mitchum, Jr., H.W. Posamentier, and P.R. Vail, 1987, Part 2: Key definitions of sequence stratigraphy, in A.W. Bally, ed., AAPG Atlas of Seismic Stratigraphy, v. 1, p. 11-14.

Varga, L.L., and W. B. Harrison, 1982, Dolomitization of Brassfield Formation (abs.): American Association of Petroleum Geologists Bulletin, v. 66, p. 638.

Warn, G.F., 1941, Silurian stratigraphic relations and Brassfield correlations: unpublished MS thesis, Northwestern University, Evanston, Illinois, 237 pp.

Weaver, C.E., 1958, Geologic interpretation of argillaceous sediments: American Association of Petroleum Geologists Bulletin, v. 42, p. 254-309.

Walker, R.G., 1984, Shelf and shallow marine sands, in R.G. Walker, ed., Facies Models, 2nd edition Geoscience Reprint Series 1, p. 141-170.

Weir, G.R., W.L. Peterson, and W.C. Swadley, 1984, Lithostratigraphy of Upper Ordovidian strata exposed in Kentucky: United Stated Geological Survey Professional Paper 1151-E, 121 pp.

Weiss, M.P., and W.C. Sweet, 1962, Contributions of facies analysis to Ordovician History of Cincinnati Arch provence (abs): Geological Society of American Special Paper 68, p. 294.

Wednt, J., 1970, Stratigraphische Kondensation in tradischen und jurassichen Cephalopodenkalken der Tethys: N. Jb. Geol. Palaont. Abh., v. 135, p. 171-189.

Wilgus, C.K., B.S. Hastings, C.G.St.C. Kendall, H.W. Posamentier, C.A. Ross, and J.C. Van Wagoner, eds., 1988, Sea-Level Changes: An Integrated Approach: Society of Economic Paleontologists and Mineralogists Special Publication 42, 407 pp.

Wilkinson, B.H., 1982, Cyclic cratonic carbonates and Phanerozoic calcite seas: Journal of Geological Education, v. 30, p. 189-203.

Wilson, J.L., 1975, *Carbonate Facies in Geologic History*: Springer-Verlag, New York, 471 p.

Woodward, H.P., 1961, Preliminary subsurface study of southeastern Appalachian interior plateau: American Association of Petroleum Geologists Bulletin, v. 45, p. 1634-1655.

Woolnough, W.G., 1942, Geological extrapolation and psudo-abyssal sediments: American Association of Petroleum Geologists Bulletin, v. 26, no. 5, p. 765-792.

Zenger, D.H., 1973, Syntaxial calcite borders on dolomite crystals, Little Falls Formation (Upper Cambrian), New York: Journal of Sedimentary Petrology, v. 43, p. 118-124.

Ziegler, A.M., L.R.M. Cocks, and R.K. Bambach, 1968, The composition and structure of Lower Silurian marine communities: Lethaia, v. 1, p. 1-27.

Ziegler, A.M., K.S. Hansen, M.E. Johnson, M.A. Kelly, C.r. Scoteese, and R. Van Der Voo, 1977, Silurian continental distributions, palegeography, climatology, and biogeography: Tectonophysics, v. 40, p. 13-51.

Ziegler, A.M., C.R. Scoteese, W.S. McKerrow, M.E. Johnson, and R.K. Bambach, 1979, Paleozoic paleogeography: Annual Review of Earth and Planetary Sciences, v. 7, p. 473-502.

Ziegler, A.M., M.L. Hulver, A.C. Lotts, and W.F. Schmachtenberg, 1984, Uniformitarianism and paleoclimate inferences from the distribution of carbonate rocks, in P. Brenchely, ed., *Fossils and Climate*: Wiley, New York, p. 3-23.

APPENDIX 1

OUTCROP LOCATIONS

1) Roadcut on the east side of Rt. 527, on the north edge of Raywick, Marion Co., KY.
2) Roadcut on the east side of Rt. 49, 3.9 miles south of Rt. 150, south of Bardstown, Marion Co. KY.
3) Several roadcuts along the south side of Blue Grass Parkway just east of the bridge across the Rolling Fork, Nelson Co., KY.
4) Roadcut along Blue Grass Parkway west of Bardstown where it crosses Beach Fork, Nelson Co., KY.
5) Roadcut 2.2 miles west of Bardstown on Rt. 62, just east of a small lake, Nelson Co., KY.
6) Roadcut on Rt. 480 about 1 mile west of where the highway crosses Cox's Creek and 3 miles west of the Bullit-Nelson Co. line, near Solitude, Bullit Co., KY.
7) Roadcut just above a small abandoned quarry on the north side of Seatonville Rd.on Floyds Fork Creek, about 1 mile west of Seatonville, Jefferson Co., KY.
8) Exposure on the west side of Brownsboro Road, 0.4 miles south of the bridge over South Fork Harrod's Creek, Oldham Co., KY.
9) Large roadcut on the north side of Indiana Highway 62 on the east bluff of Fourteen Mile Creek, 3 miles northeast of Charlestown Clark Co., IN.
10) Small outcrop on the northeast side of the road near top of Ohio River bluff, 1.3 miles west of Bethlehem, Clark Co., IN.

11) Near the top of Ohio River bluff about 200 yards above Hearts Falls Creek, Jefferson Co. IN.

12) Natural exposure above a waterfall about 0.3 miles along the road leading into the north side of Hanover College campus, Jefferson Co., IN.

13) Roadcut on northwest side of Rt. 56 (Powerhouse Road), 1.8 miles west of the entrance to Clifty Falls State Park near Madison, Jefferson Co., IN.

14) Several roadcuts along the south side of River Road on Devils Backbone, Jefferson Co., IN.

15) Exposure at the top of a long outcrop on Rt. 7 (Hanging Rock Road), 1 mile north of Madison, Jefferson Co., IN.

16) Exposures in the cut in the hill north of Madison on Rt. 421 above a small creek that passes below the highway, Jefferson Co., IN.

17) Exposures on the north side of Indiana highway 62, 1.5 miles west of Canaan, Jefferson Co., IN.

18) Outcrops above and below Rt. 225 East, 2 miles east of Rexville, Ripley Co., IN.

19) Quarry of the Tri-County Stone Company, 4 miles south of Cross Plains (Ripley Co.), Switzerland Co., IN.

20) Stream bed exposure 10 meters north of its intersection with county road 1150 N., 1.5 miles east of Rt. 421, and about 2 miles northeast of Bryantsburg, Ripley Co., IN.

21) Small (6 foot) waterfall 100 meters west of Rt. 129, 1.5 miles north of Olean, Ripley Co. IN.

22) Stream cut along a small east-west stream about 2.3 miles north-northeast of Osgood, Ripley Co. IN.

23) The Napoleon Quarry of the New Point Stone Co., 0.9 miles east of Napoleon on Indiana 229, Ripley Co., IN.

24) New Point Stone Co. Quarry, 1 mile north of the Village of New Point on county road 800 E, 0.6 miles west of the access road to I-74, Decatur Co., IN.

25) Exposure near the top of the east bluff of Righthand Fork, 1/4 mile upstream from where the stream crosses the road, marked by a small power station; no road name, but located on line between NE1/4 SW1/4 and NW 1/4 SE1/4 sec. 22, T 11 N, R 11 E, Franklin Co., IN.

26) Derbyshire Quarry on Rt. 52 3.3 miles west of its intersection with Rt. 121, Franklin Co., IN.

27) Natural exposure in the northeast fork of Sains Creek, 2.3 miles west of Laurel, Franklin Co., IN.

28) Abandoned quarry of Fall Creek Stone Co. (Sarha Johnson's Property on Bunker Hill); SE1/4 NW1/4 sec. 5, T 13 N, R 12 E.

29) Rt. 227 and Elkhorn Creek at Elkhorn falls, 2.5 miles south of Richmond, just before 227 reaches Wolf Road, Wayne Co., IN.

30) Natural exposure on Sevenmile Creek, about 2 miles south of Eaton Preeble Co., where Ohio Rt. 127 crosses the creek.

31) Piqua - Aramco Steel Co. Quarry, off the state road 1.1 miles west of Piqua, Miami Co., OH.

32) Ludlow Crush Stone Quarry, Ludlow Falls, Miami Co., OH.

33) Roadcut on Ohio Rt. 71, 0.25 miles east of West Milton, Miami Co., OH.

34) Ernst Quarry, 100 yards south of Ohio Rt. 440, 0.5 miles east of Taylorsville Dam, Montgomery Co., IN.

35) Wright Brothers Memorial, exposure above railroad tracks and below the Memorial where it faces Huffman Dam, Montgomery Co., OH.

36) Core, archived at Wright State University, taken on the Antioch College campus, Green Co., OH.

37) Stream cut and very small abandoned quarry about 1000 feet east of McKay Rd., 0.2 miles south of where McKay Rd. crosses Anderson Fork Creek, Clinton Co., OH.

38) Stream cut and small abandoned quarry on the north side of Todd Fork 400 yards upstream from Center Rd., Clinton Co., IN.

39) Exposure in an abandoned quarry and stream cuts southwest and northeast of intersection between Quarry Rd. and Sharpsville Rd., 1.5 miles east of Lynchburg, Highland Co., OH.

40) Intersection of Ohio Rt. 73 and Cucko Rd. 50 yards from where 73 crosses Flat Run, and 1.6 miles west of Louden, Adams Co., OH.

41) Roadcut on the west side of Ohio Rt. 41, on the south bluff of Ohio Brush Creek, 1.4 miles south of Jacksonville, Adams Co., OH.

42) Roadcut on the north side of US 52 where Ohio Brush Creek enters the Ohio River, 9 miles east of Manchester, Adams Co., OH.

43) Roadcuts on both sides of Kentucky Rt. 10, 2.5 miles east of intersection with Kentucky Rt. 57 in Tollesboro, Lewis Co., KY.

44) Roadcut on Kentucky Rt. 32 about 1 mile northwest of Goddard and 6.5 miles southeast of Flemingsburg, Flemming Co., KY.

45) Exposure on the north side of Kentucky Rt. 111, 0.5 miles north of Grange City, Fleming Co., KY.

46) Roadcuts on the south bluff of a tributary to Storey Creek, 0.7 miles north from the road junction in Colfax, Fleming Co., KY.

47) Roadcuts along I-64 just west of the Owingsville/Fredricksburg exit (exit #121), Bath Co., KY.

48) Roadcut on the east side of Stepstone Rd. just south of the I-64 underpass at Sugargrove Church, Bath Co., KY.

49) Roadcut on the north side of Mountain Parkway where the highway crosses Howards Creek, Clark Co., KY.

50) Exposures in a roadcut on the east side of Kentucky Highway 89 near the top of the south bluff of the Red River, Estill Co., KY.

51) Exposures on both sides of Rt. 52 on the east bluff of Drowning Creek near the Estil/Madison Co. line and near Winston, Madison Co., KY.

52) Exposure along Rt. 52, 0.5 miles west of Waco, on the east side of a bridge over Muddy Creek, Madison Co., KY.

53) Exposure along Rt. 52, 1 mile southeast of Bybee, Madison Co., KY.

54) Railroadcut exposure on the west side of Louisville and Nashville tracks where they are crossed by a secondary road 0.5 miles north of the Farristown Church, Madison Co., KY.

55) Exposure in a roadcut on the east side of I-75 about 500 feet north of the overpass of Rt. 595, about 3 miles northwest of Berea, Madison Co., KY.

56) Exposure on Rt. 150 on the east side of a bridge where it crosses Cedar Creek, 2.5 miles west of Crab Orchard, Lincoln Co., KY.

APPENDIX 2

PETROGRAPHIC TABLES

2A - GENERAL PETROGRAPHIC

2B - BIOCLAST CONSTITUENTS

2C - TEXTURE

2D - DOLOMITE CHARACTER

APPENDIX 2A

PETROGRAPHIC CONSTITUENTS

EXPLANATION OF ABRIVIATIONS

ROCK TYPE :

M = MICSTONE

S = SILTSTONE

D = DOLOMITE (COULD NOT DETERMINE ORIGINAL TEXTURE)

W = WACKESTONE

P = PACKSTONE

G = GRAINSTONE

APPENDIX TABLE 2A
PETROGRAPHIC CONSTITUENTS

LOCATION	SAMPLE	FACIES	ROCK TYPE	BIOCLASTS	INTRACLASTS	PEBBLES	PELLETS	Fe OOIDS	QTZ SILT	MICRITE	CCT CEMENT	DOLOMITE	CHERT	PYRITE	NO ID
36	AC128	1	S				tr		tr			100			
36	AC131	1	S									100			tr
29	EF1	1	D									83		17	
29	EF1.2	1	D				3			tr	tr	96		1	
29	EF1.8	1	W	3							16	81			
29	EF1.9	1	D						tr		tr	97	2	1	
34	EQ1.1	1	S						4		1	95			tr
37	L2B	1	S						3		2	95			
37	L4A	1	S				tr		1		1	98			
41	OBC14	1	S						10			90			
35	WBM5.5	1	S				3		1		tr	96			
35	WBM5.6	1	S	3							7	90			tr
	AVERAGE	N/A	N/A	0.50	0.0	0.0	0.50	0.0	1.58	0.0	2.25	93.42	0.17	1.58	0.0
41	OBC12	2A	P	44						32	17	7	tr		
41	OBC13	2A	G	52						10	32	6			
39	TC1	2A	S/G				4		1		2	92	tr	1	
	AVERAGE	N/A	N/A	32.00	0.0	0.0	1.33	0.0	0.33	14.00	17.00	35.00	0.0	0.33	0.0
41	OBC10	2B	G	54			1				45	tr			
41	OBC11	2B	P	21					tr	35	10	4	30		
	AVERAGE	N/A	N/A	37.50	0.0	0.0	0.50	0.0	0.0	17.50	27.50	2.00	15.00	0.0	0.0
41	OBC2	3	mG	40			2	12		10	29	7			
41	OBC3	3	G	39	25		tr	tr		1	32	3			
41	OBC4	3	G	11			1	47			41				
41	OBC5	3	G	53			6			4	37				
41	OBC8	3	mG	60							37	3			
41	OBC9	3	P	47			1		tr	9	11	32			
	AVERAGE	N/A	N/A	41.67	4.17	0.0	1.67	9.83	0.00	4.00	31.17	7.50	0.0	0.0	0.0
36	AC115	4	mG	56	1		tr			9	20	14			
36	AC120	4	mG	57						8	29	6		tr	
36	AC123	4	D									100			
36	AC125	4	D								1	99			tr
34	EQ2.5	4	G/P	43			6			12	16	23			
34	EQ3.0A	4	mG	61			4			8	22	5			
34	EQ3.0B	4	G	30							7	63			
32	LF2	4	W								6	94			
32	LFLW	4	P	49						27	10	14			
30	SMC1A	4	mG	60						5	31	4		tr	
30	SMC2B	4	mG	56			tr		tr	4	27	13			
38	TF3B	4	G	62			10		tr		24	4			
38	TF5	4	P	46			19			11	18	6		tr	
35	WBM3.0	4	G/P	52		tr					12	36			
33	WM1A	4	G	61			12				26	tr		1	
33	WM1B	4	G	59			3			4	24	10			
33	WM2A	4	G	66			2			1	30	1			tr
33	WM3	4	G	66			4			1	20	9			
33	WN4A	4	G	54			11			tr	34	1			tr
	AVERAGE	N/A	N/A	46.21	0.05	0.0	3.74	0.0	0.0	4.74	18.79	26.42	0.0	0.05	0.0

APPENDIX 2A
PETROGRAPHIC CONSTITUENTS
-Continued-

LOCATION	SAMPLE	FACIES	ROCK TYPE	BIOCLASTS	INTRACLASTS	PEBBLES	PELLETS	Fe OOIDS	QTZ SILT	MICRITE	CCT CEMENT	DOLOMITE	CHERT	PYRITE	NO ID
36	AC107	5	P	42					tr	5	25	28		tr	
36	AC99	5	B	21						70	5	4			
29	EF2.0B	5	G	53			tr				23	23		1	
29	EF2.0B'	5	D				1					96		3	
29	EF2.3	5	G/P	48			tr				8	44		tr	
29	EF3.5	5	mG	59							tr	41		tr	
29	EF3.7	5	G	58			2			tr	39	1		tr	
29	EF3.8	5	G	56			1			1	40	1		1	
29	EF3.9	5	mG	38			5			3	40	14			
29	EF4.0	5	mG	61			2				27	10			
29	EF4.2	5	G	33			3				26	38			
29	EF4.5	5	G	51			3			1	42	3			
29	EF4.9	5	G	58			6				34	2		tr	
29	EF5.3	5	G	40						1	31	27		1	
29	EF5.5	5	G	45							39	16			
29	EF6.0	5	G	54			2				34	10			
29	EF6.1	5	G	56							37	6		1	
29	EF6.2	5	G	55			tr				29	16			
34	EQTM	5	G	61			2	3		6	21	2			5
34	EQTOP	5	G	59			1			1	28	7			4
37	L5B	5	P	55			2			41	1	1			
37	L6	5	G	31			30		tr	4	34	1			
37	L7A	5	G	56			tr			2	42	tr			
37	L7B	5	P	48			1		tr	18	33	tr			
37	L7T	5	G	79			2			2	16	tr			1
32	LF7	5	mG	78						10	10	2	tr	tr	
32	LF8	5	M/W				1		tr		5	94			
32	LFB	5	W	18					tr	49	9	24	tr		
30	SMC3C	5	mG	62			tr		tr	7	27	3			1
30	SMC4B	5	G/P	54			tr			8	29	9			
38	TF6A	5	G	45			12			6	34	2			1
38	TF6C	5	G	42			23			1	33				
38	TF7A	5	G	71			1			2	20	6			
38	TF8A	5	G	73			5				22	tr			
38	TF8B	5	G	55			8				31	5			1
38	TF9A	5	G	23	1			39			37	tr			
38	TF9B	5	G	58			tr	2			39	tr			1
38	TF9C	5	G	12				44			43	1			
35	WBM1.7	5	G/P	71			tr			9	12	8			
35	WBM2.0	5	G	67			7			5	21	tr			
33	WM6	5	G	81			3				15	1		tr	
33	WM7	5	G	60			6		tr	tr	31	3		tr	
33	WMBC	5	B	73						19	1	7		tr	
33	WMBHT	5	mG	76						9	14	1			
	AVERAGE	N/A	N/A	50.82	0.02	0.0	2.93	2.00	0.0	6.36	24.70	12.66	0.0	0.16	0.34

APPENDIX TABLE 2A

PETROGRAPHIC CONSTITUENTS
-Continued-

LOCATION	SAMPLE	FACIES	ROCK TYPE	BIOCLASTS	INTRACLASTS	PEBBLES	PELLETS	Fe OOIDS	QTZ SILT	MICRITE	CCT CEMENT	DOLOMITE	CHERT	PYRITE	NO ID
8	BR1.65	6	M/P	51	tr		1			22	26	tr	tr		
8	BR2.65	6	G	53		tr	4			4	39	tr			
17	C2.6	6	G	58			tr				42				
17	C2.7	6	W	17			3		2	37	4	37			
11	FC2.0	6	G	72			1			tr	24	2		1	
11	FC2.25	6	G	66			3				27	4		tr	
15	HR2.16	6	mG	55			4			11	26	3		1	
16	M1A	6	G	69			tr		tr			31			
16	MB1	6	G/P	46			tr		1	17	30	6			
16	MB2	6	G	59						3	37	1	tr		
16	MN2.2	6	G	37							25	38			
16	MN2.85	6	D								21	78		1	
24	MPQ2.3	6	W/P	17			2			62	19	tr			
24	NPQ2.95	6	G	38		26	2			1	33	tr			
24	NPQ2.3B	6	G	68						4	28				
24	NPQ2.45	6	P/W	22			tr			66	9	2		1	
23	NPQ	6	P	15					1	65		17		2	
23	NQ1	6	P/W	34					1	32		33			
23	NQ2	6	W	37					1	31		31			
23	NQ3	6	P	49				6	tr	36	2	7			
23	NQ4	6	mG	27	17			20		9	21	6			
23	NQ5	6	G/P	50	25		6		tr		19	tr			
23	NQ6	6	P/G	42			6		2	25	19	4		2	
23	NQ7	6	G	59	2		1		tr		38				
23	NQBASE	6	G/P	51	1					15	24	9			
23	NQS	6	G	44	5					1	49	1			
21	01.8	6	G/P	42	tr		4		tr	11	35	8			
21	03.0	6	G	46			3			7	44	tr			
22	PC2.0	6	G/P	48	3		4			20	19	6			
20	PQ	6	G	54	tr		4		tr		41	tr		1	
13	PR1.6	6	P	46			3			35	12	4			
18	R2.2	6	W	10						90	tr	tr			
18	R2.3	6	P	36		11	7			38	8	tr			
18	R2.35	6	G	34	49		3			2	12				
18	R2.3	6	P	45	8		1			44	1	1			
18	R2.75	6	G	57						8	34	1		tr	
25	RHF2.1	6	G	56			2				42	tr			
25	RHF2.8	6	G	49			2				49	tr			
25	RHF3.9	6	G	54			3			17	26	tr			
25	RHF4.4	6	mG	34						32	33	tr		1	
6	S1.9	6	mG	41			tr			12	26	21			
6	S2.1	6	mG	35			19				29	17			
6	S.25	6	P	35					tr		1	64			
6	S2.6	6	G/P	44			4			16	35	1			
6	SR2.4	6	G	56							36	8			
6	SR2.7	6	G/P	42					tr	tr	8	40	10		
19	TCS1.7	6	G/P	34			12			13	29	12		tr	
19	TCS1.8	6	G	45	25						25	5			
19	TCS1.9	6	G/P	22			5				20	53		tr	
19	TCS3.0	6	G/P	25			1				19	55			
	AVERAGE	N/A	N/A	42.52	2.70	0.74	2.20	0.52	0.16	15.72	22.92	12.12	0.20	0.20	0.0

APPENDIX TABLE 2A

PETROGRAPHIC CONSTITUENTS
-Continued-

LOCATION	SAMPLE	FACIES	ROCK TYPE	BIOCLASTS	INTRACLASTS	PEBBLES	PELLETS	Fe OOIDS	QTZ SILT	MICRITE	CCT CEMENT	DOLOMITE	CHERT	PYRITE	NO ID
14	DBLC	7	W/M			tr	2		1		3	92	2		
14	DBLC2	7	D	tr		tr	1		2		2	81	14		
15	HR2.7	7	D				1				tr	91		tr	8
16	MN2.9	7	D				3		tr		1	96			
13	PR2.0	7	W/M			1	3		2			92	2		
7	SR2.8	7	W				tr		tr			99	1		
7	SR3.3	7	D								3	71	tr		26
19	TCS3.4	7	D		tr	1	tr					97	1	1	
	AVERAGE	N/A	N/A	0	0	.25	1.25	0.0	.63	0.0	1.13	89.88	2.50	0.13	4.25
31	AC93	DAY	M				tr		1			99			
31	AC96	DAY	M								6	94			
24	NPQ2.6	DAY	P	11						tr	4	85			
41	OBC1	DAY	P	58			1			19	17	5			
25	RHF4.6	DAY	D								13	87		tr	
33	WM8	DAY	M								3	97			
	AVERAGE	N/A	N/A	11.50	0.0	0.0	0.17	0.0	0.17	3.17	7.17	77.83	0.0	0.0	0.0
8	BRO.7	ORD	D						4			96			
8	BR1.6	ORD	W/M	12						64	2	22			
16	MN1.8	ORD	D								14	85		1	
16	MO	ORD	P	35						44	6	15	tr		
23	NQW	ORD	P	28					tr	48	5	19			
21	01.55	ORD	W/P	13			1			37	14	35			
41	OBC15	ORD	D	tr					3		14	83		tr	
22	PG1.5	ORD	P	29	8		6			40	5	12			
13	PR1.3	ORD	G	58			9			6	21	6			
13	PR1.3'	ORD	G/P	35			1			43	20	1			
25	RHF1.1	ORD	G	49	5		tr				26	20	tr	tr	
25	RHF1.7	ORD	P												
25	RHF1.9	ORD	P	33			3			51	11	2			
50	RR1.3	ORD	W/M	12					tr	42	2	44			
6	St.6	ORD	D						10			90			
6	SB	ORD	P/G	11							13	76	tr	tr	
7	SR2.0	ORD	D								1	99			
7	SR2.3	ORD	W	11					tr	47	18	24			
	AVERAGE	N/A	N/A	19.18	0.76	0.0	1.18	0.0	1.00	24.82	10.12	42.88	0.0	0.06	0.0
8	BR3.5	OSG	D	tr					tr			100			
8	BR3.7	OSG	D						1			99			
15	HR2.8	OSG	D								tr	100		tr	
23	NQ056	OSG	D	7					1			92			
18	R2.9	OSG	P	16						10	tr	74			
18	R3.5	OSG	W									100		tr	
6	S3.0	OSG	D									100		tr	
6	S3.4	OSG	D			tr			1			99			
6	S4.0	OSG	D	tr					1			99			
	AVERAGE	N/A	N/A	2.56	0.0	0.0	0.0	0.0	0.44	1.11	0.0	95.89	0.0	0.0	0.0

APPENDIX 2B
BIOCLAST CONSTITUENTS

APPENDIX TABLE 2B

BIOCLASTS CONSTITUENTS

LOCATION	SAMPLE	FACIES	ROCK TYPE	% BIOCLASTS	CRINOID	CORAL	BRYOZOAN	BRACHIOPOD	GASTROPOD	TRILOBITE	OSTRACOD	STROMATOPOROID	NO ID
	EF1.8	1	P/W	3	100			tr					
	AVERAGE	N/A	N/A	0.0	100	0.0	0.0	0.0	0.0	0.0	0.0	0.0	0.0
	OBC12	2B	P/G	44	76	1	2	11		5	tr		5
	OBC13	2B	G	52	72	8	2	13		1	4		
	AVERAGE	N/A	N/A	48	74.0	4.5	2.0	12.0	0.0	3.0	2.0	0.0	2.5
	OBC10	3	G	54	82	10	6	2					
	OBC11	3	P	21	76	10	8			1			5
	OBC2	3	G	40	58	2	30	3	2	3	2		
	OBC3	3	G	39	64	1	10	15	3	5	tr		2
	OBC4	3	G	45	78	11	9			2			
	OBC5	3	G	53	58	tr	24	8		4	3		3
	OBC8	3	G	60	87		tr	2			4		7
	OBC9	3	P	47	76		4	4					16
	AVERAGE	N/A	N/A		72.4	4.3	11.4	4.3	0.6	1.9	1.1	0.0	4.1
	AC115	4	mG	56	75		25	tr		tr		tr	
	EQ2.5	4	G/P	43	62	tr	36	1		tr			1
	EQ3.0A	4	mG	61	86		10	2		1			1
	EQ3.0B	4	G		100								
	LFLW	4	G/P	49	100			tr					
	SMC2B	4	mG	56	98			1					1
	SMC1A	4	mG	60	100								
	SMC2B	4	mG	56	98		1	1					
	TF3B	4	G	62	90		5	tr		2			3
	TF5	4	G	46	98		2	tr		tr	tr		
	WBM3.0	4	mG	52	100								
	WM1A	4	G	61	92		7	tr		tr			1
	WM1B	4	G	59	98		1						1
	WM2A	4	G	66	68		32	tr		tr	tr		
	WM3	4	G	66	63		35						2
	WM4A	4	G	54	68	tr	32			tr	tr		
	AVERAGE	N/A	N/A		87.3	0.0	11.6	0.3	0.0	0.2	0.0	0.0	0.6

APPENDIX TABLE 2B

BIOCLASTS CONSTITUENTS
-Continued-

LOCATION	SAMPLE	FACIES	ROCK TYPE	% BIOCLASTS	CRINOID	CORAL	BRYOZOAN	BRACHIOPOD	GASTROPOD	TRILOBITE	OSTRACOD	STROMATOPOROID	NO ID
31	AC107	5	P/G	41	34	29	27	3	7				
31	AC99	5	B	21	24		71			5			
29	EF2.0B	5	G	53	100								
29	EF2.3	5	G	47	100								
29	EF3.5	5	P/G	59	100								
29	EF3.7	5	G	58	91		4	4		tr			1
29	EF3.8	5	G	56	81		7	9		2	1		
29	EF3.9	5	mG	38	79		11	10		tr	tr		
29	EF4.0	5	mG	61	78	13	6	2		1			
29	EF4.2	5	G	33	100		tr	tr					
29	EF4.5	5	G	51	60		29	8		1	tr		2
29	EF4.9	5	G	58	64	21	7	6		2			
29	EF5.3	5	G	39	92	5	3	tr					
29	EF5.5	5	G	48	57	30	9						4
29	EF6.0	5	G	54	75	4	9	8					4
29	EF6.1	5	G	56	78	2	13	5		2			
29	EF6.2	5	G	55	62	tr	32	tr		tr		6	
34	EQTM	5	G	61	77	2	14	2		2	1		2
34	EQTOP	5	G	59	79	16	4	1		tr			
37	L5B	5	G	55	85		13	2			tr		
37	L6	5	G	31	68	tr	26	tr		6			
37	L7A	5	G	56	48	5	34	5		2	2		4
37	L7B	5	G/P	48	88		9			2	1		
37	L7T	5	G	79	54	40	4	1		tr			1
32	LF7	5	G/P	78	67	8	6			tr		19	
32	LFB	5	W	18	22	42	36	tr		tr			
30	SMC3C	5	mG	62	70	5	25						
30	SMC4B	5	G/P	54	87		13						
38	TF6A	5	G	45	98		2	tr		tr	tr		
38	TF6C	5	G	42	81		12	2		2		2	1
38	TF7A	5	G	71	50	33	1	2				14	
38	TF8A	5	G	73	66	14	17	3				tr	
38	TF8B	5	G	55	73		11	14		2	tr		
38	TF9B	5	G	60	85		2	12					1
38	TF9C	5	G	56	82		1	4		7	5		1
35	WBM1.7	5	G/P	71	79	tr	14			tr		6	1
35	WBM2.0	5	G	67	83		15	2		tr			
33	WM6	5	G	81	63	14	19	2		1	tr		1
33	WM7	5	G	60	77	11	10	2		tr	tr		
35	WMBC	5	B	73	2	98	tr				tr		
35	WMBHT	5	P/G	76	51	24	20					4	1
		N/A	N/A		71.0	10.1	13.1	2.7	0.2	0.9	0.2	1.2	0.6

APPENDIX TABLE 2B

BIOCLASTS CONSTITUENTS
-Continued-

LOCATION	SAMPLE	FACIES	ROCK TYPE	% BIOCLASTS	CRINOID	CORAL	BRYOZOAN	BRACHIOPOD	GASTROPOD	TRILOBITE	OSTRACOD	STROMATOPOROID	NO ID
8	BR1.65	6	W/G	51	80		5	4		4			7
8	BR2.65	6	G	53	73		11	13	1	2			
17	C2.6	6	G	58	76	tr	10	9		2			3
11	FC2.0	6	G	72	89	tr		8					3
11	FC2.25	6	G	66	86		3	6		1			4
15	HR2.16	6	G	55	58	15	20	7					
16	M1A	6	G	69	91		5	4					
16	MB1	6	G/P	46	89		1	5		4			1
16	MB2	6	G	59	93			7					
16	MN2.2	6	G	37	100		tr	tr					
24	NPQ2.3	6	P/W	17	65	6	tr	29		tr			
24	NPQ2.35	6	G	38	53		21	3				21	2
24	NPQ2.3B	6	G	68	88		4	2		1			5
24	NPQ2.45	6	P/W	22	73		14	5		4			4
23	NQ1	6	W	34	41		3	30			24		2
23	NQ2	6	W	37	58			17		3		16	6
23	NQ3	6	P	49	64	4	14	10	1	6	tr		1
23	NQ4	6	G	27	56	1	7	12		15	1		8
23	NQ6	6	P/G	40	70		9	6			2	9	4
23	NQ7	6	G	59	86		3	7			tr	tr	4
23	NQBASE	6	G/P	51	73	1	21	4		tr	1	1	
23	NQS	6	G	44	48	tr	29	9	5		7	7	2
21	01.8	6	G/P	42	63	10	5	20					2
21	03.0	6	G	46	85	2	4	9		tr			
22	PC2.0	6	G/P	48	77	8	4	6					5
20	PO	6	G	54	89	tr	7	2		1		1	
13	PR1.6	6	P	46	80	tr	4	4			2		10
18	R2.3	6	P	36	53	tr	22	19		tr	3		3
18	R2.35	6	G	34	37	33	3	1		tr	tr	26	
18	R2.3'	6	P	45	69	18	4	4		2		1	2
18	R2.75	6	G	57	70	9	7	4		2	2	tr	6
25	RHF2.1	6	G	56	71		23	4					2
25	RHF2.8	6	G	49	71		23	4					2
25	RHF3.9	6	G	54	88		4	8		tr			
6	S1.9	6	mG	41	93		2	1		2			2
6	S2.1	6	mG	35	96		3	1					
6	S2.5	6	P	35	93			5	tr			2	
6	S2.6	6	G/P	44	86		9	4	1		tr		
6	SR2.4	6	G	56	98	1	1	tr					
6	SR2.7	6	G/P	52	36			1				63	
19	TCS1.7	6	G/P	34	59	tr	24	11	6				
19	TCS1.8	6	G	45	69	tr	29	2		tr			
19	TCS1.9	6	G/P	22	83		5	9					3
19	TCS3.0	6	G/P	25	92			8					
	AVERAGE	N/A	N/A		74.3	2.5	8.3	7.4	0.3	1.1	0.8	3.3	2.1

APPENDIX TABLE 2B

BIOCLASTS CONSTITUENTS
-Continued-

LOCATION	SAMPLE	FACIES	ROCK TYPE	% BIOCLASTS	CRINOID	CORAL	BRYOZOAN	BRACHIOPOD	GASTROPOD	TRILOBITE	OSTRACOD	STROMATOPOROID	NO ID
41	OBC1		P	58	60		7	7		14	3		9
25	RHF4.6	DAYTN	G	34	29		28	5	34	4			
	AVERAGE	N/A	N/A		44.5	0.0	17.5	6.0	17.0	9.0	1.5	0.0	4.5
16	MO	ORDVC	P	35	83		3	11		3			
22	PC1.5	ORDVC	P	29	10	34	21	27	7	1			
13	PR1.3	ORDVC	G	58	81			12	7		tr		
25	PHF1.9	ORDVC	P	33	78	tr	3	16		3			
13	PR1.3'	ORDVC	G/P	35	37	3	31	14		3	1		11
8	BR1.6	ORDVC	W/M	12							89		11
27	RHF1.1	ORDVC	G	47	61	4	6	26	2	1			
7	SR2.3	ORDVC	W	11	2			23	30		45		
21	01.55	ORDVC	W	13	48	8		44					
6	SB	ORDVC	D	11	100	tr							
23	NQW	ORDVC	P	28	48	1	6	43					2
	AVERAGE	N/A	N/A		49.8	4.5	6.4	19.6	4.2	1.0	12.3	0.0	2.2

APPENDIX 2C

TEXTURE

EXPLANATION OF ABBREVIATIONS

SORTING : W = WELL

M = MODERATE

P = POOR

GRAIN ABRASION AND CHEMICAL ALTERATION:

H = HIGH (QUALITATIVE)

M = MODERATE

L = LOW

APPENDIX TABLE 2C

TEXTURE

LOCATION	SAMPLE	FACIES	ROCK TYPE	GRAIN SIZE MICRONS	GRAIN SIZE MODE	SORTING	GRAIN ABRASION	CHEM ALTERATION	POPROSITY
30	SMC1A	1	mG	200-600	500	W	H	L	13
32	LF2	1	W	ND					tr
29	EF1.8	1	P/W	250-260		P			10
29	EF1.9	1	D	ND					12
35	WBM5.6	1	D	250-300	250			M-H	2
35	WBM5.5	1	D	50-150	150			H	3
31	AC12B	1	D	ND					7
31	AC131	1	D	ND					17
37	L2B	1	D	ND					40
34	EQ1.1	1	S	ND					6
41	OBC14	1	D	40-80					18
29	EF1.2	1	D	50-mm	500+	M		H	11
29	EF1	1	D	ND					5
37	L4A	1	D	ND					12
41	OBC12	2	P/G	50-mm	500	P	M	M	tr
43	TC1	2	D	ND	125				10
41	OBC13	2	G	100-cm	400	P	M	H	
41	OBC10	2.5	G	150-cm	mm	W	M	M-H	5
41	OBC11	2.5	P	100-mm	225	P	M	M-H	2
41	OBC4	3	G	75-mm	350	M-W	L-M	VH	9
41	OBC8	3	G	30-750	250	VW	L-M	L	tr
41	OBC5	3	G	150-100	300	M	M	L-M	tr
41	OBC9	3	P	50-350	200	P	L-M	L-H	4
41	OBC2	3	G	150	750	P	M	VH	1
41	OBC3	3	G	200-cm	mm	W	L-M	L	tr

APPENDIX TABLE 2C

TEXTURE
-Continued-

LOCATION	SAMPLE	FACIES	ROCK TYPE	GRAIN SIZE MICRONS	GRAIN SIZE MODE	SORTING	GRAIN ABRASION	CHEM ALTERATION	POPROSITY
34	EQ2.5	4	G/P	150-mm	500	W	L	L	1
31	AC115	4	mG	150-mm	350	M	L-M	L	tr
34	EQ3.0A	4	mG	150-mm	750	M-W	L	L	4
34	EQ3.0B	4	G	300-mm	750				15
33	WM4A	4	G	150-mm	750	W	L-M	L	2
38	TF3B	4	G	150-1000	250	W	L-M	L	7
32	LFLW	4	P/G	100-mm	500	P	L	L	0
31	AC125	4	D	ND					11
30	SMC2B	4	mG	350-mm	750	M	L-M	L-M	14
31	AC120	4	mG	100-750	350	M	L	L	tr
33	WM1A	4	G	150-mm	500	W	L	L	tr
31	AC123	4	D	ND					4
35	WMB3.0	4	mG	250-1000	500	M-W	L-M	L-M	tr
38	TF5	4	G	100-1000	400	W	L	L	2
33	WM2A	4	G	200-mm	750	W	L	L	tr
33	WM1B	4	G	300-mm	750	W	L	L	12
33	WM3	4	G	150-mm	750	W	L	L	1

APPENDIX TABLE 2C

TEXTURE
-Continued-

LOCATION	SAMPLE	FACIES	ROCK TYPE	GRAIN SIZE MICRONS	GRAIN SIZE MODE	SORTING	GRAIN ABRASION	CHEM ALTERATION	POPROSITY
35	WMB	5	B	cm	cm	P	L	L	2
38	TF9B	5	G	100-500	175	W	M	M-H	tr
35	WMBHT	5	P	200-cm	1000+	P	L	L	1
30	SCM4B	5	G/P	350-mm	750	P	L	L	2
37	L7T	5	G	500-cm	750	P	L-M	L	1
29	EF2.0B	5	G	300-2000	500	W	M-L	L	1
31	AC99	5	B	100-cm	cm	P	L	L	
33	WM7	5	G	350-mm	750	M	L-M	L	6
37	L7B	5	G/P	25-500	250	P	L	L	tr
32	LFB	5	W	500-mm	1000	P	L	L	0
32	LF7	5	G/P	150-cm	500+	M	L	L	0
38	TF8B	5	G	75-500	175	W	M	M	tr
36	AC107	5	P/G	100-cm	500	M-P	L	L	1
29	EF2.3	5	P/G	200-1500	500	P	M-L	L	1
38	TF9C	5	G	150-mm	500	M	M-H		1
33	WM6	5	G	150-mm	750	W	L-M	L	1
29	EF3.8	5	G	150-mm	400	W	M	L	3
38	TF9A	5	G	100-100	500	W	L-M	VH	2
32	LF8	5	M/W	ND					4
38	TF6C	5	G	50-mm	150	M-W	M	L	
38	TF7A	5	G	150-cm		P	L-H	L	2
38	TF8A	5	G	150-cm	650	M-W	L	L	1
37	L5B	5	G	150-1500	350	M	M	L	2
37	L6	5	G	50-300	150	W	M	L	tr
37	L7A	5	G	150-mm	500	M-W	L-M	L	1
34	EQTM	5	G	150-mm	300/600	M	M-H	VH	3
34	EQTOP	5	G	300-mm	650	W	L-M	M-H	4
30	SMC3C	5	mG	250-mm	700	M-P	L-M	L-H	5
29	EF3.9	5	mG	100-1000	250	M-P	M	L	1
38	TF6A	5	G	100-mm	150/400	W	L-M	L	1
35	WBM1.7	5	G/P	150-mm	625	P	M-L	L	2
35	WBM2.0	5	G	150-mm	500	M	L-M	L	3
29	EF4.9	5	G	100-mm	275	W	M	L	1
29	EF5.3	5	G	200-mm	750	W	L	L	1
29	EF2.0B'	5	D	150-500					9
29	EF6.0	5	G	300-cm	750	W	L-M	L	1
29	EF3.5	5	P/G	200-cm	500	P	L	L	12
29	EF3.7	5	G	150-mm	500	W	L	L	3
29	EF6.2	5	G	150-cm	750+	M-W	L	L	4
29	EF4.2	5	G	175-250	200	W	M-H	L	tr
29	EF4.0	5	mG	125-1500	250	M-W	M	L	1
29	EF5.5	5	G	150-cm	500	W	L	L	2
29	EF4.5	5	G	150-500	200	W	M	L	1
29	EF6.1	5	G	200-mm	750+	W	L	L	3

APPENDIX TABLE 2C

TEXTURE
-Continued-

LOCATION	SAMPLE	FACIES	ROCK TYPE	GRAIN SIZE MICRONS	GRAIN SIZE MODE	SORTING	GRAIN ABRASION	CHEM ALTERATION	POPROSITY
25	RHF2.8	6	G	150-mm	350	W	L	L	2
8	BR1.65	6	W/P/G	150-1000	350	M	L-H	L	
25	RFH4.6	6	G	750-mm	mm	M-P	L	L	10
16	M1A	6	G	100-mm	500	W	M	M	7
22	PC2.0	6	G/P	ND	300	W	M-H	L-M	
11	FC2.0	6	G	150-1000	600	W	L	M	tr
11	FC2.25	6	G	ND	550	W	M	M	3
17	C2.7	6	W	100-350		P	M	M-H	
23	NQ4	6	G	250-cm	500	M	M-H	M-H	6
16	MN2.2	6	G	150-mm	500	W	M-H	M	
25	RHF2.1	6	G	150-mm	500	W	L-M	L	tr
23	NQ6	6	P/G	250-500	250	M	M	L-H	4
25	RHF3.9	6	G	150-mm	600	M-W	M	M	4
15	HR2.16	6	G	100-mm	350	M-W	M-H	M	
21	03.0	6	G	150-cm	400	M-W	H	M	
24	NPQ2.3	6	P/W	100-1500	400	P	L	L-H	
24	NPQ2.3B	6	G	150-900	400	W	M	M	tr
24	NPQ2.35	6	G	100-cm		M	M	M-H	
24	NPQ2.45	6	G	ND				M-H	1
16	MB2	6	G	100-2000	600	H	H	L	2
6	S2.1	6	mG	150-300	200	M-H	M-H	M	5
23	NQBASE	6	G/P	250-750	500	M-P	L	L	
20	PO	6	G	150-mm	350	W	M	M	tr
23	NQ7	6	G	150-mm	750	W	M	M-H	
19	TCS1.8	6	G	150-mm	750	M-W	M-H	L-M	
23	NQO	6	P	ND					1
23	NQS	6	G	100-cm	750	M	M	L	
23	NQ1	6	W	75-600	150	P	L	M	
23	NQ2	6	W	75-600	150	P	M-L	M-H	1
23	NQ3	6	P	250-mm	750	M-L		VH	tr
8	BR2.65	6	G	150-mm	300	W	M-H	M	
23	NQ5	6	G/P	ND				M	1
16	MN2.85	6	D	ND					
13	PR1.6	6	P	ND	300	P	M-H	M	
15	HR2.15	6	P/G	ND		P	M	M	
21	01.8	6	G/P	150-mm	500	M-W	M	M	1
7	SR2.7	6	G/P	150-mm		P	L-M	L-M	tr
18	R2.2	6	W	mm	mm	P	L	M	
18	R2.3	6	P	150-mm	300	M-P	M	M-H	
18	R2.35	6	G	150-cm	300	M-W	M-H	M-H	
18	R2.75	6	G	150-mm	750	W	H	H	
18	R2.3'	6	P	100-mm		P			
19	TCS1.9	6	G/P	300-400	300	W	M-H	L	
6	S2.5	6	P	300-1500	900	M	L-M	M	1
6	S2.6	6	G/P	ND					
19	TCS1.7	6	P/G	250-500	400	P-W	M	M	
7	SR2.4	6	G	300-750	500	W	M-H	L-M	
6	S1.9	6	mG	200-mm	500	M-W	M	M	tr
19	TCS3.0	6	G/P	150-mm	Varies	P	M-L	L	
16	MB1	6	G/P	150-1500	500	M	M-L	N	
17	C2.6	6	G	150-350	250	W	M	M	

APPENDIX TABLE 2C

TEXTURE
-Continued-

LOCATION	SAMPLE	FACIES	ROCK TYPE	GRAIN SIZE MICRONS	GRAIN SIZE MODE	SORTING	GRAIN ABRASION	CHEM ALTERATION	POPROSITY
19	TCS3.4	7	D	ND				M-H	2
19	DBLC	7	D	30-500	500	P	H	H	4
15	HR2.7	7	D	ND					
7	SR2.8	7	W	ND					
16	MN2.9	7	D	ND					
13	PR2.0	7	D	ND				H	
14	DBLC2	7	D	ND			H	H	2
7	SR3.3	7	D	ND					8
41	OBC1	DAY	G/P	50-150	100	W	M	L	tr
24	NPQ2.6	DAY	P	100-350	200	P	L	L	
31	AC96	DAY	D	ND					10
31	AC93	DAY	M	ND					4
33	WM8	DAY	M	ND					14
25	RHF4.4	DAY	D	ND					9
22	PC1.5	ORD	P	mm-cm	mm	P	L-M	L	1
41	OBC15	ORD	D	ND	40				
23	NQW	ORD	P	50-mm	Varies	P	L	L	
25	RHF1.9	ORD	P	50-mm	150-600	P	L	L-H	3
13	PR1.3	ORD	G	250-350	300	W	H	M	
13	PR1.3'	ORD	G/P	200-2000	750	M	H	M	
50	RR1.3	ORD	M/W	ND					4
21	01.55	ORD	P/W	ND					
25	RHF1.1	ORD	G	cm	cm	M	L	L	4
25	RHF1.7	ORD	P	to cm	cm	P	M	M	ND
8	BR0.7	ORD	D	ND	30	P			
7	SR2.3	ORD	W	50-cm	Poly Modal	P	M	L	
8	BR1.6	ORD	M/W	ND					7
16	MN1.8	ORD	D	ND					
6	SB	ORD	P/G	300-mm	Poly Modal	P-M	L-M	L	
16	MO	ORD	P	50-1500	600	P	L-M	L	1
6	S1.6	ORD	D	25-75	50	P			20
7	SR2.0	ORD	D	ND					2

APPENDIX TABLE 2C

TEXTURE
-Continued-

LOCATION	SAMPLE	FACIES	ROCK TYPE	GRAIN SIZE MICRONS	GRAIN SIZE MODE	SORTING	GRAIN ABRASION	CHEM ALTERATION	POPROSITY
15	HR2.8	OSG	D	ND					1
8	BR3.7	OSG	D	ND					5
8	BR3.5	OSG	D	ND					7
23	NQO5G	OSG	D	ND					6
18	R3.5	OSG	W	ND					[illegible]
18	R2.9	OSG	P	250-1000	POLYMODAL	P	L	L	
6	S3.0	OSG	D	ND					5
6	S3.4	OSG	D	ND					19
6	S4.0	OSG	D	0					9

APPENDIX 2D

DOLOMITE CHARACTER

EXPLANATION OF ABBREVIATIONS

RHOMB MORPHOLOGY:	Pe = planar euhedral
	Ps = planar subhedral
ZONES:	N = non zoned
	tr = occasional zone
	2 = 2 zones
IRON CONTENT:	N = non ferroan
	SF = slightly ferroan
	F = ferroan
	FZ = ferroan zones
TEXTURE SELECTIVE:	M = after micrite
	WR = whole rock
	C/B = after cement and bioclasts
POROSITY TEXTURE:	D = porosity around individule rhombs
	I = interrhombic
	N = non dolomite related porosity only
	DM = dolomoldic
	L = interlaminar
	R/A = unspecific rhomb related

APPENDIX TABLE 2D

DOLOMITE

LOCATION	SAMPLE	FACIES	ORIG. TEXTURE	PELLETS	QTZ	CHERT	PYRITE	RHOMB SIZE MODE - MICRONS	RHOMB MORPHOLOGY	ZONES	IRON CONTENT	TEXTURE SELECTIVE	DOLO POROSITY	POROSITY TEXTURE	% DOLOMITE	% CALCITE
30	SMC4B	1	G					125-200	Pe	N	N	M	2	D/I	9	91
30	SMC3C	1	G	tr			tr	150-200	Pe	N	N	M	5	D/I	3	97
32	LFLW	1	P/G					150-300	Pe	tr	N	M	0		14	86
32	LF	1	P	4.0	7.0		tr	100-150	Pe	tr	N	M	2	I	17	74
32	LF8	1	W	tr	1.0		tr	50-100	Ps-e	N	N	WR	4	I	92	7
32	LF2	1	W					10-100	Pe	N	SF	WR	0		6	94
32	LFB	1	W	tr		1.0		50-100	Pe	N	N	M	0		24	75
33	WMBC	1	B				tr	10-100	Pe	N	N	M	2	N/D	7	93
33	WMBHT	1	P					100	Pe	N	N	M	1	D	1	99
33	WM8	1	M					30	Pe	N	SF	WR	14	I	97	3
33	WM7	1	G	tr			tr	150	Pe	N	N	M	6	DM	3	97
33	WM3	1	G					100-150	Pe	N	N	M	1	I/D	9	91
33	WM1B	1	G					100-150	Pe	N	N	M	12	DM	9	91
34	EQ1.1	1	S	3.0				80	Pe	N	N	WR	6	I/L	97	
34	EQ2.0	1	G				tr	150-300	Pe	N	N	C/B	10	I/D	41	59
34	EQ2.5	1	G		tr		tr	100-300	Pe	N	N	M	1	I	23	77
34	EQ3.0	1	G					200	Pe	N	N	C/B	tr	N	14	86
34	EQ3.0B	1	G					150-300	Pe	N	N	C/B	29	I/D	63	37
34	EQ3.0A	1	G					50-150	Pe	N	N	M	4	D	5	
34	EQTM	1	G					25-150	Pe	N	N	?	5	D/F	4	nd
34	EQTOP	1	G					50-200	Pe	2-3	N	M	7	D/I	13	nd
35	WBM3.0	1	G					300	Pe	N	SF	C/B	tr	I	36	64
35	WBM5.6	1	S					250	Pe	N	SF	WR	2	I	89	10
35	WBM5.5	1	S	1.0	3.0			75	Ps/e	N	N	WR	3	I	96	
35	WBMB	2	S	4.0				75	Pe-s	N	N	WR	11	I/L	95	1
35	WBM1.7	2	G/P					150	Pe	4	N	M	2	I	8	92
36	AC93	2	?	tr	tr			40	Ps	N	N	WR	4	I	100	
36	AC96	2	?					100	Ps	N-tr	Fz	WR	10	I	94	6
36	AC99	2	B					50	Pe	N	N	M			4	96
36	AC107	2	P	tr				100-200	Pe	N	N	M	1		28	72
36	AC115	2	Q					75-300	Pe	N	N	M	tr		14	86
36	AC120	2	G					150-300	Pe	tr	Fz	M	tr	D	6	94
36	AC123	2	?					150-500	Pe	1+	Fz	WR	4	I	100	
36	AC125	2	?					200 mm	Ps/e	1+	Fz	WR	11	I	100	

APPENDIX TABLE 2D

DOLOMITE
-Continued-

LOCATION	SAMPLE	FACIES	ORIG. TEXTURE	PELLETS	QTZ	CHERT	PYRITE	RHOMB SIZE MODE - MICRONS	RHOMB MORPHOLOGY	ZONES	IRON CONTENT	TEXTURE SELECTIVE	DOLO POROSITY	POROSITY TEXTURE	% DOLOMITE	% CALCITE
36	AC128	2.5	?	tr	tr			80-125	Pe-s	tr	Fz	WR	7	I/D	100	
37	L2B	2.5	S	3+				150	Pe-s	tr	SF		12	I	95	2
37	L4A	2.5	?	1.0				250	Pe	1	F-SF	WR	7	F/L	98	1
38	TF3A	2.5	G	tr				125-300	Pe	1-2	Fz	WR	2	I	93	7
38	TF3B	2.5	?				tr	75-200	Pe	1	F	WR	15	I	4	96
38	TF5	2.5	G/P					150-50	Pe	1-2	N	M/F	1	I	6	94
38	TF7A	2.5	G					150-50	Pe	1-2	N	M	1	I	6	94
38	TF9C	2.5	G					25-150	Pe	tr-1	Fz-F	M	1	D/I	1	nd
38	TC1	2.5	G		4.0			75-350	Pe-s	2-3	F	M	10	I/I	94	2
39	OBC15	2.5	S	3.0				20-80	Pe	N	SF	WR	1	F	83	14
41	OBC14	2.5	S	10.0				30-80	Pe	N	SF	WR	18	I/L	90	
41	OBC12	2.5	P					50-150	Pe	2-3	SF	M	tr	I/D	7	93
41	OBC11	2.5	P					75-150	Pe	4-5	SF	M	2	DM	4	96
41	OBC9	2.5	P	tr	tr			30-100	Pe	1	F	M	4	L	32	68
41	OBC8	3.0	mG					50-100	Pe	1	F	M	tr		3	97
41	OBC3	3.0	G					50-100	Pe-s	N	F	M	tr		3	97
41	OBC2	3.0	G					50-75	Pe	N	F	M	1		7	nd
41	OBC1	3.0	G/P					50-100	Pe	1-2	F	M	tr		5	95
43	TO1-0	3.0	P/W					175-75	Pe	1-2	F	WR		I	85	15
43	T2A	3.0	S	1.0	4.0	tr		100-500	Ps	N	F	WR	1	I	95	
43	T2B	3.0	S	tr	1.0			72-250	Ps	N	F	WR	4	L/I	99	
43	T2C	3.0	S	1.0	tr	tr		150-75	Pe-s	1-2	F	WR	5	I	93	6
43	T3A	3.0	W/P	tr	tr			150-00	Ps	2	F	WR	1	I	100	
43	T3B	3.0	W/P	tr	tr			150-50	Pe-s	2	SF	WR	7	I	86	32
43	TA-4	3.0	W/P	tr		tr		150-00	Pe-s	1-2	F	WR	4	I	100	
43	T5	3.0	P/G	tr		tr		150-350	Pe-s	2-3	F-NF	WR	4	I	100	tr
43	T6	3.0	P/G	tr				200-75	Pe-s	2	F-NF	WR	4	I	80	20
43	T6B	3.0	P/G	tr				75-150	Pe-s	N	F	WR	19	I	100	
43	T7	3.0	P/G	tr	tr		tr	50-75	Ps	N	F	WR	3	A/I	100	
43	T7'	3.0	P/G	tr	tr		tr	150	Pe	1-2	F-SF	WR	3	I	90	10
43	T8	3.0	P/G	tr				75-150	Pe-s	1-2	F	WR	5	I	94	6
43	T9	3.0	P/G	tr	tr			150-100	Pe-s	1-2	F	WR	4	I	75	25
43	T9B	3.0	P/G	1.0	tr		tr	125-100	Ps	N	F	WR	3	I	99	
43	T10	3.0	P/G	1.0				25-75	Ps	N	F	WR	22	D/I	99	

APPENDIX TABLE 2D

DOLOMITE
-Continued-

LOCATION	SAMPLE	FACIES	ORIG. TEXTURE	PELLETS	QTZ	CHERT	PYRITE	RHOMB SIZE MODE - MICRONS	RHOMB MORPHOLOGY	ZONES	IRON CONTENT	TEXTURE SELECTIVE	DOLO POROSITY	POROSITY TEXTURE	% DOLOMITE	% CALCITE
43	T11	3.0	G	tr	tr	tr	tr	150-150	Ps	N	F	W	2	I	100	
43	T12	3.0	P		tr	1.0		50-200	Pe-s	1-2	F-NF	W	12	I	75	24
45	GC0.5	3.0	M/S	tr	tr	tr	tr	150-300	Ps	tr	F-NF	W	2	I	98	2
45	GC1	3.0	M/S	2.0	2.0		1.0	50-100	Ps	N	F	W	11	I/L	95	
47	64 2.6	3.0	P	3.0				50-200	Pe	N	F	W	20	I	94	
47	64B	3.0	P/W	tr	3.0	tr	1.0	75-400	Ps-e	N	F	W	4	I	96	
47	64 1.5	3.0	P/G	1.0	1.0	tr	1.0	m/125/m	Ps-e	N	F	W	1	I	96	
50	RR3.0	3.0	?	2.0	2.0	tr	tr	75-200	Ps-e	N	F	W	3	L	96	
50	RR3.1	3.0	?	1.0	tr	tr	tr	m/100	Ps	N	F	W	3	L	98	
50	RR4.1	3.0	G	tr				150-300	Ps	N	SF	W	1	I	100	
50	RR4.5	3.0	G/P				tr	125-650	Ps	N	SF	W	2	I	100	
50	RR5.5	3.0	G/P	tr	tr			75/mm	Ps	N	SF	W	3	I	100	
50	RR5.9	3.0	W/P	tr				20-150	Ps	N	SF/F Z	W	3	I	99	1
50	RR6.2	3.0	G					225/mm	Ps-e	tr	SF-F	W	17	I	100	
50	RR6.5	3.0	G/P	tr				75-500	Ps	tr	F	W	tr		100	
55	52 1.5	4.0	?	9.0	6.0			100	Ps	N	F	W	3	I	85	
55	52 2.4	4.0	?	tr	tr		tr	100-250	Ps	N-tr	F	W	1	I	100	
55	52 2.8	4.0	G	tr				150-170	Ps-e	N-tr	F-SF	W	3	I/M	100	
55	52 3.4	4.0	P/G	2.0				150-750	Ps-e	N-tr	F-SF	W	4	I	98	
55	52 4.4	4.0	W	tr				30-300	Ps	N	F	W	tr	I	100	
55	52 6.2	4.0	G	tr	1.0			100-mm	Ps	N-tr	F	W	2	I	99	
56	C01.0	4.0	S	12.0	tr		tr	50-150	Pe	N-tr	F-SF	W	23	I	88	
56	C02.3	4.0	?	4.0	1.0			100-750	Ps	N-tr	F-SF	W	7	I	95	
56	C02.4	4.0	?	2.0				50-150	Ps	N-tr	F-SF	W				
56	C02.8	4.0	G	tr	tr			50/200/m	Ps	tr	F-SF	W	5	I	100	
56	C05.2	4.0	G	tr				200/mm	Ps-e	1	FZ	W	1	I	99	1
56	C05.5	4.0	P	tr	tr			150/mm	Ps	tr	FZ	W	tr		100	tr
29	EF1.0	4.0	M/S				16.0	50-150	Ps	N-tr	FZ	W	5	I	84	
29	EF1.3	4.0	S/W	tr	1.0	tr	2.0	m/200	Ps-e	N-tr	FZ	W	8	D/I	89	
29	EF1.8	4.0	P/W					75-200	Ps-e	N-tr	FZ	W	1	I	81	19
29	EF2.0B	4.0	G		tr		1.0	150	Pe	1	FZ	C	1	I	23	76
29	EF2.3	4.0	G/P		tr		tr	100-250	Pe	1	FZ	C	1	I	44	56
29	EF3.8	4.0	G		0.0		1.0	100-150	Pe	N	N	M	3	DM	1	98
29	EF3.9	4.0	G		0.5			150	Pe	N	N	M	1		14	86

APPENDIX TABLE 2D

DOLOMITE
-Continued-

LOCATION	SAMPLE	FACIES	ORIG. TEXTURE	PELLETS	QTZ	CHERT	PYRITE	RHOMB SIZE MODE - MICRONS	RHOMB MORPHOLOGY	ZONES	IRON CONTENT	TEXTURE SELECTIVE	DOLO POROSITY	POROSITY TEXTURE	% DOLOMITE	% CALCITE
29	EF4.2	5.0	G				1.0	100	Pe	N	N	G/M	tr		38	61
29	EF4.5	5.0	G		3.0			200	Pe	N	N	M	tr		3	97
29	EF4.9	5.0	G		6.0			50-150	Pe	N	N	M	1	D	2	98
29	EF5.3	5.0	G				tr	100-300	Pe	1	FZ	M	1	G/I	27	72
29	EF6.0	5.0	mG				1.0	25-150	Pe-s	N	N	M	1	I	10	90
29	EF6.2	5.0	G					25-250	Pe	N	N	M	1	I	6	94
11	FC2.25	5.0	G		3.0			75	Pe			M	4	I	4	96
25	RHF1.1	5.0	G/P		5.0	tr	tr	125	Pe	N	N	M	3	I	20	75
25	RHF4.6	5.0	G				1.0	50-100	Pe	N	N	M	4		tr	99
25	RHF4.4	5.0	W				tr	30-100	Pe	N	N	WR			87	13
24	NPQ2.4	5.0	P/W		tr		1.0	30	Pe	N	N	M			2	
23	NQ6	5.0	P					20-50	Pe-s	N	N	WR			85	15
23	NQW	5.0	P	tr				50	Pe	N	N	M			19	81
23	NQB	5.0	G/P					75	Pe	tr-1	FZ	M			9	91
23	NQ056	5.0	W	1.0				20-50	Ps	N	S-F	WR	6	I	92	7
23	NQ1	5.0	W/P	1.0				20-50	Pe	N	N	M			33	66
23	NQ4	5.0	G					20	Pe	N	N	M	6	I	6	
22	PC2.0	5.0	G/P					20-50	Pe	N	N	M			6	
18	R2.75	5.0	G					30-50	Pe	N	N	M			1	
18	R.29	5.0	W					25-75	Pe	N	N	M			74	26
18	R3.5	5.0	W					20-60	Pe	N	N	M			100	
19	TCS1.7	5.0	G					125	Ps	tr-1	F	M	tr	A	12	87
19	TCS1.9	5.0	G				tr	200	Pe	1	N	M			25	47
19	TCS3.3	6.0	W		1.0	1.0	1.0	25-150	Ps	N	S-N	WR			97	
19	TCS1.9	6.0	M					25	Ps	N	F-S	WR			100	
17	C2.7	6.0	S/W	2.0	3.0			75	Pe	1	N	M			37	58
16	MN1.8	6.0	S				1.0	100	Pe	N	N	WR			85	14
16	MN2.2	6.0	G/P					125	Pe	N	N	WR			38	62
16	MN2.85	6.0	P				1.0	100	Pe	tr	N-S	WR			78	21
16	MN2.9	6.0	W		3.0			100	Ps	N	N-S	WR			96	1
13	PR1.3	6.0	G		9.0			100	Pe	N	N	M			6	94
13	PR1.3'	6.0	G/P					25	Pe	N	N	M			1	99
13	PR2.0	6.0	M	2.0	4.0	2.0		75	Ps	N	N	WR			92	
14	DBLC	6.0	M	1.0	2.0	2.0		25-125	Ps-e	N	N	WR			92	3
8	BR0.7	6.0	S	3.0				50-150	Ps-e	N	N	WR			97	
8	BR1.6	6.0	W					25-125	Pe	N	N	M			22	88
8	BR2.95	6.0	W	tr	tr	tr		75	Pe	N	N	M			3	97
8	BR3.5	6.0	M/S	tr				20	Ps	tr	FZ	M	7	I	100	
7	SR2.0	6.0	?					100-750	Ps	tr	FZ	WR	2	I	99	1
7	SR2.3	6.0	W	tr				50-125	Pe	N	N	M			24	76
7	SR2.4	6.0	G					75-150	Pe	N	N	M			8	92
7	SR2.7	6.0	G	tr		10.0		175	Pe	tr	N	M	tr		40	50
7	SR2.8	6.0	M/W	tr	tr	1.0		25-75	Ps-e	N	N	WR	1		99	
6	S1.6	6.0	?	8.0				50	Ps-e	N	N	WR	20	I	92	

APPENDIX TABLE 2D

DOLOMITE
-Continued-

LOCATION	SAMPLE	FACIES	ORIG. TEXTURE	PELLETS	QTZ	CHERT	PYRITE	RHOMB SIZE MODE - MICRONS	RHOMB MORPHOLOGY	ZONES	IRON CONTENT	TEXTURE SELECTIVE	DOLO POROSITY	POROSITY TEXTURE	% DOLOMITE	% CALCITE
6	SB	7.0	P/G			tr	tr	100-500	Pe-s	1	FZ	WR			76	
6	S1.9	7.0	G		tr			50-150	Pe	N	N	M			21	79
6	S2.5	7.0	P/G	tr				40-125	Pe-s	N	N	M			64	36
6	S2.6	7.0	G					60-125	Pe	N	N	M			1	99
6	S3.0	7.0	?					100-500	Pe-s	1	F	WR	5	I	100	
6	S3.4	7.0	?	1.0	tr			25-100	Pe-s	1	FZ	WR	19	I	99	
3	BGP3	DAY	S/W	4.0	tr		tr	50-75	Ps	tr	FZ	WR	1			
3	BGP6	DAY	S/W	4.0	tr		tr	75-150	Pe-s	1	FZ	WR	18	I/A	96	
3	BPG7	DAY	R/W/	1.0	1.0		tr	50-150	Pe-s	tr	FZ	WR	7	I/A	99	
3	BPG8	DAY	G/P	tr	1.0	tr		50-250	Ps	tr	FZ	WR	9	I/A	95	4
3	BPG8/9	DAY	W/P	1.0	tr		1.0	50-100	Ps	tr	FZ	WR	9	A	97	
3	BPG9	DAY	?	2.0				150-400	Ps-e	tr	FZ	WR	15	I	98	
3	BPG6/7	ORD	?	1.0	1.0			25-150	Ps	tr	FZ	WR	4	A	98	
3	BPG5.8	ORD	?	1.0			1.0	25-150	Ps	tr	FZ	WR	13	I/A	98	
5	62B	ORD	?	1.0	tr		tr	25-300	Ps-e	tr	FZ	WR	28	A/I	99	
5	62 1.7	ORD	W	1.0				50-150	Ps-e	tr	FZ	WR	19	A/I	98	
5	62 2/3	ORD	?		1.0	tr		30-300	Ps-e	tr	FZ	WR	17	A/IR	100	tr
5	62 4.6	ORD	?				1.0	20-350	Pe	1	FZ	WR	19	A/I	99	tr
5	62 8.5	ORD	?	tr				30	Ps	N	S	WR	8	I	100	tr
4	BFB1	ORD	S/M	2.0	1.0		3.0	50-150	Ps-e	tr	FZ	WR	9	A/R	94	tr
4	BFM	ORD	?	tr		tr		225	Pe	tr	FZ	WR	29	A/R	94	6
4	BF10	ORD	P/G	tr	1.0			50	Ps-e	tr	S	WR	14	I	92	7
4	BFT	ORD	P/G	tr	tr			50-150	Pe	N	N	WR	1	I	100	tr
1	RWK1.5	ORD	P/W				tr	50-250	Pe	1	FZ	WR	13	A/I	93	7
1	RWK2.5	ORD	W	tr	tr		tr	50-150	Pe	tr	FZ	WR	8	I/A	100	
1	RWK3.5	ORD	G/P	tr	tr	tr	tr	100-200	Ps-e	1	FZ	WR	7	A	98	2
1	RWK6.2	OSG	P	1.0			tr	25-150	Ps-e	1	FZ	WR	15	A/I	99	
1	RWK6.7	OSG	G/P	1.0	1.0			25-150	Ps-e	1	FZ	WR	25	A/I	98	
1	RWKTO	OSG	P/W	tr			tr	50-150	Ps-e	N	S	WR	18	A/I	99	1

APPENDIX 3 - XRD PEAK SEARCH DATA

LOCATION 34 - SAMPLE EQT

NO.	2THETA	D	INTEG. I (%)	INTEG. I	MAX. I	FWHM
1	20.149	4.4035	0.5	87	15	0.295
2	21.268	4.1743	0.9	138	31	0.220
3	23.086	3.8495	3.2	515	115	0.225
4	24.141	3.6837	1.0	156	30	0.259
5	29.458	3.0298	100.0	15922	4192	0.190
6	30.847	2.8964	5.3	841	245	0.172
7	31.527	2.8354	1.2	191	45	0.214
8	33.231	2.6938	3.7	583	93	0.314
9	35.667	2.5152	3.2	503	96	0.261
10	36.043	2.4899	5.4	859	197	0.218
11	36.777	2.4418	0.7	104	19	0.269
12	39.501	2.2795	8.0	1271	230	0.276
13	40.944	2.2025	1.4	215	20	0.544
14	43.256	2.0899	8.6	1365	261	0.261
15	47.616	1.9082	11.3	1798	240	0.374
16	48.596	1.8720	8.9	1421	229	0.311
17	49.557	1.8379	1.4	224	30	0.373
18	56.663	1.6231	1.5	234	38	0.305
19	57.502	1.6014	3.4	542	85	0.319

LOCATION 38 - SAMPLE TF9C

NO.	2THETA	D	INTEG. I (%)	INTEG. I	MAX. I	FWHM
1	21.379	4.1529	1.0	207	39	0.262
2	23.198	3.8312	3.3	673	137	0.245
3	24.327	3.6559	0.2	43	17	0.128
4	29.589	3.0166	100.0	20671	5199	0.199
5	30.960	2.8860	2.6	546	209	0.131
6	31.567	2.8319	0.3	56	25	0.111
7	33.349	2.6846	0.5	111	21	0.262
8	33.504	2.6725	0.2	48	25	0.095
9	35.763	2.5087	0.3	66	27	0.123
10	36.159	2.4821	4.5	933	226	0.206
11	36.870	2.4359	0.2	38	15	0.131
12	39.598	2.2741	6.7	1385	301	0.230
13	43.359	2.0852	6.4	1326	300	0.221
14	47.316	1.9196	1.7	349	102	0.171
15	47.714	1.9045	8.3	1713	329	0.261
16	48.700	1.8683	8.4	1732	321	0.270
17	56.794	1.6197	0.8	169	44	0.192
18	57.595	1.5991	3.2	661	126	0.263

LOCATION 34 - SAMPLE EQT

NO.	2THETA	D	INTEG. I (%)	INTEG. I	MAX. I	FWHM
1	21.313	4.1656	2.2	327	79	0.207
2	23.115	3.8467	2.7	397	106	0.187
3	24.095	3.6906	0.4	61	24	0.126
4	29.501	3.0254	100.0	14755	4396	0.168
5	30.885	2.8930	2.8	417	98	0.213
6	31.549	2.8336	0.7	106	33	0.163
7	33.223	2.6945	4.0	594	102	0.292
8	33.354	2.6842	2.3	340	106	0.160
9	35.678	2.5145	4.2	613	121	0.254
10	36.101	2.4860	3.9	581	138	0.210
11	36.813	2.4395	1.0	152	40	0.192
12	39.518	2.2786	6.2	917	255	0.180

LOCATION 38 - SAMPLE TF9C

NO.	2THETA	D	INTEG. I (%)	INTEG. I	MAX. I	FWHM
1	23.158	3.8377	2.5	478	117	0.204
2	26.467	3.3649	0.5	101	21	0.237
3	29.543	3.0212	100.0	18827	5327	0.177
4	31.586	2.8303	1.1	201	55	0.183
5	33.316	2.6871	0.5	99	33	0.151
6	34.854	2.5721	0.4	81	24	0.168
7	36.119	2.4848	3.0	567	146	0.194
8	36.826	2.4387	0.8	153	57	0.135
9	39.566	2.2759	4.7	887	220	0.201
10	43.314	2.0873	5.4	1013	215	0.236
11	47.306	1.9200	1.2	221	58	0.191
12	47.692	1.9054	6.8	1287	241	0.267
13	48.698	1.8683	8.0	1507	262	0.288
14	56.762	1.6206	1.1	215	40	0.268
15	57.575	1.5996	1.6	294	104	0.141
16	57.746	1.5953	0.2	40	14	0.144

LOCATION 43 - SAMPLE T

NO.	2THETA	D	INTEG. I (%)	INTEG. I	MAX. I	FWHM
1	21.257	4.1764	1.9	271	41	0.334
2	23.981	3.7078	1.0	152	27	0.285
3	25.872	3.4409	1.8	261	60	0.217
4	26.786	3.3255	0.7	105	29	0.181
5	28.181	3.1640	0.5	79	29	0.137
6	29.629	3.0126	11.3	1652	374	0.221
7	30.860	2.8952	100.0	14656	3702	0.198
8	32.060	2.7896	2.2	320	85	0.189
9	33.288	2.6893	2.7	401	67	0.298
10	34.219	2.6183	0.9	127	28	0.225
11	35.191	2.5482	2.0	298	49	0.306
12	37.293	2.4092	1.4	198	55	0.179
13	40.212	2.2408	1.1	167	30	0.281
14	41.048	2.1971	3.6	534	114	0.233
15	43.390	2.0838	0.8	120	27	0.220
16	44.873	2.0183	1.9	276	51	0.270
17	47.017	1.9311	0.9	134	32	0.209
18	49.666	1.8342	1.3	198	38	0.258
19	50.272	1.8135	2.2	322	46	0.347
20	50.898	1.7926	3.9	576	70	0.414
21	53.191	1.7206	1.2	172	25	0.339

LOCATION 24- SAMPLE NPQ2.3W

NO.	2THETA	D	INTEG. I (%)	INTEG. I	MAX. I	FWHM
1	23.085	3.8496	2.5	746	176	0.212
2	26.667	3.3402	0.2	60	14	0.214
3	29.497	3.0259	100.0	29700	7740	0.192
4	30.901	2.8914	0.8	233	48	0.241
5	31.516	2.8364	0.7	194	58	0.167
6	36.052	2.4893	4.0	1174	285	0.206
7	39.487	2.2803	5.9	1176	329	0.269
8	43.249	2.0902	5.4	1619	354	0.229
9	46.968	1.9330	0.2	56	23	0.124
10	47.213	1.9236	0.9	260	105	0.124
11	47.608	1.9085	8.6	2558	481	0.266
12	48.602	1.8718	3.9	1149	366	0.157
13	56.655	1.6234	0.5	153	56	0.136
14	57.486	1.6019	2.5	733		0.221
15	58.162	1.5848	0.2	61	41	0.074

LOCATION 24 - SAMPLE NPQ2.3BRN

NO.	2THETA	D	INTEG. I (%)	INTEG. I	MAX. I	FWHM
1	23.077	3.8510	3.9	815	174	0.235
2	26.660	3.3410	0.3	66	16	0.206
3	27.554	3.2346	0.3	61	15	0.200
4	29.455	3.0301	100.0	21056	5659	0.186
5	31.477	2.8398	0.8	171	51	0.166
6	36.036	2.4903	4.6	978	209	0.234
7	39.474	2.2810	7.3	1527	301	0.253
8	43.223	2.0915	6.9	1459	330	0.221
9	47.215	1.9235	1.8	385	100	0.192
10	47.574	1.9098	8.6	1807	314	0.288
11	48.599	1.8719	7.9	1672	322	0.260
12	56.674	1.6229	1.9	392	44	0.445
13	57.464	1.6024	3.5	745	160	0.232

LOCATION 23 - SAMPLE NQCRUST

NO.	2THETA	D	INTEG. I (%)	INTEG. I	MAX. I	FWHM
1	10.157	8.7016	2.5	243	29	0.414
2	10.579	8.3561	3.4	325	27	0.592
3	11.080	7.9791	2.3	222	24	0.464
4	12.009	7.3638	2.0	194	21	0.470
5	23.165	3.8366	8.8	841	187	0.225
6	26.738	3.3315	3.9	371	81	0.230
7	29.549	3.0206	100.0	9567	2393	0.200
8	30.945	2.8875	18.0	1726	313	0.276
9	34.966	2.5641	2.5	238	21	0.576
10	36.124	2.4845	11.7	1123	243	0.231
11	39.574	2.2755	17.3	1659	343	0.242
12	41.172	2.1908	2.7	260	43	0.301
13	43.329	2.0866	15.4	1474	333	0.221
14	44.944	2.0153	1.2	115	19	0.297
15	47.320	1.9195	6.9	657	117	0.281
16	47.681	1.9058	17.7	1693	351	0.241
17	48.691	1.8686	19.9	1902	327	0.291

LOCATION 41 - SAMPLE OBC16T

NO.	2THETA	D	INTEG. I (%)	INTEG. I	MAX. I	FWHM
1	20.111	4.4118	0.6	97	18	0.269
2	21.251	4.1775	2.5	387	65	0.298
3	23.066	3.8528	3.5	551	124	0.222
4	29.444	3.0311	100.0	15740	4068	0.193
5	30.740	2.9062	1.0	164	29	0.280
6	31.480	2.8396	0.9	138	31	0.220
7	32.026	2.7924	0.9	139	21	0.327
8	36.025	2.4911	6.4	1005	209	0.241
9	36.754	2.4433	2.1	329	54	0.305
10	39.476	2.2809	9.6	1512	298	0.254
11	40.984	2.2004	0.3	51	17	0.152
12	43.241	2.0906	8.7	1372	258	0.266
13	47.613	1.9084	15.3	2412	298	0.404
14	48.062	1.8916	0.8	119	33	0.183
15	48.613	1.8714	11.9	1880	295	0.318
16	53.335	1.7163	0.9	135	27	0.249
17	56.652	1.6234	1.3	207	39	0.268
18	57.511	1.6012	3.4	530	82	0.321
19	58.217	1.5835	1.1	180	26	0.346
20	59.108	1.5617	0.6	93	16	0.292

LOCATION 47 - SAMPLE 64B

NO.	2THETA	D	INTEG. I (%)	INTEG. I	MAX. I	FWHM
1	6.208	14.2247	2.9	217	48	0.226
2	7.763	11.3800	3.8	278	41	0.341
3	8.791	10.0512	100.0	7372	559	0.659
4	12.513	7.0682	3.8	279	48	0.289
5	15.897	5.5706	2.2	165	29	0.281
6	17.864	4.9613	6.5	478	72	0.330
7	20.887	4.2496	2.7	202	42	0.240
8	26.806	3.3232	24.5	1809	195	0.465
9	27.624	3.2265	3.7	272	59	0.232

LOCATION 39 - SAMPLE TC1

NO.	2THETA	D	INTEG. I (%)	INTEG. I	MAX. I	FWHM
1	8.744	10.1042	100.0	5519	442	0.624
2	12.461	7.0980	4.7	260	37	0.352
3	17.804	4.9780	10.0	549	45	0.611
4	26.812	3.3224	31.7	1751	120	0.730

LOCATION 32 - SAMPLE LFM

NO.	2THETA	D	INTEG. I (%)	INTEG. I	MAX. I	FWHM
1	4.701	18.7831	7.8	107	51	0.105
2	8.075	10.9397	17.9	246	60	0.205
3	8.257	10.6997	1.6	22		0.138
4	8.861	9.9711	70.5	967	220	0.220
5	20.915	4.2439	32.2	442	150	0.147
6	26.705	3.3355	100.0	1372	301	0.228
7	31.002	2.8823	84.8	1164	280	0.208

LOCATION 24 - SAMPLE NPQGLAUC

NO.	2THETA	D	INTEG. I (%)	INTEG. I	MAX. I	FWHM
1	5.065	17.4316	3.9	194	44	0.220
2	8.820	10.0181	100.0	5009	383	0.655
3	17.791	4.9814	11.1	557	76	0.366
4	20.923	4.2424	2.6	129	49	0.132
5	26.746	3.3305	37.2	1865	324	0.288
6	30.900	2.8916	10.9	544	124	0.219

LOCATION 24 - SAMPLE NPQ2.45

NO.	2THETA	D	INTEG. I (%)	INTEG. I	MAX. I	FWHM
1	2.132	41.4075	100.0	7454	589	0.633
2	2.889	30.5538	95.2	7099	212	1.671
3	6.422	13.7530	9.8	730	83	0.442
4	8.760	10.0861	44.3	3304	230	0.719
5	17.845	4.9665	18.8	1404	64	1.091
6	18.817	4.7121	5.2	390	41	0.472
7	19.988	4.4386	2.7	200	37	0.270
8	26.724	3.3332	29.2	2173	337	0.322
9	27.931	3.1918	2.6	192	28	0.348
10	29.466	3.0289	14.3	1064	278	0.192
11	30.979	2.8844	19.8	1476	225	0.328

LOCATION 1 - SAMPLE RWKGLAUC

NO.	2THETA	D	INTEG. I (%)	INTEG. I	MAX. I	FWHM
1	8.827	10.0098	20.5	2073	192	0.504
2	13.253	6.6750	1.6	161	27	0.301
3	17.774	4.9863	3.5	354	47	0.380
4	20.887	4.2495	32.5	3280	1467	0.112
5	26.699	3.3363	34.1	3445	940	0.183
6	27.960	3.1866	2.1	216	62	0.174
7	30.960	2.8861	100.0	10098	2078	0.243

LOCATION 29 - SAMPLE EF1.0

NO.	2THETA	D	INTEG. I (%)	INTEG. I	MAX. I	FWHM
1	20.858	4.2555	1.7	302	72	0.209
2	21.965	4.0433	0.6	116	26	0.220
3	23.970	3.7096	2.1	379	72	0.262
4	25.828	3.4467	0.4	72	25	0.142
5	26.652	3.3420	7.7	1379	430	0.160
6	28.496	3.1297	0.2	44	22	0.100
7	30.842	2.8969	100.0	17862	3581	0.249
8	32.031	2.7920	1.2	217	48	0.227
9	32.280	2.7710	0.5	93	31	0.149
10	33.351	2.6844	2.9	510	78	0.326
11	35.169	2.5497	1.6	294	51	0.290
12	36.608	2.4528	0.5	96	26	0.185
13	37.289	2.4095	2.7	489	101	0.242
14	39.497	2.2797	0.3	56	20	0.140
15	41.027	2.1982	8.5	1526	244	0.312
16	43.743	2.0678	0.7	124	29	0.213
17	43.911	2.0603	0.2	36	21	0.085
18	44.825	2.0203	5.7	1011	190	0.266
19	47.463	1.9140	0.5	84	41	0.102
20	49.144	1.8524	0.8	145	29	0.247
21	50.270	1.8135	5.7	1015	233	0.218
22	50.362	1.8104	1.2	206	61	0.167
23	50.865	1.7937	6.0	1079	260	0.208
24	51.012	1.7889	1.1	201	62	0.161
25	56.327	1.6320	0.4	71	27	0.130
26	58.757	1.5702	0.8	148	35	0.209
27	59.667	1.5484	0.7	117	45	0.131

LOCATION 43 - SAMPLE T2A

NO.	2THETA	D	INTEG. I (%)	INTEG. I	MAX. I	FWHM
1	2.769	31.8789	35.0	336	93	0.181
2	8.060	10.9600	25.3	243	52	0.234
3	8.567	10.3128	100.0	961	183	0.262
4	8.658	10.2048	56.2	540	239	0.113
5	12.512	7.0691	22.6	217	51	0.212
6	26.698	3.3363	64.0	615	152	0.202
7	26.897	3.3122	15.6	150	85	0.088
8	30.754	2.9049	19.3	185	40	0.232
9	30.952	2.8869	6.3	60	44	0.068

LOCATION 34 - SAMPLE EQCLAY

NO.	2THETA	D	INTEG. I (%)	INTEG. I	MAX. I	FWHM
1	3.909	22.5853	9.5	330	59	0.281
2	8.824	10.0129	100.0	3468	319	0.543
3	12.499	7.0761	11.0	381	49	0.386
4	17.828	4.9713	11.9	413	49	0.420
5	26.911	3.3104	28.4	986	97	0.506

LOCATION 23 - SAMPLE NQTOP

NO.	2THETA	D	INTEG. I (%)	INTEG. I	MAX. I	FWHM
1	3.639	24.2579	11.3	333	64	0.260
2	8.819	10.0186	100.0	2935	256	0.573
3	17.806	4.9773	22.6	663	97	0.341
4	21.284	4.1711	41.5	1219	156	0.391
5	26.863	3.3163	32.9	966	128	0.378
6	33.305	2.6881	13.5	395	55	0.356
7	36.167	2.4816	5.9	174	37	0.238
8	36.756	2.4432	10.6	310	48	0.323
9	45.470	1.9932	11.7	342	46	0.369

LOCATION 56 - SAMPLE CO2.3

NO.	2THETA	D	INTEG. I (%)	INTEG. I	MAX. I	FWHM
1	36.655	2.4497	9.1	218	61	0.179
2	37.467	2.3984	30.9	741	148	0.250
3	39.608	2.2736	4.6	110	37	0.149
4	41.256	2.1865	100.0	2402	523	0.230
5	42.573	2.1219	2.8	67	31	0.110
6	43.922	2.0598	12.3	297	63	0.234
7	45.048	2.0109	39.9	958	189	0.254

LOCATION 56 - SAMPLE CO5.2

NO.	2THETA	D	INTEG. I (%)	INTEG. I	MAX. I	FWHM
1	36.110	2.4854	3.2	83	14	0.295
2	36.609	2.4527	4.9	125	26	0.240
3	37.403	2.4024	34.9	889	145	0.306
4	41.158	2.1915	100.0	2550	421	0.303
5	42.507	2.1250	2.9	73	20	0.183
6	43.839	2.0635	9.3	237	47	0.254
7	44.965	2.0144	53.4	1361	220	0.309

LOCATION 50 - SAMPLE RR3.1

NO.	2THETA	D	INTEG. I (%)	INTEG. I	MAX. I	FWHM
1	36.102	2.4859	3.5	74	13	0.278
2	36.646	2.4503	6.2	131	35	0.185
3	37.476	2.3979	37.2	778	124	0.314
4	39.601	2.2740	6.7	141	33	0.215
5	41.245	2.1871	100.0	2092	401	0.261
6	42.554	2.1227	11.4	239	62	0.192
7	43.922	2.0598	15.0	315	60	0.262
8	45.050	2.0108	56.8	1189	215	0.277

LOCATION 50 - SAMPLE RR4.1

NO.	2THETA	D	INTEG. I (%)	INTEG. I	MAX. I	FWHM
1	37.444	2.3999	44.4	969	176	0.275
2	41.205	2.1891	100.0	2185	410	0.266
3	43.095	2.0605	8.3	182	35	0.263
4	45.002	2.0128	62.9	1375	225	0.305

LOCATION 43 - SAMPLE T2A

NO.	2THETA	D	INTEG. I (%)	INTEG. I	MAX. I	FWHM
1	36.118	2.4849	6.4	121	21	0.284
2	36.653	2.4498	7.4	141	27	0.260
3	37.299	2.4088	35.7	681	126	0.270
4	40.374	2.2322	2.6	49	19	0.128
5	41.050	2.1970	100.0	1906	316	0.301
6	43.672	2.0710	3.8	73	22	0.167
7	44.846	2.0195	56.1	1070	158	0.338

LOCATION 43 - SAMPLE T5

NO.	2THETA	D	INTEG. I (%)	INTEG. I	MAX. I	FWHM
1	36.101	2.4860	3.4	63	15	0.204
2	37.441	2.4001	42.6	775	125	0.309
3	41.180	2.1903	100.0	1820	287	0.318
4	43.894	2.0610	7.0	127	24	0.267
5	44.989	2.0134	75.8	1379	227	0.304

LOCATION 43 - SAMPLE T11

NO.	2THETA	D	INTEG. I (%)	INTEG. I	MAX. I	FWHM
1	37.247	2.4121	29.0	583	93	0.312
2	41.005	2.1933	100.0	2008	275	0.365
3	43.692	2.0701	9.3	187	27	0.350
4	44.811	2.0209	55.7	1118	160	0.349

LOCATION 41 - SAMPLE OBC11D

NO.	2THETA	D	INTEG. I (%)	INTEG. I	MAX. I	FWHM
1	36.100	2.4861	68.2	1068	220	0.243
2	39.550	2.2768	100.0	1565	282	0.278
3	41.002	2.1955	7.7	121	19	0.313
4	42.911	2.1059	91.5	1432	304	0.236

LOCATION 41 - SAMPLE 0BC14

NO.	2THETA	D	INTEG. I (%)	INTEG. I	MAX. I	FWHM
1	36.598	2.4534	32.0	416	102	0.204
2	37.290	2.4094	23.6	307	61	0.250
3	39.534	2.2777	20.2	262	74	0.178
4	40.349	2.2336	14.1	183	46	0.200
5	40.979	2.2006	100.0	1299	183	0.354
6	42.504	2.1251	31.0	403	87	0.230
7	44.817	2.0207	65.1	846	142	0.297
8	45.810	1.9792	9.0	117	44	0.133

LOCATION 39 - SAMPLE TC1B

NO.	2THETA	D	INTEG. I (%)	INTEG. I	MAX. I	FWHM
1	36.708	2.4463	11.0	163	36	0.228
2	37.401	2.4026	45.8	676	119	0.284
3	39.610	2.2735	6.6	97	33	0.149
4	41.122	2.1933	100.0	1477	275	0.268
5	43.410	2.0829	5.1	75	16	0.235
6	43.844	2.0632	8.2	121	21	0.294
7	44.949	2.0151	72.4	1070	185	0.290

LOCATION 37 - SAMPLE L6

NO.	2THETA	D	INTEG. I (%)	INTEG. I	MAX. I	FWHM
1	36.200	2.4794	64.2	1176	224	0.263
2	39.646	2.2715	100.0	1832	358	0.256
3	40.615	2.2195	2.4	44	11	0.194
4	43.402	2.0832	95.4	1747	378	0.231

LOCATION 36 - SAMPLE AC96

NO.	2THETA	D	INTEG. I (%)	INTEG. I	MAX. I	FWHM
1	36.107	2.4856	18.2	293	68	0.216
2	36.448	2.4605	7.0	113	22	0.258
3	37.382	2.4037	39.0	627	119	0.263
4	39.557	2.2764	20.5	329	68	0.242
5	41.109	2.1940	100.0	1609	290	0.277
6	43.308	2.0876	22.1	355	70	0.254
7	43.828	2.0640	6.5	105	24	0.218
8	44.904	2.0170	44.5	717	144	0.248

LOCATION 36 - SAMPLE AC107

NO.	2THETA	D	INTEG. I (%)	INTEG. I	MAX. I	FWHM
1	37.436	2.4004	7.7	121	24	0.253
2	39.514	2.2788	100.0	1558	318	0.245
3	41.200	2.1893	25.4	395	80	0.246
4	43.260	2.0897	79.1	1232	317	0.194
5	45.016	2.0122	15.0	233	38	0.307

LOCATION 32 - SAMPLE LFLW

NO.	2THETA	D	INTEG. I (%)	INTEG. I	MAX. I	FWHM
1	36.104	2.4858	56.8	922	226	0.204
2	37.493	2.3968	12.3	199	51	0.194
3	39.545	2.2771	100.0	1623	363	0.223
4	41.255	2.1866	15.6	252	68	0.186
5	43.294	2.0882	87.8	1425	329	0.217

LOCATION 29 - SAMPLE EF5.3

NO.	2THETA	D	INTEG. I (%)	INTEG. I	MAX. I	FWHM
1	37.396	2.4029	23.3	341	66	0.259
2	39.511	2.2790	81.3	1194	275	0.217
3	41.169	2.1909	46.3	679	125	0.271
4	43.259	2.0898	100.0	1468	362	0.203
5	44.996	2.0131	16.2	238	45	0.264

LOCATION 16 - SAMPLE MN2.2

NO.	2THETA	D	INTEG. I (%)	INTEG. I	MAX. I	FWHM
1	37.341	2.4062	23.2	270	49	0.274
2	39.511	2.2790	100.0	1166	239	0.244
3	41.098	2.1945	48.7	568	77	0.370
4	43.252	2.0901	97.9	1142	263	0.217
5	44.875	2.0182	32.2	376	57	0.332

LOCATION 7 - SAMPLE SR2.8

NO.	2THETA	D	INTEG. I (%)	INTEG. I	MAX. I	FWHM
1	36.614	2.4523	4.9	109	22	0.251
2	37.313	2.4080	37.3	839	172	0.244
3	39.495	2.2798	5.4	121	21	0.294
4	41.059	2.1965	100.0	2250	399	0.282
5	43.747	2.0676	8.0	180	40	0.227
6	44.866	2.0186	63.9	1439	254	0.283

LOCATION 7 - SAMPLE SR3.3

NO.	2THETA	D	INTEG. I (%)	INTEG. I	MAX. I	FWHM
1	36.327	2.4711	25.2	367	51	0.358
2	37.404	2.4023	37.4	546	99	0.275
3	39.808	2.2626	32.5	475	55	0.434
4	41.154	2.1917	100.0	1459	232	0.314
5	43.568	2.0757	34.4	501	47	0.530
6	44.964	2.0144	48.5	708	123	0.289

LOCATION 8 - SAMPLE BR2.65

NO.	2THETA	D	INTEG. I (%)	INTEG. I	MAX. I	FWHM
1	36.144	2.4831	88.4	1519	347	0.219
2	39.596	2.2743	94.7	1627	291	0.280
3	41.117	2.1936	7.7	132	17	0.379
4	43.344	2.0859	100.0	1718	313	0.274

LOCATION 6 - SAMPLE S2.1

NO.	2THETA	D	INTEG. I (%)	INTEG. I	MAX. I	FWHM
1	36.196	2.4797	76.2	1099	260	0.211
2	39.650	2.2713	100.0	1442	298	0.242
3	41.163	2.1912	13.3	191	37	0.261
4	43.409	2.0829	90.3	1301	270	0.241
5	44.977	2.0139	19.3	278	35	0.393

LOCATION 6 - SAMPLE S3.0

NO.	2THETA	D	INTEG. I (%)	INTEG. I	MAX. I	FWHM
1	36.231	2.4774	5.4	106	16	0.331
2	37.381	2.4077	51.4	1015	165	0.308
3	41.067	2.1961	100.0	1974	335	0.294
4	43.762	2.0669	13.6	268	34	0.394
5	44.878	2.0181	56.7	1119	172	0.325

LOCATION 3 - SAMPLE BGP#9

NO.	2THETA	D	INTEG. I (%)	INTEG. I	MAX. I	FWHM
1	36.683	2.4479	4.3	101	19	0.263
2	37.406	2.4022	29.5	688	129	0.267
3	39.611	2.2734	2.7	62	19	0.164
4	40.445	2.2285	5.2	122	21	0.296
5	41.128	2.1930	100.0	2333	353	0.331
6	43.789	2.0657	7.1	165	38	0.218
7	44.915	2.0165	53.8	1256	233	0.270

LOCATION 1 - SAMPLE RWK6.7*

NO.	2THETA	D	INTEG. I (%)	INTEG. I	MAX. I	FWHM
1	36.689	2.4475	5.4	121	28	0.218
2	37.474	2.3980	32.1	714	139	0.256
3	39.595	2.2743	4.5	100	27	0.185
4	41.247	2.1869	100.0	2225	469	0.237
5	42.657	2.1179	5.7	126	31	0.205
6	43.909	2.0604	10.0	223	48	0.234
7	45.045	2.0110	60.0	1336	250	0.267

LOCATION 18 - SAMPLE R2.3BLK/BRN

NO.	2THETA	D	INTEG. I (%)	INTEG. I	MAX. I	FWHM
1	2.943	29.9984	35.6	183	56	0.164
2	5.294	16.6791	24.5	126	57	0.111
3	8.885	9.9445	100.0	513	83	0.308
4	10.558	8.3725	13.7	70	30	0.117
5	26.027	3.3359	58.3		85	0.177

LOCATION 25 - SAMPLE RHF3.9

NO.	2THETA	D	INTEG. I (%)	INTEG. I	MAX. I	FWHM
1	8.853	9.9803	100.0	652	79	0.411
2	12.384	7.1416	49.8	325	88	0.184
3	24.935	3.5681	46.4	303	65	0.231

LOCATION 23 - SAMPLE NQ CRUST/CLAY

NO.	2THETA	D	INTEG. I (%)	INTEG. I	MAX. I	FWHM
1	8.812	10.0268	100.0	848	92	0.461
2	12.341	7.1666	30.9	262	57	0.231
3	26.721	3.3355	29.8	252	48	0.264
4	27.025	3.2967	23.5	199	47	0.210

LOCATION 18 - SAMPLE R2.3

NO.	2THETA	D	INTEG. I (%)	INTEG. I	MAX. I	FWHM
1	3.628	24.3360	19.7	179	49	0.184
2	5.255	16.8046	18.3	166	46	0.181
3	7.904	11.1761	8.1	74	38	0.097
4	8.770	10.0749	41.7	379	107	0.176
5	20.886	4.2498	13.0	118	54	0.108
6	26.704	3.3357	100.0	908	295	0.154
7	30.848	2.8963	18.5	168	54	0.155

DATA FOR LIMESTONE DOLOMITE RATIO CURVE

SAMPLE 100%DOLO-XTAL

NO.	2THETA	D	INTEG. I (%)	INTEG. I	MAX. I	FWHM
1	22.182	4.0044	0.2	152	34	0.224
2	24.197	3.6752	0.5	433	101	0.215
3	28.466	3.1330	0.5	403	96	0.210
4	29.734	3.0023	0.6	493	44	0.563
5	31.089	2.8745	100.0	8248	15420	0.267
6	33.643	2.6618	0.7	546	80	0.343
7	35.432	2.5314	0.6	497	78	0.319
8	37.534	2.3934	1.0	809	171	0.237
9	41.281	2.1852	3.0	2444	435	0.281
10	43.960	2.0581	0.4	309	50	0.309
11	45.086	2.0093	1.3	1112	195	0.285
12	47.191	1.9244	0.1	107	19	0.287

SAMPLE 95%DOLO/5%CCT

NO.	2THETA	D	INTEG. I (%)	INTEG. I	MAX. I	FWHM
1	37.652	2.3871	30.5	821	141	0.292
2	41.414	2.1785	100.0	2689	456	0.295
3	43.490	2.0792	2.2	59	19	0.157
4	44.052	2.0540	6.8	183	37	0.249
5	45.213	2.0039	44.6	1198	176	0.340

SAMPLE 80%DOLO/20%CCT

NO.	2THETA	D	INTEG. I (%)	INTEG. I	MAX. I	FWHM
1	22.160	4.0082	0.2	162	37	0.217
2	23.249	3.8229	0.3	219	39	0.278
3	24.178	3.6780	0.5	343	81	0.212
4	28.442	3.1356	0.6	413	143	0.144
5	29.614	3.0141	15.3	10446	3225	0.162
6	31.066	2.8765	100.0	68287	14154	0.241
7	33.561	2.6681	0.1	79	31	0.127
8	35.409	2.5330	0.4	273	67	0.205
9	36.203	2.4793	0.5	353	107	0.164
10	37.538	2.3941	1.0	666	149	0.223
11	39.633	2.2722	0.5	325	70	0.233
12	41.263	2.1861	2.4	1605	324	0.248
13	43.401	2.0833	0.3	225	51	0.222
14	45.038	2.0113	2.0	1349	273	0.256
15	47.721	1.9043	0.9	647	177	0.182
16	48.756	1.8622	0.4	259	75	0.172
17	49.377	1.8442	0.1	84	38	0.111

SAMPLE 70%DOLO/30%CTT

NO.	2THETA	D	INTEG. I (%)	INTEG. I	MAX. I	FWHM
1	36.280	2.4741	19.7	316	57	0.276
2	36.582	2.4544	1.8	28	12	0.118
3	37.617	2.3892	18.4	295	82	0.179
4	39.769	2.2648	34.7	557	134	0.208
5	41.378	2.1803	100.0	1605	302	0.266
6	43.522	2.0778	24.0	385	100	0.192
7	45.201	2.0044	31.3	502	101	0.249

SAMPLE 60%DOLO/40%CCT

NO.	2THETA	D	INTEG. I (%)	INTEG. I	MAX. I	FWHM
1	22.016	4.0341	0.2	101	34	0.148
2	23.102	3.8469	0.6	275	98	0.140
3	24.057	3.6963	0.3	140	46	0.151
4	29.467	3.0288	67.5	29680	9050	0.164
5	30.923	2.8894	100.0	43962	8677	0.253
6	33.427	2.6785	0.2	86	31	0.140
7	35.320	2.5392	0.3	139	31	0.227
8	35.506	2.5263	0.1	46	18	0.127
9	36.056	2.4890	1.0	435	133	0.163
10	37.360	2.4051	0.7	329	91	0.182
11	39.486	2.2804	1.6	692	181	0.192
12	41.126	2.9131	2.5	1079	212	0.255
13	43.256	2.0899	1.4	614	242	0.127
14	43.774	2.0664	0.2	69	31	0.111
15	44.932	2.0158	1.6	687	140	0.245

SAMPLE 50%DOLO/50%CCT

NO.	2THETA	D	INTEG. I (%)	INTEG. I	MAX. I	FWHM
1	22.127	4.0141	0.3	92	25	0.186
2	23.195	3.8317	0.8	245	71	0.171
3	24.144	3.6831	0.3	85	23	0.183
4	29.587	3.0168	76.4	23778	6175	0.193
5	31.105	2.8811	100.0	31124	6393	0.243
6	33.572	2.6673	0.4	125	36	0.173
7	35.368	2.5358	0.3	83	30	0.139
8	36.156	2.4823	1.4	450	131	0.172
9	37.464	2.3986	1.1	342	89	0.191
10	39.596	2.2743	2.5	785	265	0.148
11	41.204	2.1891	2.1	667	187	0.178
12	43.318	2.0871	2.0	621	153	0.203
13	45.007	2.0126	1.9	598	118	0.253
14	47.172	1.9252	0.6	202	88	0.115
15	47.706	1.9048	3.9	1215	557	0.109
16	48.676	1.8691	3.3	1033	227	0.228
17	49.327	1.8460	0.2	73	27	0.134
18	49.563	1.8377	0.1	46	17	0.133

SAMPLE 40%DOLO/60%CCT

NO.	2THETA	D	INTEG. I (%)	INTEG. I	MAX. I	FWHM
1	22.195	4.0020	0.3	100	19	0.268
2	23.252	3.8224	1.2	362	76	0.239
3	24.181	3.6776	0.6	171	39	0.217
4	29.639	3.0116	100.0	30848	9343	0.165
5	31.095	2.8739	88.7	27351	4936	0.277
6	33.651	2.6612	0.4	123	31	0.197
7	35.470	2.5288	0.6	189	32	0.295
8	36.197	2.4797	1.6	499	115	0.217
9	37.549	2.3934	0.8	249	46	0.274
10	39.648	2.2714	2.8	876	193	0.227
11	41.298	2.1844	2.3	704	108	0.327
12	43.407	2.0830	3.2	996	251	0.198
13	45.102	2.0086	1.8	567	104	0.272
14	47.352	1.9183	0.8	256	59	0.216
15	47.752	1.9031	3.8	1174	234	0.251
16	48.751	1.8644	3.0	923	179	0.258

SAMPLE 30%DOLO/70%CTT

NO.	2THETA	D	INTEG. I (%)	INTEG. I	MAX. I	FWHM
1	36.416	2.4652	55.0	501	92	0.272
2	37.695	2.3844	15.4	141	32	0.220
3	39.853	2.2602	100.0	912	226	0.202
4	41.486	2.1749	49.7	454	63	0.358
5	43.606	2.0740	75.4	688	171	0.201
6	44.219	2.0466	9.9	90	17	0.260
7	45.295	2.0005	26.3	240	35	0.340

SAMPLE 20%DOLO/80%CCT

NO.	2THETA	D	INTEG. I (%)	INTEG. I	MAX. I	FWHM
1	20.089	4.4166	0.1	47	12	0.194
2	23.193	3.8320	1.3	502	126	0.199
3	29.546	3.0209	100.0	39053	12723	0.153
4	30.998	2.8827	30.5	11897	2582	0.230
5	31.582	2.8307	0.6	219	81	0.136
6	36.123	2.4846	1.6	622	144	0.216
7	37.463	2.3987	0.2	95	52	0.091
8	39.562	2.2761	3.5	1372	411	0.167
9	41.241	2.1873	0.9	339	61	0.277
10	43.316	2.0872	3.3	1273	345	0.184
11	47.302	1.9202	0.8	311	100	0.156
12	47.674	1.9060	5.9	2290	601	0.191
13	48.680	1.8690	3.9	1509	533	0.141
14	49.317	1.8463	0.2	83	21	0.195

SAMPLE 05%DOLO/95%CTT

NO.	2THETA	D	INTEG. I (%)	INTEG. I	MAX. I	FWHM
1	36.137	2.4836	56.5	866	157	0.275
2	39.595	2.2743	82.6	1265	249	0.254
3	43.351	2.0856	100.0	1533	359	0.214

SAMPLE 100%CTT-SPAR

NO.	2THETA	D	INTEG. I (%)	INTEG. I	MAX. I	FWHM
1	23.274	3.8188	1.3	593	113	0.262
2	29.669	3.0087	100.0	47381	13222	0.179
3	31.674	2.8227	0.5	251	49	0.258
4	36.237	2.4770	1.6	751	159	0.236
5	39.665	2.2704	2.7	1276	292	0.218
6	43.445	2.0813	3.1	1460	309	0.236
7	47.383	1.9171	0.9	420	86	0.246
8	47.799	1.9013	4.9	2317	509	0.227
9	48.761	1.8661	4.2	1999	563	0.178

APPENDIX 4

CLAY MINERALOGY

The clay mineral content of selected carbonate samples (and one clay sample from locality 34) are shown in Table 2. Data from Ehlers and Hoover (1961) and O'Donnel (1967), who analyzed clays from the shaly portions of the Brassfield, are also presented. Clays found in the Brassfield include illite, glauconite, kaolinite, and chlorite. Illite is most common and was present in all samples. Ehlers and Hoover (1961) and O'Donell (1967) determined that kaolinite and chlorite occur only in eastern and southeastern outcorp areas.

Chlorite is only found to the north. Samples from the west side of the Cincinnati Arch do not contain kaolinite or chlorite. This trend was noted by O'Donell and verified in this study (with the exception of locality 25, where chlorite is present). The presence of kaolinite (and absence of glauconite) is thought to indicate proximity of source area (Weaver, 1958; Odin and Letolle, 1980). In the Brassfield, high kaolinite contents are found to the east and southeast, where shale is in greatest abundance, suggesting a clastic source in this direction.

GLAUCONITE

Literature addressing the formation and mineralogical variations of glauconite minerals is extensive. Only an abbreviated treatment of the subject is given here.

TABLE 2

CLAY MINERALOGY OF SELECT OUTCROPS

LOCALITY	O'DONNEL 1967	EHLERS & HOOVER 1961	THIS REPORT
34			Illite/Glauconite/ Chlorite
32			Illite/Glauconite
37	Illite/Chlorite		
38	Illite/Chlorite		
39			Illite/Glauconite/ PossibleKaolinite/ Chlorite
40	Illite/Kaolinite	Illite/Kaolinite/ Possible Chlorite	
41	Illite/Kaolinite	Illite/Kaolinite/ Possible Chlorite	
36		Illite/Kaolinite/ Possible Chlorite	
42			
43	Illite/Kaolinite		Illite/Glauconite Possible Kaolinite
45	Illite/Kaolinite		
47			Illite/Glauconite Possible Kaolinite/ Chlorite
1			
5	Illite		Illite/Glauconite
18			Illite/Glauconite
23			Illite/ Glauconite
24			Illite/Glauconite
25			Illite/Glauconite
27	Illite		

"Glauconite," as it is commonly used, is a rather ambiguous term that refers to a wide variety of earthy, green, commonly pelloidal, hydrous silicates of iron and potassium. In fact, glauconite refers to a specific mineral: a hydrated ferric mica with less than 5% expandable layers (Burst, 1958). True "mineral gluaconite" is rare in most sediments, however.

The suite of glauconites commonly found in sediments can be regarded as an iron-rich analogue of the illite-smectite crystallogrpahic family. According to this scheme, glauconite begins growth as glauconitic illite-smectite and eventually evolves into a glauconitic mica. The length of sedimentary hiatus required for its formation has been estimated between thousands to millions of years (Odin and Letolle, 1980).

Glauconites have been thought to form by:

(1) absorption of bases by hydrated gelatinous silica (Takahashi, 1939);

(2) alteration of biotite and iron mica (Galliher, 1935); and

(3) absorption of potassium and iron by three-layer silica lattice minerals ("layer lattice" theory of Brust,. 1958).

However, the necessity for a particular parent material has been shown to be erroneous. It is the environment -- or microenvironment -- that controls the formation of glaucontie (Odin and Matter, 1981; Hein et al., 1974).

Conditions of very low sediment input over long periods of time in a normal marine environment are essential elements of glauconite formation. The mineralology of glauconite is thought to be related to the duration of its formation, and may provide a relative estimate of length of sedimentary hiatus. Rapid deposition interferes with the exchange of ions necessary for the mineralogical evolution of glauconite minerals (Odin and Letolle, 1980). The geochemical environment for authigenic gluaconite formation occurs at the interface between oxidizing and reducing conditions (Hein et al., 1974).

Fe^{+++} is the dominant oxidation state of iron incorporated into the octahedral layer, but some Fe^{++} is also taken up. Odin and Letolle (1981) suggest that semi-confined microenvironments, such as exist inside microtests, in pores of carbonate clasts, in fecal pellets, or on various minerals, would provide favorable control of redox conditions and a minimal exchange of iron and potassium ions with sea water.

BRASSFIELD GLAUCONITE

Glauconite in the Brassfield occur in three forms:

(1) well-formed pellets;

(2) glauconitized bioclasts (usually in crinoid stereom pores); and

(3) disseminated masses.

Well-formed pellets are most common in facies I, facies VII, in fine grained flaser beds of facies VI, and at the base of facies II and III. These horizons represent

considerable sedimentary hiatus and the well-formed glauconite pellets they are associated with may represent a highly evolved form that began as glauconitized bioclasts.

Glauconitized bioclasts are most common toward the middle and tops of facies II, III, V, and VI, and are probably not as evolved as well formed pellets. In short, well formed pellets are common at the base of shoaling-upward cycles, and glauconitized bioclasts occur toward the tops of the cycles. The base of shoaling cycles may maintain low rates of sedimentation for longer periods than cycle tops, and allow for the development of more highly evolved pellets. Disseminated glauconite is present in only a few samples and occurs as gray-green to green masses or as coatings on broad substrates.

All samples with green pellets and bioclasts contained glauconite. The high amount of octrahedral Fe+++ causes a scattering of the 002 reflection resulting in a weak to non-existent peak for pure or evolved glauconites. Most Brassfield glauconite samples showed a small reflection at this position, indicating a glauconite composition similar to illite (an iron rich illite).